CHALMERS

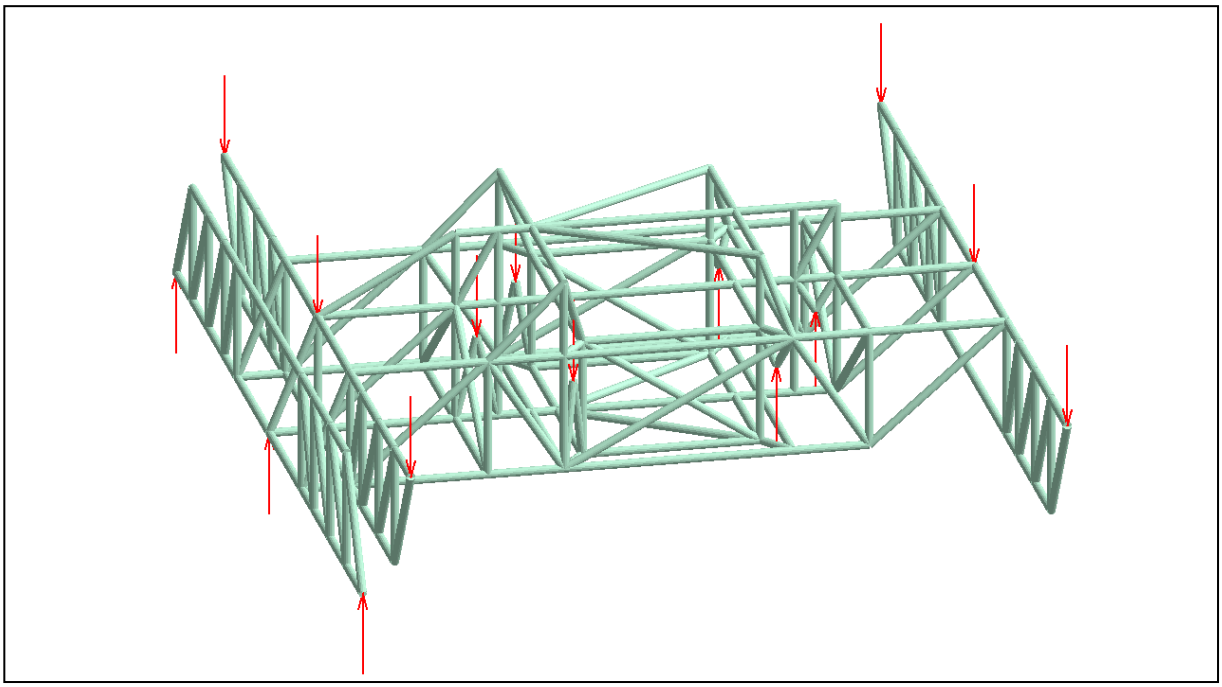

Three-dimensional strut-and-tie modelling of wind power plant foundations

Master of Science Thesis in the Master's Programme Structural engineering and building performance design

NICKLAS LANDÉN
JACOB LILLJEGREN

Department of Civil and Environmental Engineering
Division of Structural Engineering
Concrete Structures
CHALMERS UNIVERSITY OF TECHNOLOGY
Göteborg, Sweden 2012
Master's Thesis 2012:49

MASTER'S THESIS 2012:49

Strut-and-tie modelling of wind power plant foundations

Master of Science Thesis in the Master's Programme Structural engineering and building performance design

NICKLAS LANDÉN

JACOB LILLJEGREN

Department of Civil and Environmental Engineering
Division of Structural Engineering
Concrete Structures
CHALMERS UNIVERSITY OF TECHNOLOGY
Göteborg, Sweden 2012

Strut-and-tie modelling of wind power plant foundations

Master of Science Thesis in the Master's Programme Structural engineering and building performance design

NICKLAS LANDÉN JACOB LILLJEGREN

© NICKLAS LANDÉN, JACOB LILLJEGREN, 2012

Examensarbete / Institutionen för bygg- och miljöteknik,
Chalmers tekniska högskola, 2012:49

Department of Civil and Environmental Engineering
Division of Structural Engineering
Concrete Structures
Chalmers University of Technology
SE-412 96 Göteborg
Sweden
Telephone: + 46 (0)31-772 1000

Cover:
Established 3D strut-and-tie model for a wind power plant foundation.

Chalmers Reproservice Göteborg, Sweden 2012

Master of Science Thesis in the Master's Programme Structural engineering and building performance design

NICKLAS LANDÉN
JACOB LILLJEGREN
Department of Civil and Environmental Engineering
Division of Structural Engineering
Concrete structures
Chalmers University of Technology

ABSTRACT

With an increasing demand for renewable energy sources worldwide, a promising alternative is wind power. During the last decades the number of wind power plants and their size has increased. Wind power plant foundations are subjected to a centric load, resulting in a 3D stress distribution. Even though this is known, the common design practice today is to design the foundation on the basis of classical beam-theory. There is also an uncertainty of how to treat the fatigue loading in design. Since a wind power plant is highly subjected to large variety of load amplitudes the fatigue verification must be performed.

The purpose with this master thesis project was to clarify the uncertainties in the design of wind power plant foundations. The main objective was to study the possibility and suitability for designing wind power plant foundations with 3D strut-and-tie modelling. The purpose was also to investigate the appropriateness of using sectional design for wind power plant foundations.

A reference case with fixed loads and geometry was designed according to Eurocode with the two different methods, i.e. beam-theory and strut-and-tie modelling. Fatigue assessment was performed with Palmgren-Miners law of damage summation and the use of an equivalent load. The shape of the foundation and reinforcement layout was investigated to find appropriate recommendations.

The centric loaded foundation results in D-regions and 3D stress flow which make the use of a strut-and-tie model an appropriate design method. The 3D strut-and-tie method properly simulates the 3D stress flow and is appropriate for design of D-regions. Regarding the common design practice the stress variation in transverse direction is not considered. Hence the design procedure is incomplete. If the linear-elastic stress distribution is determined, regions without stress variation in transverse direction can be distinguished. Those regions can be designed with beam-theory while the other regions are designed with a 3D strut-and-tie model.

Further, clarifications of fatigue assessment regarding the use of an equivalent load for reinforced concrete need to be recognized. The method of using an equivalent load in fatigue calculations would considerably simplify the calculations for both reinforcement and concrete.

We found the use of 3D strut-and-tie method appropriate for designing wind power plant foundations. But the need for computational aid or an equivalent load are recommended in order to perform fatigue assessment.

Key words: wind power plant foundation, gravity foundations, 3D, three-dimensional strut-and-tie model, fatigue, equivalent load, concrete

Dimensionering av vindkraftsfundament med tredimensionella fackverksmodeller
Examensarbete inom Structural engineering and building performance design
NICKLAS LANDÉN
JACOB LILLJEGREN
Institutionen för bygg- och miljöteknik
Avdelningen för Konstruktionsteknik
Betongbyggnad
Chalmers tekniska högskola

SAMMANFATTNING

I takt med ökad efterfrågan på förnyelsebara energikällor de senaste decennierna har både antalet vindkraftverk och dess storlek vuxit. De större kraftverken har resulterat i större laster och därmed större fundament. På grund av en ständigt varierande vindlast måste fundamenten dimensioneras för utmattning. Vidare är fundamenten centriskt belastade vilket ger upphov till ett 3D spänningsflöde. Det verkar dock vanligt att dimensionera fundamenten genom att anta att spänningarna är jämt utspridda över hela fundamentet och använda balkteori. Ett sätt att ta större hänsyn till det 3D spänningsflödet är att dimensionera fundamentet med en 3D fackverksmodell.

Det huvudsakliga syftet med examensarbetet var att undersöka möjligheten att dimensionera vindkraftsfundament med en 3D fackverksmodell, men även undersöka om det är lämpligt att basera dimensioneringen på balkteori. Dessutom har olika armeringsutformningar studerats.

För att utreda nämnda frågeställning utfördes en dimensionering av ett vindkraftsfundament med givna laster och dimensioner grundat på Eurocode. Fundamentet dimensionerades både med en 3D fackverksmodell och genom att använda balkteori. Utmattningsberäkningarna utfördes med Palmgren-Miners delskadehypotes och med en ekvivalent spänningsvariation.

Med hänsyn till lastförutsättningen, vilket förutom att ge upphov till ett 3D spänningsflöde också resulterar i D-regioner. Därav finner vi det lämpligt att använda sig av 3D fackverksmodeller. Gällande dimensionering grundad på balkteori är denna ogiltig då spänningsvariationen den transversella riktningen inte beaktas.

Vi anser att det är lämpligt att använda sig av 3D fackverksmodeller, det krävs dock en automatiserad metod eller en ekvivalent last för att kunna hantera hela lastspektrumet. Gällande användandet av en ekvivalent last krävs vidare studier på hur denna skall beräknas.

Nyckelord: vindkraftsfundament, gravitationsfundament, 3D, tredimensionell, fackverksmodell, ekvivalent last, betong

Contents

ABSTRACT I
SAMMANFATTNING II
CONTENTS III
PREFACE VII
NOTATIONS VIII

1 INTRODUCTION 1
1.1 Background 1
1.2 Purpose and objective 2
1.3 Limitations 2
1.4 Method 3

2 WIND POWER PLANT FOUNDATIONS 4
2.1 Design aspects of wind power plant foundations 4
2.2 Function of gravity foundations 4
2.3 Connection between tower and foundation 5

3 DESIGN ASPECTS OF REINFORCED CONCRETE 6
3.1 Shear capacity and bending moment capacity 6
3.2 Fatigue 9
3.2.1 Fatigue in steel 9
3.2.2 Fatigue in concrete 10
3.2.3 Fatigue in reinforced concrete 10

4 STRUT-AND-TIE MODELLING 12
4.1 Principle of strut-and-tie modelling 12
4.2 Design procedure 12
4.3 Struts 14
4.4 Ties 14
4.5 Strut inclinations 15
4.6 Nodes 15
4.7 Three-dimensional strut-and-tie models 17
4.7.1 Nodes and there geometry 18

5 REFERENCE CASE AND DESIGN ASSUMPTIONS 19
5.1 Design codes 19
5.2 General conditions 20

5.3 Geometry and loading 20
5.4 Tower foundation connection 22
5.5 Global equilibrium 25

6 DESIGN OF THE REFERENCE CASE ACCORDING TO COMMON PRACTICE ON THE BASIS OF EUROCODE 29
6.1 Bending moment and shear force distribution 29
6.2 Bending moment capacity 32
6.3 Shear capacity 34
6.4 Crack width limitation 37
6.5 Fatigue 37
6.6 Results 41
6.7 Conclusions on common design practice 42

7 DESIGN OF REFERENCE CASE WITH 3D STRUT-AND-TIE MODELS AND EUROCODE 2 45
7.1 Methodology 45
7.2 Two-dimensional strut-and-tie model 45
7.3 Three-dimensional strut-and-tie models 46
7.4 Reinforcement and node design 51
7.5 Fatigue 53
7.6 Results 53
7.7 Conclusions on the 3D strut-and-tie method 55

8 CONCLUSIONS AND RECOMMENDATIONS 56
8.1 Reinforcement layout and foundation shape 56
8.2 Suggestions on further research 56

9 REFERENCES 58

APPENDICES

A IN DATA REFERENCE CASE 60
A.1 Geometry 60
A.2 Loads 62
A.3 Material properties 64

B GLOBAL EQUILIBRIUM 65
B.1 Eccentricity and width of soil pressure 65

B.2 Shear force and bending moment distribution 68
B.3 Sign convention 74

C DESIGN IN ULTIMATE LIMIT STATE 75
C.1 Sections 75
C.2 Design of bending reinforcement 77
C.3 Star reinforcement inside embedded anchor ring 80
C.4 Minimum and maximum reinforcement amount 82
C.5 Shear capacity 82
C.6 Local effects and shear reinforcement around steel ring 86

D CRACK WIDTHS SERVICE ABILITY LIMIT STATE 91
D.1 Loads 91
D.2 Crack control 92

E FATIGUE CALCULATIONS WITH EQUIVALENT LOAD CYCLE METHOD 97
E.1 Loads and sectional forces 97
E.2 Fatigue control bending moment 102
E.3 Fatigue control local effects 109

G FATIGUE CONTROL WITH THE FULL LOAD SPECTRA 112
G.1 Loads and sectional forces 112
G.2 Fatigue in bending reinforcement 121
G.3 Shear force distribution 132
G.4 Fatigue in U-bows 135

H UTILISATION DEGREE AND FINAL REINFORCEMENT LAYOUT 138

I FATIGUE LOADS 140

J SECTIONS OF STRUT AND TIE MODEL 1 146

K REINFORCEMENT CALCULATIONS AND FORCES IN STRUTS AND TIES 149

Preface

This master's thesis project was carried out at Norconsults office in Gothenburg in cooperation with the department of structural engineering at Chalmers University of Technology.

We would like to thank team 'Byggkonstruktion' for making the stay so pleasant. We especially would like to thank our supervisor at Norconsult Anders Bohiln for always taking the time needed to answer questions and give useful feedback.

We are also grateful to our examiner Professor Björn Engström and supervisor Doctor Rasmus Rempling for aiding us in this master's thesis project.

Notations

Roman upper case letters

A_s	Cross sectional area of reinforcement in bottom
A'_s	Cross sectional area of reinforcement in top
A_{sw}	Cross sectional area of shear reinforcement
F_k	Characteristic load
F_{soil}	Soil pressure
F_c	Compressive force component from moment
F_t	Most eccentric tensile force component from moment
F_x	Horizontal component of wind force in x direction
F_y	Horizontal component of wind force in y direction
F_{xy}	Resulting horizontal component of wind force
G	Total self-weight of foundation including filling material
M	Bending moment
M_x	Bending moment around x-axis
M_y	Bending moment around y-axis
M_{xy}	Resulting bending moment
$M_{xy,k}$	Characteristic moment
N_{eq}	Equivalent number of allowed cycles
N	Normal force
S_r	Range of load cycles
$S_{r,eq}$	Equivalent range of load cycle
V	Shear force
$V_{Rd,c}$	Shear capacity for concrete without shear reinforcement

Roman lower case letters

b	Width of soil pressure
c	Concrete cover
d	Effective depth
d_s	Distance between force couple from resisting moment
d_{sr}	Diameter of anchor ring eccentricity
e	Eccentricity of soil pressure resultant
g	Self-weight of slab including filling material

f_c Concrete compressive strength

f_{cd} Design value of concrete compressive strength

f_{ck} Characteristic value of concrete compressive strength

f_{yd} Design yield strength of steel

k_1 Design yield strength of steel

m Exponent that defines the slope of the S-N curve

n Number of cycles

r_0 Radius of anchor ring

z Length of internal lever arm

Greek upper case letters

σ Stress

$\sigma_{Rd,max}$ Design strength for a concrete strut or node

Greek lower case letters

ε_c Concrete strain

ε_s Steel strain

γ_f Load partial factor

γ_F Fatigue load partial factor

γ_m Material partial factor

υ Reduction factor for the compressive strength for cracked strut (EC2)

1 Introduction

There is a growing demand for renewable energy sources in the world and wind power shows a large growth both in Sweden and globally. Both the number of wind power plants and their sizes have increased during the last decades.

1.1 Background

In the beginning of 1980 the first wind power plants were built in Sweden. In 2009 about 1400 wind power plants produced 2.8 TWh/year, which corresponds to 2 % of the total production in Sweden, Vattenfall (2011). The Swedish government's energy goal for 2020 is to increase the use of renewable energy to 50 % of total use. This means that the energy produced only from wind power has to increase to 30 TWh/year. As wind has become a more popular source of energy the development of larger and more effective wind power plants has gone rapidly.

The sizes of wind power plants have increased from a height of 30 m and a diameter of the rotor blade of 15 m in 1980 to a height of 120 m and a diameter of the rotor blade of 115 m in 2005, se Figure 1.1.

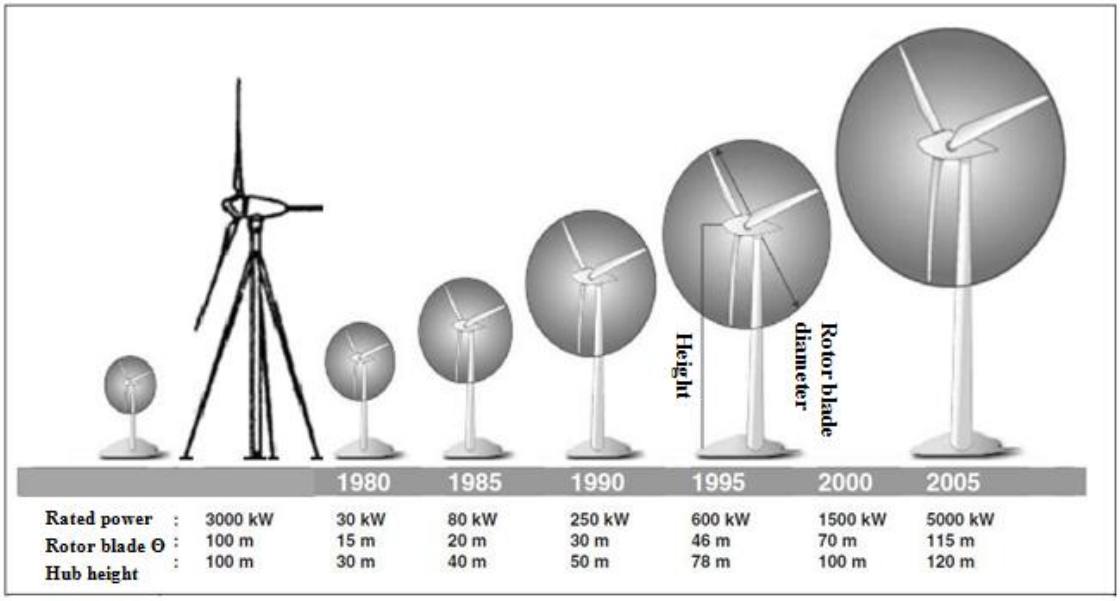

Figure 1.1 How the size of rotor blade and height have changed from 1980 to 2005 adopted from Faber, T. Steck, M. (2005).

The increased sizes have led to larger loads and consequently larger foundations. In addition to the need for sufficient resting moment capacity the foundations are subjected to cyclic loading due the variation in wind loads. The cyclic loading requires that the foundations are designed with regard to fatigue.

The tower is connected to the centre of the foundation where the rotational moment is transferred to the foundation according to Figure 1.2. The concentrated forces cause stress variations in three directions and also result in a Discontinuity region (D-region) where beam-theory no longer is valid.

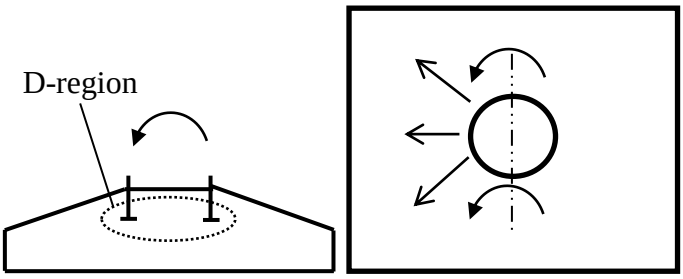

Figure 1.2 The foundation is subjected to concentrated forces and centric loading causing need for load transfer in two directions.

In contrast to B-regions (Bernoulli- or Beam-regions) the assumption that plane sections remain plane in bending is not valid in D-regions. Figure 1.3 shows how a centric loading resulting in a stress variation in three directions, similar to a flat slab.

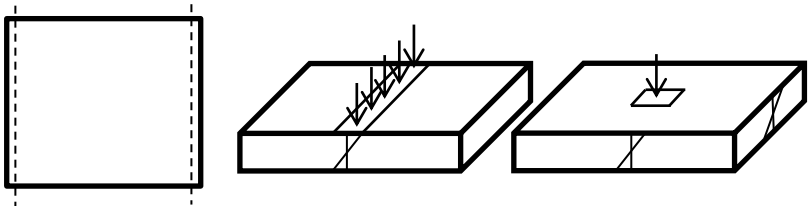

Figure 1.3 Left: boundary conditions. Middle: Loading applied along the full width, no stress variations along the width. Right: Centric loading results in stress variation in three directions.

Despite the centric concentrated load it appears to be common practice to assume that the internal forces are spread over the full width of the foundation and base the design on classical beam-theory.

D-regions can be designed with the so called strut-and-tie model, which is a lower bound approach for designing cracked reinforced concrete in the ultimate limit state. The method is based on plastic analysis and is valid for both D-regions and B-regions. In addition the strut-and-tie model can be established in three dimensions to capture the 3D stress flow. For this reason the strut-and-tie method seem to be a suitable approach to design wind power plant foundations.

1.2 Purpose and objective

The purpose with this master thesis project was to clarify the uncertainties in the design of wind power plant foundations. The main objective was to study the possibility and suitability for designing wind power plant foundations with 3D strut-and-tie modelling. The purpose was also to investigate the appropriateness of using sectional design for wind power plant foundations.

1.3 Limitations

In the project, focus will be directed to the foundation, the behaviour of the surrounding soil and its properties should not be investigated in detail. The master thesis project only considers on-shore gravity foundations.

1.4 Method

Initially a litterateur study was performed to gain a better understanding of the difficulties in designing wind power plant foundations. Today's design practice was identified and the various design aspects were studied. Further information about the strut-and-tie method was acquired from literature. For the purpose of studying the suitability for designing wind power plant foundations with the different approaches a reference case was used. The reference foundation was designed with both today´s design practice, i.e. using sectional design, and the use of a 3D strut-and-tie model. The design of the reference foundation with fixed geometry and loading was performed according to Eurocode. The two different design approaches was compared in order to find advantages and disadvantages with the alternative methods. To handle the complex 3D strut-and-tie models the commercial software *Strusoft FEM-design 9.0 3D frame* was used.

2 Wind power plant foundations

This chapter presents general information about the function and loading of gravity foundations.

2.1 Design aspects of wind power plant foundations

The location of a wind power plant affects the design of the foundation in many different ways. One of the most important is obviously the wind conditions. The design of the foundation changes depending whether the foundation is located on- or off-shore. On-shore foundation design is affected by the geotechnical properties of the soil. Three different types of on-shore foundations can be distinguished, gravity foundations, rock anchored foundations and pile foundations. In addition to the geotechnical conditions off-shore foundations must also be designed for currents and uplifting forces.

The most common type is gravity foundations, which is the only type of foundations studied in this project. Gravity foundations can be constructed in many different shapes such as square, octagonal and circular. The upper part of the slab can be flat, but often has a small slope of up to 1:5 from the centre towards the edges to reduce the amount of concrete and to divert water.

2.2 Function of gravity foundations

The height of modern wind power plant can be over 100 m with almost the same diameter of the rotor blades. Consequently the foundation is subjected to large rotational moments. As the name gravity foundations suggest, the foundation prevents the structure from tilting by its self-weight. In addition to restrain the rotational moment the foundation must bear the self-weight of turbine and tower. Depending on the height of the tower, size of the turbine and location of the wind power plant the foundation usually varies between a thickness of 1.5 - 2.5 m and a width of 15 - 20 m. Figure 2.1 shows how the structure resists the rotational moment with a level arm between the self-weight and reaction force of the soil.

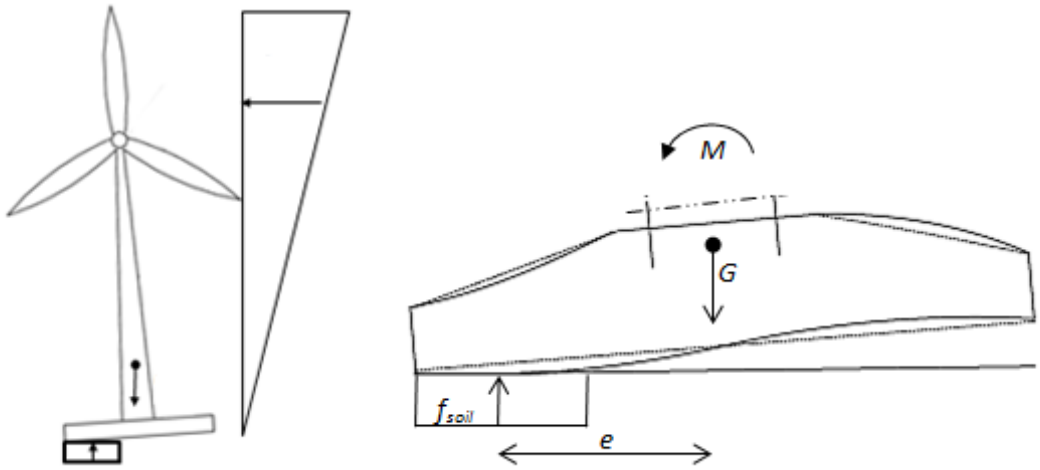

Figure 2.1 The structure is prevented from tilting by a level arm (e) between the self-weight (G) and the eccentric reaction force of the soil (F_{soil}).

Depending on load magnitude and soil pressure distribution the eccentricity varies. To transfer the load, the foundation must have sufficient flexural and shear force capacity, which must be provided for with reinforcement. Since the wind loads vary, the foundation is subjected to cyclic loads which make a fatigue design mandatory to ensure sufficient fatigue life. Figure 2.2 shows a wind power plant where the loss of equilibrium has led to failure, even though the flexural capacity appears to be sufficient.

Figure 2.2 A collapsed power plant due to loss of equilibrium SMAG (2011).

2.3 Connection between tower and foundation

There are different methods used to connect the tower to the foundation Faber, T. Steck, M. (2005). Figure 2.3 shows three common connection types, so called anchor rings or embedded steel rings. All consist of a top flange prepared for a bolt connection to the tower. The anchor rings is located in the centre of the foundation surrounded by concrete. The first type (a) consists of an anchor ring in steel with an I-section. Alternative (b) only has one flange casted in the concrete and is often used in smaller foundations. This solution requires suspension reinforcement to lift up the compressive load to utilise the concrete. The last solution (c) consists of a pre-stressed bolt connection between two flanges.

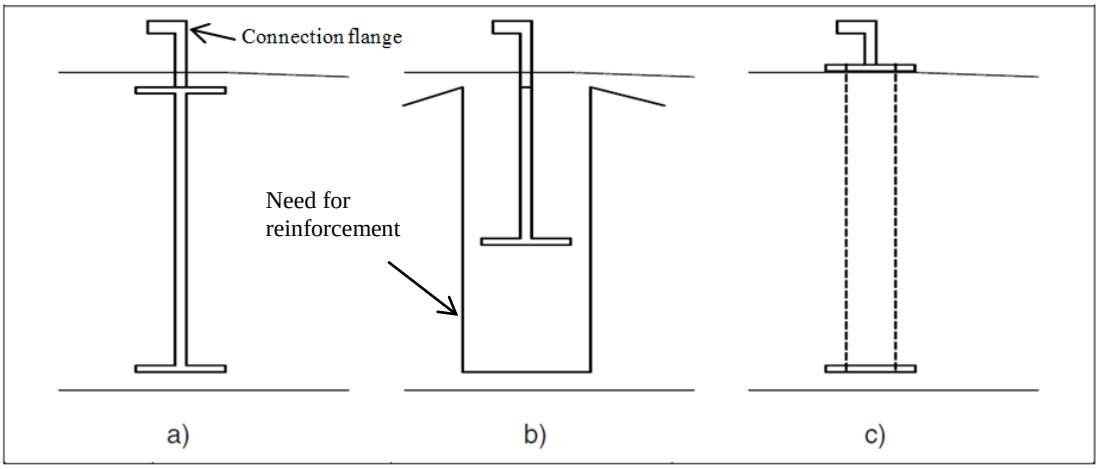

Figure 2.3 Three common types of connections between the tower and foundation, adopted from Faber, T. Steck, M. (2005).

3 Design aspects of reinforced concrete

This chapter gives a general description of design aspects regarding internal force transfer and fatigue in reinforced concrete.

3.1 Shear capacity and bending moment capacity

For beams and slabs a linear strain distribution can be assumed since the reinforcement is assumed to fully interact with the concrete. Hence sectional design using Navier's formula can be used for design of reinforced concrete beams and slabs. The design must ensure that both the flexural and shear capacity is sufficient. In addition limitations on crack widths and deformations must be fulfilled to achieve an acceptable behaviour in serviceability limit state.

Three types of cracks can be distinguished in beams:

- Shear cracks, Figure 3.1 (1): develop when principal tensile stresses reach the tensile strength of concrete in regions with high shear stresses.
- Flexural cracks, Figure 3.1 (3): develop when flexural tensile stresses reach the tensile strength of concrete in regions with high bending stresses.
- Flexural-shear-cracks, Figure 3.1 (2). A combination of shear and flexural cracks in regions with both shear and bending stresses

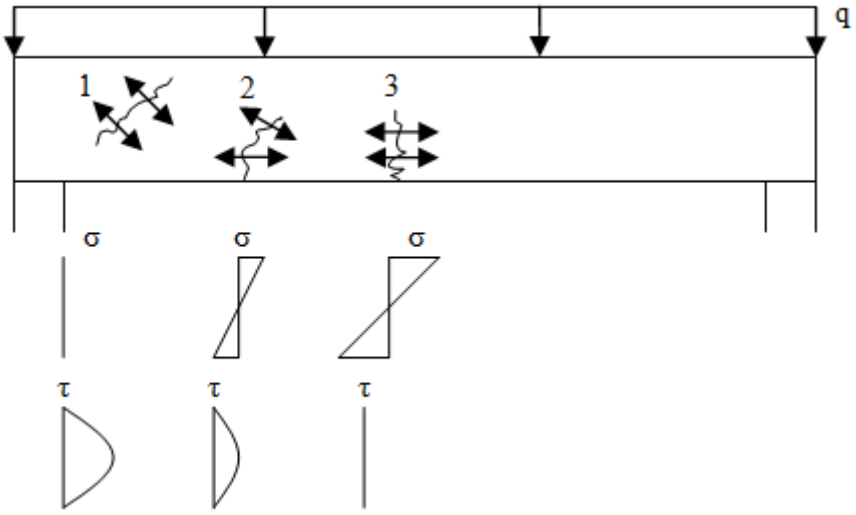

Figure 3.1 Example of crack-types in a simply supported beam. (1) Shear crack (2) flexural-shear-crack (3) flexural crack.

To avoid failure due to flexural cracks, bending reinforcement is placed in regions with high tensile stresses. The model shown in Figure 3.2 can be used to calculate bending moment capacity, assuming compressive failure in concrete. In the model tensile strength of concrete is neglected and linear elastic strain distribution is assumed.

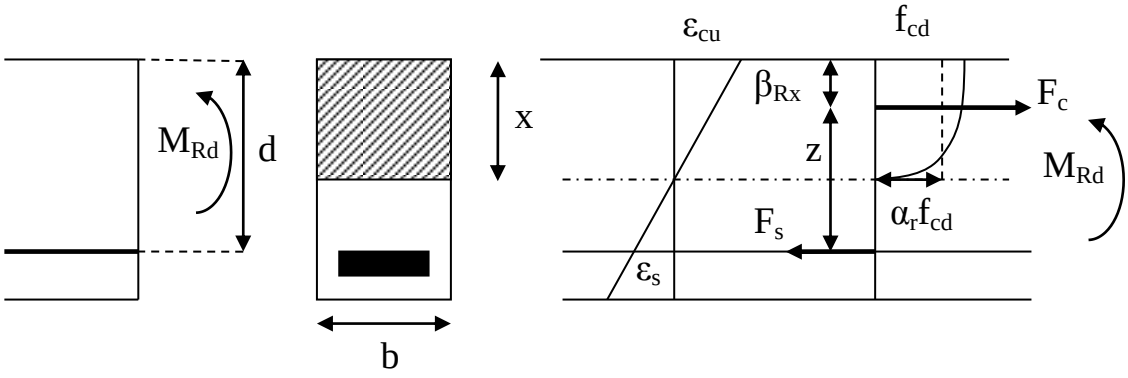

Figure 3.2 Calculation model for moment capacity in reinforced concrete assuming full interaction between steel and concrete. This results in a linear strain distribution.

The ultimate bending moment capacity can be calculated with the following equations:

$$F_s = F_c \rightarrow \sigma_s A_s = \alpha_R f_{cd} x b \tag{3.1}$$

$$\rightarrow M_{Rd} = \alpha_R f_{cd} x b (d - \beta_R x) \tag{3.2}$$

where:

α_R Stress block factor for the average stress

β_R Stress block factor for the location of the stress resultant

Shear forces in crack concrete with bending reinforcement are transferred by an interaction between shear transferring mechanisms shown in Figure 3.3.

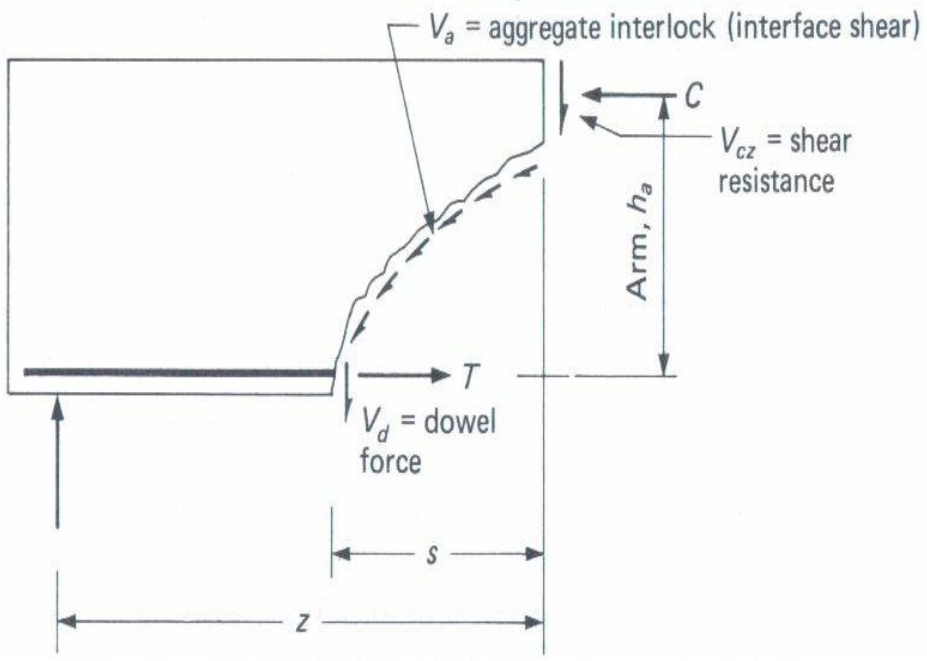

Figure 3.3 Shear transferring mechanisms in a beam with bending reinforcement.

The shear capacity for beams without vertical reinforcement is hard to calculate analytically and many design codes are based on empirical calculations. To increase the shear capacity vertical reinforcement (stirrups) can be used resulting in a truss–action as shown in Figure 3.4.

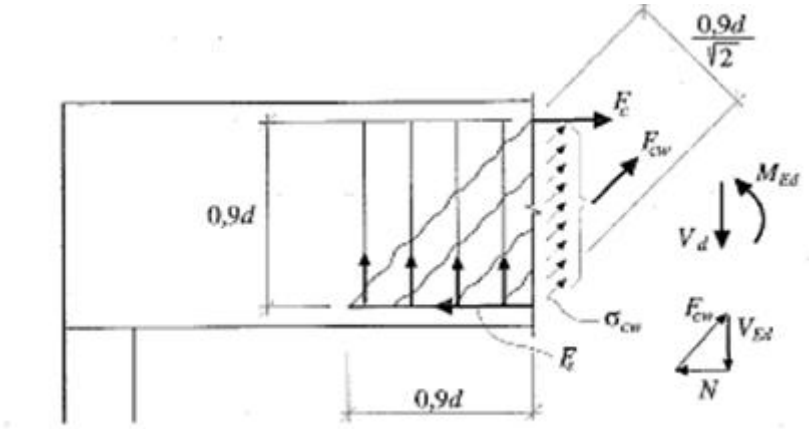

Figure 3.4 Truss action in a concrete beam with shear reinforcement.

The model in Figure 3.4 is used to calculate the shear capacity for beams with vertical or inclined reinforcement; in calculations according to Eurocode effects from dowel force and aggregate interlock are neglected. The inclination of the compressive stress field (F_{cw}) depends on the amount of shear reinforcement; an increased amount increases the angle. In order to achieve equilibrium an extra normal force (N) appears in the bending reinforcement. The relationship between the additional tensile force of the shearing force and the angle of F_{cw} is that if one increases, the other decreases and vice versa.

To ensure sufficient shear capacity the failure modes described in Figure 3.5 must be checked.

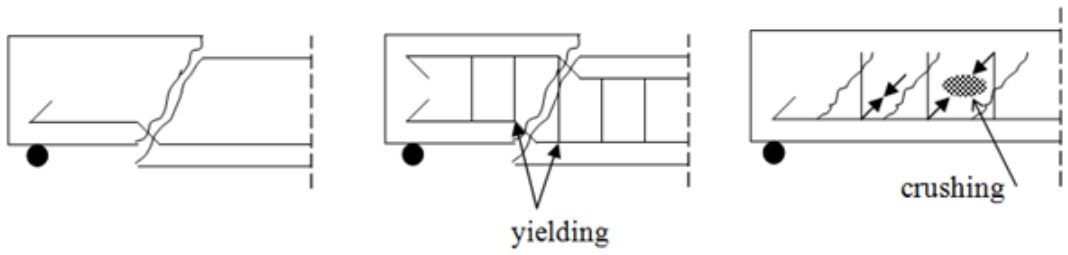

Figure 3.5 Different shear failure modes. Left: shear sliding. Middle: Yielding of stirrups. Right: Crushing in concrete.

A special case of shear failure is punching shear failure which must be considered when a concentrated force acts on a structure that transfers shear force in two directions. When failure occurs a cone is punched through with an angle regularly between 25 and 40 degrees, exemplified in Figure 3.6.

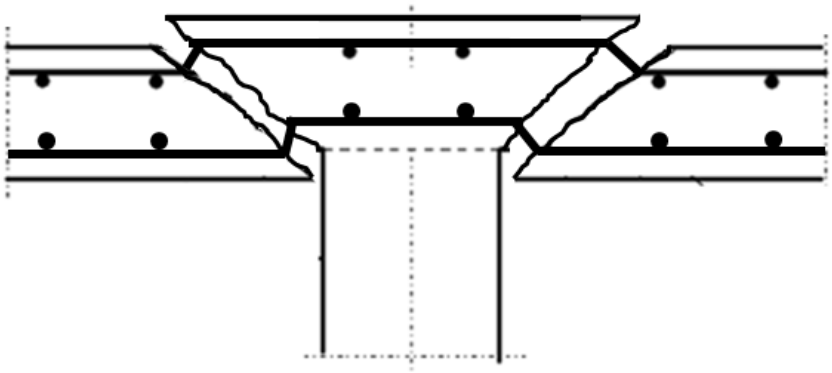

Figure 3.6 Punching shear failure in a slab supported by a column. A cone is punched through the slab.

3.2 Fatigue

Failure in materials does not only occur when it is subjected to a load above the ultimate capacity, but also from cyclic loads well below the ultimate capacity. This phenomenon is known as fatigue and is a result of accumulated damage in the material from cyclic loading, fatigue is therefore a serviceability limit state problem. American Society for Testing and Materials (ASTM) defines fatigue as:

> *Fatigue: The process of progressive localized permanent structural change occurring in a material subjected to conditions that produce fluctuating stresses and strains at some point or points and that may culminate in cracks or complete fracture after a sufficient number of fluctuations.*

The fatigue life is influenced by a number of factors such as the number of load cycles, load amplitude, stress level, defects and imperfections in the material. Even though reinforced concrete is a composite material, the combined effects are neglected when calculating fatigue life. Instead the fatigue calculations are carried out for the materials separately according to Eurocode 2. Concrete and steel behave very differently when subjected to fatigue loading. One important aspect of this is that the steel will have a strain hardening while the concrete will have a strain softening with increasing number of load cycles. Another is the effect of stress levels which affects the fatigue life of concrete more than steel.

Cyclic loaded structures such as bridges and machinery foundations are often subjected to complex loading with large variation in both amplitude and number of cycles. A wind power plant foundation loaded with wind is obviously such a case. Therefore, there are simplified methods for the compilation of force amplitude, one such example is the rain flow method. The basic concept of the rain flow method is to simplify complex loading by reducing the spectrum. The fatigue damage for the different load-amplitudes can then be calculated and added with the Palmgren-Minor rule.

3.2.1 Fatigue in steel

Fatigue damage is a local phenomenon; it starts with micro cracks increasing in an area with repeated loading which then grow together forming cracks. Fatigue loading accumulate permanent damage and can lead to failure. Essentially two basic fatigue

design concepts are used for steel, calculation of linear elastic fracture mechanics and use of S-N curves. In general fatigue failure is divided in three different stages, crack initiation, crack propagation and failure. Calculations of the fatigue life with fracture mechanics is divided into crack initiation life and crack propagation life. These phases behave differently and are therefore governed by different parameters. The other method is Whöller diagram or S-N curves which are logarithmic graphs of stress (S) and number of cycles to failure (N), see Figure 3.7. These graphs are obtained from testing and are unique for every detail, Stephens R (1980).

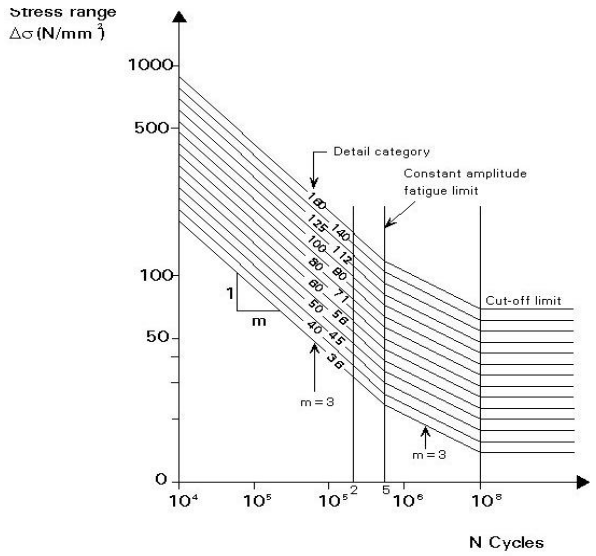

Figure 3.7 S-N curves for different steel details. Note that the cut-off limit shows stress amplitudes which do not result in fatigue damage.

3.2.2 Fatigue in concrete

Concrete is a much more inhomogeneous material than steel, Svensk Byggtjänst (1994). Because of temperature differences, shrinkage, etc. during curing micro cracks develop even before loading. These cracks will continue growing under cyclic loading and other cracks will develop simultaneously in the loaded parts of the concrete. The cracks grow and increase in numbers until failure. It should be noted that is very hard to determine where cracking will start and how they will spread.

3.2.3 Fatigue in reinforced concrete

As stated before the fatigue capacity of reinforced concrete is determined by checking concrete and steel separately. When a reinforced concrete structure is subjected to cyclic load the cracks will propagate and increase, resulting in stress redistribution of tensile forces to the reinforcement Svensk Byggtjänst (1994). Fatigue can occur in the interface between the reinforcement bar and concrete which can lead to a bond failure. There are different types of bond failure such as splitting and shear failure along the perimeter of the reinforcement bar.

Regarding concrete without shear reinforcement the capacity is determined by the friction between the cracked surfaces. The uneven surfaces in the cracks are degraded by the cyclic load which can result in failure. When shear reinforcement is present, it is the fatigue properties of the shear reinforcement that will determine the fatigue life.

Fatigue failure in reinforcement can be considered more dangerous than in concrete, since there might not be any visual deformation prior to failure. For concrete on the other hand there is often crack propagation and an increased amount of cracks along with growing deformations, which form under a relatively long time.

4 Strut-and-tie modelling

In this chapter the basic principles of strut-and-tie modelling will be described. Design of the different parts of strut-and-tie models will be explained, such as ties, struts and nodes.

4.1 Principle of strut-and-tie modelling

The strut-and-tie model simulates the stress filed in reinforced cracked concrete in the ultimate limit state. The method provides a rational way to design discontinuity regions with simplified strut-an-tie models consisting of compressed struts, tensioned ties and nodes in-between and where external concentrated forces act.

A strut-and-tie model is well suited for Bernoulli regions (B-regions) as well as in shear critical- and other disturbed (discontinuity) regions (D-regions). A D-region is where the Euler-Bernoulli assumption that plane sections remain plane in bending is not valid. Consequently, the strain distribution is non-linear and Navier's formula is not valid. The stress field is indeterminate and an infinite number of different stress distributions are possible with regard to equilibrium conditions. A D-region extends up to a distance of the sectional depth of the member.

The strut-and-tie model is a lower bound solution in theory of plasticity, which means that the plastic resistance is at least sufficient to withstand the design load. For this to be true the following criteria must be fulfilled:

- The stress field satisfies equilibrium with the external load
- Ideally plastic material response
- The structure behaves ductile, i.e. plastic redistribution can take place

The strut-and-tie method is beneficial to use when designing D-regions since it takes all load effects into consideration simultaneously i.e. N, V and M. Another advantage is that the method describes the real behaviour of the structure. Hence, it gives the designer an understanding of cracked reinforced concrete in ultimate limit state in contrary to many of the empirical formulas found in design codes.

4.2 Design procedure

When designing structures with the strut-and-tie method, it is important to keep in mind that it is a lower bound approach based on theory of plasticity. This means that many solutions to a problem may exist and be acceptable, even if for example the reinforcement amount or layout become different. The reason for this is that in the ultimate limit state all the necessary plastic redistribution has taken place and the reinforcement provided by the designer is utilised. However, it is still important that the structure is designed so that the need of plastic redistribution is limited. This can be achieved by designing the structure on the basis of a stress field close to the linear elastic stress distribution, which will give an acceptable performance in serviceability limit state.

There are no unique strut-and-tie models for most design situations, but there are a number of techniques and rules which help the designer to develop a suitable model. To find a reasonable stress flow there are different methods that can be used such as the 'load path method' purposed by Schlaich, J. et.al (1987), 'stress field approach'

according to Muttoni, A. et.al. (1997) or by linear finite element analysis. These methods can aid the designer in choosing an appropriate stress feild.

In order to show how a strut-and-tie model can be established the methodology will be used on a simple 2D problem. The first step is to determine the B- and D-region. The second step is to choose a model to simulate the stress field. To find the stress filed the load path method will be used in the example bellow. When using the load path method there are certain rules that must be fulfilled:

- The load path represents a line through which the load is transferred in the structure, i.e. from loaded area to support(s)
- Load paths do not cross each other
- The load path deviates with a sharp bent curve near concentrated loads and supports
- The load path should deviate with a soft bent curve **further away** from supports and concentrated loads
- At the boundary of the D-region the load path starts in the same direction as the load or support reaction
- The load must be divided in an adequate amount to avoid an oversimplistic representation

When a load paths that fulfil all these requirements have been established, areas where transverse forces are needed to change the direction of the load paths are located. These are areas where there is a need for either a compressive or tensile force in transversal direction. It is also important to note if the change in transverse direction should develop abruptly or gradually, since this will decide if the corresponding nodes will be concentrated or distributed, which is further explained in Section 4.6 about nodes.

Figure 4.1 illustrates the creation of a strut-and-tie model by means of the load path method. However before the strut-and-tie model can be accepted angle limitations and control of concentrated nodes described below must be fulfilled.

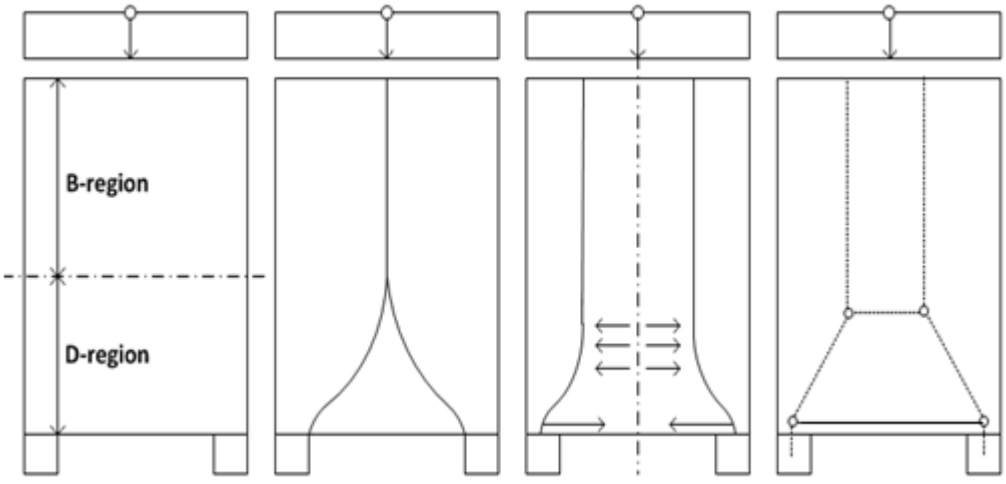

Figure 4.1 Example of how a strut-and-tie model can be established by means of the load path method.

4.3 Struts

The struts represent the compressed concrete stress field in the strut-and-tie model, often represented by dashed lines in the model. Struts are generally divided in three types, prismatic-, bottle- and fan-shaped struts, see Figure 4.2. The prismatic-shaped strut has a constant width. The bottle-shaped strut contracts or expands along the length and in the fan-shaped strut a group of struts with different inclinations meet or disperse from a node.

The capacity of a strut is in Eurocode related to the concrete compressive strength under uniaxial compression. The capacity of the strut must be reduced, if the strut is subjected to unfavourable multi-axial effects. On the other hand, if the strut is confined in concrete (i.e. multi-axial compression exists), the capacity of the strut becomes greater.

If the compressive capacity of a strut is insufficient, it can be increased by using compressive reinforcement.

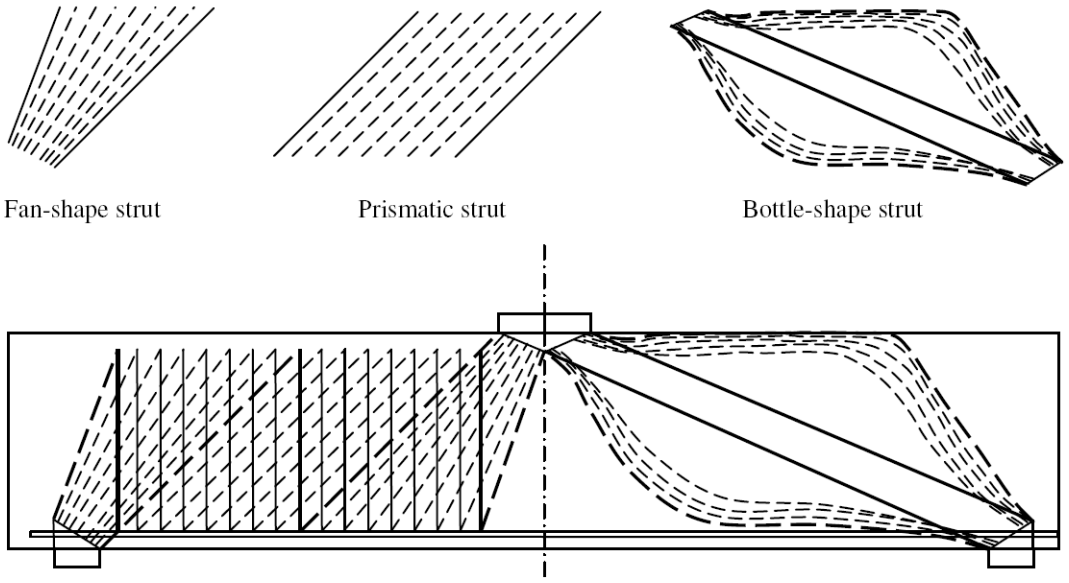

Figure 4.2 The different strut shapes with examples in a beam, Chantelot, G. and Alexandre, M. (2010).

4.4 Ties

Ties are the tensile members in a strut-and-tie model, which represent reinforcement bars and stirrups. Although concrete has a tensile capacity, its contribution to the tie is normally neglected. There are two common types of ties, concentrated and distributed. Concentrated ties connected concentrated nodes and are usually reinforced with closely spaced bars. Distributed ties are in areas with distributed tensile stress fields between distributed nodes and here the reinforcement is spread out over a larger area.

A critical aspect when detailing especially concentrated ties is to provide sufficient anchorage. It can be beneficial to use stirrups, since the bends provide anchorage.

4.5 Strut inclinations

When a strut-and-tie model is established, it needs to fulfil rules concerning the angle between the struts and ties. The reason for this limitation is that too small or large angles influence the need for plastic redistribution and the service state behaviour. The recommended angles vary between design codes, but also depending on how the strut(s) and tie(s) intersect.

When designing on the basis of more complex strut-and-tie models, a situation may arise where all angle requirements cannot be satisfied. Then the heavily loaded struts should be prioritised and the requirements for less critical struts may be disregarded, Engström (2011).

Recommended angles according to Schäfer, K. (1999)

- Distribution of forces shall take place directly, with approximately 30° but not more than 45°

Recommended minimum angles between struts and ties, Schäfer, K. (1999)

- Between strut and tie, approximately 60° but not less than 45° Figure 4.3 (a) and (b)
- In case of a strut between two perpendicular ties, preferred 45°but not smaller than 30°, see Figure 4.3 (c) and (d)

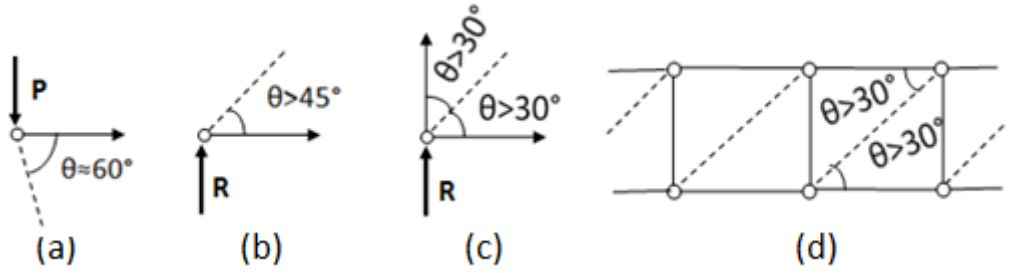

Figure 4.3 Angle limitations adopted from Schäfer (1999).

4.6 Nodes

Nodes represent the connections between struts and ties or the positions where the stresses are redirected within the strut-and-tie model. Nodes are generally divided in two categories, concentrated and distributed. Distributed nodes are not critical in design and therefore not further explained. The concentrated nodes are divided into three major node types, CCC-, CCT- and CTT-nodes illustrated in Figure 4.4, Martin, B. and Sanders, D (2007). The letter combinations explain which kind of forces that acts on the node, C for compression and T for tension.

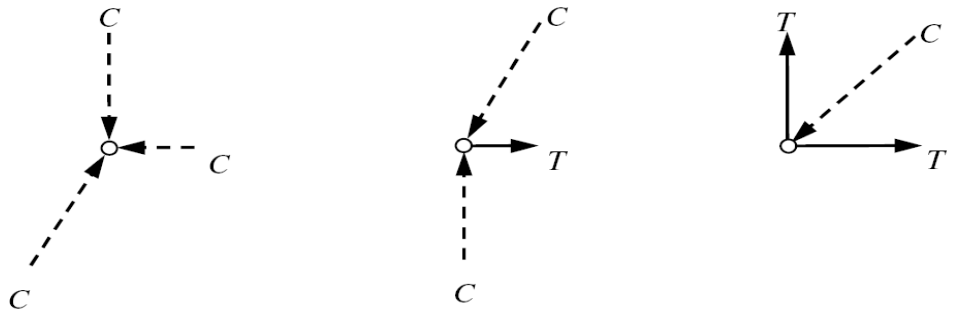

Figure 4.4 The different nodes, from left to right CCC-node, CCT-node and CTT-node.

When nodes are designed they are influenced by support condition, loading plate, geometrical limitations etc. The node geometry for two common nodes is shown in Figure 4.5.

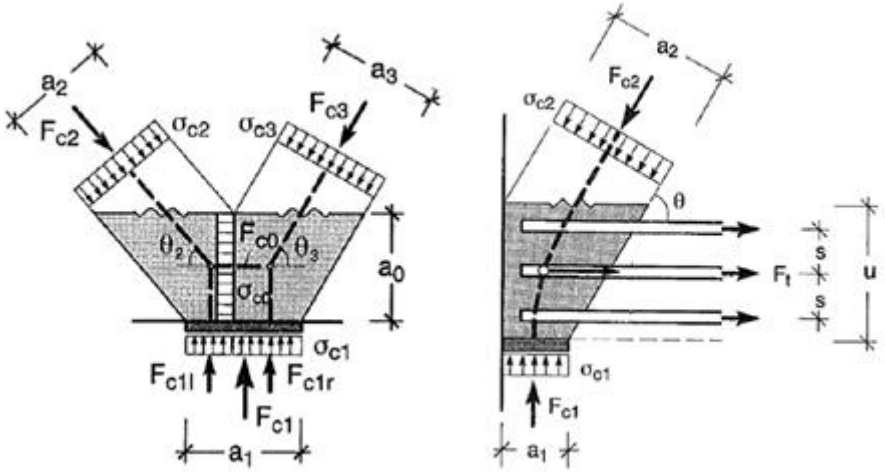

Figure 4.5 Left: node region of a CCC-node. Right: node region for a CCT-node, Schäfer, K. (1999).

An example of idealised node geometries for a CCC-node and a CCT-node is shown in Figure 4.5. The nodal geometry can be defined by determining the location of the node and the width of the bearing plate. It is important that the detailing of concentrated nodes are designed in an appropriate way, especially nodes subjected to both compression and tension forces. For example it is important to provide sufficient anchorage for reinforcement and confining the anchored reinforcement with for instance stirrups.

Concentrated nodes should be designed with regard to the following stress limitations according to Eurocode 2. The compressive strength may be increased with 10 % if at least one of the conditions in Eurocode is fulfilled, EN 1992-1-1:2005 6.5.4. For example, if the reinforcement is placed in several layers the compressive strength can be increased with 10 %. Note that nodes with three-axial compression may have a compressive strength up to three times larger than for a CCC-node.

CCC-nodes without anchored ties in the node

$$\sigma_{Rd,max} = k_1 v f_{cd} \tag{4.1}$$

where:

$$k_1 = 1$$

$$v = 1 - \frac{f_{ck}}{250}$$

CCT-nodes with anchored ties in one direction

$$\sigma_{Rd,max} = k_2 v f_{cd} \tag{4.2}$$

where:

$$k_2 = 0.8$$

$$v = 1 - \frac{f_{ck}}{250}$$

CTT-nodes with anchored ties in more than one direction

$$\sigma_{Rd,max} = k_3 v f_{cd} \tag{4.3}$$

where:

$$k_3 = 0.75$$

$$v = 1 - \frac{f_{ck}}{250}$$

4.7 Three-dimensional strut-and-tie models

Structures subjected to load that result in a 3D stress variation are not adequate to model in 2D. Examples of structures with a 3D stress variation are pile caps, wind power plant foundations and deep beams. There are two different approaches for construction a 3D strut-and-tie model, by model in 3D or by combining 2D models. A 3D strut-and-tie model for a centric loaded pile cap is shown in Figure 4.6.

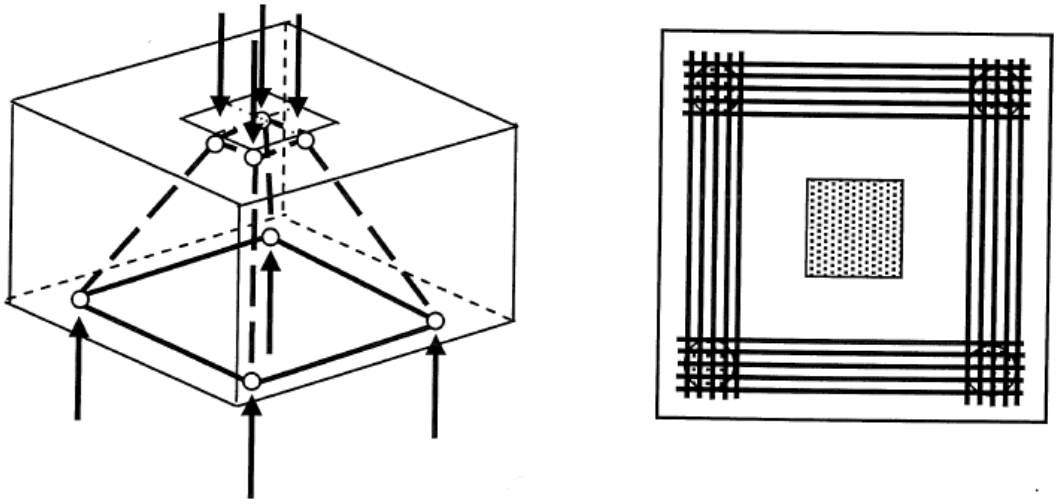

Figure 4.6 Example of a 3D strut-and-tie model and corresponding reinforcement arrangement for a pile plinth, Engström, B. (2011).

Figure 4.7 illustrates how two 2D strut-and-tie models can be used, one in plane of the flanges and one in plane of the web. For such a model each strut-and-tie model transfers the load in its own plane. The two models are joined with common nodes. The result is a combination of 2D models which is applicable on structures with a 3D behaviour.

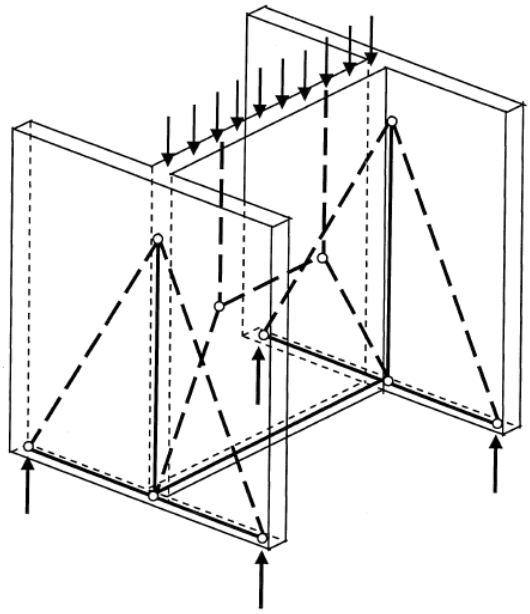

Figure 4.7 A combination of 2D strut-and-tie models, Engström, B. (2011).

4.7.1 Nodes and there geometry

A 3D strut-and-tie model can results in nodes with multi-axial stress for which there are no accepted design rules or recommendations. This is not the case for angle limitations in 3D which often can be adopted from the 2D recommendations. A solution for designing 3D node regions is proposed in a master thesis '*Strut-and-tie modelling of reinforced concrete pile caps*', Chantelot, G. and Alexandre, M. (2010). The basic concept was to simulate 3D nodal regions with rectangular parallelepiped and struts with a hexagonal cross-section shown in Figure 4.8.

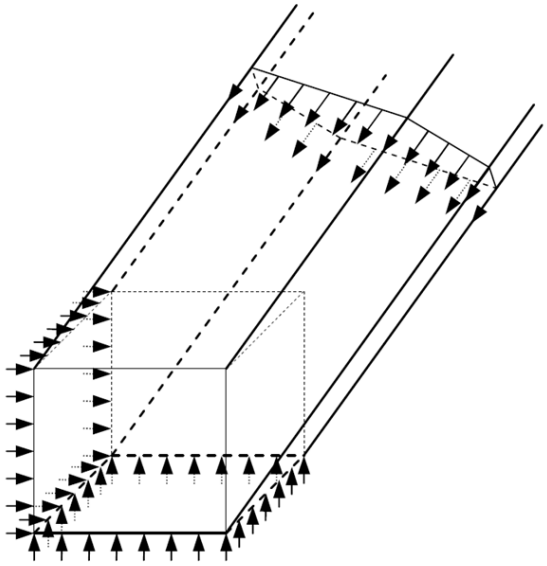

Figure 4.8 Geometry of the 3D nodal zone above the piles, Chantelot, G. and Alexandre, M. (2010)

5 Reference case and design assumptions

This chapter contains a description of the reference case, used design codes and assumptions made in design. The fixed parameters in design such as loads and the geometry are presented along with specifications on concrete strength class and minimum shear reinforcement prescribed by the turbine manufacturer is also presented. The design of the foundation was performed with Eurocode 2 and IEC 61400-1. These codes were used for different design aspects. The design was mainly performed with Eurocode 2, but the partial safety factors for the loads are calculated according to IEC standard.

5.1 Design codes

Eurocode is a relatively new common standard in the European Union and replaced in Sweden the old Swedish design code BKR in May 2011. The standard is divided in 10 different main parts, EC0-EC9, each with national annexes. EC0 and EC1 describe general design rules and rules for loads respectively. The other eight codes are specific for various structural materials or structural types and EC2 "Design of concrete structures" together with EC0 and EC1 are relevant for this project. In order to ensure safe design Eurocode uses the so called 'partial coefficient method'. The partial coefficients increase the calculated load effect and decrease the calculated resistance, in order to account for uncertainties in design. This is done to ensure that the probability of failure is sufficiently low, shown in Figure 5.1.

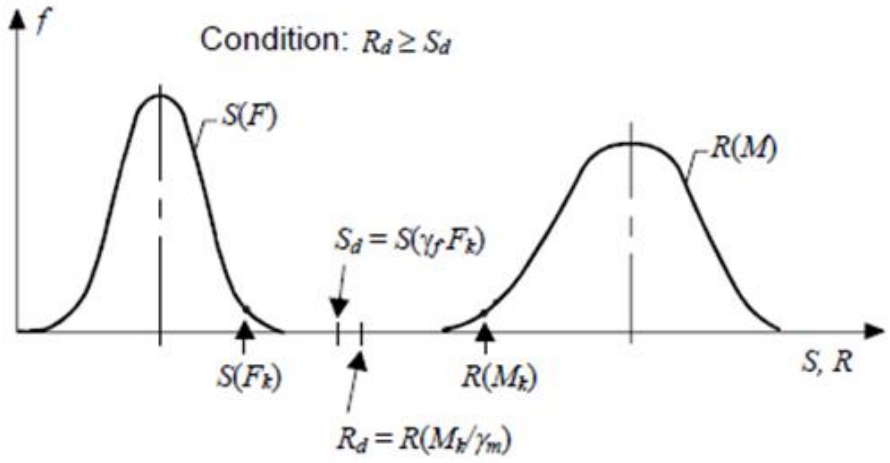

Figure 5.1 Method of partial safety factors. S is the load effect and R the resistance. The d index indicates the design value.

IEC 61400-1 is an international standard for designing wind turbines; the standard is developed by the International Electrotechnical Commission, IEC (2005). The IEC standard is based on the same principles as Eurocode concerning partial factors on both materials and loads. The loads given by the turbine manufacturer follow the IEC-standard and the standard was therefore used for load calculations. The standard allows the designer to implement partial factors based on Eurocode.

The partial safety factors for loads are in IEC classified with regard to the type of design situation and if the load is favourable or unfavourable. Instead of classifying the loading in serviceability limit state and ultimate limit state, IEC uses normal and abnormal load situations. The used partial factors for loads are presented in Table 5.1.

Table 5.1 Partial safety factors on loads according to IEC 61400-1

Design situation	Abnormal (ULS)	Normal (SLS)	Fatigue
$Wind\ loads$	$\gamma_f = 1.1$ unfavourable	$\gamma_f = 1$	$\gamma_f = 1$
$Dead\ loads$	$\gamma_f = 0.9$ favourable	$\gamma_f = 1$	-

5.2 General conditions

The considered wind power plant foundation located in Skåne in the south of Sweden. The soil consists of sand and gravel. The project has been limited to only study the foundation and the ground conditions are assumed good and are not further investigated.

5.3 Geometry and loading

The foundation is square shaped with 15.5 m long sides and a height that varies with a slope of approximately 4.5 %. The tower is 68.5 m high and both the tower and turbine are supplied by the turbine manufacturer. The wind power plant is designed for a life time of 50 years. The foundation consists of concrete strength class C45/55 and is designed for the exposure class XC3. Figure 5.2 shows the section and plan of the foundation with fixed geometry from the reference case. After construction the foundation is to be covered with filling material, which in the design was included in a constant surface load (g).

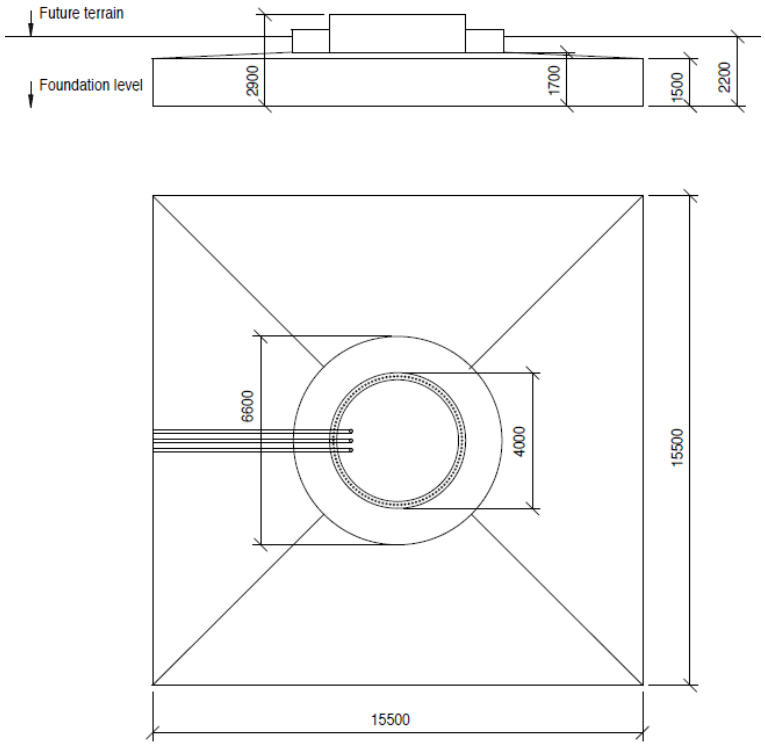

Figure 5.2 Section and plan of the foundation.

The sectional forces at the connection between tower and foundation are specified by the turbine supplier with safety factors according to the standard IEC 61400-1. The following loads must be resisted; rotational moment from wind forces and the unintended inclination of the tower, a twisting moment from wind forces (which are excluded in this project), a transverse load from wind forces and a normal force from self-weight of the tower (including turbine and blades). Besides the loads acting on the anchor ring, described in Chapter 2 the foundation, is subjected to self-weight of reinforcement, concrete and potential filling materials. Figure 5.3 shows the definition of the load from the tower and the characteristic values are presented in Table 5.2. The design loads are calculated in Appendix A.

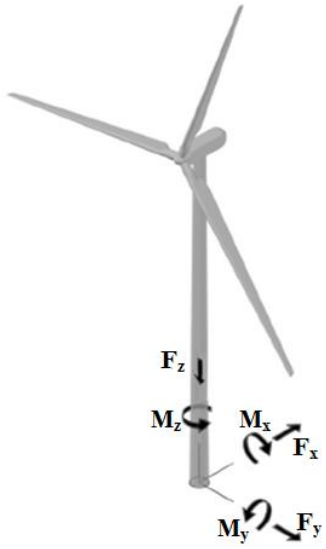

Figure 5.3 *Definition of sectional forces from the tower at the connection between tower and foundation, adopted from ASCE/AWEA (2011).*

Table 5.2 *Characteristic values of sectional forces acting on top in the centre of the anchor ring and self-weight of foundation. The load effects are based on "design load case 6.2 extreme wind speed model" with a recurrence period of 50-years.*

Load type	Size	Remark
F_z	2 121 kN	
$M_{xy} = \sqrt{{M_x}^2 + {M_y}^2} + \Delta M_1 + \Delta M_2$	51 115 kNm	Including moment from misalignment of 8mm/m and dynamic amplification
$F_{xy} = \sqrt{{F_x}^2 + {F_y}^2}$	800 kN	
M_z	5 863 kNm	Excluded
G	12 575 kN	Including filling material

In serviceability limit state the characteristic crack width should be limited to 0.4 mm specified in the national annex of Eurocode 2. The crack width limitation given in Eurocode 2 depends on exposure class (XC3) and life time (50 years).

Since the wind power plant is subjected to large wind loads of variable magnitude, the foundation's fatigue capacity is of great importance. The fatigue load amplitudes are supplied by the turbine manufacturer, consisting of 280 unique loads (presented in Appendix I). The fatigue load amplitudes are presented in a table with number of cycles. It is however unclear for how long time the presented load amplitudes are valid. The mean values are also presented along with the used safety factor see Table 5.3.

Table 5.3 Mean values of sectional forces for fatigue design of reinforced concrete structures

F_x [kN]	$\lvert F_y \rvert$ [kN]	M_x [kN]	M_y [kN]	$\lvert M_z \rvert$ [kN]	γ_F
316	4	1 888	21 293	222	1.0

5.4 Tower foundation connection

The reference case is designed with an anchor ring of type (b) described in Section 2.3. This type of anchor ring has only one flange in the bottom, which means that both the compressive and tensile force is applied at the same level in the foundation. The anchor ring used in the reference case is shown in Figure 5.4.

Figure 5.4 The anchor ring in the reference case during reinforcement installation.

In the calculations the resulting moment (M_{xy}) was replaced by a force couple consisting of a compressive and tensile resultant. In order to calculate the level arm between the force couple a linear elastic stress distribution was assumed at the interface between concrete and the steel flange.

Navier's formula was used to calculate the maximum stresses in concrete subjected to compression by the flange of the anchor ring:

$$\sigma_{max} = \left({}^{M_{xy}}/_{I}\right) \cdot r_2 + {}^{F_z}/_{(\pi r_2^2 - \pi r_1^2)} \tag{5.1}$$

The second moment of inertia (I) for an annular ring with dimension of the bottom flange of the anchor ring is calculated as:

$$I = \frac{\pi}{4} \cdot (r_2^4 - r_1^4) \tag{5.2}$$

where:

$r_1 =$ inner radius of flange

$r_2 =$ outer radius of flange

To verify the assumption of linear elastic behaviour the calculated stresses were compared with the stress-strain relationship for concrete shown in Figure 5.5. According to Figure 5.5 the stress strain relation is almost linear to about 50% of f_{cd}. The maximum stress was calculated to approximately 56% of f_{cd} and a linear elastic stress distribution in the compressed concrete could be assumed.

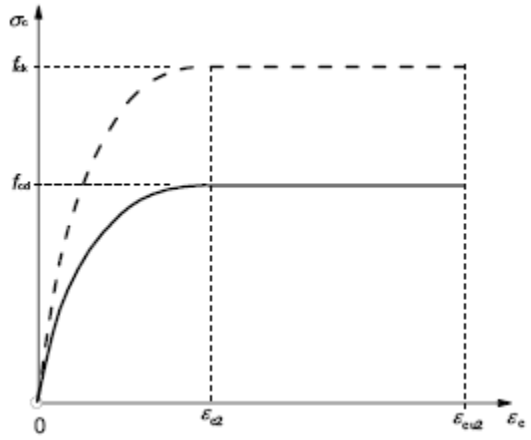

Figure 5.5 Stress-strain relation for concrete in compression according to EC2

As a simplification the linear stress distribution was assumed to correspond to a uniform stress distribution in two quarters of the anchor ring according to Figure 5.6. The level arm was then calculated as the distance between the arcs centres of gravities according to equation 5.3.

$$d_s = 2\left(\frac{2}{\pi r_0}\right)\int_{-\frac{\pi}{4}}^{\frac{\pi}{4}} r_{sr} \cos\varphi \, d\varphi = 3.6m \tag{5.3}$$

where:

$r_{sr} = \frac{r_1 + r_2}{2} =$ radius of anchor ring$=2m$

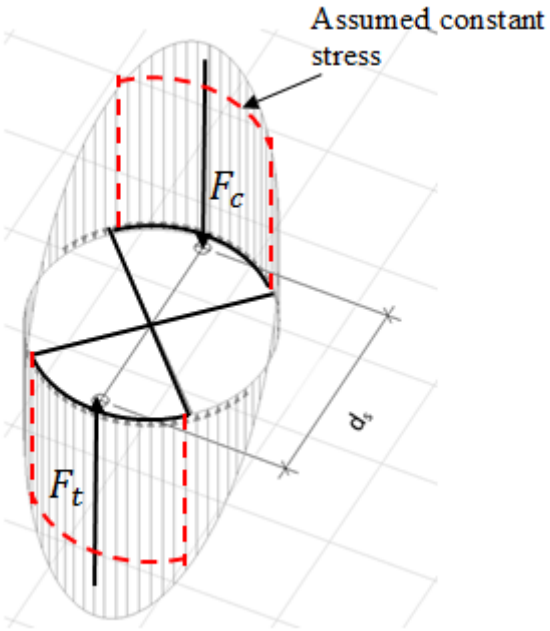

Figure 5.6 *Resisting moment acting on the anchor ring with resulting force couple and simplified stress distribution, d_s=3.6m*

The self-weight of the tower and turbine was assumed to be equally spread over the anchor ring and the resultant, F_z, was divided in 4 equal parts. Two of the F_z components coincide with the force couple from the moment. The model shown in Figure 5.7 was used in calculations.

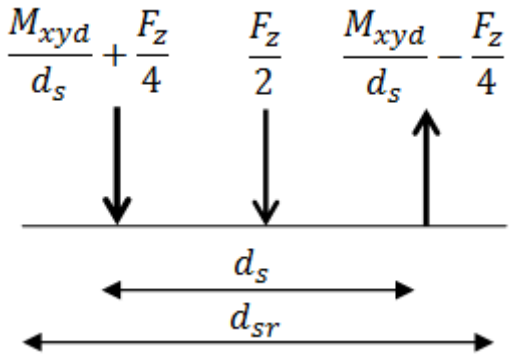

Figure 5.7 *Idealised model of the forces acting on the anchor ring, where d_{sr} is the diameter of the anchor ring (4m) and d_s is the distance between the resulting force couple from the rotational moment (3.6m).*

As described in Section 2.1 anchor type (b) requires reinforcement in order to lift up the compressive force and to pull down the tensile force. The compressive force is lifted in order to utilise the full height of the section. The two other types of anchor rings that are presented in Section 2.1 take the compressive force directly in the top of the slab, i.e. does not need to be lifted by reinforcement to utilise the full height of the section. The distance between the vertical bars of the suspension reinforcement or U-bow reinforcement was prescribed by the turbine manufacture to be minimum 500 mm. How the compressive and tensile forces from the anchor ring are assumed to be transferred is shown in Figure 5.8. Calculations are found in Appendix B.

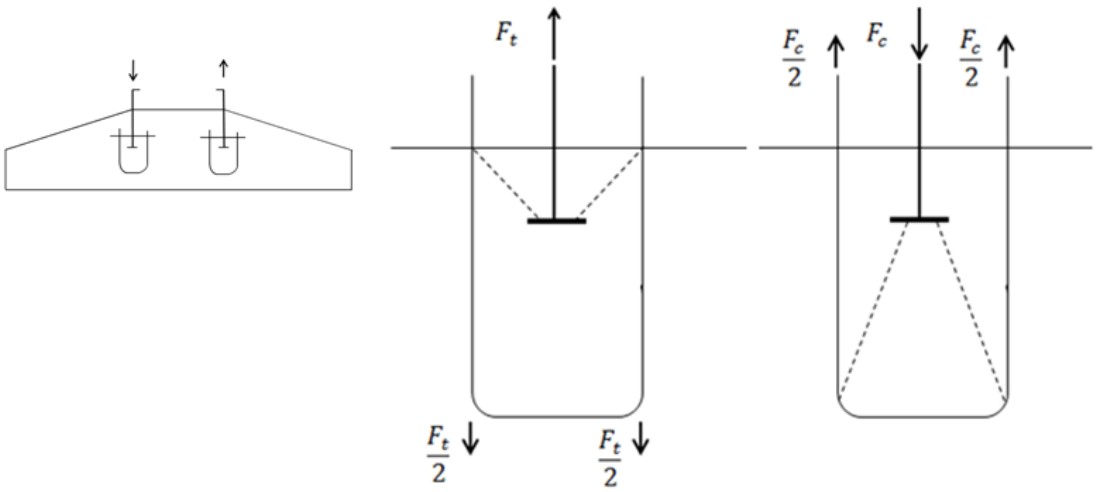

Figure 5.8 *Force couple from the rotational moment acting in the bottom of the anchor ring. The compressive force (F_c) is lifted by the U-bow and the tensile force (F_t) pulled down by the U-bow.*

5.5 Global equilibrium

As briefly described in Section 2.1 the foundation must prevent the tower from tilting by a resisting moment created by an eccentric reaction force (F_{soil}). To ensure stability in arbitrary wind directions the stability was checked with two wind directions, perpendicular and diagonal (wind direction 45 degrees), see Figure 5.9. By fulfilling equilibrium demands these two load cases, stability for all intermediate load directions were assumed to be satisfied.

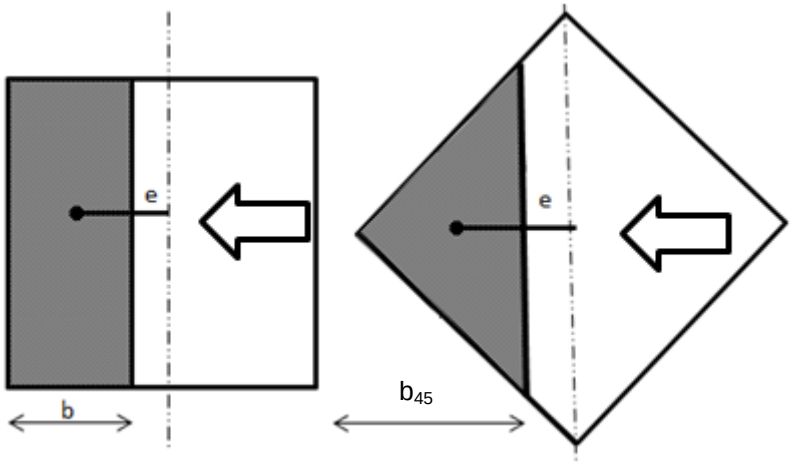

Figure 5.9 *Left: Wind direction perpendicular to foundation Right: Wind direction 45 degrees direction to foundation.*

In order to be able to determine the soil pressure (σ_{soil}) and its eccentricity (e), the stress distribution of the soil pressure needed to be assumed. The exact distribution of the soil pressure is hard to determine, because of the complex loading situation, with concentrated load at the centre of the foundation. As a simplification the soil pressure was assumed to be equally spread in the transverse direction (over the full width of

the foundation). In the longitudinal direction two different assumptions are considered; uniform soil pressure and triangular soil pressure, see Figure 5.10.

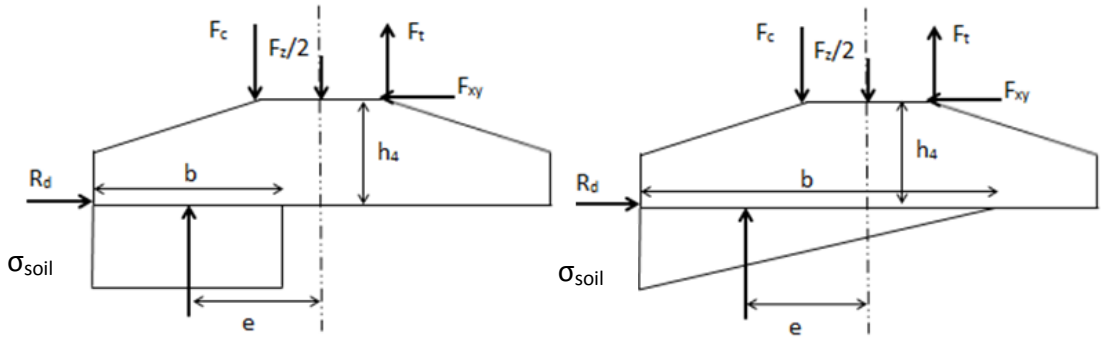

Figure 5.10 Different distributions of soil pressure within the length (b). Left: Uniform soil pressure distribution. Right: Triangular soil pressure distribution.

The resultant of the soil pressure (F_{soil}) and its eccentricity (e) can be determined from global equilibrium with the following equations:

$$F_{soil} = F_z + G \tag{5.4}$$

$$e = \frac{M_{xy}+F_{xy}\cdot h_4}{F_{soil}} \tag{5.5}$$

With triangular distribution the size of the soil pressure varies over the length. The soil pressure is distributed over the length *b*, which is determined by the eccentricity. The maximum soil pressures per unit width for a perpendicular wind direction can be calculated as:

$$\sigma_{soil,uni} = \frac{F_z+G}{b_{uni}} \tag{5.6}$$

$$\sigma_{soil,tri} = \frac{F_z+G}{b/_2} \tag{5.7}$$

With a wind direction of 45 degrees and an assumed uniformed stress distribution the soil pressure can be calculated in a similar manner as for the triangular soil distribution in case of perpendicular wind direction. The uniformed soil pressures resultant is then triangular because of the shape of the loaded area.

$$\sigma_{45,soil,uni} = \frac{F_z+G}{b_{45,uni}/_2} \tag{5.8}$$

With known eccentricity and assumed soil distribution the bending moment and shear force distributions in the foundation slab can be calculated. To identify the most critical wind direction the different bending moment and shear force distributions are compared in Figure 5.11 and Figure 5.12. These distributions was only used for compression and the width of the slab is not considered.

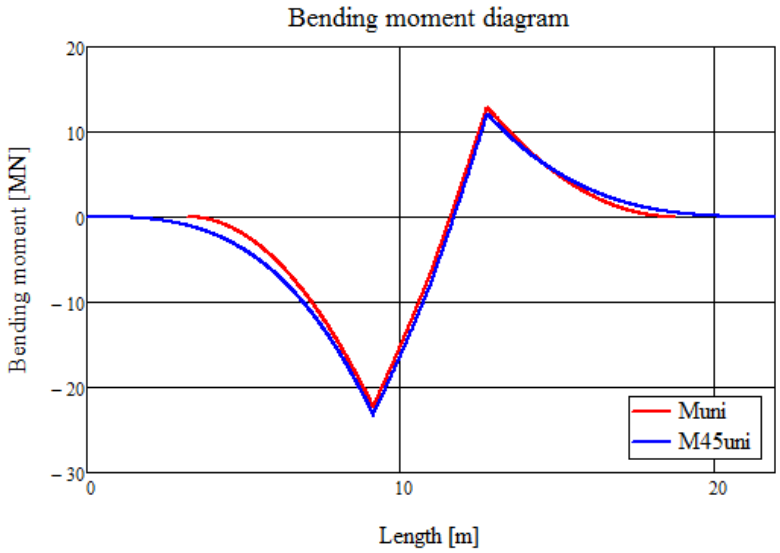

Figure 5.11 *Bending moment distributions for different load cases. The index uni correspond to uniform soil distribution and index 45 is with a wind direction of 45 degrees.*

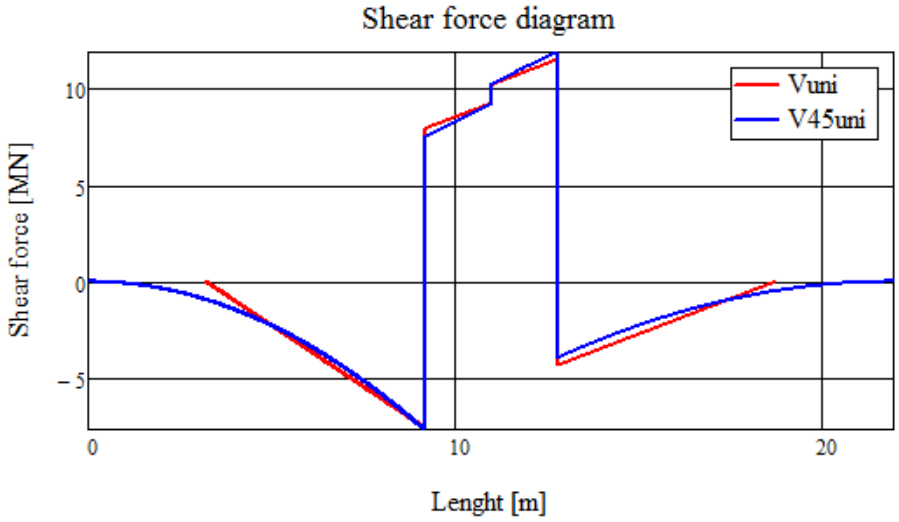

Figure 5.12 *Shear force distributions for different load cases. The index uni correspond to uniform soil distribution and index 45 is with a wind direction of 45 degrees.*

The conclusions that can be drawn from the diagrams are that the differences are small and it was assumed sufficient to design the foundation for a perpendicular wind direction. To simplify calculations the largest need for bending and shear reinforcement is provided all the way to the edges of the foundation. By providing reinforcement to the edges, more than sufficient capacity is assumed in the corners, see Figure 5.13.

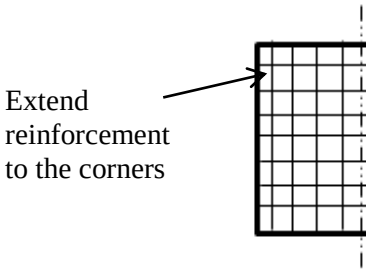

Figure 5.13 To achieve sufficient capacity all reinforcement should be extended to the corners.

Regarding the soil pressure distribution it is common to assume a uniform distribution when designing in the ultimate limit state. In the serviceability limit state and for fatigue calculations, a triangular soil pressure distribution is more appropriate. The distributions with uniform soil pressure and triangular soil pressure was compared, see Figure 5.14.

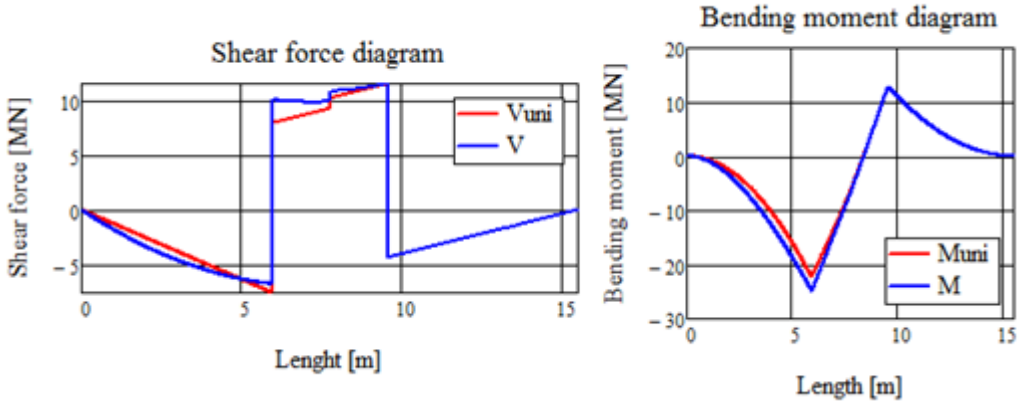

Figure 5.14 Shear and bending moment distribution for uniform and triangular soil pressure distribution.

The triangular soil pressure distribution resulted in slighter higher bending moment and shear force. The differences are however small and in addition the real soil pressure distribution is rather a combination of the two distributions, see Figure 5.15.

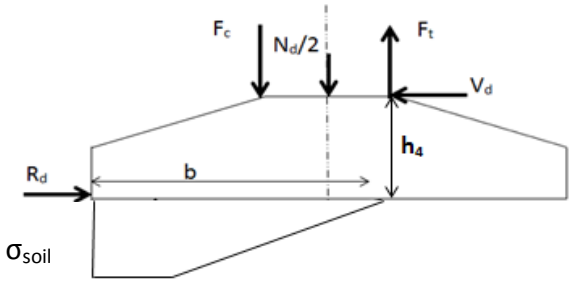

Figure 5.15 A combination of uniformed and triangular soil pressure distribution.

Therefore the design in the ultimate limit state was performed assuming uniform soil pressure distribution, while the triangular distribution was used in the serviceability limit state and for fatigue assessment. The full calculations are found in Appendix B.

6 Design of the reference case according to common practice on the basis of Eurocode

In this chapter it is described how the reference case is designed according to Eurocode 2 considering the conditions and assumptions presented in Chapter 5. Obtained results are presented. Detailed calculations are shown in Appendix A-H.

The sectional design was performed in various sections which are presented in Figure 6.1.

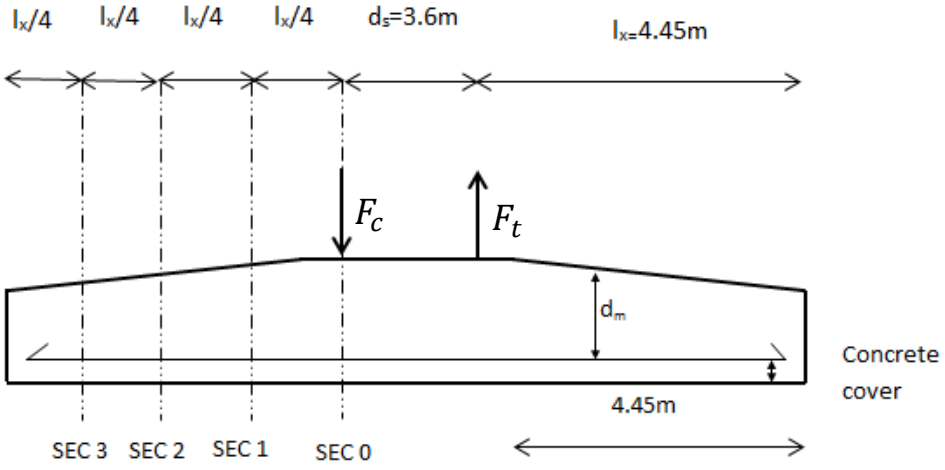

Figure 6.1 *The sectional design was performed in four different sections on each side of the foundation.*

The design was performed according to the following design steps:

- Design of top and bottom reinforcement in the ultimate limit state using sectional design (Appendix C).
- Design of shear reinforcement and the zone around the anchor ring in the ultimate limit state (Appendix C)
- Design with regard to serviceability limit state (Appendix D)
- Design with regard to fatigue of reinforcement and compressed concrete (Appendix E using equivalent stress range and G using full load spectra)

6.1 Bending moment and shear force distribution

The foundation was regarded similar to a flat slab where the load is transferred to the support using crossed reinforcement in two perpendicular directions, see Figure 6.2.

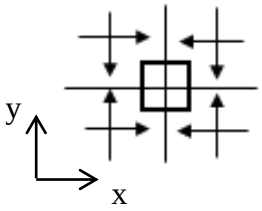

Figure 6.2 *Reinforcement in principal direction transfers the load in two directions separately.*

The design of bending reinforcement was based on the assumption that the bending moment in a section is uniformly distributed over the full width of the slab. The assumption requires a redistribution of sectional forces since the linear elastic stress distribution has a stress variation in the transverse direction. The assumption is used when designing flat slabs according to the strip method. Hillerborg suggests that the reinforcement should be concentrated over interior supports in flat slabs in order to achieve a better flexural behaviour in the serviceability limit state, shown in Figure 6.3.

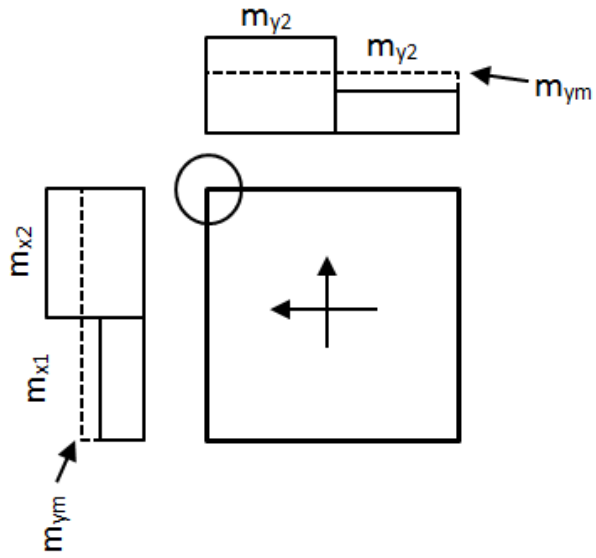

Figure 6.3 Bending moment capacity in a corner supported slab with reinforcement concentrated over the column

In design practise it appears to be common to assume that the sectional shear force is uniformly distributed over the full width of the slab, i.e. the same assumption as for bending moment. However, this assumption is not true near the reaction of the anchor ring. Figure 6.4 illustrates the loaded slab with two different sections, 1 and 2.

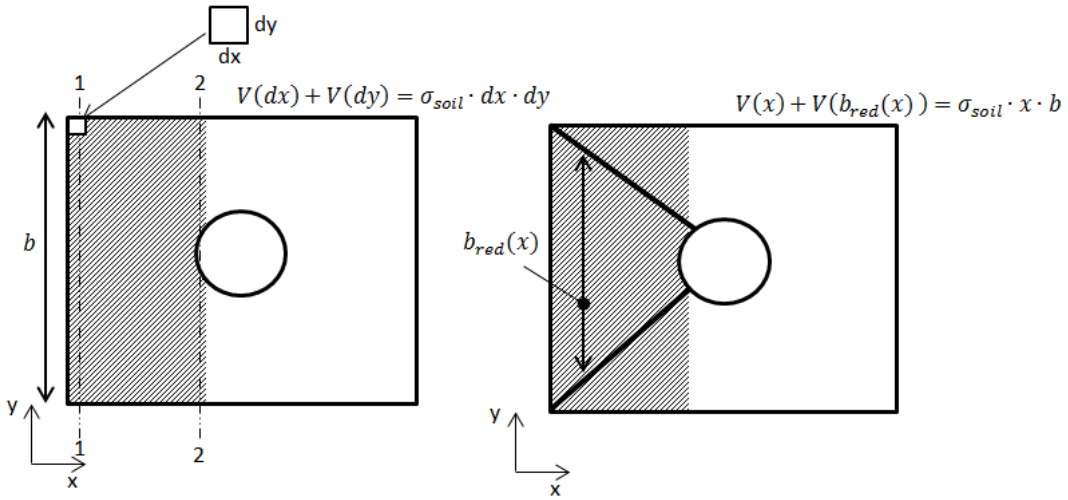

Figure 6.4 Equilibrium conditions in a slab

Section 1 is far away from the anchor ring and it is therefore reasonable to assume that the sectional shear force is uniformly distributed over the full width of the slab:

$$V(x) + 0 = \sigma_{soil} \cdot x \cdot b \tag{6.1}$$

where:

b full width of the slab

Along section 2 this assumption is not reasonable because of the concentrated load, i.e. the shear force varies in y-direction along section 2:

$$V(x) + V(b_{red}(x)) = \sigma_{soil} \cdot x \cdot b \tag{6.2}$$

The equilibrium condition is statically undetermined and it is hard to assume a distribution without determining the linear elastic stress distribution. It is doubtful if a redistribution of the sectional shear forces is possible in the same manner as for bending moment. Since the common practice is to assume that the internal forces are spread over the full width the assumption was used despite the lack of a transition from a uniformed distribution to a more concentrated near the anchor ring. The bending moment and shear force distribution are shown Figure 6.5 and Figure 6.6. As previously stated a uniform soil distribution was assumed for design in the ultimate limit state.

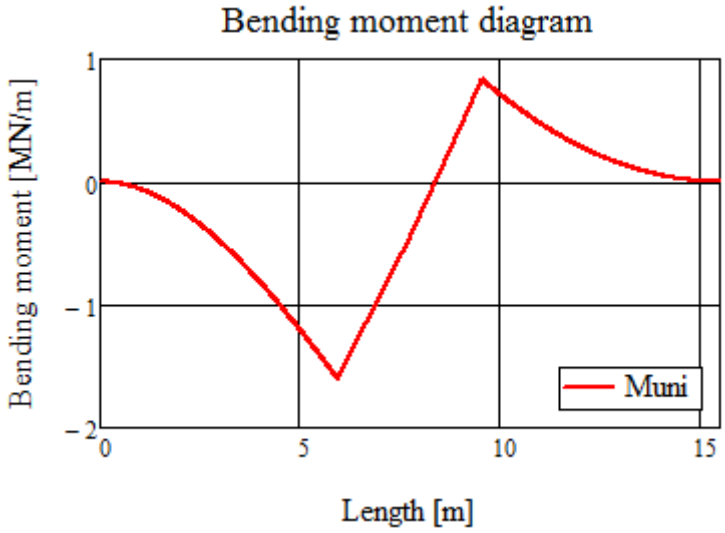

Figure 6.5 *Bending moment distribution used for sectional design. The moment was assumed to be uniformly distributed in the transverse direction and a uniform soil pressure is assumed.*

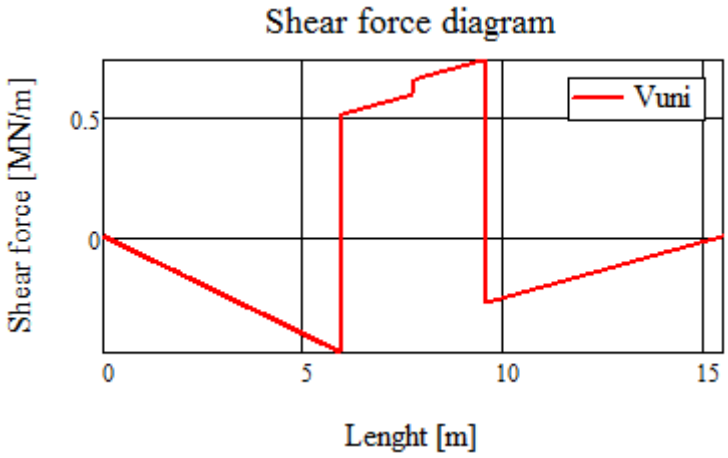

Figure 6.6 *Shear force distribution used for sectional design. The shear force was assumed to be uniformly distributed in the transverse direction and a uniform soil pressure is assumed.*

6.2 Bending moment capacity

The reinforcement was designed according to Eurocode 2 assuming an ideal elasto-plastic material model of the steel. For concrete the stress-strain relation presented in Figure 5.5 was used. Since the height of the foundation varies both over the length and across the foundation, the mean height over the width was used in each section, see Figure 6.7.

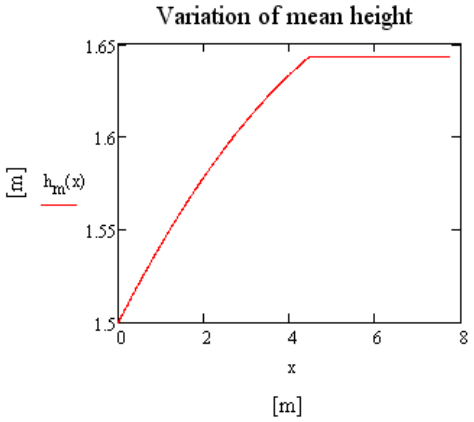

Figure 6.7 *Variation of mean height along the length. The variation is equal on both sides of the foundation.*

To simplify both calculations and reinforcement arrangement required reinforcement amounts was calculated only in section 0 shown in Figure 6.1. Special consideration of the top reinforcement near the anchor ring was required, since it is not possible to continue the bars through the anchor ring. The effect of the inclination of top reinforcement with approximately 4.5 % was neglected.

The design of top reinforcement near the anchor ring was performed using so called star reinforcement. Figure 6.8 shows the anchor ring and the layout of the star reinforcement.

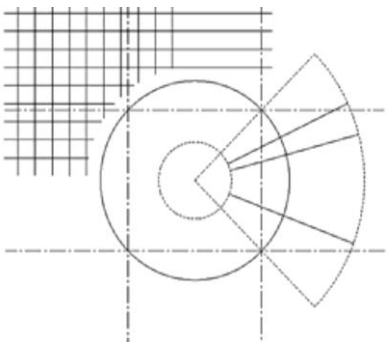

Figure 6.8 *Left: Example of an anchor ring with holes where star reinforcement is placed. ESB International (2010). Right: Principle arrangement of star reinforcement.*

The star reinforcement was placed within 56 holes spread equally around the upper part of the anchor ring. The capacity of the star reinforcement was determined by calculating an equivalent reinforcement area of the star reinforcement. The equivalent reinforcement area was then multiplied with the number of bars in the anchor ring. The product corresponds to the equivalent amount of reinforcement bars, which can be compared to the required amount of straight bars. If the equivalent star reinforcement is greater than the required amount of straight bars, sufficient capacity of star reinforcement was assumed. The following calculations were performed:

$$A_{s,req} = A_{si,top}\frac{d_{sr}}{a}\frac{M_{Ed}}{M_{Rd,top}} \tag{6.3}$$

$$A_{s,ekv} = A_{si,ring}\sum\cos(\varphi_i) \tag{6.4}$$

where:

$A_{si,top}$	Area of top reinforcement bar
d_{sr}	Diameter of anchor of ring
a	Spacing of top reinforcement
M_{Ed}	Design moment in critical section
$M_{Rd,top}$	Moment capacity in controlled section (with bars only in x-direction)
$A_{si,ring}$	Area of star reinforcement bar
φ_i	Angle of each bar, see Figure 6.9

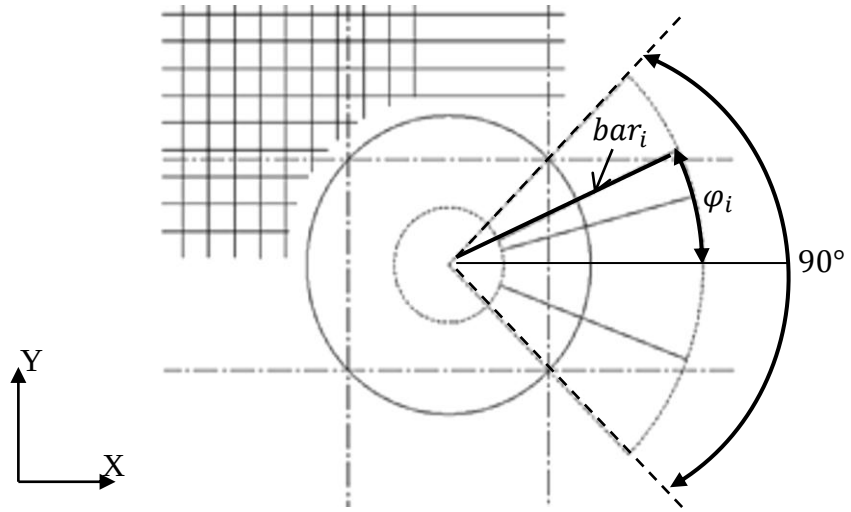

Figure 6.9 The equivalent amount of reinforcement is calculated as the equivalent number of bars in x-direction within a 90 degree circle sector.

6.3 Shear capacity

The region near the anchor ring must be designed with regard to concentrated anchor and compressive forces and with regard to punching shear. In other regions the design with regard to shear capacity was based on the assumption that the shear force was uniformly distributed in the transverse direction

The shear capacity without shear reinforcement was calculated according to EN 1992-1-1:2005 6.2.2 equation 6.2.a:

$$V_{Rd,c} = \left[C_{Rd,c} k (100 \rho_l f_{ck})^{1/3}\right] b_w d \geq v_{min} \quad (6.5)$$

$$k = 1 + \sqrt{\frac{d}{200}} < 2 \text{ , d in mm} \quad (6.6)$$

$$\rho_l = \frac{A_{sl}}{b_w d} \quad (6.7)$$

$$v_{min} = 0.035 k^{3/2} f_{ck}^{1/2} \quad (6.8)$$

where:

f_{ck}	Characteristic concrete compression, in MPa
$C_{Rd,c}$	Constant found in national annex
A_{sl}	Area of horizontal bars
b_w	Width of section
d	Effective depth

According to the calculations the capacity without shear reinforcement was sufficient except in the area closest to the anchor ring. Even though no shear reinforcement was required in outer parts of the foundation, the turbine manufacturer specified a minimum shear reinforcement amount depending on the concrete class. This is the

reason for the chosen minimum shear reinforcement of $\phi 25$ mm with spacing 500 mm.

In the analysis of the region near the anchor ring the maximum stress (σ_{max}) was calculated according Section 5.4 with Navier's formula and the second moment of inertia for an annular ring. A bar diameter of $\phi 25$ mm was used and the required spacing was calculated according to the model in Figure 6.10. The maximum compressive stress (σ_{max}) was also compared with the compressive strength of concrete.

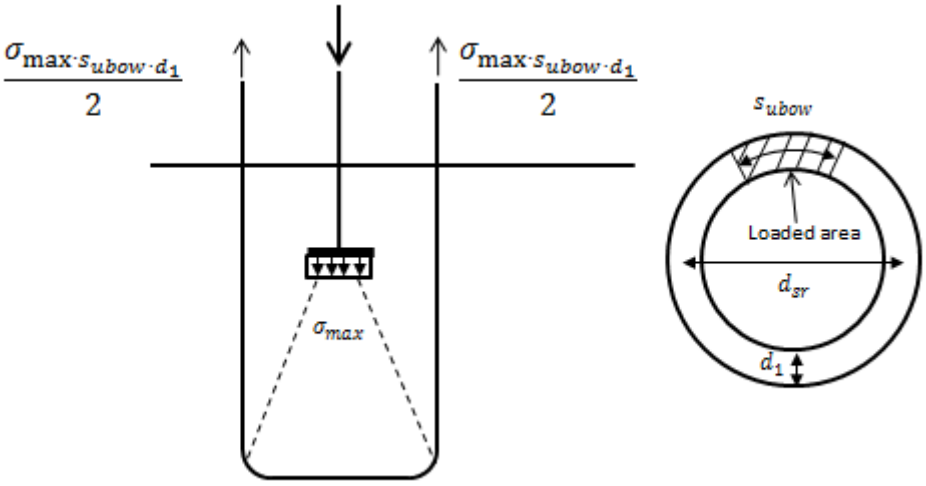

Figure 6.10 Model for calculating required spacing of the U-bows.

Regarding punching shear it is not obvious how the capacity should be verified. The large bending moment could result in a punching failure where half the anchor ring is punched down while the other half is punched up. Eurocode provides methods for verification of punching shear at columns subjected to bending moment, but the actual situation differs from the one described in Eurocode since the bending moment dominates. Instead of treating the loaded area as a column that is punched, a cone along the perimeter of the anchor ring was assumed to be punched according to Figure 6.11.

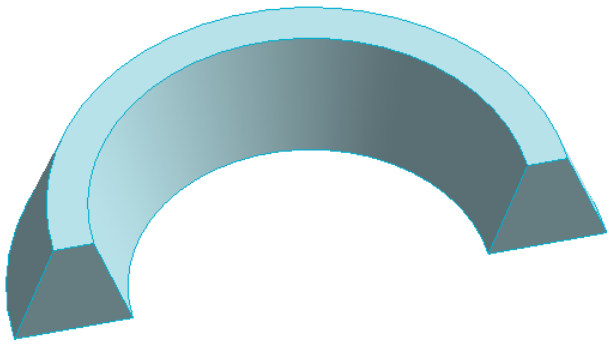

Figure 6.11 A cone under the anchor ring was assumed to be punched out. Note that a similar cone must also punch through the upper part of the foundation slab for punching shear to occur.

The critical sections were chosen according to EC2 and are shown in Figure 6.12.

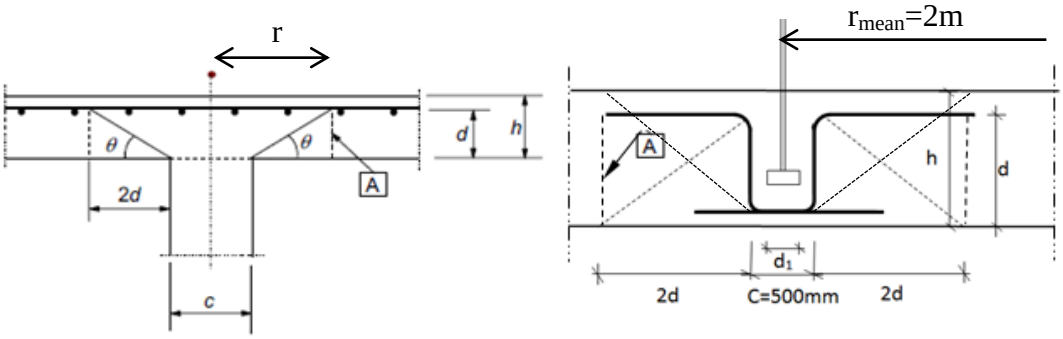

Figure 6.12 Left: Control perimeter for punching shear according to EC2. Left: The used model.

The described assumptions were used together with equation 6.2 for determining the punching shear capacity for concrete without shear reinforcement, see equation 6.2. Instead of using the sectional area $A = b_w d$ the perimeter area in Figure 6.12 was used. The area of the control perimeter section, 2d from the applied load, marked A in Figure 6.12 was calculated as:

$$A = 2\pi r d \tag{6.9}$$

For this special type of punching shear the two control perimeters sections have different radius and the total area was calculated using the mean radius. Observe that it is only the perimeter of a half circle according to Figure 6.11 that should be considered.

$$A = 2\left(\frac{2\pi r_{mean}}{2} d\right) \tag{6.10}$$

To have sufficient punching shear capacity the result must be greater than the resultant of the compressive force(F_c). The edge areas of the "cone" shown in Figure 6.11 may contribute to the capacity. Since half of the ring is punched up and half is punched down, parts of the edge area will coincide, see Figure 6.13.

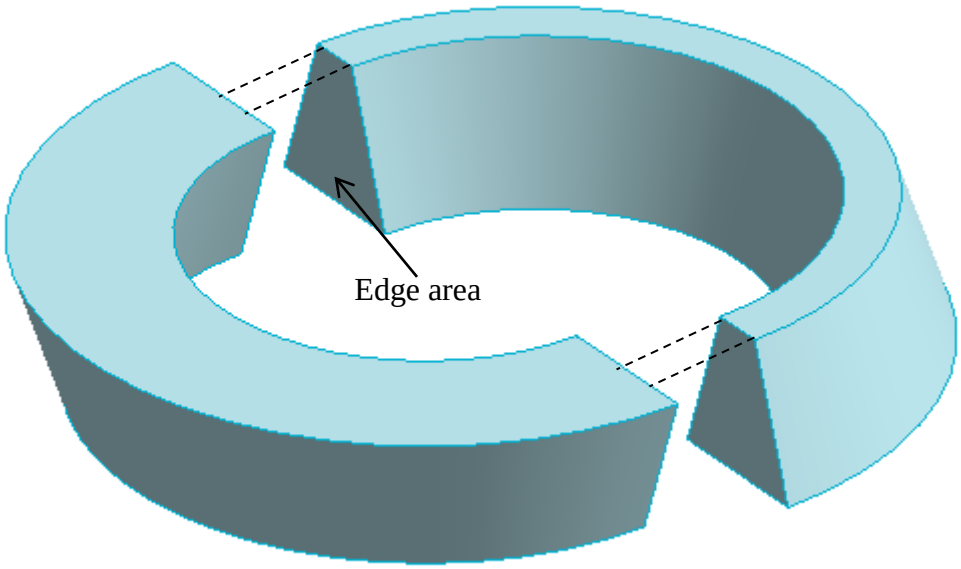

Figure 6.13 One cone is punched up while the other is punched down.

It is therefore uncertain how the contribution from the edges should be handled. If this edge area was included the capacity was sufficient and no extra shear reinforcement was needed. However without the contribution from this area the capacity was insufficient and extra reinforcement was needed. The minimum reinforcement, with spacing 500 mm, is enough to ensure that the cracks cross at least two reinforcement bars which is enough to provide sufficient capacity.

6.4 Crack width limitation

The design with regard to permissible crack width was performed in the serviceability limit state assuming a triangular soil pressure. The crack width calculations were performed by first determining the maximum steel stresses in state II, i.e. assuming that the tensile part of the concrete section is fully cracked. The characteristic crack width w_k was then calculated according to EN 1992-1-1:2005 7.3.4.

$$w_k = s_{r,max} \cdot (\varepsilon_{sm} - \varepsilon_{cm}) \leq w_{k,max} \tag{6.11}$$

$$s_{r,max} = k_3 \cdot c_{soil} + k_1 \cdot k_2 \cdot k_4 \cdot \phi / \rho_{p,eff} \tag{6.12}$$

where:

$s_{r,max}$	Maximum crack spacing
c_{soil}	Concrete cover thickness
k_1	Coefficient considering the bond properties between concrete and reinforcement
k_2	Coefficient considering the strain distribution
k_3	Value from national annex
k_4	Value from national annex
ϕ	Reinforcement bar diameter
$\Delta\varepsilon$	Strain difference between the mean values for steel and concrete
$\rho_{p,eff}$	Reinforcement ratio in effective concrete area

The reinforcement amount needed for flexural resistance was not sufficient to fulfil the crack width limitations. As expected a larger reinforcement amount was needed both in the top and bottom. The most critical part of the foundation with regard to crack widths was the bottom side of the slab close to the anchor ring where the largest bending moment was located. In addition to the need of bending reinforcement the foundation needed reinforcement near the edges to limit the crack widths.

6.5 Fatigue

When designing a wind power plant foundation the fatigue analysis cannot be omitted. In this project the fatigue analysis have been performed separately for concrete and reinforcement. The fatigue life was verified for bending reinforcement, U-bows and the compressed concrete under the flange of the anchor ring. The need for shear reinforcement was small, except for the region near the anchor ring. Fatigue verification is therefore only performed on the U-bows with a local analysis. The

shear capacity outside the local area around the anchor ring was assumed to be sufficient.

The fatigue analysis for steel was performed with two approaches, 'Palmgren-Miner cumulative damage law' and the use of an equivalent load. Both mentioned approaches exist in Eurocode, but no description for establishing the equivalent load exists. However, the fatigue life of concrete can only be verified with an equivalent load since there are no S-N curves for concrete, which are necessary in order to use 'Palmgren-Miner cumulative damage law'.

In order to calculate an equivalent load a method described in *'Fatigue equivalent load cycle method'* by H.B Hendriks and B.H. Bulder was used, Hendriks and Bulder (2007). They purpose a method to calculate one equivalent load amplitude ($S_{r,eq}$) which is based on the full load spectra. This equivalent load can be used to calculate equivalent stress variations which then can be used to verify the capacity according to Eurocode. With an equivalent stress range both fatigue verification of reinforcement and compressed concrete are possible. Equation 6.13 shows the equation used for determine $S_{r,eq}$, and the equations used for verification is shown in equation 6.13.

$$S_{r,eq} = \left(\sum_{i=0}^{n} \frac{S_{r,i}^{m}}{N_{eq}}\right)^{\frac{1}{m}} \tag{6.13}$$

$Where$:

$S_{r,eq}$	Equivalent range of load cycle
N_{eq}	Equivalent number of allowed cycles
m	Exponent that defines the slope of the S-N curve
S_r	Range of load cycles
n	Number of cycles

The method is developed "to compare different fatigue load spectrum on a quantitative basis", Hendriks and Bulder (2007). From our understanding the equivalent fatigue load in Equation 6.12 is not intended for fatigue calculation of reinforcement, but instead for other components of the wind power plant such as the rotor blades, Stiesdal, H (1992).

Equation 6.13 can only be used with the slope of one S-N curve. In Eurocode two different slopes are presented depending on the load magnitude. The two different slopes presented in Eurocode for reinforcement are $m = 5$ and $m = 9$ ($m = k$ in Eurocode EN1992-1-1 2005). The value m was assumed to be the mean value of the given slopes, i.e. $m = 7$. The equivalent stress range was calculated for $N_{eq} = 10^6$ load cycles, which was used together with the mean value given by turbine manufacturer to calculate a minimum and a maximum of fatigue loads. The complete calculation together with the load spectra can be found in Appendix I.

The variation of moment load was calculated as:

$$\Delta M = M_{xy,mean} \pm S_{r,eq} \tag{6.14}$$

where:

$S_{r,eq}$=13049.8kNm

$M_{xy,mean} = 21380kNm$

Calculation of ΔF_{xy} was performed in the same manner. The determined maximum and minimum loads are used to calculate different eccentricities for the different loads as described in Section 5.5 but with a triangular distribution of the soil pressure. The smaller loads results in smaller eccentricities, hence the soil pressure is distributed over the full length, shown in Figure 6.14.

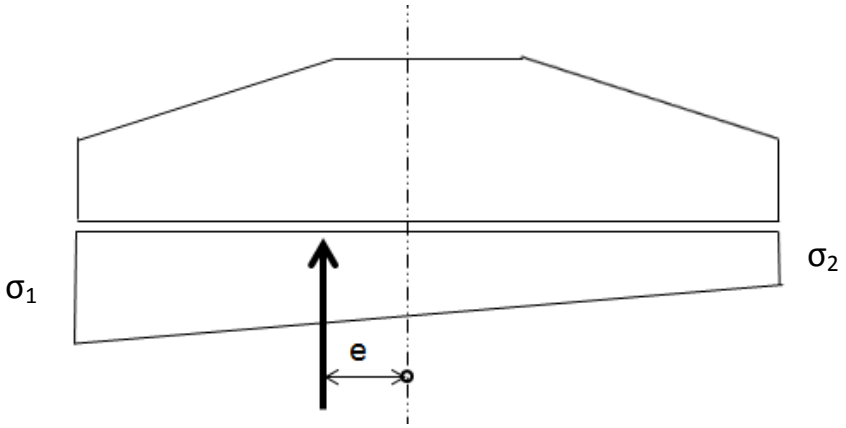

Figure 6.14 Soil pressure distribution used in fatigue calculations.

The size of σ_1 and σ_2 can be determined by establishing the expression for the distance to the gravity centre and horizontal equilibrium. The equivalent moment and shear force distribution is presented in Figure 6.15.

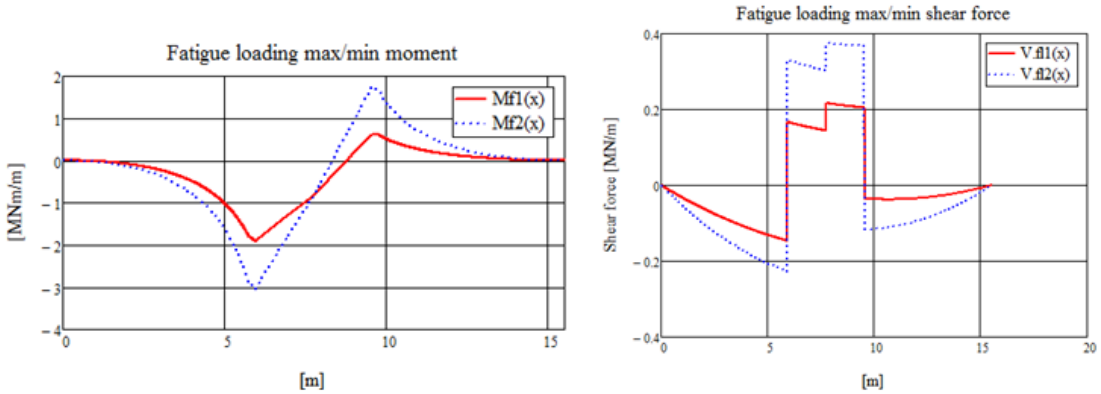

Figure 6.15 Variation in bending moment and shear force for the two used equivalent fatigue loads.

The stress-amplitudes for reinforcement and concrete can be determined from the moment and shear force distribution. The stress-amplitudes in reinforcement can be used in Equation 6.14 (EN 1992-1-1:2005 6.8.5) to determine the fatigue damage for the reinforcement.

$$\gamma_{F,fat} \cdot \Delta\sigma_{\mathrm{S,equ}}(N^*) \leq \frac{\Delta\sigma_{\mathrm{Rsk}}(N^*)}{\gamma_{s,fat}} \tag{6.14}$$

where:

$\Delta\sigma_{Rsk}(N^*)$	Stress range of N^* load cycles
$\Delta\sigma_{S,equ}(N^*)$	Damage equivalent stress range for N^* cycles
$\gamma_{s,fat}$	Partial safety factor for fatigue loading
$\gamma_{F,fat}$	Partial safety factor for material uncertainties

The 'Palmgren-Miner cumulative damage law' approach was used with the full load spectrum supplied from the turbine manufacturer to calculate accumulated damage with both slopes of the S-N curves for reinforcement. To do this the complete load spectra are exported to Mathcad, where the bending moment and shear force distribution for each different load is calculated in order to determine the stress variations for each unique load. The size of the load is then checked to see which slope of the S-N curve that should be used. The two different slops given in Eurocode are presented below.

$k = 5$ For $\Delta\sigma \cdot \gamma_{F,fat} < \frac{\Delta\sigma_{Rsk}}{\gamma_{s,fat}}$

$k = 9$ For $\Delta\sigma \cdot \gamma_{F,fat} \geq \frac{\Delta\sigma_{Rsk}}{\gamma_{s,fat}}$

The total damage D_{Ed} can then be calculated as:

$$D_{Ed} = \sum_i \frac{n(\Delta\sigma_i)}{N(\Delta\sigma_i)} < 1 \quad (6.15)$$

Where $N(\Delta\sigma_i)$ is the total number of cycles until failure for the stress range ($\Delta\sigma_i$) calculated as:

$$N(\Delta\sigma_i) = 10^6 \left(\frac{\Delta\sigma_{Rsk}/\gamma_{s,fat}}{\gamma_{F,fat} \cdot \Delta\sigma_i} \right)^k \quad (6.16)$$

For the fatigue verification of the compressed concrete, two approaches exist in Eurocode. The used method is based on the equivalent load, where a reference number of load cycles, $N_{eq} = 10^6$, is used instead of the full load spectra. There is an alternative method of calculating equivalent load described in the bridge part of Eurocode EN1992-1-1:2005 that takes account for the frequency of the load. However, there was no time to evaluate this method within the limited time for this project. The used equations for fatigue verification of concrete are, EN1992-1-1:2005 6.8.7:

$$E_{cd,max,equ} + 0.43\sqrt{1 - R_{equ}} \leq 1 \quad (6.17)$$

$$R_{equ} = \frac{E_{cd,min,equ}}{E_{cd,max,equ}} \quad (6.18)$$

$$E_{cd,min,equ} = \frac{\sigma_{cd,min,equ}}{f_{cd,fat}} \quad (6.19)$$

$$E_{cd,max,equ} = \frac{\sigma_{cd,max,equ}}{f_{cd,fat}} \quad (6.20)$$

where:

R_{equ}	Stress ratio
$E_{cd,min,equ}$	Lowest compressive level
$E_{cd,max,equ}$	Highest compressive level
$f_{cd,fat}$	Concretes design strength
$\sigma_{cd,min,equ}$	Lowest compressive at stress change for 10^6 cycles
$\sigma_{cd,max,equ}$	Highest compressive at stress change for 10^6 cycles

6.6 Results

In the static design of the reference case both the bottom and top reinforcement amounts calculated in ultimate limit state had to be increased in order to fulfil the crack width limitations.

Shear reinforcement was only required to avoid punching shear failure. The provided U-bows and minimum shear reinforcement prescribed by the turbine manufacturer was however sufficient to avoid punching shear failure and no extra reinforcement was needed. The highest degrees of utilisation are presented in Table 6.1.

Wind power plants are subjected to a large number of load cycles and the fatigue analysis becomes of great importance. Two different fatigue verification methods were performed; 'Fatigue equivalent load cycle method' and 'Palmgren-Miner cumulative damage law'. The 'Palmgren-Miner cumulative damage law' can only be used together with full load spectra and requires applicable S-N curves. Hence, this method cannot be used to check compressed concrete, since no S-N curves for concrete exist. Further, the 'Fatigue equivalent load cycle method' is more straight-forward and requires less calculations. Though it is unclear if this method is suitable for fatigue analysis of reinforced concrete structures.

Both fatigue calculation methods resulted in less damage than expected, in all checked regions and components apart from the U-bows. However, there are uncertainties regarding which time period the load spectra provided by the turbine manufacturer represent which make the results hard to evaluate.

The fatigue calculations performed with the equivalent load gave higher damage than the damage summation method in all checks, except for the analysis of the U-bows. In analysis of the U-bows the equivalent load method gave a damage of 80 % and the 'Palmgren-Miners damage summation law' resulted in fatigue failure ($D_{Ed} = 1.06$). Since the calculation was performed only on the outermost U-bow, which is subjected to the largest stress variations, the results were accepted even if the damage was above 1. Since the U-bows are evenly distributed around the perimeter of the anchor ring and stress redistribution is possible in case of failure.

The difference in result between the two calculation methods indicates that the 'Fatigue equivalent load cycle method' may be improper for reinforced concrete structures. At least the method must be investigated regarding which assumptions the method is based on.

The concrete fatigue life was only calculated with the equivalent load, the full load spectra could not be used since S-N curves for concrete do not exist. The calculated fatigue damage for concrete was low. The reason for this could be the high required concrete strength class C45/55 specified by the turbine manufacturer.

Table 6.1 presents some utilisation ratios from the design. All results are presented in Appendix H. The utilisation ratios are calculated by dividing required capacity divided by provided capacity.

Table 6.1 present utilisation ratios from the design, all results are presented in Appendix H.

Table 6.1 Highest utilisation ratios

Part	ULS	Fatigue	Remark
Bending reinforcement bottom	30 %	26 %	Section 0, Equivalent load
Bending reinforcement top	31 %	35%	Section 0, Equivalent load
Star reinforcement	66 %	32%	calculated with required area compared to the used
U-bow reinforcement	94 %	106 %	Local analysis, Palmgren-Miner
Concrete compression	51 %	56 %	Local analysis under anchor ring, Equivalent load
Shear reinforcement	73 %	-	Section 0
Crack width	92 %	-	Section 0, at the bottom

Table 6.1 clearly shows that the critical design aspects of the reference foundation were the crack width limitation and the U-bows subjected to fatigue loading. The utilisation ratio for shear reinforcement was calculated with shear reinforcement spacing 500 mm, which was specified by the turbine manufacturer. Shear reinforcement was however only needed with regard to punching shear failure.

Besides the result for the star reinforcement, the ultimate limit state utilisation ratio and the fatigue life is rather similar. The low utilisation ratios in the ultimate limit for bending reinforcement are an effect of the crack limitations in the serviceability limit state, may explain the rather small fatigue damage. The result for star reinforcement was calculated differently and could not be compared with the other results for bending reinforcement. The U-bow reinforcement is not designed with regard to crack width limitations, which explains the large utilisation, both in the ultimate limit state and in case of fatigue.

6.7 Conclusions on common design practice

Design according to common practice is based on the idea of distributing the sectional forces uniformly across the full width of the foundation and using sectional design. However, this assumption is unreasonable near the anchor ring because of the concentrated reaction from the anchor ring. By concentrate the reinforcement to the

centre of the slab the effects of stress variation in transverse direction is accounted for. The bending capacity can be regarded as sufficient as long as the total bending reinforcement is enough and plastic redistribution is possible. Regarding the shear design it is necessary to construct a truss model in order to ensure sufficient shear resistant. Therefore a 3D truss model is recommended in order to consider the 3D behaviour of the slab. In common design practice the stress variation in transverse direction is disregarded and the design procedure is incomplete.

If the linear elastic stress field is known, regions where 3D-aspects need to be considered can be identified. Hence, regions where beam-theory is valid can be recognised and designed with sectional design.

Sectional design is straight forward and it is easy to determine how sectional forces change depending on load magnitude. This makes fatigue calculations based on the full load spectra and 'Palmgren-Miners damage summation law' rather simple. The 3D aspects must also be considered in the fatigue assessment. Because of the relative small fatigue loads it is unreasonable to assume that the internal forces will redistribute. Therefore it is recommended to assume that both the shear force and bending moment are concentrated to the centre of the foundation.

There are uncertainties regarding which time period the load spectra used for fatigue assessment represent, which make the results from these calculations hard to evaluate. It is also uncertain if an equivalent load is reasonable for design of reinforced concrete structures. The results from the calculations with 'Palmgren-Miners damage summation law' differ from the one performed with an equivalent load. The equivalent load was used, because the fatigue verification of concrete in Eurocode requires one equivalent stress range.

Because of the large bending moment in the anchor ring the verification of capacity against punching shear failure is conducted with a modified version of the one proposed in Eurocode. The used method for verification of capacity against punching shear failure must be studied further before it can be accepted in design.

The square shape of the foundation is well suited for a reinforcement layout with bars placed only perpendicular and parallel with the edges. In case of circular foundations a design where the reinforcement is placed radial may be more suitable.

With a circular foundation the length of radially placed bars can be constant, while they need to be shortened in a square foundation. With the same reasoning a circular foundation is less suited for reinforcement with crossed bars, se Figure 6.16.

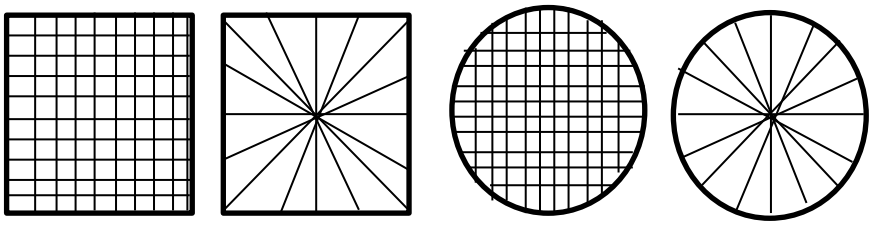

Figure 6.16 Different reinforcement layouts in square and circular foundations

Unlike crossed bars the use of bars placed radially results in problem with the spacing in the centre of the foundation. If the bars are placed radially the need of reinforcement is reduced due to the fact that the loads do not need to be transferred in two directions separately. In Figure 6.17 this is exemplified with a corner supported slab.

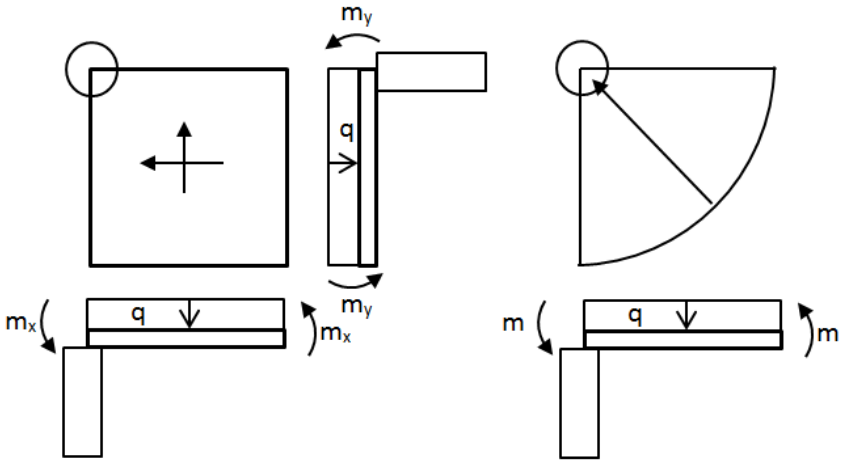

Figure 6.17 *Left: Reinforcement in x- and y-direction. Left: Radially placed reinforcement. With radially placed reinforcement the need for reinforcement decreases.*

7 Design of reference case with 3D strut-and-tie models and Eurocode 2

With regard to the boundary conditions and the concentrated centric load a 3D-model was used to capture the behaviour of the foundation. This chapter describes the design methodology that was used to establish 3D strut-and-tie models for the reference object described in Chapter 5.

7.1 Methodology

The previously described methodology in Chapter 4 to describe the stress flow in D-regions known as the load-path method can be used in 3D. There is however a very complex loading situation and without great experience or advanced computer analysis a reasonable stress field is hard to assume. The chosen procedure was to simplify the loading and start to construct a suitable 2D model that then was developed into a 3D model.

The self-weight and soil pressure needed to be divided in an adequate amount of nodes to avoid an oversimplistic model. With a chosen division of loads the models were established based on the load path method. The models were constructed in the commercial software *Strusoft FEM-design 9.0 3D frame*. Strut-and-tie models are only based on equilibrium conditions, i.e. no deformations should be assumed in the struts or ties. Therefore the elements were represented by "*truss members*" with properties chosen to according to Figure 7.1.

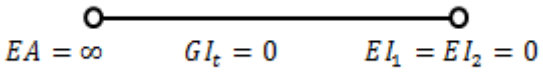

Figure 7.1 Used elements in analysis.

The first models in FEM-design were constructed with "fictitious bars", but because of problems with setting the flexural rigidly to zero ordinary "*truss members*" were used instead. These elements can only transfer normal forces and all connections are hinged. In order to avoid influence from deformations or buckling the loads were scaled to 1/100 and large steel sections of high strength were used. To verify the results from *FEM-design* the freeware *Fachwerk 0.4.1* was used, developed by *Vontobel, A (2010). Fachwerk* is designed for analysing strut-and-tie models and uses only equilibrium conditions, i.e. does not consider any material behaviour.

7.2 Two-dimensional strut-and-tie model

To simplify the loading situation the self-weight was represented by two resultants acting on top of the structure. The soil pressure was modelled as uniformly distributed and represented by one resultant in the strut-and-tie model. The position of the U-bows is fixed and the distance between vertical bars is 500 mm. The first model was established with only the criterion of equilibrium and did not consider angle limitations or node stresses. In order to keep balance so called "u-turns" were needed above the resultants F_c and F_t in order to take care of the bending moment. Only vertical and horizontal ties were accepted with regard to practical reinforcement arrangement. The developed 2D model along with used loading conditions is shown

in Figure 7.2. This 2D model was used as the base for development to 3D models.

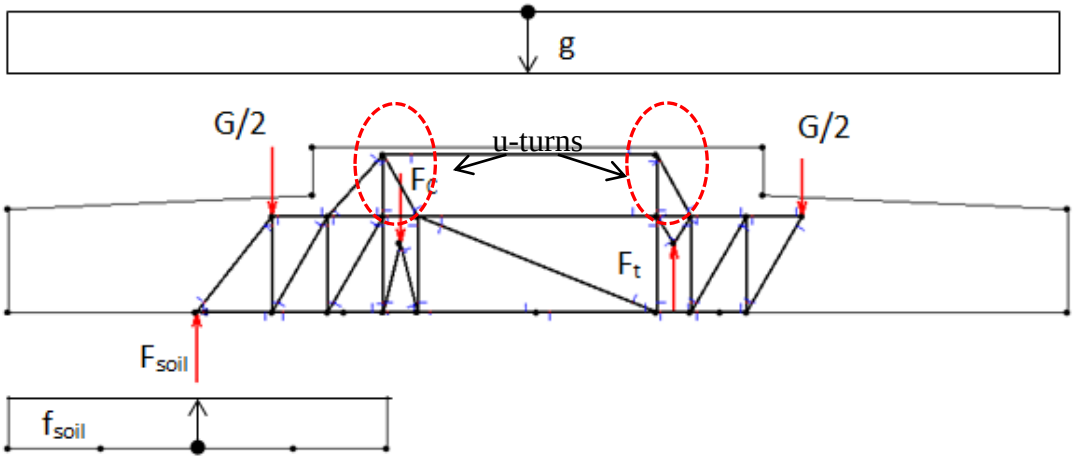

Figure 7.2 Established 2D strut-and-tie model for the wind power plant foundation.

7.3 Three-dimensional strut-and-tie models

A wind power plant foundation is subjected to many different load amplitudes and a unique strut-and-tie model could be established for each load case both in 2D and 3D. The 3D strut-and-tie models were established for the ultimate limit state. The difference in the serviceability limit state is the location of F_{soil} since the soil pressure and eccentricity varies with the load magnitude.

When developing the 2D model to 3D, the reactions acting on the foundation must be represented by an adequate amount of nodes over the width of the foundation. The soil pressure was assumed to be evenly distributed over the width of the foundation. Choices made regarding the distribution of nodes were the following:

- The self-weight including the filling material was divided into six parts of the same size
- The soil pressure was divided into three equal parts over the width

How the loads were divided is shown in Figure 7.3. In the strut-and-tie models a node were placed in the centre of each loaded area.

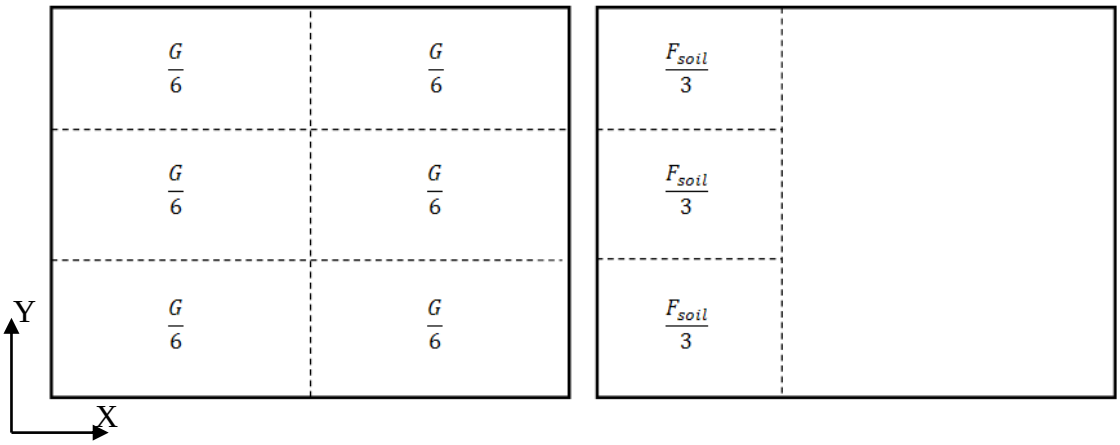

Figure 7.3 Load dividing lines for the nodes.

With the chosen load distribution two different load paths were used, one with load transferred in one plane at a time (model 1) and another with load transfer radial (model 2). Model 1 was based on the idea to only use reinforcement parallel or perpendicular to the edges, i.e. in x- and y-directions. Model 2 transfers the load in diagonal paths to and from the anchor ring. The different models are illustrated in Figure 7.4.

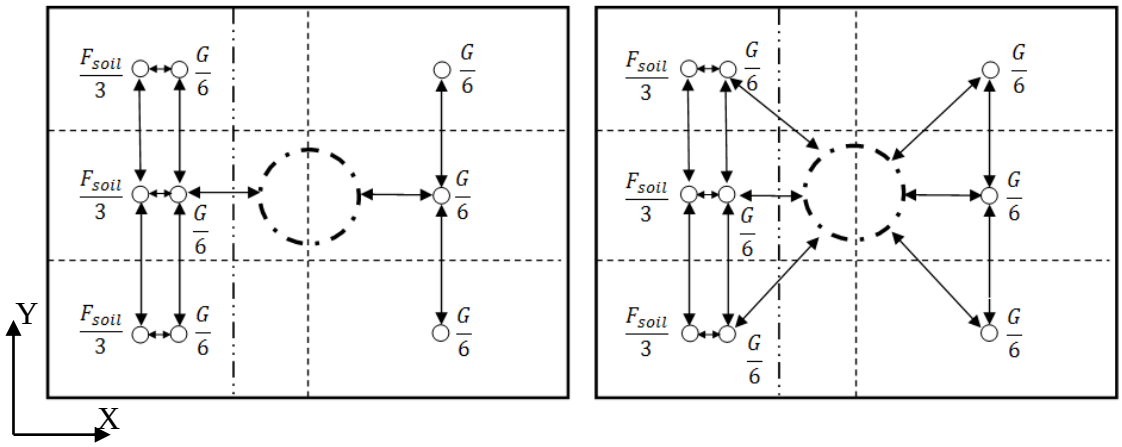

Figure 7.4 The different load path models. Left: model 1 load paths in x- and y-directions. Right: model 2 with diagonal load paths. Dotted line: division of G, dot-dashed line division of f_{soil}.

As stated earlier the 2D strut-and-tie model was used as a base for the 3D model. The diagonal "legs" and the parallel "legs" are similar to the 2D model. These "legs" were connected with a strut-and-tie model for the anchor ring. Figure 7.5 shows the principle ideas for the establishment of the strut-and-tie models and the so called 'legs'.

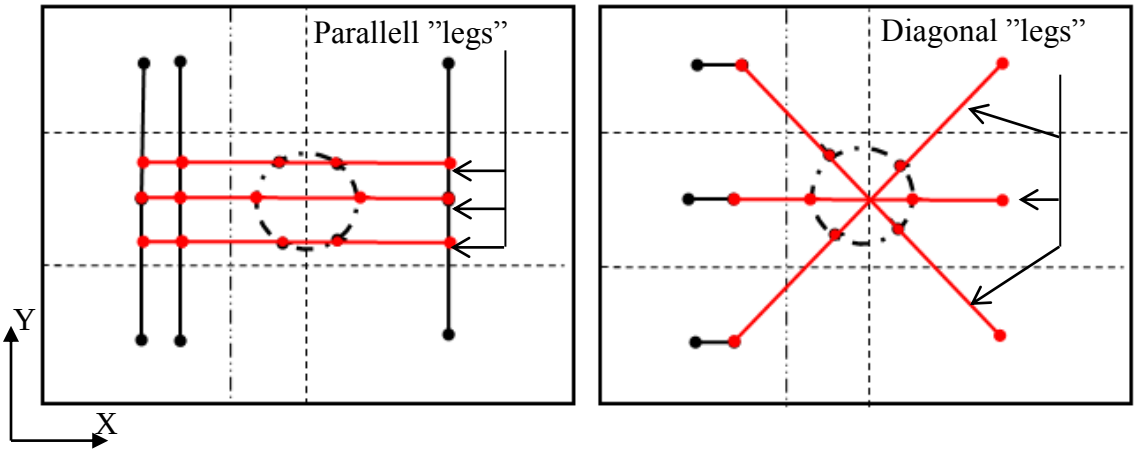

Figure 7.5 *Principle of the 3D strut-and-tie models. Left: The loads are transferred in x- and y-direction separately. Right: Load transferred diagonally. The parallel and diagonal “legs” are marked red.*

In order to achieve equilibrium the nodes representing the soil pressure must be connected with the reaction force of the anchor ring. In the model that transfer loads in x- and y- directions the “legs” is connected with the anchor ring in the middle and on the edges to utilise the full width of the anchor ring. In the diagonal model the position of “legs” were chosen to go between the positions of the nodes representing the self-weight.

In the 2D model the bending moment was represented by a force couple. The same method was used in the 3D model, but instead 3 force couples represented the bending moment. To determine the magnitude of each force a similar approach was used as in the design based on common practice, i.e. assume that plane sections remain plane in the interface between the anchor ring and the concrete. In this case, six components must be determined and their resultants must act in the node position corresponding to the connection between the ‘legs’ and the anchor ring. The calculation of the forces was carried out with a FEM-analysis. The FEM model consisted of a thick anchor ring to avoid deformations in the anchor ring. It was supported with point supports placed at the chosen node positions and loaded with the bending moment. The model is shown in Figure 7.6, where the stress resultants of the supports were placed at the corresponding nodes in the strut-and-tie models. The largest resultants were located in the most eccentric part of the anchor ring. The magnitudes of the different forces are presented in Table 7.1 and their location in Figure 7.6.

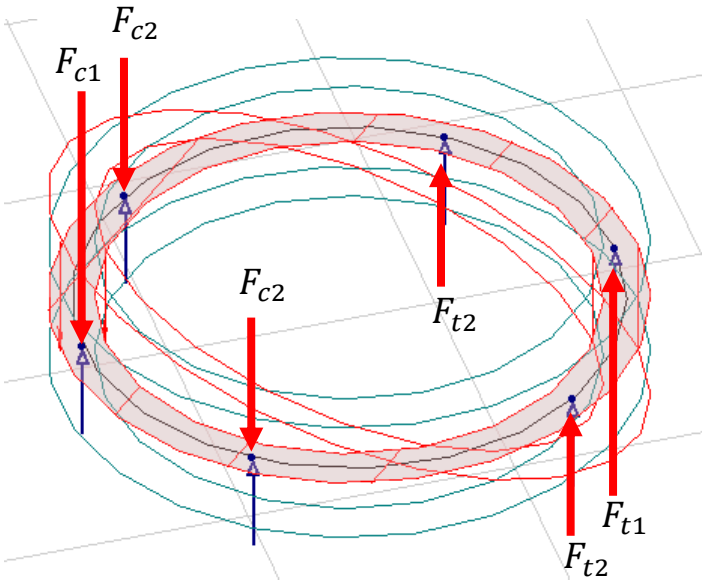

Figure 7.6 *Used model to determine F_{c1}, F_{c2}, F_{t1} and F_{t2} in the 3D strut-and-tie model.*

Table 7.1 *Ultimate loads calculated with the FEM-analysis including F_z*

F_{c1}	90 400 kN
F_{c2}	52 700 kN
F_{t1}	85 900 kN
F_{t2}	45 300 kN

With chosen load distribution on the foundation, positions and size of the forces corresponding to the rotational moment two strut and tie models were established. These 3D strut-and-tie models are presented in Figure 7.7 and Figure 7.8. Figure 7.7 shows model 1 that was established from the concept of using ties in x- and y-direction for simplified reinforcement layout.

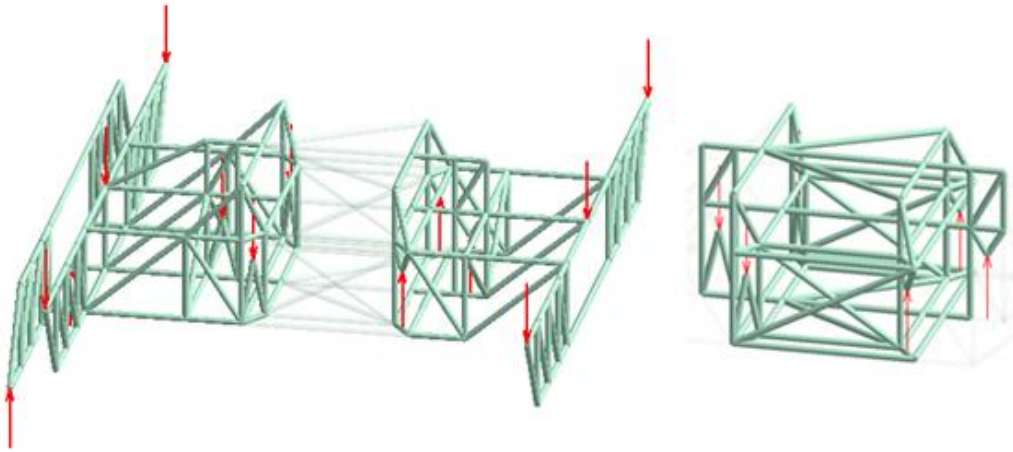

Figure 7.7 *Model 1, were the detailing for the centre of the strut-and-tie model is shown separately.*

Figure 7.8 shows model 2 established with the idea of transferring the load radial.

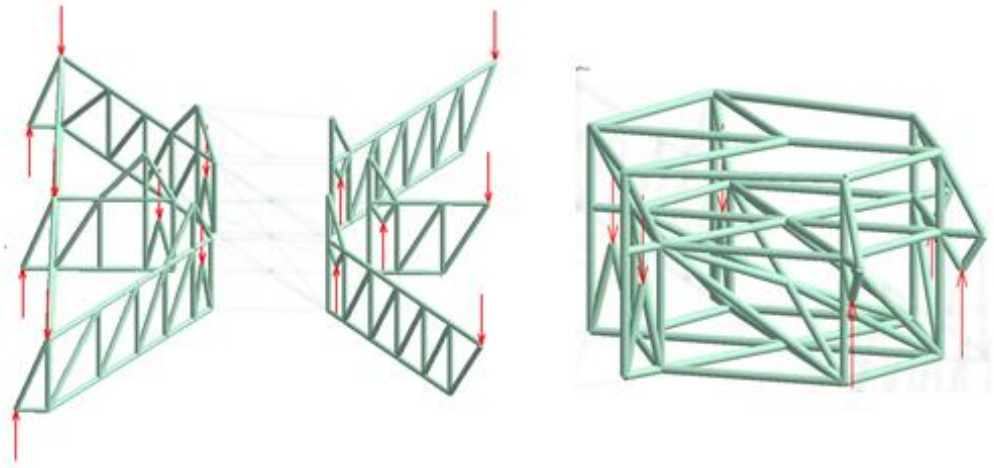

Figure 7.8 Model 2, were the detailing for the centre of the strut-and-tie model is shown separately.

Note that the models have different centre, the reason for this was to achieve equilibrium by only using straight bars for Model 1. When the 3D strut-and-tie models are established, the angles and node capacities should be checked. The angle recommendations used in 2D can be adapted to 3D, by checking the angle in each plane separately.

The foundation must be able to resist arbitrary wind directions, but the strut-and-tie models can only be established for one load case at a time. As described in Section 6.1, performing the design of the foundation for all parallel wind directions is regarded as sufficient since the reinforcement is crossed. If model 1 is rotated to restrain all perpendicular wind directions the model is assumed to resist all wind directions. Model 1 becomes double symmetric when rotated, which is not the case for model 2. In Figure 7.9 both models are rotated. For model 2 it is not sufficient to only check parallel wind directions, since the load is not transferred in two directions the diagonal wind direction can result in larger need for reinforcement and therefore it must be verified separately.

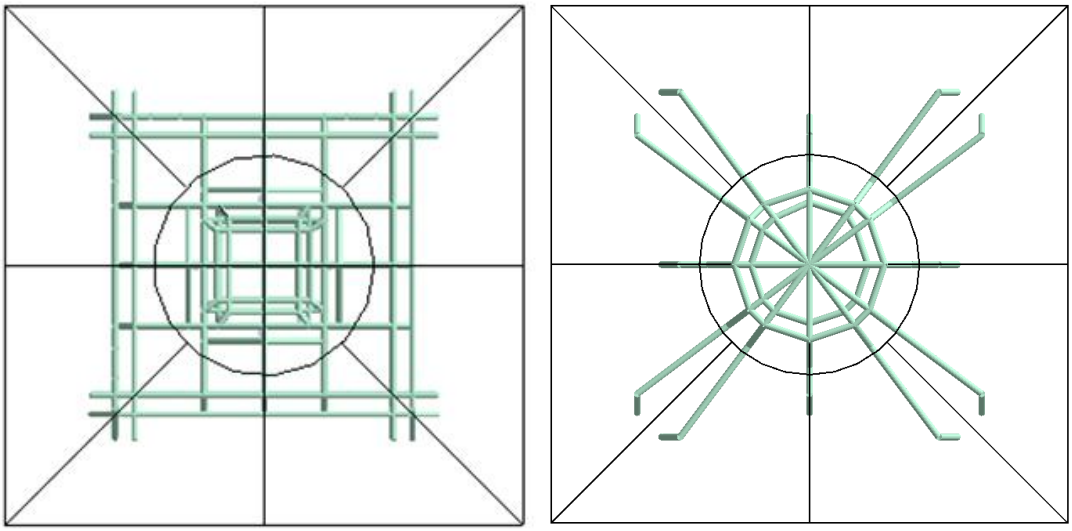

Figure 7.9 Rotated strut-and-tie models: Left: model 1 Right: Model 2.

Since the foundation of the reference case is square Model 1 is preferable due to the problematic connection in the centre of the foundation.

7.4 Reinforcement and node design

Designing the reference foundation with radial placed reinforcement was regarded as inappropriate because of the square shape. Therefore the reinforcement calculations were only performed for Model 1. Model 1 was divided into different sections, which were designed separately. The definition of sections is shown in Figure 7.10 and the corresponding forces and sections can be found in Appendix J.

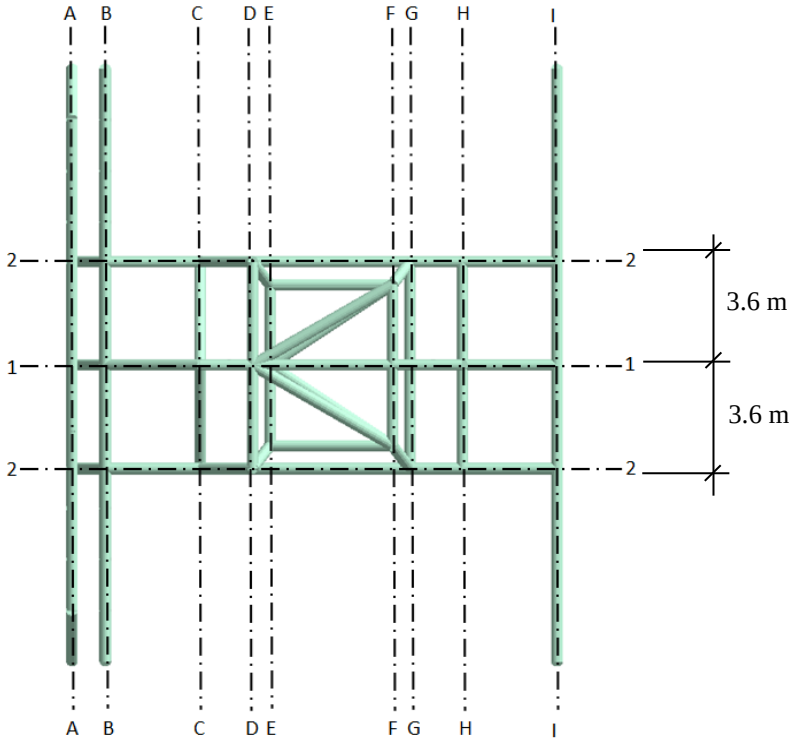

Figure 7.10 Definitions of sections for Model 1, each section is presented in Appendix J.

The design of shear, top and bottom reinforcement in each section was performed according to the following steps:

1. Determine the largest tensile force for vertical, top and bottom tie separately.
2. Calculate the amount of shear, top and bottom reinforcement required for the corresponding ties.
3. Spread the needed reinforcement over the width of the approximated tensile stress field, which the corresponding tie represents.

For example Section 1-1's largest tensile force in the bottom layer is spread over a width of 3.6 m, see Figure 7.10. This resulted in a spacing of 200 mm of $\phi 25$ bars. 3.6 m is the distance between Sections 1-1 and 2-2, which is the width where the corresponding tensile stress field of the tie is assumed to occur. The reinforcement needed to transfer the soil pressure and self-weight are spread over the same widths as

used for the load paths, shown in Figure 7.4. To resist load from arbitrary wind directions the reinforcement calculated must also be provided in the transverse direction.

The suspension reinforcement was designed under the same assumptions and with the same design procedure as described in Section 6.3. Accordingly U-bows with a bar diameter of $\phi 25$ mm and a spacing of 100 mm were chosen. An example of detailing around the anchor ring is illustrated in Figure 7.11.

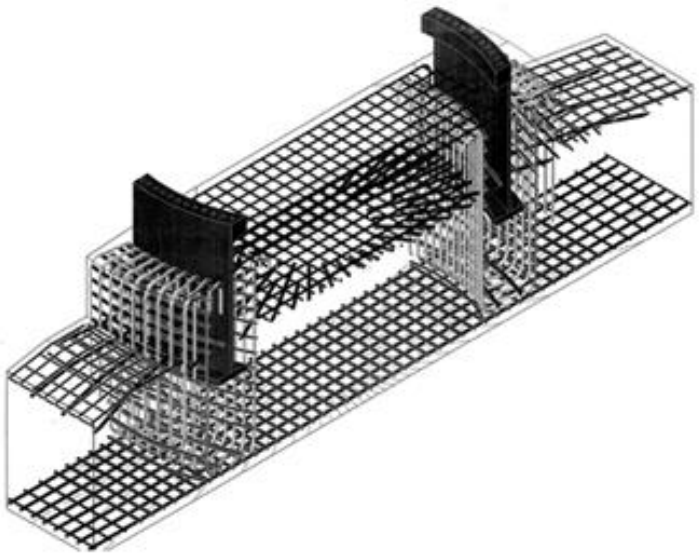

Figure 7.11 Example of U-bows that are placed very dense around the anchor ring.

In 3D complex node geometries can arise which cannot be designed by directly adapting the design rules from 2D design. There are no accepted design rules for how to design these nodes. However, a solution for designing complex 3D node regions is purposed by Chantelot, G. and Alexandre, M. (2010) and is briefly described in Section 4.7.1.

The wind power plant foundation is subjected to distributed forces from the soil pressure and self-weight. The sectional forces are distributed over the circumference of the anchor ring flange at the interface to concrete. The sectional forces at the anchor ring interface connection are distributed over the circumference of the anchor ring flange. Hence, the corresponding nodes are distributed and do not need to be checked.

When confirming the strut-and-tie model it is not enough to verify the concentrated nodes. The compressive force in the struts does also need to be limited. This can be done by calculating the concrete area required to take the compressive forces in the struts and compare it to the available. The struts are assumed to be spread over the same width as the corresponding tie. To verify the capacity of the struts the required concrete area for each strut is calculated in Appendix K. There are however, struts that are critical within the anchor ring but the established model of the detailing around the anchor ring needs to be refined. This can be achieved by subdividing the force couple in more than six nodes. In addition the design should be improved with minimum reinforcement.

The tensile forces in the vertical ties in the strut-and-tie model outside the anchor ring are assumed to be spread over the same length as the bottom and top reinforcement. This gave the required spacing of the shear reinforcement which were larger than the required, $\phi 25$ bars spaced 500 mm from the turbine manufacturer. But since the design only have been performed for the ultimate limit state the design must be supplemented with service ability calculations.

7.5 Fatigue

No fatigue verification has been performed on the strut-and-tie models, since every different load case would result in a unique strut-and-tie model. Without an automatic routine it is unreasonable to establish a 3D strut-and-tie model for every load case. Two strut-and-tie models could be established for the two equivalent loads to find the stress amplitude in these cases, but with regard to uncertainty of the accuracy of these loads this has not been performed.

With either an automatic routine or a reduced number of load cases the strut-and-tie method is well suited for fatigue calculations, since the 3D behaviour of the foundation is taken into consideration. However, if the strut-and-tie model is used for fatigue calculations the model must be close to the linear elastic stress field, i.e. have a small need for plastic redistribution. Further, the reinforcement layout cannot change between the models, i.e. one reinforcement solution must fit all load cases and corresponding models.

The master thesis "*Fatigue Assessment of Concrete Foundations for Wind Power Plants*" Göransson, F. Nordenmark, A. (2011) describes how fatigue verification of 2D strut-and-tie models can be performed. Instead of using one equivalent load as in our project a reduced load spectrum was used, which was provided by the turbine manufacturer. To simulate the stress field four unique 2D strut-and-tie models were established in the fatigue analysis. The strut-and-tie models were different, but all models had the same reinforcement layout.

7.6 Results

The design of the foundation with a 3D strut-and-tie model resulted in a reinforcement layout shown in Figure 7.12 and Figure 7.13.

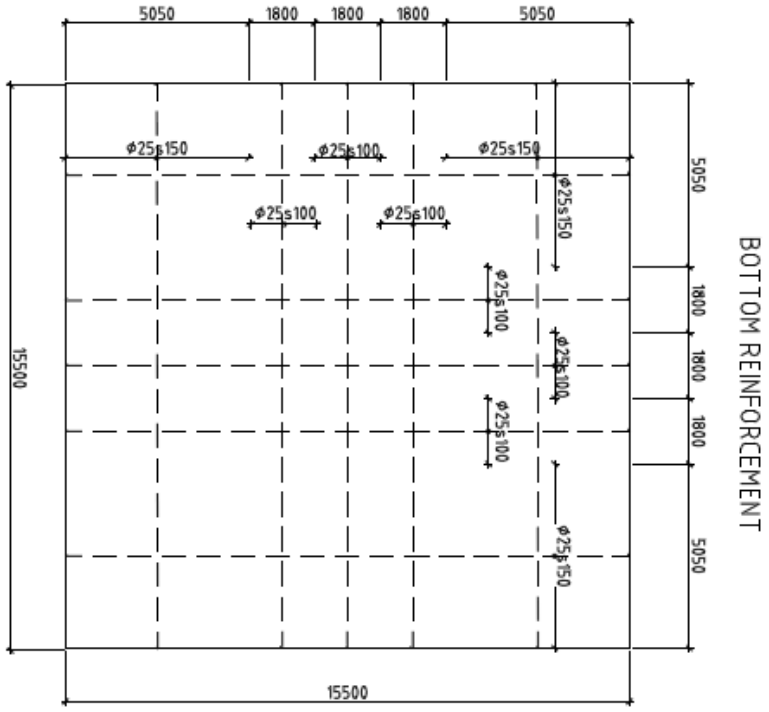

Figure 7.12 Bottom reinforcement layout, all measurements are in mm.

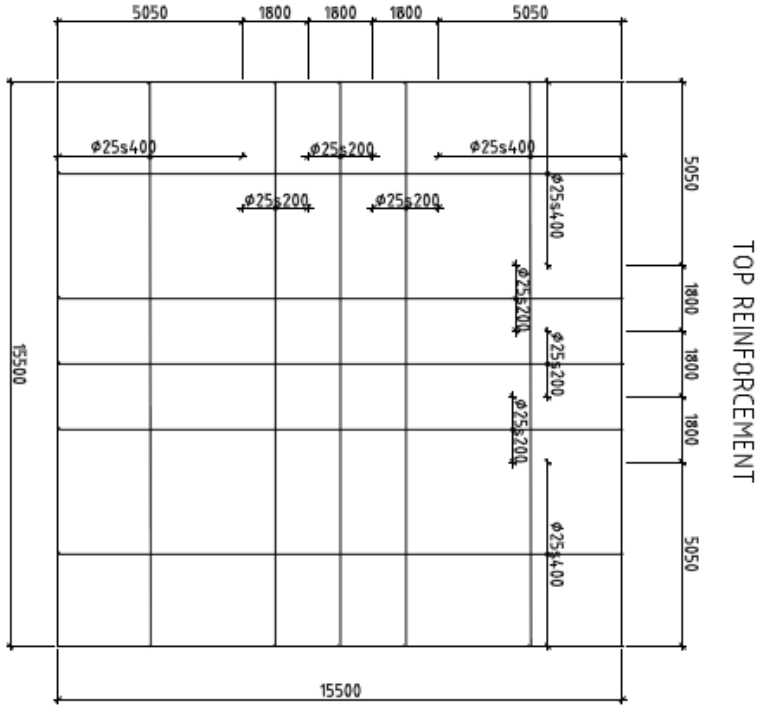

Figure 7.13 Top reinforcement layout, all measurements are in mm.

The reinforcement layout shows that the horizontal reinforcement is placed denser in the centre of the foundation. The need for bottom reinforcement is considerable larger than the need for top reinforcement. The shear reinforcement is placed with a spacing of 500 mm, Figure 7.14 illustrates the type of shear reinforcement that was used.

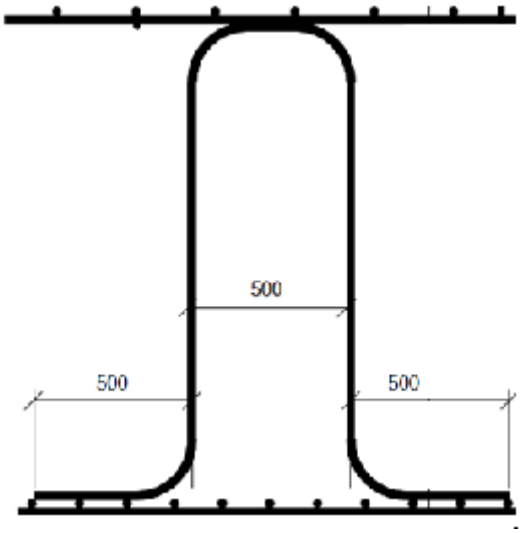

Figure 7.14 Shear reinforcement

7.7 Conclusions on the 3D strut-and-tie method

By designing the wind power plant foundation based on a 3D strut-and-tie model the 3D stress distribution is taken into consideration.

By conducting a linear elastic FEM-analysis of the foundation the linear elastic stress field could be calculated and a more refined model can be established. A more refined strut-and-tie model better simulates the elastic stress field and reduce the need of plastic redistribution. A reduced need for plastic redistribution will improve the behaviour of the foundation in the serviceability limit state.

The established model results in two different reinforcement layouts: one with radially placed reinforcement bars and one with reinforcement bars only in parallel and perpendicular directions to the edges. Due to the square shaped foundation reinforcement placed only in parallel and perpendicular directions to the edges was preferable.

Without an automatic routine for establishment of strut-and-tie models or a reduced load spectra it is very time consuming to perform fatigue calculations on a strut-and-tie model. The reason for this is that a unique model must be established for each fatigue load case. Except for these requirements the strut-and-tie model is well suited for fatigue calculations since the stress variations is easy to evaluate. It should be kept in mind that the strut-and-tie model is designed for the ultimate limit state and the fatigue loads are well below the ultimate loads. It is therefore of great importance that the model is based on a stress field close to the linear elastic. If the strut-and-tie model is based on a stress field far away from the elastic, the model will not simulate the stress field for the relative small fatigue loads and plastic redistributions are small or non-existing.

8 Conclusions and recommendations

The centrically loaded foundation results in D-regions and 3D stress flow which make the use of a 3D strut-and-tie model an appropriate design method. The 3D strut-and-tie model properly simulates the 3D stress flow of reinforced concrete and is appropriate for design of both B-and D-regions. The design according to common practice does not capture the 3D behaviour and is therefore unsatisfactory. Shear design with a sectional model is not possible, i.e. a truss model is required. And in order to capture the 3D behaviour a 3D truss model is necessary.

By conducting a linear elastic FEM-analysis of the foundation the linear elastic stress field can be calculated and D-regions can be distinguished. With this known a more refined strut-and-tie model can be established that follow the linear elastic stress flow more accurately. It also possible to distinguishes where sectional design can be used, i.e. where the stress variation in transverse direction do not need to be considered.

We found it rather complex to establish the 3D strut-and-tie models, it was particularly hard to model the region around the anchor ring in an appropriate way. This might be due to lack of experience of modelling in 3D. Suitable software might simplify the establishment of 3D strut-and-tie models. Another difficulty with strut-and-tie modelling for the design of the wind power plant foundation is the fatigue verification. Fatigue verification with the full load spectra are not reasonable to perform with strut-and-tie models without an automated routine since a unique model must be established for each fatigue load. Without an automated routine the use of an equivalent load becomes necessary. The uncertainties regarding the equivalent load results in a need for a separately research before it can be accepted in design.

8.1 Reinforcement layout and foundation shape

A square foundation seems more suitable for the use of reinforcement in the two main directions than radially placed reinforcement. It is an easier layout that avoids problematic connection in the centre of the foundation and the need of reinforcement bars in many different lengths. One disadvantage is that it requires more reinforcement since the load must be transferred in two directions separately. If a circular foundation instead is used, radially arrangement of the reinforcement bars appears to be more appropriate.

The reinforcement layout from the design according to common practice was suggested to be concentrated towards the centre of the foundation for both top and bottom reinforcement. This choice is motivated by the similarities with a flat slab, where the solution is used to improve the behaviour in service state. The results from the strut-and-tie model also imply that this is a good reinforcement arrangement, with regard to the concentration of internal forces near the anchor ring.

8.2 Suggestions on further research

In this thesis only one type of connection between the tower and foundation has been studied. It would be interesting to study alternative connection types and how they influence the design. Also how to perform relevant verification of punching shear failure of the anchor ring need to be further studied. Further a design for serviceability limit state is desirable.

The uncertainties regarding how to handle the fatigue loads, i.e. if an equivalent load can be used for design of reinforced concrete needs to be clarified. If the use of an equivalent load could be verified, this would make the fatigue calculations considerably simpler. Further the interaction between the soil and the foundation influence the design and studies about the actual soil pressure distribution is of great interest.

9 References

ASCE/AWEA (2011): *Recommended Practice for Compliance of Large Onshore Wind Turbine Support Structures (draft),* American society of civil engineering and American wind energy association, USA.

Martin, B. and Sanders, D. (2007): *Verification and Implementation of Strut-and-Tie Model in LRFD Bridge Design Specifications*, 1-14pp

Boverket (2004): *Boverkets handbok om betongkonstruktioner BBK 04* (Boverket´s handbook on Concrete Structures BBK 04, Vol. 3 Design. In Swedish), Boverket, Byggavdelningen, Karlskrona, Sweden, 181 pp.

Chantelot, G. and Alexandre, M. (2010): *Strut-and-tie modelling of reinforced concrete pile caps*. Master's Thesis. Department of Structural Engineering, Chalmers University of Technology, Publication no. 2010:51, Göteborg, Sweden, 51-53 pp.

Engström, B. (2011): *Design and analysis of deep beams, plates and other discontinuity regions*. Department of Structural Engineering, Chalmers University of Technology, Göteborg, Sweden, 2011.

ESB International (2010): *Wind Turbine Foundations Risk Mitigation of Foundation Problems in the Industry (Electronic),* ESB International. Accessible at< http://www.iwea.com/contentFiles/events/ElecTEC10/10.Eoin_O_Brien_WTG_Foundations2010.pdf?uid=1276273700726> (2012-02-13).

Faber, T. Steck., M. (2005): *Windenenergiealagen zu. Wasser und zu Lande Entwicklung und Bautechnik der Windenergie* (Construction development of offshore and onshore wind energy. In German), Germanischer Lloyd WindEnergie GmbH, Hamburg, 2005

fib (1999): *Bulletin 3 Structural Concrete, fib* (fédération international du béton) Vol. 3, Stuttgart, Germany, 1999, 141 pp.

Göransson, F. Nordenmark, A. (2011): *Fatigue Assessment of Concrete Foundations for Wind Power Plants*. Master's Thesis. Department of Structural Engineering, Chalmers University of Technology, Publication no. 2011:119, Göteborg, Sweden.

Hendriks, H.B., Bulder, B.H. (1995): *Fatigue Equivalent Load Cycle.* ECN, ECN-C-95-074, pp. 3.

IEC (2005): *IEC 61400-1 (International Electrotechnical Commission).* third edition, Geneva, Switzerland, 2005.

Muttoni, A., Schwartz, J., and Thürlimann, B. (1997): *Design of Concrete Structures with Stress Fields*. Birkhäuser Verlag, Basel, Boston and Berlin, Switzerland, 1997, 145 pp.

Rogowsky, M. MacGregor, J. (1983): *Shear strength of deep reinforced concrete continuous beams.* Structural engineering report no 110 Department of civil engineering, University of Alberta. Edmonton, Alberta Candada.

Russo, G., Venir, R., Pauletta, M. (2005): *ACI Structural journal*, Vol. 102, No. 3, May-June 2005, pp. 429-437.

Sanad, A., Saka, M. (2001): *Journal of structural engineering*. Vol. 127, No. 7, July 2001, pp. 818-828.

Schlaich, J., Schäfer, K., and Jennewein, M. (1987): *Toward a Consistent Design of Structural Concrete*. Journal of Prestressed Concrete Institute, V. 32, No. 3, May-June 1987, pp. 74-150.

Schäfer, K. (1999): *Nodes.* Section 4.4.4 in Structural Concrete, Vol. 2, fédération internationale du béton (fib), Bulletin 2, Lausanne, Suisse, pp. 257-275.

SMAG (2011): *Wind Turbines Are Safe. (Electronic), Saddleworth Moors Action Group* Accessible at: < http://www.noturbinesin.saddleworth.net/pictures5.htm> (2011-10-13)

Stephens R, et al. (1980): *Metal fatigue in engineering*. John Wiley & sons, inc, New York.

Stiesdal, H. (1992): *Journal of Wind Engineering & Industrial Aerodynamics*. Vol. 39, No. 1, pp. 303-315.

Svensk Byggtjänst (1994): *Betonghandbok Material* (Concrete Handbook Material. In Swedish), Svensk Byggtjänst, Stockholm.

Vattenfall (2011): *Vind i framtiden* (Wind in the future. In Swedish) *(Electronic),* Vattenfall. Accessible at: <http://www.vattenfall.se/> (2011-10-13)

Vontobel, A. (2010): *Fachwerk 0.4.1 (Electronic),* Accessible at: <http://fachwerk.sourceforge.net> (2011-12-13)

A In data reference case

A.1 Geometry

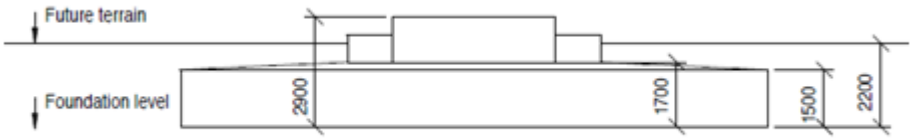

Section

$h_1 := 1500mm$

$h_2 := 1700mm$

$h_3 := 2200mm$

$h_4 := 2900mm$

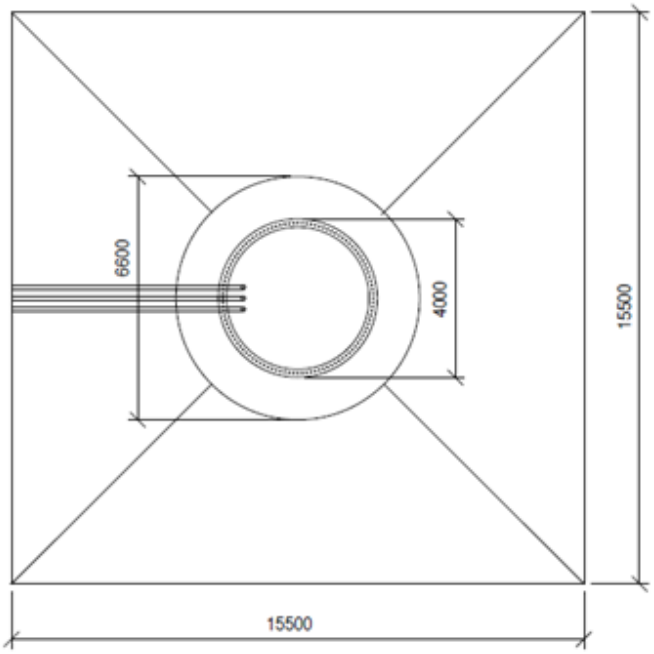

plane

$l := 15500mm$ Length of foundation

$l_{45} := \sqrt{l^2 + l^2}$ Diagonal of foundation

$d_{sr} := 4m$ Outer diameter of steel ring

$c := 50mm$ Concrete cover template

$c_{soil} := 100mm$ Concrete cover to soil (bellow)

$x := 0, 0.01m .. 15.5m$

Variation of foundation section height

$$h(x) := \begin{cases} \left[h_1 + \left(\frac{h_2 - h_1}{\frac{l}{2} - 3.3m}\right)\cdot x\right] & \text{if } x < \frac{l}{2} - 3.3m \\ \left[h_2 - \left(\frac{h_2 - h_1}{\frac{l}{2} - 3.3m}\right)\cdot\left(x - \frac{l}{2} - 3.3m\right)\right] & \text{if } \frac{l}{2} + 3.3m < x \\ h_2 & \text{otherwise} \end{cases}$$

$$x := 0, 0.01m .. \frac{15.5}{2}m$$

Variation of foundation mean height (height varies in two directions):

$$h_m(x) := \begin{cases} \frac{\left[h(x)\cdot 2\cdot\left(\frac{l}{2} - x\right) + \left[l - 2\left(\frac{l}{2} - x\right)\right]\cdot\frac{(h(x) + 1.5m)}{2}\right]}{l} & \text{if } x < \frac{l}{2} - 3.3m \\ \frac{1.7m\cdot 6.6m + (l - 6.6m)\cdot\frac{1.7m + 1.5m}{2}}{l} & \text{otherwise} \end{cases}$$

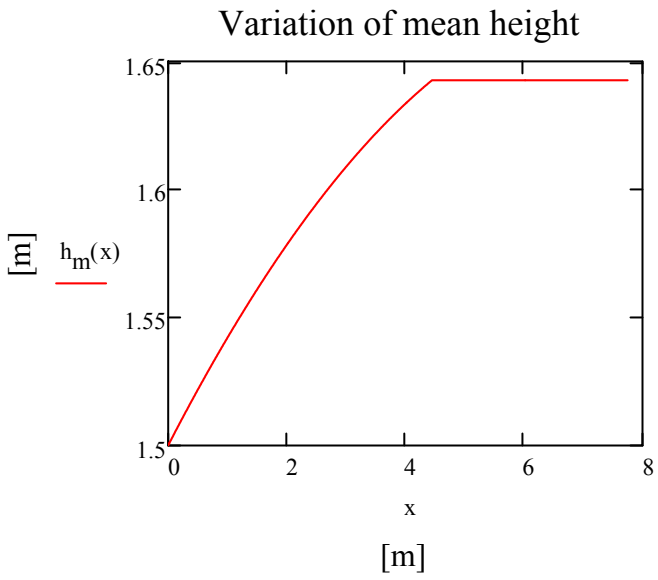

A.2 Loads

Coordinate system

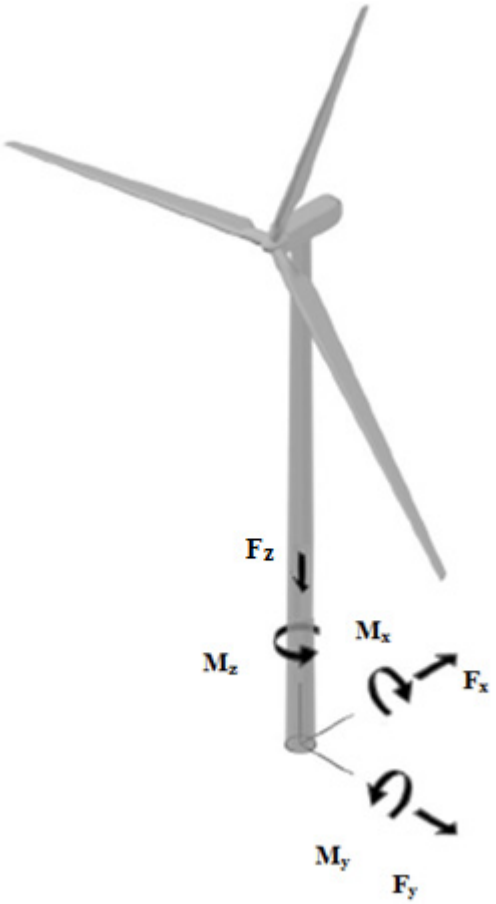

Characteristic loads

Loads from tower

$F_Z := 2121kN$

$M_Z := 5863kN \cdot m$

$M_{xy} := 51115kN \cdot m$ Included moment from misalignment

$F_{xy} := 800kN$

Loads of foundation

Dead weight of concrete foundation including filling material and reinforcement

$G := 12574.9kN$

$g := 52.341 \frac{kN}{m^2}$

Partial factors for loads according to IEC 61400-1:2005 edition 3

According to table 2 p. 35 IEC 61400-1:2005
DLC 6.2 "Extreme wind speed model 50-year recurrence period"
Ultimate analysis, Abnormal

IEC use another standard where:
Abnormal corresponds to ULS
Normal corresponds to SLS

Live loads:		**Dead loads:**	
ULS			
$\gamma_Q := 1.1$	Unfavourable	$\gamma_G := 1.0$	Unfavorable
$\gamma_{Qf} := 0.9$	Favourable	$\gamma_{Gf} := 0.9$	Favorable
SLS			
$\gamma_{Qsls} := 1.0$		$\gamma_{Gsls} := 1.0$	
Fatigue			
$\gamma_f := 1.0$		-	

Partial factors for consequences of failure to IEC 61400-1:2005 edition 3

Component class 1: $\gamma_n := 1.0$

Design loads

ULS

$M_{xyd} := \gamma_Q \cdot M_{xy} = 56.227 \cdot MN \cdot m$

$F_{xyd} := \gamma_Q \cdot F_{xy} = 0.88 \cdot MN$

$F_{zd} := \gamma_{Gf} \cdot F_z = 1.909 \cdot MN$

$M_{zd} := \gamma_Q \cdot M_z = 6.449 \cdot MN \cdot m$

$G_d := \gamma_{Gf} \cdot G = 11.317 \cdot MN$

$g_d := \gamma_{Gf} \cdot g = 47.107 \cdot \frac{kN}{m^2}$

SLS

$M_{xySLS} := \gamma_{Qsls} \cdot M_{xy} = 51.115 \cdot MN \cdot m$

$F_{xySLS} := \gamma_{Qsls} \cdot F_{xy} = 0.8 \cdot MN$

$F_{zSLS} := \gamma_{Gsls} \cdot F_z = 2.121 \cdot MN$

$M_{zSLS} := \gamma_{Qsls} \cdot M_z = 5.863 \cdot MN \cdot m$

$G_{dSLS} := \gamma_{Qsls} \cdot G = 12.575 \cdot MN$

$g_{dSLS} := \gamma_{Qsls} \cdot g = 52.341 \cdot \frac{kN}{m^2}$

A.3 Material Properties

Material properties and partial factors according to Eurocode

Partial safety factors [EN 1992-1-1:2005 2.4.2.4 table 2.1N]

$\gamma_{mc} := 1.5$ Material partial factor for concrete

$\gamma_{ms} := 1.15$ Material partial factor for steel

Concrete strength class C45/55

[EN 1992-1-1:2005 3.1.3 table 3.1]

$f_{ck} := 45MPa$ Characteristic compressive strength

$f_{cm} := 53MPa$ Mean compressive strength

$f_{ctm} := 3.8MPa$ Mean tensile strength

$E_{cm} := 36GPa$ Mean Young's modulus

$\varepsilon_{cu} := 3.5 \cdot 10^{-3}$ Ultimate strain

Reinforcement KS600S

$f_{yk} := 600MPa$ Characteristic yield strength

$E_s := 200GPa$ Young's modulus for steel

Design values

$f_{cd} := \frac{f_{ck}}{\gamma_{mc}}$ $f_{cd} = 30 \cdot MPa$ Design compressive strength of concrete

$f_{yd} := \frac{f_{yk}}{\gamma_{ms}}$ $f_{yd} = 521.739 \cdot MPa$ Design yield strength of steel

$\alpha := \frac{E_s}{E_{cm}}$ $\alpha = 5.556$

Note that the fatigue loads are presented in respective chapter

B Global equilibrium

B.1 Eccentricity and width of soil pressure

Find minimum eccentricity of soil pressure resultant with extreme loads.

$$e := \frac{M_{xyd} + F_{xyd} \cdot h_4}{F_{zd} + G_d} = 4.444\ \text{m}$$ Minimum eccentricity for soil pressure

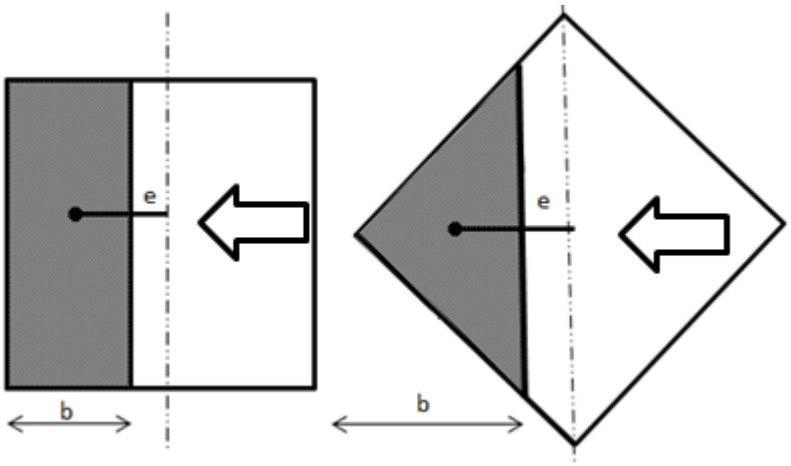

Soil pressure (shaded area) in case of different wind direction Left: Wind direction 90 degree. Right: Wind direction 45 degree. All intermediate direction is assumed to be fulfilled when those two are checked.

Width of soil pressure with uniform soil pressure and wind direction 90 degree (the soil resultant at $\frac{b}{2}$

$$b_{uni} := 2\left(\frac{l}{2} - e\right) = 6.612\ \text{m}$$

Width of soil pressure with triangular soil pressure and wind direction 90 degree (the soil resultant at $\frac{2b}{3}$)

$$b := 3\left(\frac{l}{2} - e\right) = 9.918\ \text{m}$$

Width of soil pressure with uniform soil pressure and wind direction 45 degree.

$$b_{45.uni} := \frac{3\left(\frac{\sqrt{l^2 + l^2}}{2} - e\right)}{2} = 9.774\ \text{m}$$

Width of soil pressure with triangular soil pressure and wind direction 45 degree (result in a rectangular soil pressure $(\frac{b}{2})$)

$$b_{45} := 2\left(\frac{l_{45}}{2} - e\right) = 13.032\ \text{m} \qquad b_{45} > \frac{l_{45}}{2} = 1$$

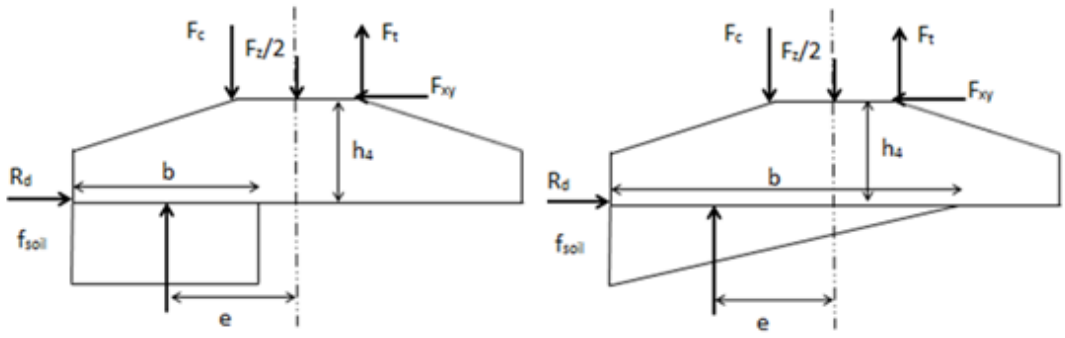

Idealisation of loading case. Moment replaced by a force couple. F_c *and* F_t *including* $\frac{F_{zd}}{4}$.

Left: rectangular soil pressure Right: Triangular soil pressure

Calculation of soil pressure

$$f_{soil} := \frac{F_{zd} + G_d}{\frac{b}{2}} = 2.667 \cdot \frac{MN}{m}$$

Resulting soil pressure with triangular soil pressure and wind direction 90 deg

$$f_{soil.uni} := \frac{F_{zd} + G_d}{b_{uni}} = 2 \cdot \frac{MN}{m}$$

Resulting soil pressure with uniform soil pressure and wind direction 90 deg

Resulting soil pressure with triangular soil pressure and wind direction 45 deg.

$$f_{45.soil.uni} := \frac{F_{zd} + G_d}{\frac{b_{45.uni}}{2}} = 2.706 \cdot \frac{MN}{m}$$

Resulting soil pressure with uniform soil pressure and wind direction 45 deg

$$g_d := \frac{G_d}{l} = 730.155 \cdot \frac{kN}{m}$$

Resulting soil pressure per meter

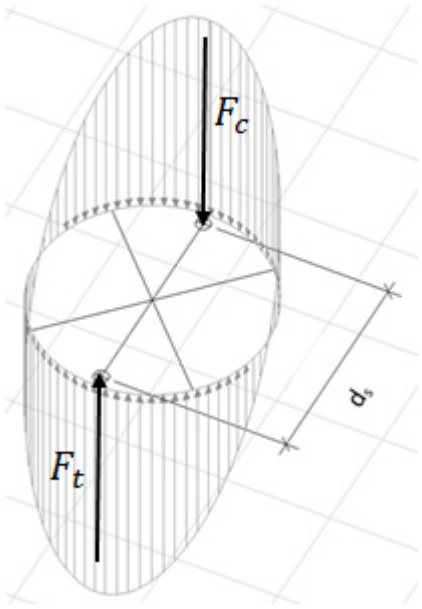

Since the calculation is made in 2D it is important to calculat
where the resultants on
the anchor ring acting. Assume that the stresses is
concentrated in two quarters of the anchor
ring with each resultant in its gravity center.

$r_o := \frac{d_{sr}}{2}$ $r_o = 2\,m$ Outer radius of steel ring

$$d_s := 2\cdot\left(\frac{2}{\pi\cdot r_o}\right)\cdot\int_{-\frac{\pi}{4}}^{\frac{\pi}{4}} r_o\cdot\cos(\varphi)\cdot r_o\,d\varphi$$

Calculation of distance between compressive and tensile forces with gravity center under the assumption of a fourth part of the steel ring being active for the compressive and tensile side

$d_s = 3.601\,m$ $r_s := \frac{d_s}{2}$

The normal force F_z is equally spread on the anchor ring and resulting in:

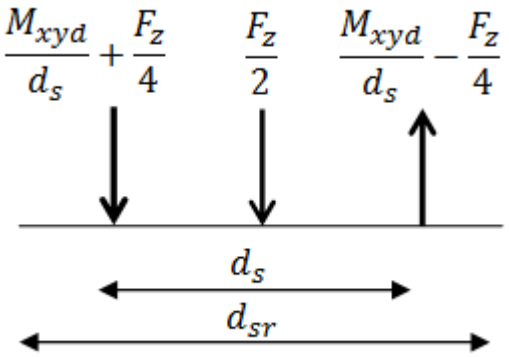

$d_s = 3.601\,m$ Distance between tensile F_t and compressive force F_c

$d_{sr} = 4\,m$ Diameter of anchor ring

Transformation of moment to force couple

$$F_c := \frac{M_{xyd} + F_{xyd} \cdot h_4}{d_s} + \frac{F_{zd}}{4} = 16.799 \cdot MN$$ Compressive force from moment and vertical force

$$F_t := \frac{M_{xyd} + F_{xyd} \cdot h_4}{d_s} - \frac{F_{zd}}{4} = 15.844 \cdot MN$$ Tensile force from moment and vertical force

$$F_c - F_t + g_d \cdot l - f_{soil} \cdot \frac{b}{2} + \frac{F_{zd}}{2} = 0 \cdot MN$$ Check of global equilibrium

$$F_c - F_t + g_d \cdot l - f_{soil.uni} \cdot b_{uni} + \frac{F_{zd}}{2} = 0 \cdot MN$$ Check of global equilibrium

$$F_c - F_t + g_d \cdot l - f_{45.soil.uni} \cdot \frac{b_{45.uni}}{2} + \frac{F_{zd}}{2} = 0 \cdot MN$$ Check of global equilibrium

B.2 Shear force and bending moment distribution

Assume that the bending moment and shear force are equally spread over the full width of the foundation

Shear force and moment distribution for wind direction 90 degree

$x := 0, 0.01m .. 15.5m$

$$V(x) := \begin{cases} f_{soil} \cdot x - \frac{f_{soil}}{b} \cdot \frac{x^2}{2} - g_d \cdot x & \text{if } x < \frac{l - d_s}{2} \\ f_{soil} \cdot x - \frac{f_{soil}}{b} \cdot \frac{x^2}{2} - g_d \cdot x - F_c & \text{if } \frac{l - d_s}{2} \le x < \frac{l}{2} \\ f_{soil} \cdot x - \frac{f_{soil}}{b} \cdot \frac{x^2}{2} - g_d \cdot x - F_c - \frac{F_{zd}}{2} & \text{if } \frac{l}{2} \le x < b \\ f_{soil} \cdot \frac{b}{2} - g_d \cdot x - F_c - \frac{F_{zd}}{2} & \text{if } b \le x < \frac{l + d_s}{2} \\ f_{soil} \cdot \frac{b}{2} - g_d \cdot x - F_c - \frac{F_{zd}}{2} + F_t & \text{if } \frac{l + d_s}{2} \le x < l \end{cases}$$

$$V_{uni}(x) := \begin{cases} f_{soil.uni} \cdot x - g_d \cdot x & \text{if } x < b_{uni} \\ f_{soil.uni} \cdot b_{uni} - g_d \cdot x & \text{if } b_{uni} \le x < \frac{l - d_s}{2} \\ f_{soil.uni} \cdot b_{uni} - g_d \cdot x - F_c & \text{if } \frac{l - d_s}{2} \le x < \frac{l}{2} \\ f_{soil.uni} \cdot b_{uni} - g_d \cdot x - F_c - \frac{F_{zd}}{2} & \text{if } \frac{l}{2} \le x < \frac{l + d_s}{2} \\ f_{soil.uni} \cdot b_{uni} - g_d \cdot x - F_c - \frac{F_{zd}}{2} + F_t & \text{if } \frac{l + d_s}{2} \le x < l \end{cases}$$

$$F_{soil}(x) := f_{soil}\cdot\frac{x^2}{2} - \frac{f_{soil}}{b}\cdot\frac{x^3}{6}$$

$$M(x) := \begin{cases} F_{soil}(x) - g_d\cdot\frac{x^2}{2} & \text{if } x < \frac{l - d_s}{2} \\ F_{soil}(x) - g_d\cdot\frac{x^2}{2} - F_c\left(x - \frac{l - d_s}{2}\right) & \text{if } \frac{l - d_s}{2} \le x < \frac{l}{2} \\ F_{soil}(x) - g_d\cdot\frac{x^2}{2} - F_c\left(x - \frac{l - d_s}{2}\right) - \frac{F_{zd}}{2}\cdot\left(x - \frac{l}{2}\right) & \text{if } \frac{l}{2} \le x < b \\ f_{soil}\cdot\frac{b}{2}\cdot\left(x - \frac{b}{3}\right) - g_d\cdot\frac{x^2}{2} - F_c\left(x - \frac{l - d_s}{2}\right) - \frac{F_{zd}}{2}\cdot\left(x - \frac{l}{2}\right) & \text{if } b \le x < \frac{l + d_s}{2} \\ f_{soil}\cdot\frac{b}{2}\cdot\left(x - \frac{b}{3}\right) - g_d\cdot\frac{x^2}{2} - F_c\cdot\left(x - \frac{l - d_s}{2}\right) \ldots & \text{if } \frac{l + d_s}{2} \le x \le l \\ \quad + -\frac{F_{zd}}{2}\cdot\left(x - \frac{l}{2}\right) + F_t\cdot\left(x - \frac{l + d_s}{2}\right) & \end{cases}$$

$$M_{uni}(x) := \begin{cases} f_{soil.uni}\cdot\frac{x^2}{2} - g_d\cdot\frac{x^2}{2} & \text{if } x < b_{uni} \\ f_{soil.uni}\cdot b_{uni}\cdot\left(x - \frac{b_{uni}}{2}\right) - g_d\cdot\frac{x^2}{2} & \text{if } b_{uni} \le x < \frac{l - d_s}{2} \\ f_{soil.uni}\cdot b_{uni}\cdot\left(x - \frac{b_{uni}}{2}\right) - g_d\cdot\frac{x^2}{2} - F_c\left(x - \frac{l - d_s}{2}\right) & \text{if } \frac{l - d_s}{2} \le x < \frac{l}{2} \\ f_{soil.uni}\cdot b_{uni}\cdot\left(x - \frac{b_{uni}}{2}\right) - g_d\cdot\frac{x^2}{2} - F_c\left(x - \frac{l - d_s}{2}\right) \ldots & \text{if } \frac{l}{2} \le x < \frac{l + d_s}{2} \\ \quad + -\frac{F_{zd}}{2}\cdot\left(x - \frac{l}{2}\right) & \\ f_{soil.uni}\cdot b_{uni}\cdot\left(x - \frac{b_{uni}}{2}\right) - g_d\cdot\frac{x^2}{2} - F_c\cdot\left(x - \frac{l - d_s}{2}\right) \ldots & \text{if } \frac{l + d_s}{2} \le x \le l \\ \quad + -\frac{F_{zd}}{2}\cdot\left(x - \frac{l}{2}\right) + F_t\cdot\left(x - \frac{l + d_s}{2}\right) & \end{cases}$$

Shear force and moment distribution for wind direction of 45 degree

The forces is assumed to be spread along the full width ($l_{eff}(x_{45})$) which vary with x, se figure

$x_{45} := 0, 0.01m .. l_{45}$

$$l_{eff}(x_{45}) := \begin{cases} 2 \cdot x_{45} & \text{if } x_{45} \le \frac{l_{45}}{2} \\ l_{45} - 2\left(x_{45} - \frac{l_{45}}{2}\right) & \text{if } x_{45} > \frac{l_{45}}{2} \end{cases}$$

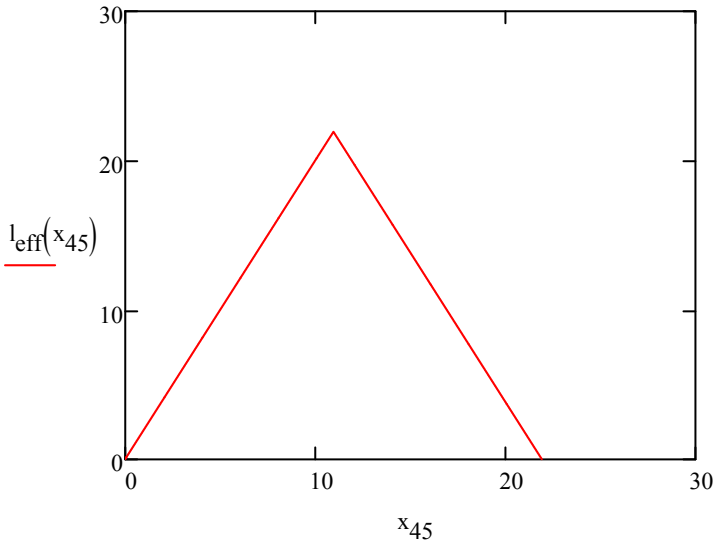

Calculate how the self-weight varies with x $g_{d.45}(x_{45})$

$g_f := \frac{G_d}{l^2}$ Self-weight per square meter

$$g_{d.45}(x_{45}) := \begin{cases} g_f \cdot x_{45}^{\,2} & \text{if } x_{45} < \frac{l_{45}}{2} \\ g_f \cdot \left(\frac{l_{45}}{2}\right)^2 + \frac{\left[l_{45} - 2\left(x_{45} - \frac{l_{45}}{2}\right)\right] + l_{45}}{2} \cdot \left(x_{45} - \frac{l_{45}}{2}\right) \cdot g_f & \text{if } x_{45} \ge \frac{l_{45}}{2} \end{cases}$$

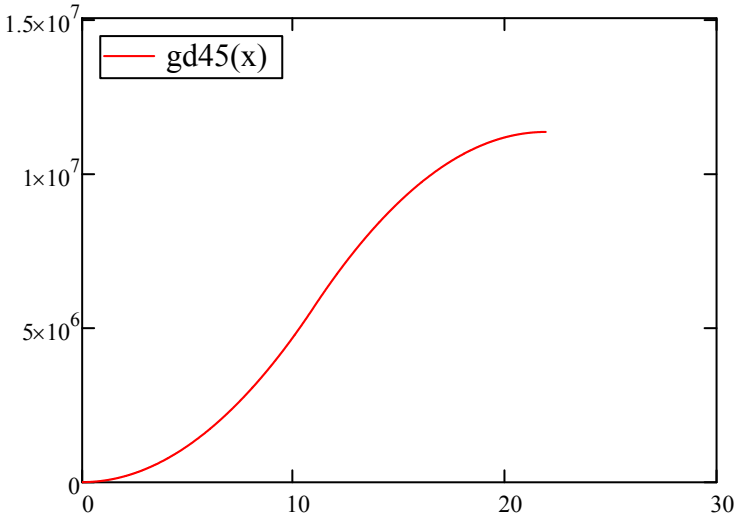

$$V_{45.uni}(x_{45}) := \begin{cases} \frac{f_{45.soil.uni}}{b_{45.uni}} \cdot \frac{x_{45}^{2}}{2} - g_{d.45}(x_{45}) & \text{if } x_{45} < b_{45.uni} \\ f_{45.soil.uni} \cdot \frac{b_{45.uni}}{2} - g_{d.45}(x_{45}) & \text{if } b_{45.uni} \le x_{45} < \frac{l_{45} - d_s}{2} \\ f_{45.soil.uni} \cdot \frac{b_{45.uni}}{2} - g_{d.45}(x_{45}) - F_c & \text{if } \frac{l_{45} - d_s}{2} \le x_{45} < \frac{l_{45}}{2} \\ f_{45.soil.uni} \cdot \frac{b_{45.uni}}{2} - g_{d.45}(x_{45}) - F_c - \frac{F_{zd}}{2} & \text{if } \frac{l_{45}}{2} \le x_{45} < \frac{l_{45} + d_s}{2} \\ f_{45.soil.uni} \cdot \frac{b_{45.uni}}{2} - g_{d.45}(x_{45}) - F_c - \frac{F_{zd}}{2} + F_t & \text{if } \frac{l_{45} + d_s}{2} \le x_{45} < l_{45} \end{cases}$$

Calculate gravity center of gravity $tp_x(x_{45})$ and the actual moment of self-weight $G_{d.45}(x_{45})$

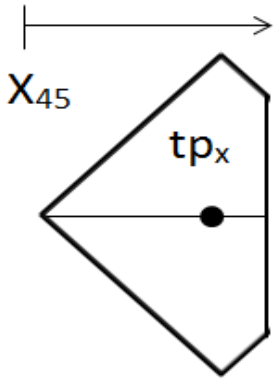

$$tp_x(x_{45}) := \frac{\left[l_{45} - 2\left(x_{45} - \frac{l_{45}}{2}\right)\right]\cdot\left(x_{45} - \frac{l_{45}}{2}\right)\cdot\frac{\left(x_{45} - \frac{l_{45}}{2}\right)}{2} + \left(x_{45} - \frac{l_{45}}{2}\right)^2\cdot\frac{\left(x_{45} - \frac{l_{45}}{2}\right)}{3}}{\left[l_{45} - 2\left(x_{45} - \frac{l_{45}}{2}\right)\right]\cdot\left(x_{45} - \frac{l_{45}}{2}\right) + \left(x_{45} - \frac{l_{45}}{2}\right)^2}$$

$$G_{d.45}(x_{45}) := \begin{cases} g_{d.45}(x_{45})\cdot\frac{x_{45}}{3} & \text{if } x_{45} < \frac{l_{45}}{2} \\ g_{d.45}\left(\frac{l_{45}}{2}\right)\cdot\left(x_{45} - \frac{2l_{45}}{2\cdot 3}\right) \ldots & \text{if } x_{45} \geq \\ + \frac{\left[l_{45} - 2\left(x_{45} - \frac{l_{45}}{2}\right)\right] + l_{45}}{2}\cdot\left(x_{45} - \frac{l_{45}}{2}\right)\cdot g_f\cdot\left(x_{45} - \frac{l_{45}}{2} - tp_x(x_{45})\right) & \end{cases}$$

$$M_{45.uni}(x_{45}) := \begin{cases} \frac{f_{45.soil.uni}}{b_{45.uni}}\cdot\frac{x_{45}^3}{6} - G_{d.45}(x_{45}) & \text{if } x_{45} < b_{45.uni} \\ f_{45.soil.uni}\cdot\frac{b_{45.uni}}{2}\cdot\left(x_{45} - \frac{2b_{45.uni}}{3}\right) - G_{d.45}(x_{45}) & \text{if } b_{45.uni} \leq x_{45} < \frac{l_{45} - d_s}{2} \\ f_{45.soil.uni}\cdot\frac{b_{45.uni}}{2}\cdot\left(x_{45} - \frac{2b_{45.uni}}{3}\right) \ldots & \text{if } \frac{l_{45} - d_s}{2} \leq x_{45} < \frac{l_{45}}{2} \\ + -G_{d.45}(x_{45}) - F_c\left(x_{45} - \frac{l_{45} - d_s}{2}\right) & \\ f_{45.soil.uni}\cdot\frac{b_{45.uni}}{2}\cdot\left(x_{45} - \frac{2b_{45.uni}}{3}\right) - G_{d.45}(x_{45}) \ldots & \text{if } \frac{l_{45}}{2} \leq x_{45} < \frac{l_{45} + d_s}{2} \\ + -F_c\left(x_{45} - \frac{l_{45} - d_s}{2}\right) - \frac{F_{zd}}{2}\cdot\left(x_{45} - \frac{l_{45}}{2}\right) & \\ f_{45.soil.uni}\cdot\frac{b_{45.uni}}{2}\cdot\left(x_{45} - \frac{2b_{45.uni}}{3}\right) \ldots & \text{if } \frac{l_{45} + d_s}{2} \leq x_{45} \leq l_{45} \\ + -G_{d.45}(x_{45}) - F_c\cdot\left(x_{45} - \frac{l_{45} - d_s}{2}\right) \ldots & \\ + -\frac{F_{zd}}{2}\cdot\left(x_{45} - \frac{l_{45}}{2}\right) + F_t\cdot\left(x_{45} - \frac{l_{45} + d_s}{2}\right) & \end{cases}$$

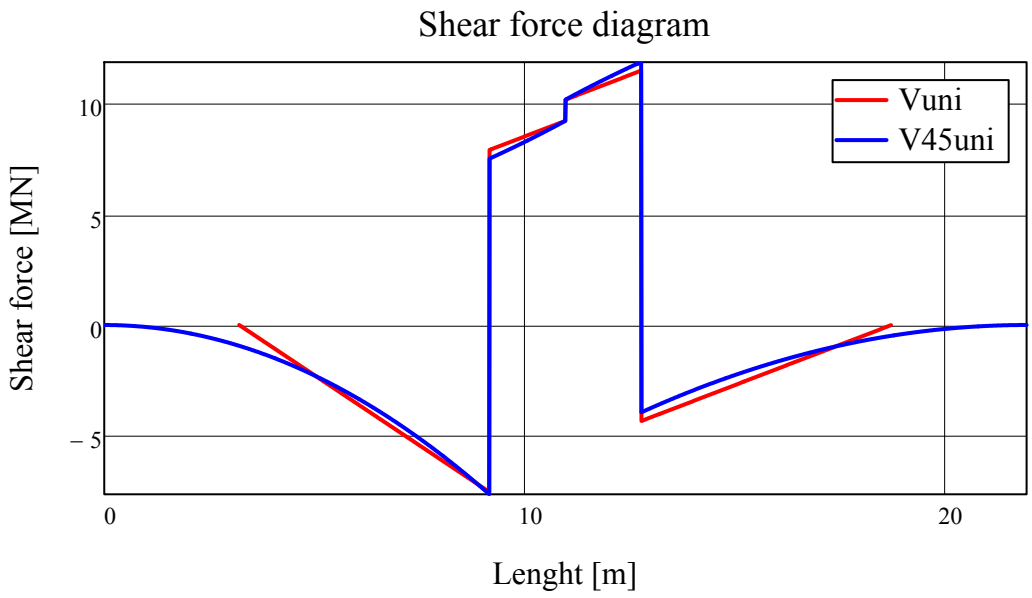

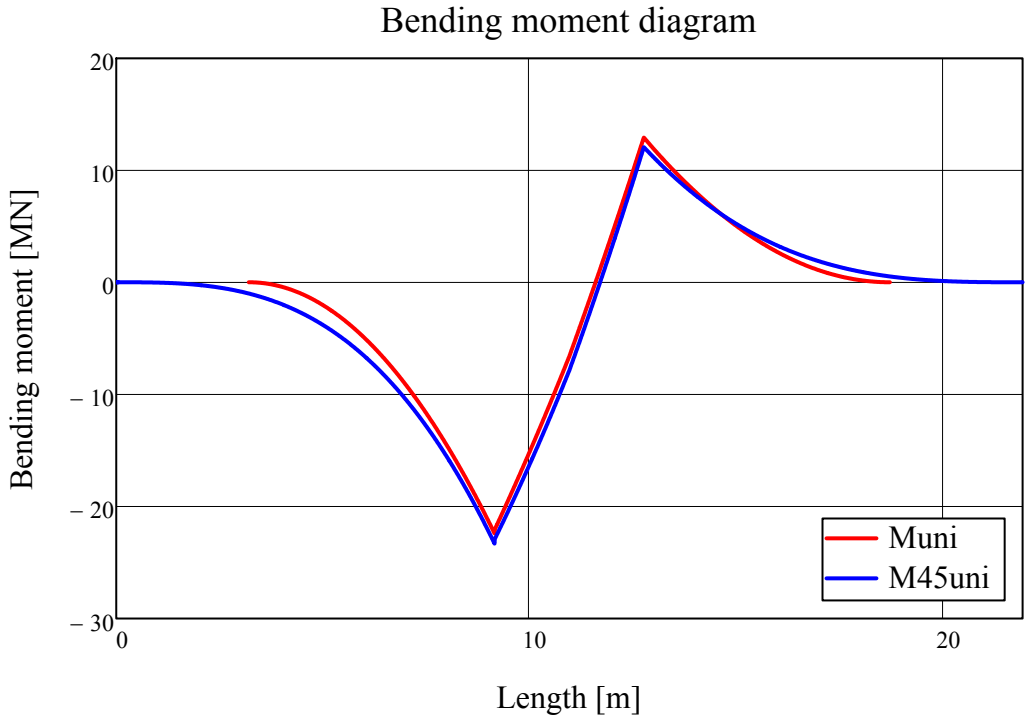

Conclusion: The moment distribution is similar independent of loading situation. Its important to extend the reinforcement in order to achieve required capacity in the corners. Since the reinforcement is crossed the capacity is satisfied also in the diagonal direction. The design will be based on the loading with uniformed soil pressure and wind direction perpendicular to the foundation. Its a common assumption to assume uniformed soil pressure in ULS calculation. The triangular soil pressure gives however slightly higher positive moment.

B.3 Sign convention

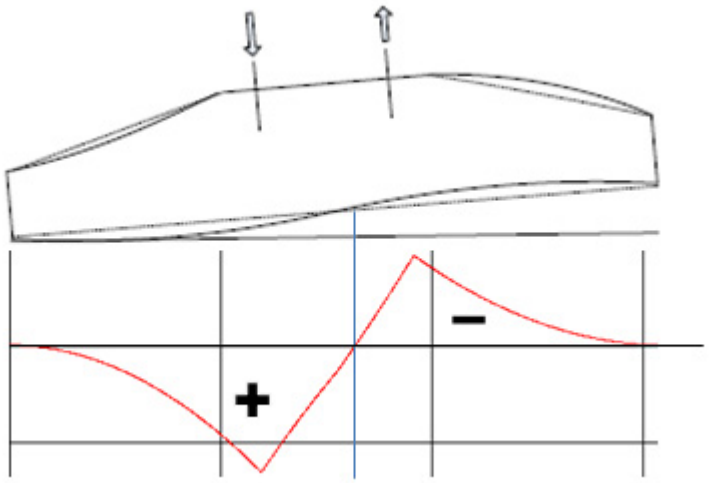

The figure above shows the sign convention. Moments resulting in tensile stresses at the bottom of the foundation is defined as positive. Observe that the diagrams shows negative downwards.

C Design in ultimate limit state

C.1 Sections

Check in four different section, se figure. bottom **U** and top **O** reinforcement. l_x starts from the embedded steel ring edges.

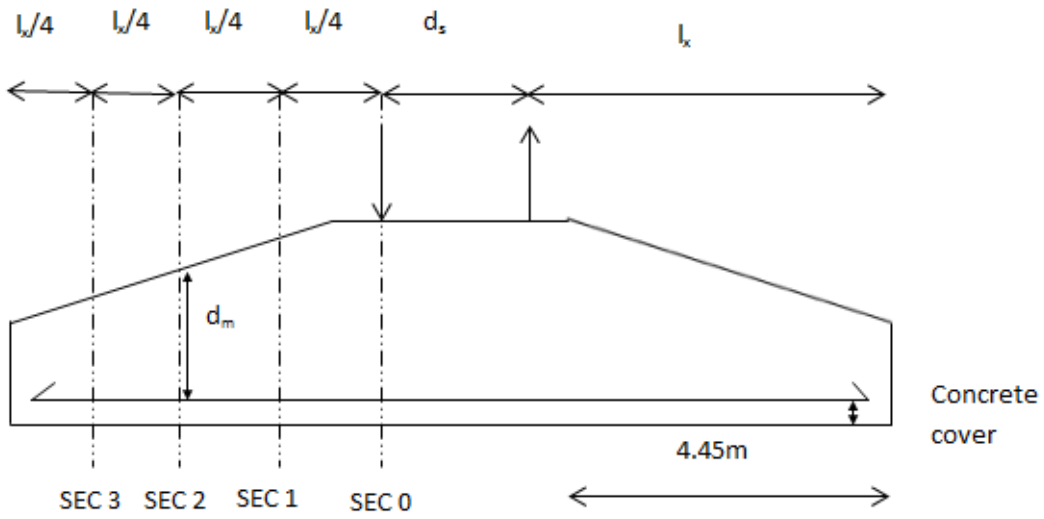

The internal forces is checked in four different sections, section 0-3.

$$l_x := \frac{l}{2} - \frac{d_s}{2} = 5.949\,\text{m}$$

M_{Edu} and M_{Edo} are the positive and negative moments in the four different section.

$$l_{section1} := \left(l_x \quad \frac{3l_x}{4} \quad \frac{2l_x}{4} \quad \frac{l_x}{4} \right) \quad l_{section2} := \left(l_x + d_s \quad l_x + d_s + \frac{l_x}{4} \quad l_x + d_s + \frac{2l_x}{4} \quad l_x + d_s + \frac{3.l_x}{4} \right.$$

$$l_{section1} := l_{section1}^{T} \quad l_{section2} := l_{section2}^{T}$$

$$h_{m_section} := \left(h_m(l_x) \quad h_m\left(\frac{3}{4}l_x\right) \quad h_m\left(\frac{2}{4}l_x\right) \quad h_m\left(\frac{l_x}{4}\right) \right)$$

$$h_{m_section} := h_{m_section}^{T}$$

Mean height of section

$x := 0, 0.01m .. 15.5m \qquad size_x := \frac{15.5}{0.01} + 1 = 1.551 \times 10^3$

$h_{m_mean} := \frac{\sum h_{m_section}}{length(h_{m_section})} = 1.613\ m$ Mean height of the four sections

$\frac{\sum h_m(x)}{size_x} = 1.625\ m$ Total mean height

Choose bar diameter

$\phi_o := 25mm \qquad \phi_u := 25mm$ Top and bottom reinforcement

$c_{soil} = 100 \cdot mm$ Concrete cover to soil

$c = 50 \cdot mm$ Concrete cover to template

$A_{sio} := \frac{\pi \cdot \phi_o^2}{4} = 490.874 \cdot mm^2$ Reinforcement area for one bar top

$A_{siu} := \frac{\pi \cdot \phi_u^2}{4} = 490.874 \cdot mm^2$ Reinforcement area for one bar bottom

Calculate mean distance to reinforcement for top and bottom reinforcement d_{mu} and

.

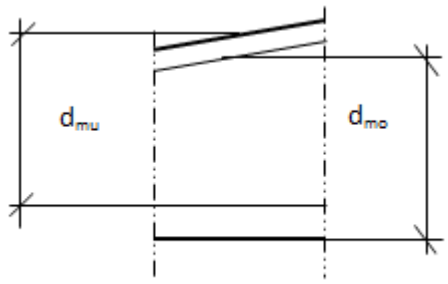

Definition of d in the four different sections . d_{mu} *is the mean distance from the top edge to the first layer bottom reinforcement.* d_{mo} *is the mean distance from the bottom edge to the first layer of top reinforcement.*

$i := 0 .. 3$

$d_{mu_i} := h_m(l_{section1_i}) - c_{soil} - \phi_u - \frac{\phi_u}{2} \qquad d_{mo_i} := h_m(l_{section1_i}) - c - \phi_o - \frac{\phi_o}{2}$

$d_{mu} = \begin{pmatrix} 1.505 \\ 1.505 \\ 1.471 \\ 1.423 \end{pmatrix} m \qquad d_{mo} = \begin{pmatrix} 1.555 \\ 1.555 \\ 1.521 \\ 1.473 \end{pmatrix} m$

Assume a ideal plastic behavior of reinforcement, i.e. no tension stiffening and no strain limit

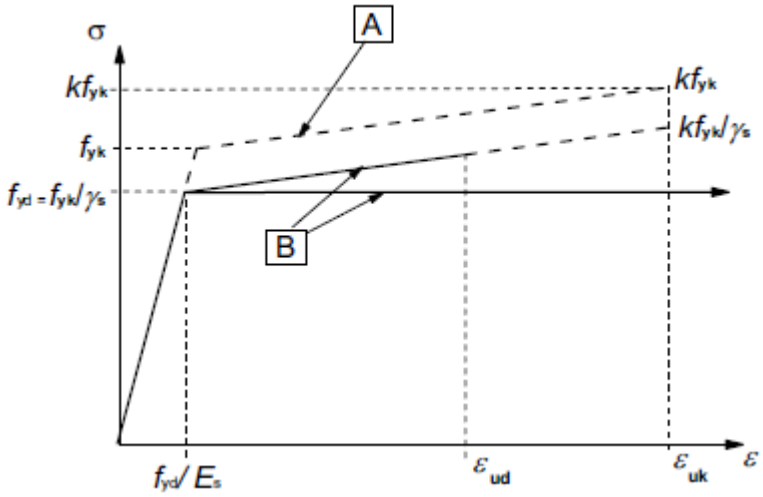

Shows different material models for reinforcement bars. Assume horizontal top branch without strain hardening and strain limit. Curve (B)

C.2 Design of bending reinforcement

$$M_{Edu_i} := \frac{M_{uni}\left(l_{section1_i}\right)}{l} \qquad M_{Edo_i} := \frac{M_{uni}\left(l_{section2_i}\right)}{l}$$

$$M_{Edu} = \begin{pmatrix} 1.422 \\ 0.816 \\ 0.363 \\ 0.091 \end{pmatrix} \cdot \frac{MN \cdot m}{m} \qquad M_{Edo} = \begin{pmatrix} -0.834 \\ -0.469 \\ -0.208 \\ -0.052 \end{pmatrix} \cdot \frac{MN \cdot m}{m}$$

Preliminary Reinforcement area and bars per meter in the different sections

$$A_{so} := \frac{M_{Edo} \cdot -1}{f_{yd} \cdot 0.9 \cdot d_{mo}} = \begin{pmatrix} 1.142 \times 10^{-3} \\ 6.422 \times 10^{-4} \\ 2.919 \times 10^{-4} \\ 7.533 \times 10^{-5} \end{pmatrix} \cdot \frac{m^2}{m} \qquad A_{su} := \frac{M_{Edu}}{f_{yd} \cdot 0.9 d_{mu}} = \begin{pmatrix} 2.012 \times 10^{-3} \\ 1.154 \times 10^{-3} \\ 5.251 \times 10^{-4} \\ 1.357 \times 10^{-4} \end{pmatrix} \cdot \frac{m^2}{m}$$

$$n_o := \frac{A_{so}}{A_{sio}} = \begin{pmatrix} 2.326 \\ 1.308 \\ 0.595 \\ 0.153 \end{pmatrix} \frac{1}{m} \qquad n_u := \frac{A_{su}}{A_{siu}} = \begin{pmatrix} 4.099 \\ 2.352 \\ 1.07 \\ 0.276 \end{pmatrix} \frac{1}{m}$$

Minimum spacing

$$a_o := \frac{1}{n_o} = \begin{pmatrix} 429.955 \\ 764.365 \\ 1.682 \times 10^3 \\ 6.516 \times 10^3 \end{pmatrix} \cdot mm \quad a_u := \frac{1}{n_u} = \begin{pmatrix} 243.966 \\ 425.247 \\ 934.844 \\ 3.618 \times 10^3 \end{pmatrix} \cdot mm$$

$a_{oreq} := \min\left(\frac{1}{n_o}\right) = 429.955 \cdot mm$ $a_{ureq} := \min\left(\frac{1}{n_u}\right) = 243.966 \cdot mm$ Required spacing with regard to bending

Choose spacing:

$a_o := 150mm$ $a_u := 110mm$ OBS This spacing is chosen with regard to crack width limitation se *D. Crack widths SLS*

Bottom reinforcement

Calculate ultimate capacity for positive moment, i.e. **bottom** reinforcement is in tension

$i := 0 .. 3$

$$d := d_{mu} = \begin{pmatrix} 1.505 \\ 1.505 \\ 1.471 \\ 1.423 \end{pmatrix} m \qquad d'_i := c_{soil} + \frac{\phi_o}{2} + \phi_o$$

Top (A'_s) and bottom (A_s) reinforcement amount

$$A_s := \frac{1}{\frac{a_u}{m}} \cdot A_{siu} = 4.462 \times 10^{-3} \cdot m^2 \quad A'_s := \frac{1}{\frac{a_o}{m}} \cdot A_{sio} = 3.272 \times 10^{-3} \cdot m^2$$

$b_1 := 1m$ Width of the section

$i := 0 .. 3$ $\alpha_r := 0.81$ $\varepsilon_{cu} = 3.5 \times 10^{-3}$

$x_{sx} := 0.001m$

$$x_{s_i} := root\left[\alpha_r \cdot f_{cd} \cdot b_1 \cdot x_{sx} + \left(\frac{x_{sx} - d'_i}{x_{sx}} \cdot \varepsilon_{cu}\right) \cdot E_s \cdot A'_s - f_{yd} \cdot A_s, x_{sx}\right]$$

$$x_s = \begin{pmatrix} 114.625 \\ 114.625 \\ 114.625 \\ 114.625 \end{pmatrix} \cdot mm$$ Size of the compressed zone of the different sections

$$\varepsilon_{s_i} := \frac{d_i - x_{s_i}}{x_{s_i}} \cdot \varepsilon_{cu} \qquad \varepsilon_s = \begin{pmatrix} 0.042 \\ 0.042 \\ 0.041 \\ 0.04 \end{pmatrix}$$ Check that compression failure in concrete have not occurred

$$\varepsilon_{sy} := \frac{f_{yd}}{E_s} = 2.609 \times 10^{-3} \qquad \varepsilon_s \geq \varepsilon_{sy} = \begin{pmatrix} 1 \\ 1 \\ 1 \\ 1 \end{pmatrix}$$

$$\varepsilon'_{s_i} := \left| \frac{x_{s_i} - d'_i}{x_{s_i}} \right| \cdot \varepsilon_{cu} \qquad \varepsilon'_s = \begin{pmatrix} 6.985 \times 10^{-4} \\ 6.985 \times 10^{-4} \\ 6.985 \times 10^{-4} \\ 6.985 \times 10^{-4} \end{pmatrix} \qquad \varepsilon'_s < \varepsilon_{sy} = \begin{pmatrix} 1 \\ 1 \\ 1 \\ 1 \end{pmatrix}$$

$\beta_r := 0.416$

$i := 0 .. 3$

$$M_{Rd_pos_i} := \alpha_r \cdot f_{cd} \cdot b_1 \cdot x_{s_i} \cdot \left(d_i - \beta_r \cdot x_{s_i} \right) + E_s \cdot \varepsilon'_{s_i} \cdot A'_s \cdot \left(d_i - d'_i \right)$$

$$M_{Rd_pos} = \begin{pmatrix} 4.685 \\ 4.685 \\ 4.573 \\ 4.418 \end{pmatrix} \cdot MN \cdot m \qquad M_{Edu} \cdot m = \begin{pmatrix} 1.422 \\ 0.816 \\ 0.363 \\ 0.091 \end{pmatrix} \cdot MN \cdot m$$

$$UR_{b.u} := \frac{M_{Edu} \cdot m}{M_{Rd_pos}} = \begin{pmatrix} 30.355 \\ 17.415 \\ 7.929 \\ 2.052 \end{pmatrix} \cdot \%$$

Degree of utilization of bottom reinforcement

Top reinforcement

Calculate ultimate capacity for negative moment, i.e. **top** reinforcement is in tension

$$d := d_{mo} = \begin{pmatrix} 1.555 \\ 1.555 \\ 1.521 \\ 1.473 \end{pmatrix} m \qquad d'_i := c_{soil} + \frac{\phi_u}{2} + \phi_u$$

$$A_s := \frac{1}{\frac{a_o}{m}} \cdot A_{sio} = 3.272 \times 10^{-3} \cdot m^2 \qquad A'_s := \frac{1}{\frac{a_u}{m}} \cdot A_{siu} = 4.462 \times 10^{-3} \cdot m^2$$

$b_1 = 1\,m$

$x_{sx} := 0.51m$

$i := 0 .. 3 \qquad \alpha_r = 0.81$

$$x_{s_i} := \text{root}\left[\alpha_r \cdot f_{cd} \cdot b_1 \cdot x_{sx} + \left(\frac{x_{sx} - d'_i}{x_{sx}} \cdot \varepsilon_{cu} \right) \cdot E_s \cdot A'_s - f_{yd} \cdot A_s, x_{sx} \right]$$

$$x_s = \begin{pmatrix} 0.107 \\ 0.107 \\ 0.107 \\ 0.107 \end{pmatrix} m$$ Size of the compressed zone of the different sections

$$\varepsilon_{s_i} := \frac{d_i - x_{s_i}}{x_{s_i}} \cdot \varepsilon_{cu} \qquad \varepsilon_s = \begin{pmatrix} 0.047 \\ 0.047 \\ 0.046 \\ 0.045 \end{pmatrix} \qquad \varepsilon_{sy} = 2.609 \times 10^{-3} \qquad \varepsilon_s \geq \varepsilon_{sy} = \begin{pmatrix} 1 \\ 1 \\ 1 \\ 1 \end{pmatrix}$$

$$\varepsilon'_{s_i} := \frac{x_{s_i} - d'_i}{x_{s_i}} \cdot \varepsilon_{cu} \qquad \varepsilon'_s = \begin{pmatrix} 6.985 \times 10^{-4} \\ 6.985 \times 10^{-4} \\ 6.985 \times 10^{-4} \\ 6.985 \times 10^{-4} \end{pmatrix} \qquad \varepsilon'_s < \varepsilon_{sy} = \begin{pmatrix} 1 \\ 1 \\ 1 \\ 1 \end{pmatrix}$$

$\beta_r = 0.416$

$$M_{Rd_neg_i} := \alpha_r \cdot f_{cd} \cdot b_1 \cdot x_{s_i} \cdot \left(d_i - \beta_r \cdot x_{s_i}\right) + E_s \cdot \varepsilon'_{s_i} \cdot A'_s \cdot \left(d_i - d'_i\right)$$

$i := 0 .. 3$

$$M_{Rd_neg} = \begin{pmatrix} 2.662 \\ 2.662 \\ 2.603 \\ 2.522 \end{pmatrix} \cdot MN \cdot m \qquad M_{Edo} \cdot m = \begin{pmatrix} -0.834 \\ -0.469 \\ -0.208 \\ -0.052 \end{pmatrix} \cdot MN \cdot m$$

$$UR_{b.o} := \frac{M_{Edo} \cdot m}{-M_{Rd_neg}} = \begin{pmatrix} 31.316 \\ 17.615 \\ 8.006 \\ 2.066 \end{pmatrix} \cdot \%$$ Degree of Utilisation of top reinforcement

C.3 Star reinforcement inside embedded steel ring

$$M_{Rd_neg} = \begin{pmatrix} 2.662 \times 10^3 \\ 2.662 \times 10^3 \\ 2.603 \times 10^3 \\ 2.522 \times 10^3 \end{pmatrix} \cdot kN \cdot m \qquad M_{Edo} = \begin{pmatrix} -833.672 \\ -468.941 \\ -208.418 \\ -52.105 \end{pmatrix} \cdot \frac{kN \cdot m}{m}$$

$d_{sr} = 4\,m$ Diameter of steel ring

$a := a_o = 150 \cdot mm$ Same spacing as top reinforcement

$\phi_o = 25 \cdot mm$ Bar diameter of top reinforcement

$$A_{s_req} := A_{sio} \cdot \frac{d_{sr}}{a} \cdot \frac{\left|M_{Edo_0}\right|}{M_{Rd_neg_0}} = 4.099 \times 10^3 \frac{1}{m} \cdot mm^2$$

$n := 56$ There is 56 holes in the anchor ring, one bar in each hole

$\phi_{star} := 25mm$ Bar diameter of star reinforcement

$$\varphi := \frac{360deg}{n} = 6.429 \cdot deg$$

Bars inside a 90 deg angle

$$n_{90} := \frac{90deg}{\varphi} = 14 \qquad n_i := \frac{-n_{90}}{2} .. \left(\frac{n_{90}}{2} - 1\right)$$

The reinforcement is placed in different direction towards the center of the anchor ring. Calculate equivalent area

$$A_{siring} := \frac{\phi_{star}^{\ 2} \cdot \pi}{4}$$

$$A_{s_eqv} := A_{siring} \cdot \sum_{n_i} \cos\left(\varphi \cdot n_i\right) = 6.181 \times 10^3 \cdot mm^2$$

$$UR_{b.star} := \frac{A_{s_req}}{A_{s_eqv}} = 66.324 \frac{1}{m} \cdot \%$$ Utilisation degree of star reinforcement

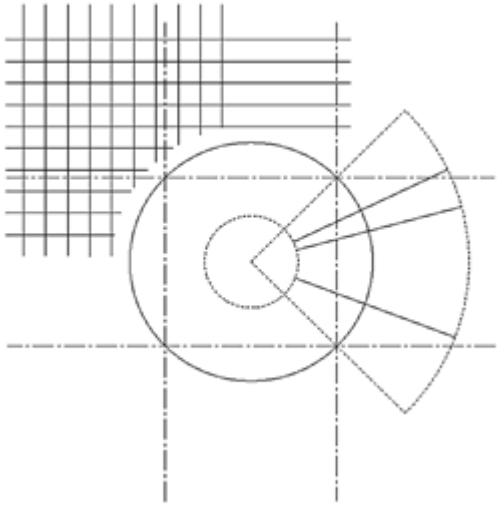

Layout of star reinforcement

C.4 Min and max reinforcement amounts

[EN 1992-1-1:2005 9.2.1.1]

Minimum reinforcement

Control of top reinforcement (lesser than bottom reinforcement)

$b_1 = 1\,m$ b_1 used for calculations per meter width

$$d_m := \frac{\sum d_{mo}}{\text{length}(d_{mo})} = 1.526\,m$$ Mean value of d of the four different sections

$$d_t := d_m$$

$$A_{smin} := \max\left(0.26\cdot\frac{f_{ctm}}{f_{yk}}\cdot b_1\cdot d, 0.0012 d_t\cdot d\right) = 2.847\times 10^{-3}\,m^2$$

$$a_{mino} := \frac{1m}{\frac{A_{smin}}{A_{siu}}} = 172.388\cdot mm$$

Maximum reinforcement

Control of bottom reinforcement (greater than top reinforcement)

$A_{cm} := h_{m_mean}\cdot b_1$ Average area of concrete cross section.

$$A_{smax} := 0.04\cdot A_{cm} = 0.065\,m^2$$

$$A_s := \frac{b_1}{a_u}\cdot A_{siu} = 4.462\times 10^{-3}\cdot m^2$$ Area of bottom reinforcement

$$A'_s := \frac{b_1}{a_o}\cdot A_{sio} = 3.272\times 10^{-3}\cdot m^2$$ Area of top reinforcement

$A'_s > A_{smin} = 1$ OK!

$A_s < A_{smax} = 1$ OK!

The chosen reinforcement amounts are within the limits

C.5 Shear capacity

Unreinforced capacity

Check if shear reinforcement is needed [EN 1992-1-1:2005 6.2.2]

Check the maximum shear force in the four different sections

$$V_{Ed} := \frac{1}{l}\cdot\begin{pmatrix} \max\left(\left|V_{uni}\left(l_x\right)\right|, \left|V_{uni}\left(l_x + d_s\right)\right|\right) \\ \max\left(\left|V_{uni}\left(\frac{3l_x}{4}\right)\right|, \left|V_{uni}\left(l_x + d_s + \frac{l_x}{4}\right)\right|\right) \\ \max\left(\left|V_{uni}\left(\frac{2l_x}{4}\right)\right|, \left|V_{uni}\left(l_x + d_s + \frac{2l_x}{4}\right)\right|\right) \\ \max\left(\left|V_{uni}\left(\frac{l_x}{4}\right)\right|, \left|V_{uni}\left(l_x + d_s + \frac{3.l_x}{4}\right)\right|\right) \end{pmatrix} = \begin{pmatrix} 510.742 \\ 365.664 \\ 243.776 \\ 121.888 \end{pmatrix}\cdot\frac{kN}{m}$$

$$V_{Rd.c} := \max\left[C_{Rd.c}\cdot k\cdot\left(100\cdot\rho_l\cdot f_{ck}\right)^{\frac{1}{3}} + k_1\cdot\sigma_{cp}\cdot b_w\cdot d, \left(V_{min} + k_1\cdot\sigma_{cp}\right)\cdot b_w\cdot d\right]$$

$$k_i := \min\left(1 + \sqrt{\frac{200}{\frac{d_{mu_i}}{mm}}}, 2.0\right) \qquad k = \begin{pmatrix} 1.365 \\ 1.365 \\ 1.369 \\ 1.375 \end{pmatrix}$$

$b_1 = 1\,m$

$k_1 := 0.15$

Area of tensioned reinforcement that reach at least (l_{bd} + d) away from current section

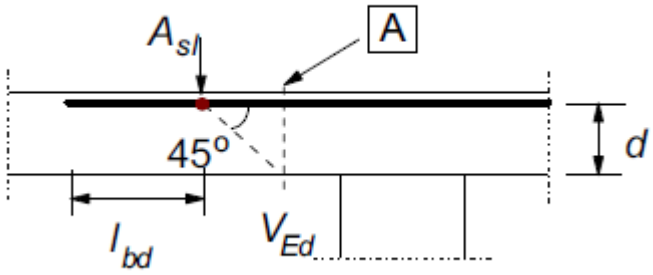

Definition of tensioned reinforcement that reach at least (l_{bd} + d*) away from current section, in this case* A_{sl} *is equal to the bottom reinforcement*

$$A_s := \frac{b_1}{a_u}\cdot A_{siu} = 4.462\times 10^{-3}\cdot m^2$$

$$A_{sl} := A_s = 4.462\times 10^{-3}\,m^2$$

$$\rho_{l_i} := \min\left(\frac{A_{sl}}{b_1\cdot d_{mu_i}}, 0.02\right) \qquad \rho_l = \begin{pmatrix} 2.965\times 10^{-3} \\ 2.965\times 10^{-3} \\ 3.035\times 10^{-3} \\ 3.136\times 10^{-3} \end{pmatrix}$$

$N_{Ed} := 0$ Normal force

$A_{c_i} := h_{m_section_i} \cdot b_1$ Concrete area

$\sigma_{cp_i} := \min\left(\frac{N_{Ed}}{A_{c_i}}, 0.2 \cdot f_{cd}\right) = ... \cdot MPa$

$C_{Rd.c} := \frac{0.18}{\gamma_{mc}} = 0.12$

$V_{min} := 0.035 \cdot k^{\frac{3}{2}} \cdot \left(\frac{f_{ck}}{MPa}\right)^{\frac{1}{2}} = \begin{pmatrix} 0.374 \\ 0.374 \\ 0.376 \\ 0.379 \end{pmatrix}$

$V_{Rd.c_i} := \max\left[C_{Rd.c} \cdot k_i \cdot \left(100 \cdot \rho_{l_i} \cdot \frac{f_{ck}}{MPa}\right)^{\frac{1}{3}} + k_1 \cdot \frac{\sigma_{cp}}{MPa} \cdot \frac{b_1}{mm} \cdot \frac{d_{mu_i}}{mm}, \left(V_{min_i} + k_1 \cdot \frac{\sigma_{cp}}{MPa}\right) \cdot \frac{b_1}{mm} \cdot \frac{d_{mu_i}}{mm}\right]$

$V_{Rd.c} := V_{Rd.c} \cdot \frac{N}{m} = \begin{pmatrix} 563.261 \\ 563.261 \\ 552.91 \\ 538.602 \end{pmatrix} \cdot \frac{kN}{m}$ $\qquad V_{Ed} = \begin{pmatrix} 510.742 \\ 365.664 \\ 243.776 \\ 121.888 \end{pmatrix} \cdot \frac{kN}{m}$

$V_{Rd.c} > V_{Ed} = \begin{pmatrix} 1 \\ 1 \\ 1 \\ 1 \end{pmatrix}$ Shear reinforcement only needed around anchor ring (U-bows) for but due to assembling, minimum reinforcement is used.

$UR_{shear.VRdc} := \frac{V_{Ed} \cdot m}{V_{Rd.c}} = \begin{pmatrix} 90.676 \\ 64.919 \\ 44.09 \\ 22.63 \end{pmatrix} m \cdot \%$

Control of concrete crushing

[EN 1992-1-1:2005 6.2.2]

$\nu := 0.6 \cdot \left(1 - \frac{f_{ck}}{250MPa}\right) = 0.492$ $\qquad V_{Ed} \cdot b_1 < 0.5 \cdot b_1 \cdot d_{mu} \cdot \nu \cdot f_{cd} = \begin{pmatrix} 1 \\ 1 \\ 1 \\ 1 \end{pmatrix}$

Shear reinforcement

Design of shear reinforcement [EN 1992-1-1:2005 6.2.3]

$V_{Rd.s} := \frac{A_{sw}}{s} \cdot z \cdot f_{ywd} \cdot \cot(\theta)$

$V_{Rd.max} := \frac{\alpha_{cw} \cdot b_w \cdot z \cdot \nu_1 \cdot f_{cd}}{\cot(\theta) + \tan(\theta)}$

$1 < \cot(\theta) < 2.5$

$\theta := 45deg$ Choose angle

$\nu := 0.6 \cdot \left(1 - \frac{f_{ck}}{250MPa}\right) = 0.492$ Reduction due to shear cracks

$\alpha_{cw} := 1$ No prestressing -> α_{cw}=1

$f_{ywd} := f_{yd}$

$\phi_w := 25mm$ Size of shear reinforcement bar

$A_{swi} := \frac{\phi_w^{\,2} \cdot \pi}{4}$ Area of one shear reinforcement bar

$z := 0.9 \cdot d_{mu}$

$$V_{Ed} \cdot b_1 = \begin{pmatrix} 510.742 \\ 365.664 \\ 243.776 \\ 121.888 \end{pmatrix} \cdot kN$$

$s_x := 0.5m$ Guessed reinforcement spacing

$s_i := root\left(\frac{A_{swi}}{s_x} \cdot z_i \cdot f_{ywd} \cdot \cot(\theta) - V_{Ed_i} \cdot b_1, s_x\right)$ Calculate the required spacing

$$s_{shear_req} := s = \begin{pmatrix} 0.679 \\ 0.949 \\ 1.39 \\ 2.691 \end{pmatrix} m$$ Required spacing with regard to shear forces

$$s := \begin{pmatrix} 0.5 \\ 0.5 \\ 0.5 \\ 0.5 \end{pmatrix} m$$ Minimum spacing of shear reinforcement according to turbine manufacturer.

$V_{Rd.s_i} := \frac{A_{swi}}{s_i} \cdot z_i \cdot f_{ywd} \cdot \cot(\theta)$

$$V_{Ed} \cdot m \le V_{Rd.s} = \begin{pmatrix} 1 \\ 1 \\ 1 \\ 1 \end{pmatrix} \quad V_{Rd.s} = \begin{pmatrix} 693.834 \\ 693.834 \\ 677.909 \\ 655.964 \end{pmatrix} \cdot kN \quad V_{Ed} \cdot b_1 = \begin{pmatrix} 510.742 \\ 365.664 \\ 243.776 \\ 121.888 \end{pmatrix} \cdot kN$$

$\nu_1 := \nu$

$$V_{Rd.max} := \frac{\alpha_{cw} \cdot b_1 \cdot z \cdot \nu_1 \cdot f_{cd}}{\cot(\theta) + \tan(\theta)} = \begin{pmatrix} 9.997 \times 10^3 \\ 9.997 \times 10^3 \\ 9.767 \times 10^3 \\ 9.451 \times 10^3 \end{pmatrix} \cdot kN \quad V_{Rd.max} > V_{Rd.s} = \begin{pmatrix} 1 \\ 1 \\ 1 \\ 1 \end{pmatrix}$$

$$V_{Rd_i} := \min\left(V_{Rd.max_i}, V_{Rd.s_i}\right) \qquad V_{Rd} = \begin{pmatrix} 6.938 \times 10^5 \\ 6.938 \times 10^5 \\ 6.779 \times 10^5 \\ 6.56 \times 10^5 \end{pmatrix} \text{N}$$

$$UR_{shear} := \frac{V_{Ed} \cdot m}{V_{Rd}} = \begin{pmatrix} 73.612 \\ 52.702 \\ 35.96 \\ 18.582 \end{pmatrix} \cdot \%$$

Utilisation ratio of shear in the different sections.

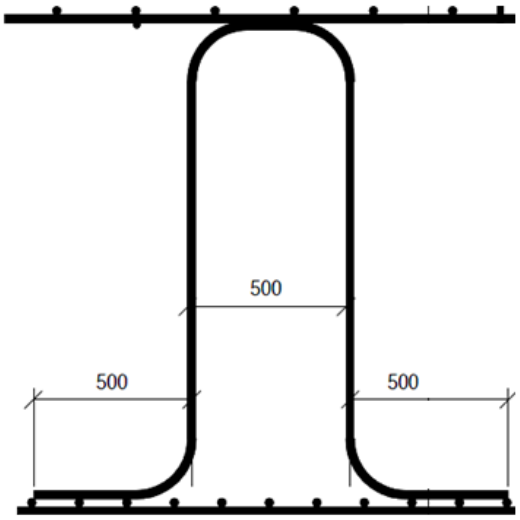

Shear reinforcement spacing 500mm diameter 25mm

C.6 Local effects and shear reinforcement around steel ring

[EN 1992-1-1:2005 6.6]

Control of U-bow reinforcement

The U-bow reinforcement is located around the embedded steel ring and will both lift up the compressive stresses and pull down the tensile stresses acting on the flange of the embedded steel ring.

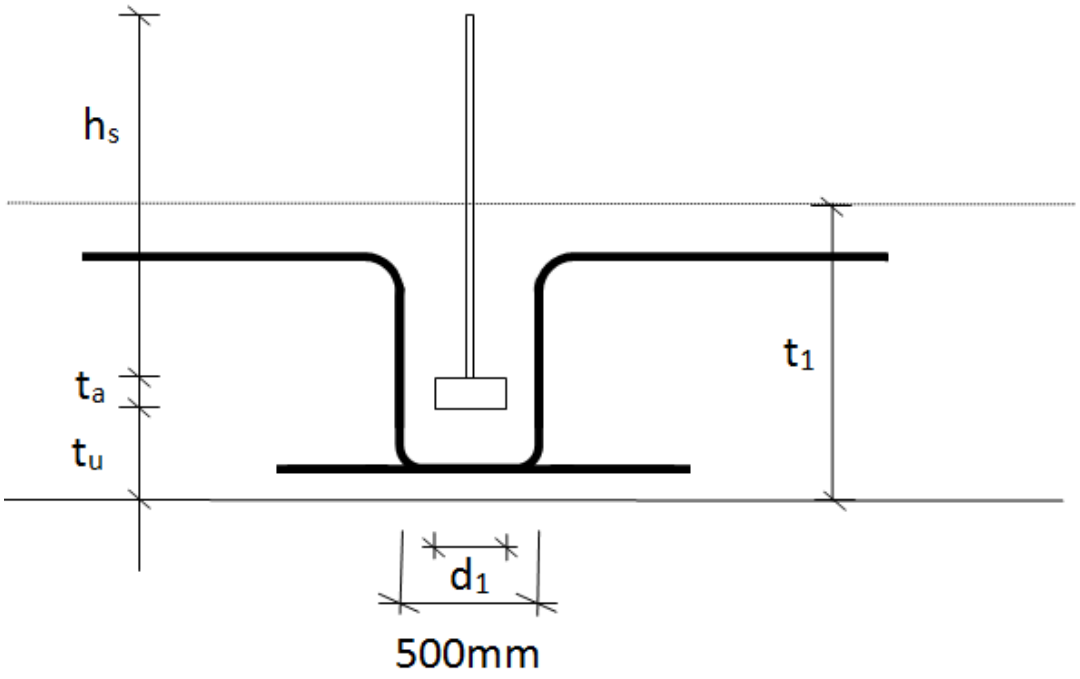

Detailing around embedded steel ring

$F_{xyd} = 880 \cdot kN$ $t_u := 1150mm$ $h_s := 1750mm$

$M_{xyd} = 56.227 \cdot MN \cdot m$ $t_1 := 2400mm$

$M_{da} := F_{xyd} \cdot h_4 + M_{xyd} = 58.779 \cdot MN \cdot m$

$\phi_{Ubow} := 25mm$ Diameter of U-bow

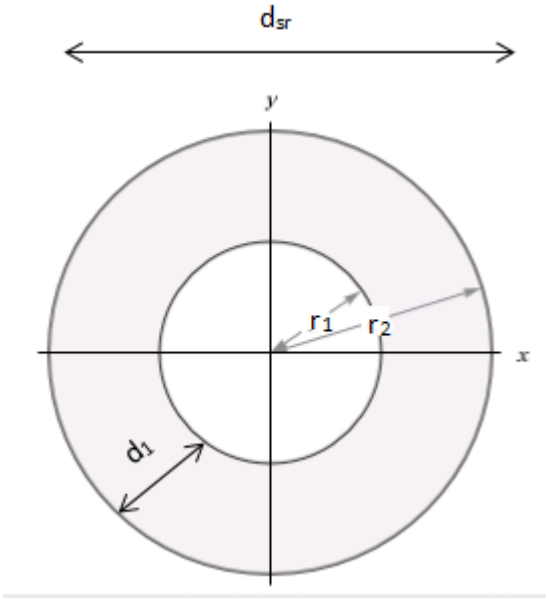

Check concrete compression (crushing)

Calculate area moment of inertia of an annulus

The stress distribution in the embedded steel ring is calculated under the assumption of linear elastic theory with Navier's formula

$$I_0 := \frac{1}{4}\cdot\pi\cdot\left(r_2^{\,4} - r_1^{\,2}\right)$$

$d_{sr} = 4\,\text{m}$

$d_1 := 340\text{mm}$

$$r_2 := \frac{d_{sr}}{2} + \frac{d_1}{2} = 2.17\,\text{m}$$

$$r_1 := \frac{d_{sr}}{2} - \frac{d_1}{2} = 1.83\,\text{m}$$

$$I_0 := \frac{\pi}{4}\cdot\left(r_2^{\,4} - r_1^{\,4}\right) = 8.607\,\text{m}^4$$

$$W_{annulus} := \frac{I_0}{r_2} = 3.966\cdot\text{m}^3$$

Stresses under the flange of the embedded steel ring

$$\sigma_{max.pos} := \frac{F_{zd}}{\pi\cdot d_{sr}\cdot d_1} + \frac{M_{da}}{W_{annulus}} = 1.527\times 10^4\cdot\text{kPa}$$

$$\sigma_{max.neg} := \frac{F_{zd}}{\pi\cdot d_{sr}\cdot d_1} - \frac{M_{da}}{W_{annulus}} = -1.437\times 10^4\cdot\text{kPa}$$

$$UR_{cc.ring} := \frac{\begin{pmatrix}|\sigma_{max.pos}|\\ |\sigma_{max.neg}|\end{pmatrix}}{f_{cd}} = \begin{pmatrix}50.888\\ 47.909\end{pmatrix}\cdot\%$$

Utilisation ratio of compression strength. No risk of crushing

Control shear reinforcement around anchor ring

Assume all shear stress is transferred by the U-bows ($V_{Ed} > V_{Rdc}$). Calculate maximum mean stress on the flange

$a_{ubow} := 0.1m \qquad \phi_{Ubow} = 25 \cdot mm$

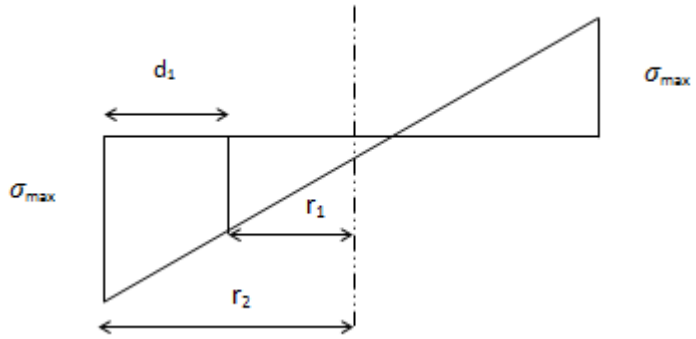

$$\sigma_{mean.pos} := \left(\frac{F_{zd}}{\pi \cdot d_{sr} \cdot d_1} + \frac{M_{da}}{I_0} \cdot r_1 + \frac{F_{zd}}{\pi \cdot d_{sr} \cdot d_1} + \frac{M_{da}}{I_0} \cdot r_2 \right) \cdot \frac{1}{2} = 14.105 \cdot MPa \qquad \text{Max stress}$$

$$\sigma_{mean.neg} := \left(\frac{F_{zd}}{\pi \cdot d_{sr} \cdot d_1} - \frac{M_{da}}{I_0} \cdot r_1 + \frac{F_{zd}}{\pi \cdot d_{sr} \cdot d_1} - \frac{M_{da}}{I_0} \cdot r_2 \right) \cdot \frac{1}{2} = -13.212 \cdot MPa \qquad \text{Min stress}$$

$$\sigma_{Ubow} := \begin{bmatrix} \left| \frac{\sigma_{mean.pos} \cdot a_{ubow} \cdot d_1}{2\left(\frac{\pi \cdot \phi_{Ubow}^2}{4} \right)} \right| \\ \left| \frac{\sigma_{mean.neg} \cdot a_{ubow} \cdot d_1}{2\left(\frac{\pi \cdot \phi_{Ubow}^2}{4} \right)} \right| \end{bmatrix} = \begin{pmatrix} 488.496 \\ 457.55 \end{pmatrix} \cdot MPa$$

$$\sigma_{Ubow} \le f_{yd} = \begin{pmatrix} 1 \\ 1 \end{pmatrix}$$

$$UR_{shear.Ubow} := \frac{\sigma_{Ubow}}{f_{yd}} = \begin{pmatrix} 93.628 \\ 87.697 \end{pmatrix} \cdot \%$$

Control shear punching

SS-EN 1992-1-1:2005 6.4

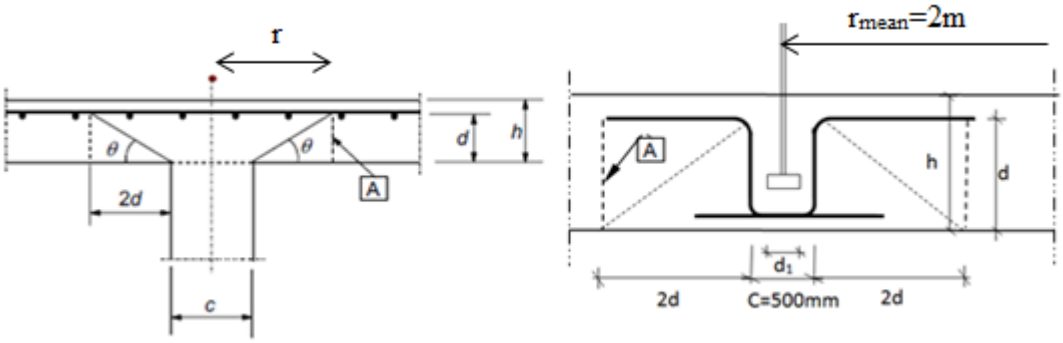

$d := 1.55m \qquad \sigma_{cp} := 0$

$$V_{Rd.c} := C_{Rd.c} \cdot k \cdot \left(100 \cdot \rho_l \cdot f_{ck}\right)^{\frac{1}{3}} + k_1 \cdot \sigma_{cp} > \left(v_{min} + k_1 \cdot \sigma_{cp}\right)$$

$$k := 1 + \sqrt{\frac{200}{\frac{d}{mm}}} = 1.359 \qquad k \le 2 = 1$$

$\rho_1 := 0.02$

$$C_{Rd.c} := \frac{0.18}{1.5} = 0.12$$

$$v_{min} := 0.035 \cdot k^{\frac{3}{2}} \cdot \left(\frac{f_{ck}}{MPa}\right)^{0.5} \cdot MPa = 0.372 \cdot MPa$$

$$V_{Rd.c.punch} := C_{Rd.c} \cdot k \cdot \left(100 \cdot \rho_1 \cdot \frac{f_{ck}}{MPa}\right)^{\frac{1}{3}} \cdot MPa = 0.731 \cdot MPa$$

$V_{Rd.c.punch} > v_{min} = 1$

$$V_{Rd.punch} := V_{Rd.c.punch} \cdot \left[2d \cdot \pi \cdot \frac{d_{sr}}{2} + d \cdot (500mm + 4d)\right] = 2.183 \times 10^4 \cdot kN$$

$V_{Rd.punch} > \sigma_{mean.pos} \cdot d_1 \cdot 100mm = 1$

$F_c = 1.68 \times 10^4 \cdot kN$

$$\frac{F_c}{V_{Rd.punch}} = 0.77$$

$$V_{Rd.punch} := V_{Rd.c.punch} \cdot 2 \cdot d \cdot \frac{\pi}{2} \cdot d_{sr} = 1.424 \times 10^4 \cdot kN$$

$V_{Rd.c.punch} \cdot 2 \cdot d \cdot \pi \cdot d_{sr} = 2.847 \times 10^7 \, N$

$$\frac{F_c}{V_{Rd.punch}} = 1.18$$

D Crack widths serviceability limit state

D.1 Loads

SLS loads equilibrium

$M_{xySLS} = 51.115 \cdot MN \cdot m$

$F_{xySLS} = 800 \cdot kN$

$M_{zSLS} = 5.863 \cdot MN \cdot m$

$G_{dSLS} = 12.575 \cdot MN$

$g_{dSLS} = 52.341 \cdot \frac{kN}{m^2}$

Sectional forces

$e_{sls} := \frac{M_{xySLS} + F_{xySLS} \cdot h_4}{F_{zSLS} + G_{dSLS}} = 3.636\,m$ Minimum eccentricity for soil pressure

$b_{sls} := 3\left(\frac{l}{2} - e_{sls}\right) = 12.342\,m$ Width of soil pressure

$G_{dSLS} = 1.257 \times 10^4 \cdot kN$

$f_{soil.sls} := \frac{F_{zSLS} + G_{dSLS}}{\frac{b_{sls}}{2}} = 2.381 \cdot \frac{MN}{m}$ Self weight and weight from soil evenly distributed over the length of the foundation

$g_{dSLS} := \frac{G_{dSLS}}{l} = 811.284 \cdot \frac{kN}{m}$

$F_{c.sls} := \frac{M_{xySLS} + F_{xySLS} \cdot h_4}{d_s} + \frac{F_{zSLS}}{4} = 15.368 \cdot MN$ Compressive force from moment and vertical force

$F_{t.sls} := \frac{M_{xySLS} + F_{xySLS} \cdot h_4}{d_s} - \frac{F_{zSLS}}{4} = 14.308 \cdot MN$ Tensile force from moment and vertical force

$F_{c.sls} - F_{t.sls} + g_{dSLS} \cdot l - f_{soil.sls} \cdot \frac{b_{sls}}{2} + \frac{F_{zSLS}}{2} = 1.863 \times 10^{-9}\,N$ Check of global equilibrium

$x := 0, 0.01m .. 15.5m$

$F_{soil.sls}(x) := f_{soil.sls} \cdot \frac{x^2}{2} - \frac{f_{soil.sls}}{b_{sls}} \cdot \frac{x^3}{6}$

$$M_{sls}(x) := \begin{cases} F_{soil.sls}(x) - g_{dSLS}\cdot\frac{x^2}{2} & \text{if } x < \frac{l - d_s}{2} \\ F_{soil.sls}(x) - g_{dSLS}\cdot\frac{x^2}{2} - F_{c.sls}\left(x - \frac{l - d_s}{2}\right) & \text{if } \frac{l - d_s}{2} \le x < \frac{l}{2} \\ F_{soil.sls}(x) - g_{dSLS}\cdot\frac{x^2}{2} - F_{c.sls}\left(x - \frac{l - d_s}{2}\right) - \frac{F_{zSLS}}{2}\cdot\left(x - \frac{l}{2}\right) & \text{if } \frac{l}{2} \le x < \frac{l + d_s}{2} \\ F_{soil.sls}(x) - g_{dSLS}\cdot\frac{x^2}{2} - F_{c.sls}\left(x - \frac{l - d_s}{2}\right) \dots & \text{if } \frac{l + d_s}{2} \le x < b_{sls} \\ \quad + -\frac{F_{zSLS}}{2}\cdot\left(x - \frac{l}{2}\right) + F_{t.sls}\cdot\left(x - \frac{l + d_s}{2}\right) & \\ f_{soil.sls}\cdot\frac{b_{sls}}{2}\cdot\left(x - \frac{b_{sls}}{3}\right) - g_{dSLS}\cdot\frac{x^2}{2} - F_{c.sls}\cdot\left(x - \frac{l - d_s}{2}\right) \dots & \text{if } b_{sls} \le x \le l \\ \quad + -\frac{F_{zSLS}}{2}\cdot\left(x - \frac{l}{2}\right) + F_{t.sls}\cdot\left(x - \frac{l + d_s}{2}\right) & \end{cases}$$

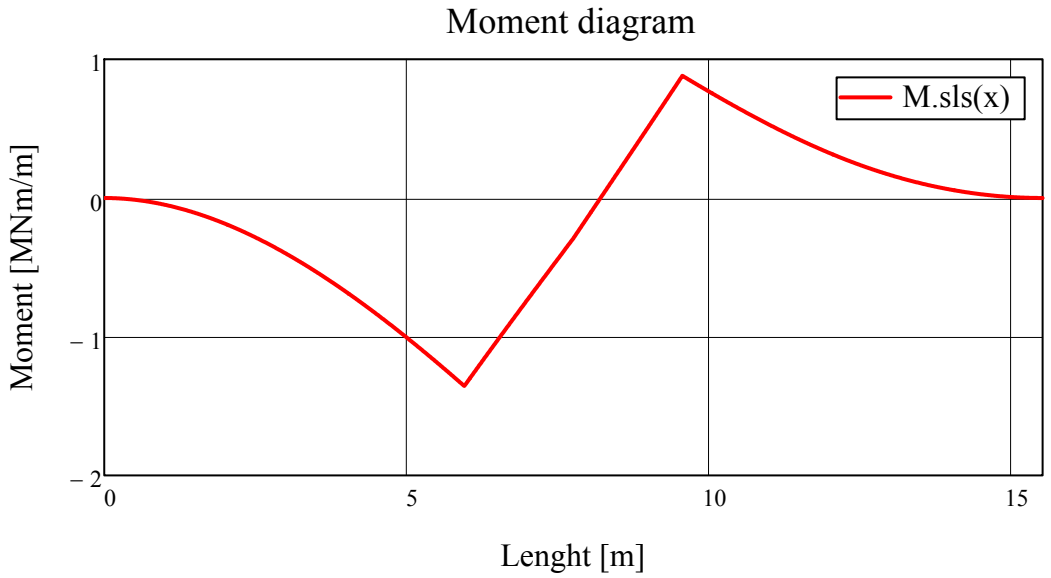

D.2 Crack width limitation

Check of allowable crack width [EN 1992-1-1:2005 7.3.4]

$b_1 = 1\,m$ Thickness of the section

$a_{sw} := 110mm$ $a_{so} := 150mm$ Spacing to fulfill crack requirement

$$M_{slsu} := \frac{b_1}{l}\begin{pmatrix} M_{sls}(l_x) \\ M_{sls}\left(\frac{3l_x}{4}\right) \\ M_{sls}\left(\frac{2l_x}{4}\right) \\ M_{sls}\left(\frac{l_x}{4}\right) \end{pmatrix} = \begin{pmatrix} 1.356 \times 10^3 \\ 824.128 \\ 393.586 \\ 105.223 \end{pmatrix} \cdot kN \cdot m$$

$$M_{slso} := \frac{b_1}{l}\begin{pmatrix} \left|M_{sls}(l_x + d_s)\right| \\ \left|M_{sls}\left(l_x + d_s + \frac{l_x}{4}\right)\right| \\ \left|M_{sls}\left(l_x + d_s + \frac{2l_x}{4}\right)\right| \\ \left|M_{sls}\left(l_x + d_s + \frac{3.l_x}{4}\right)\right| \end{pmatrix} = \begin{pmatrix} 881.183 \\ 516.446 \\ 231.576 \\ 57.894 \end{pmatrix} \cdot kN \cdot m$$

$A_{su} := \frac{b_1}{a_u} \cdot A_{siu} = 4.462 \times 10^{-3} \cdot m^2$ $\quad A'_{su} := \frac{b_1}{a_o} \cdot A_{sio} = 3.272 \times 10^{-3} \cdot m^2$

$A_{so} := \frac{b_1}{a_o} \cdot A_{sio} = 3.272 \times 10^{-3} \cdot m^2$ $\quad A'_{so} := \frac{b_1}{a_u} \cdot A_{siu} = 4.462 \times 10^{-3} \cdot m^2$

$i := 0 .. 3$

$$d_{mu} = \begin{pmatrix} 1.505 \\ 1.505 \\ 1.471 \\ 1.423 \end{pmatrix} m \quad d_{mo} = \begin{pmatrix} 1.555 \\ 1.555 \\ 1.521 \\ 1.473 \end{pmatrix} m$$

$d'o_i := c + \phi_o + \frac{\phi_o}{2}$

$d'u_i := c_{soil} + \phi_u + \frac{\phi_u}{2}$

$\alpha = 5.556$

$x_{IIu} := 0.2m$ Guess

$$x_{IIu_i} := \text{root}\left[b_1 \frac{x_{IIu}^2}{2} + (\alpha - 1) \cdot A'_{su} \cdot \left(x_{IIu} - d'u_i\right) + \alpha \cdot A_{su} \cdot \left(x_{IIu} - d_{mu_i}\right), x_{IIu}\right]$$

$x_{IIo} := 0.2m$

$$x_{IIo_i} := \text{root}\left[b_1 \frac{x_{IIo}^2}{2} + (\alpha - 1) \cdot A'_{so} \cdot \left(x_{IIo} - d'o_i\right) + \alpha \cdot A_{so} \cdot \left(x_{IIo} - d_{mo_i}\right), x_{IIo}\right]$$

$$x_{IIo} = \begin{pmatrix} 0.21 \\ 0.21 \\ 0.207 \\ 0.204 \end{pmatrix} m \quad x_{IIu} = \begin{pmatrix} 0.244 \\ 0.244 \\ 0.241 \\ 0.236 \end{pmatrix} m$$

Height of compressive zone

$$I_{IIu} := \frac{b_1 \cdot x_{IIu}^{3}}{12} + b_1 \cdot x_{IIu} \cdot \left(\frac{x_{IIu}}{2}\right)^2 + (\alpha - 1) \cdot A'_{su} \cdot \left(x_{IIu} - d'_u\right)^2 + \alpha \cdot A_{su} \cdot \left(d_{mu} - x_{IIu}\right)^2$$

$$I_{IIo} := \frac{b_1 \cdot x_{IIo}^{3}}{12} + b_1 \cdot x_{IIo} \cdot \left(\frac{x_{IIo}}{2}\right)^2 + (\alpha - 1) \cdot A'_{so} \cdot \left(x_{IIo} - d'_o\right)^2 + \alpha \cdot A_{so} \cdot \left(d_{mo} - x_{IIo}\right)^2$$

$$I_{IIo} = \begin{pmatrix} 0.043 \\ 0.043 \\ 0.041 \\ 0.039 \end{pmatrix} m^4 \qquad I_{IIu} = \begin{pmatrix} 0.055 \\ 0.055 \\ 0.053 \\ 0.05 \end{pmatrix} m^4$$

$z_{u_i} := d_{mu_i} - x_{IIu_i}$

$z_{o_i} := d_{mo_i} - x_{IIo_i}$

Steel stress

$$\sigma_{su_i} := \alpha \cdot \frac{M_{slsu_i}}{I_{IIu_i}} \cdot z_{u_i} \qquad \sigma_{su} = \begin{pmatrix} 173.258 \\ 105.309 \\ 50.893 \\ 13.825 \end{pmatrix} \cdot MPa \qquad \sigma_{so_i} := \alpha \cdot \frac{M_{slso_i}}{I_{IIo_i}} \cdot z_{o_i} \qquad \sigma_{so} = \begin{pmatrix} 153.465 \\ 89.943 \\ 40.883 \\ 10.413 \end{pmatrix} \cdot MPa$$

Maximum allowed crack width according to EN 1992-1-1:2005 NA with regard to L50 and XC3

$w_{k.max} := 0.4mm$

$$\alpha_e := \frac{E_s}{E_{cm}} = 5.556$$

$k_t := 0.4$ Depending on load duration, kt for long term load

$f_{ct.eff} := f_{ctm} = 3.8 \cdot MPa$

$A_s = 4.462 \times 10^{-3}\, m^2$

$h_{m_mean} = 1.613\, m$

Effective area for a one meter thick section

$$A_{c.effu_i} := \min\left[2.5 \cdot \left(h_{m_section_i} - d_{mu_i}\right), \frac{\left(h_{m_section_i} - x_{IIu_i}\right)}{3}\right] \cdot b_1$$

$$A_{c.effo_i} := \min\left[2.5 \cdot \left(h_{m_section_i} - d_{mo_i}\right), \frac{\left(h_{m_section_i} - x_{IIo_i}\right)}{3}\right] \cdot b_1$$

$\xi_1 := 0$ $A'_p := 0$ No pre- or post tensioned reinforcement

$$\rho_{p.effu_i} := \frac{\left(A_{su} + \xi_1^{\,2}\cdot A'_p\right)}{A_{c.effu_i}} \qquad \rho_{p.effo_i} := \frac{\left(A_{so} + \xi_1^{\,2}\cdot A'_p\right)}{A_{c.effo_i}}$$

$$\Delta\varepsilon_{u_i} := \frac{\sigma_{su_i} - k_t\cdot\frac{f_{ct.eff}}{\rho_{p.effu_i}}\cdot\left(1 + \alpha_e\cdot\rho_{p.effu_i}\right)}{E_s} \qquad \Delta\varepsilon_{o_i} := \frac{\sigma_{so_i} - k_t\cdot\frac{f_{ct.eff}}{\rho_{p.effo_i}}\cdot\left(1 + \alpha_e\cdot\rho_{p.effo_i}\right)}{E_s}$$

$$\Delta\varepsilon_{u_i} := \max\left[\Delta\varepsilon_{u_i}, \left(0.6\cdot\frac{\sigma_{su_i}}{E_s}\right)\right] \qquad \Delta\varepsilon_{o_i} := \max\left[\Delta\varepsilon_{o_i}, \left(0.6\cdot\frac{\sigma_{so_i}}{E_s}\right)\right]$$

$$\Delta\varepsilon_u = \begin{pmatrix} 5.198\times10^{-4} \\ 3.159\times10^{-4} \\ 1.527\times10^{-4} \\ 4.148\times10^{-5} \end{pmatrix} \qquad \Delta\varepsilon_o = \begin{pmatrix} 4.604\times10^{-4} \\ 2.698\times10^{-4} \\ 1.226\times10^{-4} \\ 3.124\times10^{-5} \end{pmatrix}$$

$k_1 := 0.8$ For reinforcement bars with good interactive properties

$k_2 := 1$ For reinforcement in tension

$k_{3u} := 7\cdot\frac{\phi_u}{c_{soil}} = 1.75$ $k_{3o} := 7\cdot\frac{\phi_o}{c} = 3.5$ According to EC2 1992-1-1 NA

$k_4 := 0.425$ Recommended value

$$s_{r.maxu_i} := k_{3u}\cdot c + \frac{k_1\cdot k_2\cdot k_4\cdot\phi_u}{\rho_{p.effu_i}} \qquad s_{r.maxo_i} := k_{3o}\cdot c + \frac{k_1\cdot k_2\cdot k_4\cdot\phi_o}{\rho_{p.effo_i}}$$

$w_{ku_i} := s_{r.maxu_i}\cdot\Delta\varepsilon_{u_i}$ $w_{ko_i} := s_{r.maxo_i}\cdot\Delta\varepsilon_{o_i}$ Crack width

$$w_{ku} = \begin{pmatrix} 0.386 \\ 0.235 \\ 0.113 \\ 0.031 \end{pmatrix}\cdot mm \qquad w_{ko} = \begin{pmatrix} 0.342 \\ 0.201 \\ 0.091 \\ 0.023 \end{pmatrix}\cdot mm$$

Crack width for the different sections

$w_{ku_i} \le w_{k.max} =$ $w_{ko_i} \le w_{k.max} =$ **OK!** Calculated crack width less then the allowed

1	1
1	1
1	1
1	1

Utilisation degree of crack width

$$UR_{crack.width.u} := \frac{w_{ku}}{w_{k.max}} = \begin{pmatrix} 96.453 \\ 58.625 \\ 28.332 \\ 7.696 \end{pmatrix} \cdot \%$$

$$UR_{crack.width.o} := \frac{w_{ko}}{w_{k.max}} = \begin{pmatrix} 85.539 \\ 50.133 \\ 22.788 \\ 5.804 \end{pmatrix} \cdot \%$$

E Fatigue calculations with equivalent load cycle method

E1. Loads and sectional forces

Instead of using the full load spectra one equivalent load width is calculated from the load spectra. See Appendix I

Mean amplitudes from appendix

$\Delta Mmean := 13049.8kN \cdot m$

$\Delta F_{xymean} := 218kN$

$\Delta F_z := 0kN$

Mean loads

$F_{xmean} := 316kN \qquad F_{ymean} := 4kN$

$F_{xymean} := \sqrt{F_{xmean}^2 + F_{ymean}^2} = 316.025 \cdot kN$

$M_{xmean} := 1888kN \cdot m \qquad M_{ymean} := 21293kN \cdot m$

$M_{xymean} := \sqrt{M_{xmean}^2 + M_{ymean}^2} = 2.138 \times 10^4 \cdot kN \cdot m$

$F_{zmean} := 2247kN$

min/max fatigue load

$M_{df1} := M_{xymean} - \frac{\Delta Mmean}{2} = 14.852 \cdot MN \cdot m$

$M_{df2} := M_{xymean} + \frac{\Delta Mmean}{2} = 27.901 \cdot MN \cdot m$

$F_{xydf1} := F_{xymean} - \frac{\Delta F_{xymean}}{2} = 207.025 \cdot kN$

$F_{xydf2} := F_{xymean} + \frac{\Delta F_{xymean}}{2} = 425.025 \cdot kN$

$F_{zdf1} := F_{zmean} - \frac{\Delta F_z}{2}$

$F_{zdf2} := F_{zmean} + \frac{\Delta F_z}{2}$

Equilibrium

$e_{f1} := \frac{M_{df1} + F_{xydf1} \cdot h_4}{F_{zdf1} + G_d} = 1.139\,m \qquad e_{f2} := \frac{M_{df2} + F_{xydf2} \cdot h_4}{F_{zdf2} + G_d} = 2.148\,m$ Min/max eccentricity

$b_{f1} := 3\left(\frac{l}{2} - e_{f1}\right) = 19.833\,m$ $b_{f2} := 3\left(\frac{l}{2} - e_{f2}\right) = 16.807\,m$ Width of soil pressure

$b_{f1} > l = 1$ $b_{f2} > l = 1$

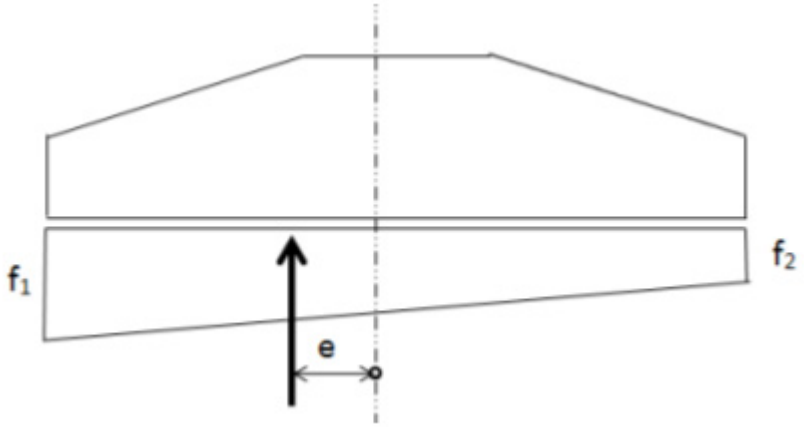

The fatigue loads are small and the soil pressure is spread over the full length. The distribution can be solved, two equations and two unknowns.

Min load (load 1)

$$f_{12} := \frac{f_{11} + f_{12}}{2}\cdot l = G_d + F_{zdf1} \quad \left|\begin{array}{l}\text{explicit}\\ \text{solve}, f_{12}\end{array}\right.\rightarrow$$

The gravity center must be equal to the eccentricity

$$\frac{\left[\frac{2\cdot\left(G_d + F_{zdf1} - \frac{f_{11}\cdot l}{2}\right)}{l}\right]\cdot\frac{l^2}{2} + \left[f_{11} - \left[\frac{2\cdot\left(G_d + F_{zdf1} - \frac{f_{11}\cdot l}{2}\right)}{l}\right]\right]\cdot\frac{2l^2}{6}}{l\cdot\frac{\left[f_{11} + \left[\frac{2\cdot\left(G_d + F_{zdf1} - \frac{f_{11}\cdot l}{2}\right)}{l}\right]\right]}{2}}$$

Expression for the distance to the gravity center

$$\frac{l}{3} + \frac{f_{11}\cdot l^2}{6\cdot\left(G_d + F_{zdf1}\right)}$$ Simplified expression

$$f_{11} := \frac{l}{3} + \frac{f_{11}\cdot l^2}{6\cdot\left(G_d + F_{zdf1}\right)} = \left(e_{f1} + \frac{l}{2}\right) \quad \left|\begin{array}{l}\text{explicit}\\ \text{solve}, f_{11}\end{array}\right.\rightarrow \frac{\left(e_{f1} + \frac{l}{6}\right)\cdot\left(6\cdot F_{zdf1} + 6\cdot G_d\right)}{l^2}$$

$f_{11} = 1.261 \times 10^3\,\frac{1}{m}\cdot kN$

$f_{12} := \left(G_d + F_{zdf1}\right)\cdot\frac{2}{l} - f_{11} = 489.225\,\frac{1}{m}\cdot kN$

Max load (load 2)

$$f_{21} := \frac{l}{3} + \frac{f_{21} \cdot l^2}{6 \cdot (G_d + F_{zdf2})} = \left(e_{f2} + \frac{l}{2}\right) \left| \begin{array}{l} \text{explicit} \\ \text{solve}, f_{21} \end{array} \right. \rightarrow \frac{\left(e_{f2} + \frac{l}{6}\right) \cdot (6 \cdot F_{zdf2} + 6 \cdot G_d)}{l^2}$$

$$f_{21} = 1.603 \times 10^3 \frac{1}{m} \cdot kN$$

$$f_{22} := (G_d + F_{zdf2}) \cdot \frac{2}{l} - f_{21} = 147.531 \frac{1}{m} \cdot kN$$

Min compressive and tensile resultant

$$F_{cf1} := \frac{M_{df1} + F_{xydf1} \cdot h_4}{d_s} + \frac{F_{zdf1}}{4} = 4.852 \cdot MN$$ Compressive force from moment and vertical force

$$F_{tf1} := \frac{M_{df1} + F_{xydf1} \cdot h_4}{d_s} - \frac{F_{zdf1}}{4} = 3.729 \cdot MN$$ Tensile force from moment and vertical force

$$F_{cf1} - F_{tf1} + g_d \cdot l - \frac{f_{11} + f_{12}}{2} \cdot l + \frac{F_{zdf1}}{2} = 0\,N$$ Check of global equilibrium

Max compressive and tensile resultant

$$F_{cf2} := \frac{M_{df2} + F_{xydf2} \cdot h_4}{d_s} + \frac{F_{zdf2}}{4} = 8.652 \cdot MN$$ Compressive force from moment and vertical force

$$F_{tf2} := \frac{M_{df2} + F_{xydf2} \cdot h_4}{d_s} - \frac{F_{zdf2}}{4} = 7.528 \cdot MN$$ Tensile force from moment and vertical force

$$F_{cf2} - F_{tf2} + g_d \cdot l - \frac{f_{21} + f_{22}}{2} \cdot l + \frac{F_{zdf2}}{2} = 0 \cdot MN$$ Check of global equilibrium

Bending moment distribution fatigue loading

$$x := 0, 0.01m .. 15.5m$$

$$F_{11}(x) := (f_{11} - f_{12}) \cdot \frac{x^2}{2} - \frac{(f_{11} - f_{12})}{l} \cdot \frac{x^3}{6}$$

$$M_{f1}(x) := \begin{cases} F_{11}(x) + f_{12}\cdot\frac{x^2}{2} - g_d\cdot\frac{x^2}{2} & \text{if } x < \frac{l - d_s}{2} \\ F_{11}(x) + f_{12}\cdot\frac{x^2}{2} - g_d\cdot\frac{x^2}{2} - F_{cf1}\left(x - \frac{l - d_s}{2}\right) & \text{if } \frac{l - d_s}{2} \le x < \frac{l}{2} \\ F_{11}(x) + f_{12}\cdot\frac{x^2}{2} - g_d\cdot\frac{x^2}{2} - F_{cf1}\left(x - \frac{l - d_s}{2}\right) - \frac{F_{zdf1}}{2}\cdot\left(x - \frac{l}{2}\right) & \text{if } \frac{l}{2} \le x < \frac{l + d_s}{2} \\ F_{11}(x) + f_{12}\cdot\frac{x^2}{2} - g_d\cdot\frac{x^2}{2} - F_{cf1}\left(x - \frac{l - d_s}{2}\right) - \frac{F_{zdf1}}{2}\cdot\left(x - \frac{l}{2}\right) \ldots & \text{if } \frac{l + d_s}{2} \le x < l \\ \quad + F_{tf1}\cdot\left(x - \frac{l + d_s}{2}\right) \end{cases}$$

$$F_{21}(x) := \left(f_{21} - f_{22}\right)\cdot\frac{x^2}{2} - \frac{\left(f_{21} - f_{22}\right)}{l}\cdot\frac{x^3}{6}$$

$$M_{f2}(x) := \begin{cases} F_{21}(x) + f_{22}\cdot\frac{x^2}{2} - g_d\cdot\frac{x^2}{2} & \text{if } x < \frac{l - d_s}{2} \\ F_{21}(x) + f_{22}\cdot\frac{x^2}{2} - g_d\cdot\frac{x^2}{2} - F_{cf2}\left(x - \frac{l - d_s}{2}\right) & \text{if } \frac{l - d_s}{2} \le x < \frac{l}{2} \\ F_{21}(x) + f_{22}\cdot\frac{x^2}{2} - g_d\cdot\frac{x^2}{2} - F_{cf2}\left(x - \frac{l - d_s}{2}\right) - \frac{F_{zdf2}}{2}\cdot\left(x - \frac{l}{2}\right) & \text{if } \frac{l}{2} \le x < \frac{l + d_s}{2} \\ F_{21}(x) + f_{22}\cdot\frac{x^2}{2} - g_d\cdot\frac{x^2}{2} - F_{cf2}\left(x - \frac{l - d_s}{2}\right) - \frac{F_{zdf2}}{2}\cdot\left(x - \frac{l}{2}\right) \ldots & \text{if } \frac{l + d_s}{2} \le x < l \\ \quad + F_{tf2}\cdot\left(x - \frac{l + d_s}{2}\right) \end{cases}$$

Fatigue loading max/min moment

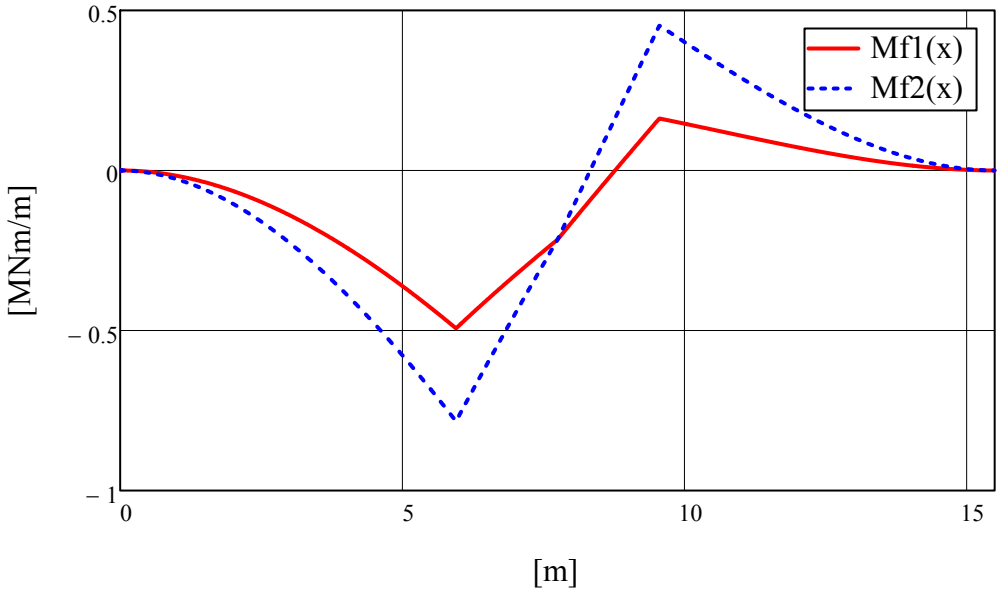

Minimum moment in section 0-3, fatigue

$$M_{1u} := \frac{b_1}{l}\begin{pmatrix} M_{f1}(l_x) \\ M_{f1}\left(\frac{3l_x}{4}\right) \\ M_{f1}\left(\frac{2l_x}{4}\right) \\ M_{f1}\left(\frac{l_x}{4}\right) \end{pmatrix} \qquad M_{1o} := \frac{b_1}{l}\begin{pmatrix} M_{f1}(l_x + d_s) \\ M_{f1}\left(l_x + d_s + \frac{l_x}{4}\right) \\ M_{f1}\left(l_x + d_s + \frac{2l_x}{4}\right) \\ M_{f1}\left(l_x + d_s + \frac{3.l_x}{4}\right) \end{pmatrix}$$

Maximum moment in section 0-3, fatigue

$$M_{2u} := \frac{b_1}{l}\begin{pmatrix} M_{f2}(l_x) \\ M_{f2}\left(\frac{3l_x}{4}\right) \\ M_{f2}\left(\frac{2l_x}{4}\right) \\ M_{f2}\left(\frac{l_x}{4}\right) \end{pmatrix} \qquad M_{2o} := \frac{b_1}{l}\begin{pmatrix} M_{f2}(l_x + d_s) \\ M_{f2}\left(l_x + d_s + \frac{l_x}{4}\right) \\ M_{f2}\left(l_x + d_s + \frac{2l_x}{4}\right) \\ M_{f2}\left(l_x + d_s + \frac{3.l_x}{4}\right) \end{pmatrix}$$

Shear force distribution fatigue loading

$$V_{fl1}(x) := \begin{cases} f_{11}\cdot x - \frac{f_{11} - f_{12}}{l}\cdot\frac{x^2}{2} - g_d\cdot x & \text{if } x < \frac{l - d_s}{2} \\ f_{11}\cdot x - \frac{f_{11} - f_{12}}{l}\cdot\frac{x^2}{2} - g_d\cdot x - F_{cf1} & \text{if } \frac{l - d_s}{2} \le x < \frac{l}{2} \\ f_{11}\cdot x - \frac{f_{11} - f_{12}}{l}\cdot\frac{x^2}{2} - g_d\cdot x - F_{cf1} - \frac{F_{zdf1}}{2} & \text{if } \frac{l}{2} \le x < \frac{l + d_s}{2} \\ f_{11}\cdot x - \frac{f_{11} - f_{12}}{l}\cdot\frac{x^2}{2} - g_d\cdot x - F_{cf1} - \frac{F_{zdf1}}{2} + F_{tf1} & \text{if } \frac{l + d_s}{2} \le x < l \end{cases}$$

$$V_{fl2}(x) := \begin{cases} f_{21}\cdot x - \frac{f_{21} - f_{22}}{l}\cdot\frac{x^2}{2} - g_d\cdot x & \text{if } x < \frac{l - d_s}{2} \\ f_{21}\cdot x - \frac{f_{21} - f_{22}}{l}\cdot\frac{x^2}{2} - g_d\cdot x - F_{cf2} & \text{if } \frac{l - d_s}{2} \le x < \frac{l}{2} \\ f_{21}\cdot x - \frac{f_{21} - f_{22}}{l}\cdot\frac{x^2}{2} - g_d\cdot x - F_{cf2} - \frac{F_{zdf2}}{2} & \text{if } \frac{l}{2} \le x < \frac{l + d_s}{2} \\ f_{21}\cdot x - \frac{f_{21} - f_{22}}{l}\cdot\frac{x^2}{2} - g_d\cdot x - F_{cf2} - \frac{F_{zdf2}}{2} + F_{tf2} & \text{if } \frac{l + d_s}{2} \le x < l \end{cases}$$

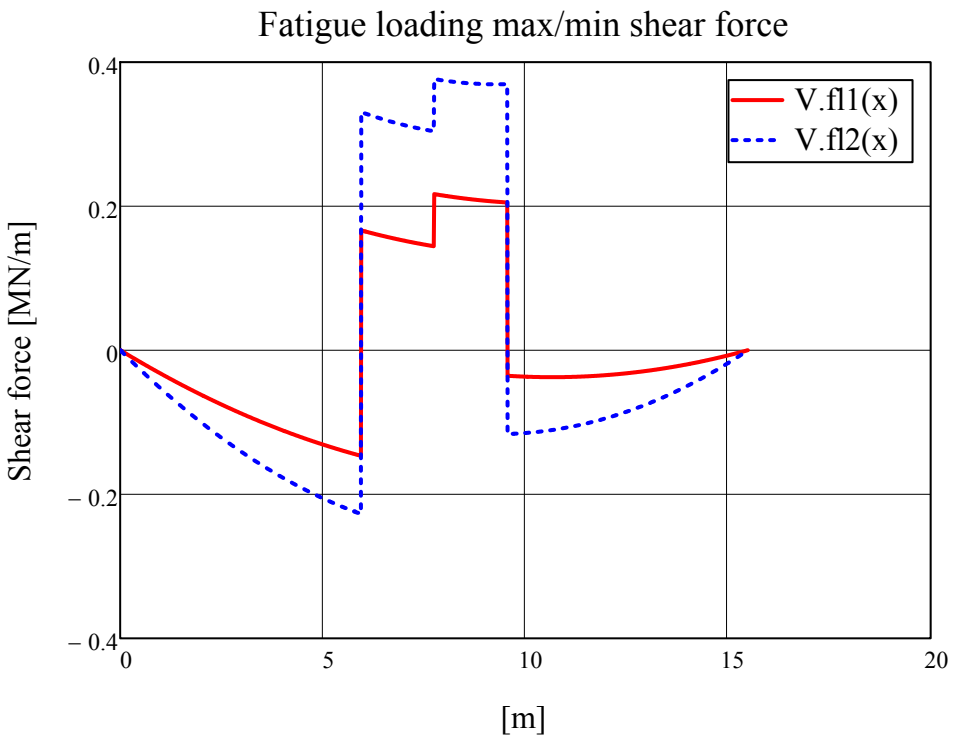

Minimum shear force in section 0-3, fatigue

$$V_{fl1_pos} := \frac{b_1}{l}\begin{pmatrix} V_{fl1}(l_x) \\ V_{fl1}\left(\frac{3l_x}{4}\right) \\ V_{fl1}\left(\frac{2l_x}{4}\right) \\ V_{fl1}\left(\frac{l_x}{4}\right) \end{pmatrix} \quad V_{fl1_neg} := \frac{b_1}{l}\begin{pmatrix} V_{fl1}(l_x + d_s) \\ V_{fl1}\left(l_x + d_s + \frac{l_x}{4}\right) \\ V_{fl1}\left(l_x + d_s + \frac{2l_x}{4}\right) \\ V_{fl1}\left(l_x + d_s + \frac{3.l_x}{4}\right) \end{pmatrix}$$

Maximum shear force in section 0-3, fatigue

$$V_{fl2_pos} := \frac{b_1}{l}\begin{pmatrix} V_{fl2}(l_x) \\ V_{fl2}\left(\frac{3l_x}{4}\right) \\ V_{fl2}\left(\frac{2l_x}{4}\right) \\ V_{fl2}\left(\frac{l_x}{4}\right) \end{pmatrix} \quad V_{fl2_neg} := \frac{b_1}{l}\begin{pmatrix} V_{fl2}(l_x + d_s) \\ V_{fl2}\left(l_x + d_s + \frac{l_x}{4}\right) \\ V_{fl2}\left(l_x + d_s + \frac{2l_x}{4}\right) \\ V_{fl2}\left(l_x + d_s + \frac{3.l_x}{4}\right) \end{pmatrix}$$

E2. Fatigue control bending moment

Check top and bottom reinforcement and compressive concrete.Use Navier's formula to calculate stresses, determine neutral axis and moment of inertia. Assume fully cracked member (stage II). According to EC compressive stresses must be checked as well.For concrete only compressive stresses is checked.

Stress range for bottom reinforcement and compressed concrete

Fatigue due to positive moment (bottom reinforcement in tension)

$A_s := \frac{b_1}{a_u} \cdot A_{siu} = 4.462 \times 10^{-3} \cdot m^2$ $A'_s := \frac{b_1}{a_o} \cdot A_{sio} = 3.272 \times 10^{-3} \cdot m^2$

$d := d_{mu} = \begin{pmatrix} 1.505 \\ 1.505 \\ 1.471 \\ 1.423 \end{pmatrix} m$ $d'_i := c + \phi_o + \frac{\phi_o}{2}$

$x_{II} := 0.23m$ Guess

$x_{II_i} := \text{root}\left[b_1 \frac{x_{II}^2}{2} + (\alpha - 1) \cdot A'_s \cdot \left(x_{II} - d'_i\right) + \alpha \cdot A_s \cdot \left(x_{II} - d_i\right), x_{II} \right]$

$x_{II} = \begin{pmatrix} 241.035 \\ 241.035 \\ 237.967 \\ 233.684 \end{pmatrix} \cdot mm$

$I_{II} := \frac{b_1 \cdot x_{II}^3}{12} + b_1 \cdot x_{II} \cdot \left(\frac{x_{II}}{2}\right)^2 + (\alpha - 1) \cdot A'_s \cdot \left(x_{II} - d'\right)^2 + \alpha \cdot A_s \cdot \left(d - x_{II}\right)^2$

$I_{II} = \begin{pmatrix} 0.055 \\ 0.055 \\ 0.053 \\ 0.05 \end{pmatrix} \cdot m^4$

Steel stress top (o) reinforcement

$z := d' - x_{II}$

$\sigma_{s1poso_i} := \alpha \cdot \frac{M_{1u_i}}{I_{II_i}} \cdot z_i$ $\sigma_{s2poso_i} := \alpha \cdot \frac{M_{2u_i}}{I_{II_i}} \cdot z_i$ Min and max stresses

$\sigma_{s1poso} = \begin{pmatrix} -7.695 \\ -4.576 \\ -2.181 \\ -0.587 \end{pmatrix} \cdot MPa$ $\sigma_{s2poso} = \begin{pmatrix} -12.222 \\ -7.341 \\ -3.53 \\ -0.957 \end{pmatrix} \cdot MPa$

Concrete stress top (o) (check top fibre on safe side)

$z := -x_{II}$

$\sigma_{c1poso_i} := \frac{M_{1u_i}}{I_{II_i}} \cdot z_i$ $\sigma_{c2poso_i} := \frac{M_{2u_i}}{I_{II_i}} \cdot z_i$ Min and max stresses

$$\sigma_{c1poso} = \begin{pmatrix} -2.174 \\ -1.293 \\ -0.621 \\ -0.169 \end{pmatrix} \cdot MPa \qquad \sigma_{c2poso} = \begin{pmatrix} -3.454 \\ -2.075 \\ -1.005 \\ -0.275 \end{pmatrix} \cdot MPa$$

Steel stress bottom (u) reinforcement

$z := d - x_{II}$

$$\sigma_{s1posu_i} := \alpha \cdot \frac{M_{1u_i}}{I_{II_i}} \cdot z_i \qquad \sigma_{s2posu_i} := \alpha \cdot \frac{M_{2u_i}}{I_{II_i}} \cdot z_i$$

Min and max stresses

$$\sigma_{s1posu} = \begin{pmatrix} 63.351 \\ 37.671 \\ 17.863 \\ 4.772 \end{pmatrix} \cdot MPa \qquad \sigma_{s2posu} = \begin{pmatrix} 100.627 \\ 60.441 \\ 28.918 \\ 7.788 \end{pmatrix} \cdot MPa$$

Star reinforcement on the top (o)

$$M_{2u_0} \cdot \frac{d_{sr}}{m} - M_{1u_0} \cdot \frac{d_{sr}}{m} = 1.161 \times 10^3 \cdot kN \cdot m$$

$$A_s := \frac{d_{sr}}{a_u} \cdot A_{siu} = 0.018 \cdot m^2 \qquad A'_s := A_{s_eqv} = 6.181 \times 10^{-3} \cdot m^2$$

$$d := d_{mu_0} = 1.505\,m \qquad d' := c_{soil} + \phi_o + \frac{\phi_o}{2}$$

$x_{II} := 0.23m$ Guess

$$x_{II} := root\left[d_{sr} \frac{x_{II}^2}{2} + (\alpha - 1) \cdot A'_s \cdot \left(x_{II} - d'\right) + \alpha \cdot A_s \cdot \left(x_{II} - d\right), x_{II} \right]$$

$x_{II} = 246.693 \cdot mm$

$$I_{II} := \frac{d_{sr} \cdot x_{II}^3}{12} + d_{sr} \cdot x_{II} \cdot \left(\frac{x_{II}}{2}\right)^2 + (\alpha - 1) \cdot A'_s \cdot \left(x_{II} - d'\right)^2 + \alpha \cdot A_s \cdot \left(d - x_{II}\right)^2$$

$z := d - x_{II}$

$$\sigma_{s1ring.pos} := \alpha \cdot \frac{M_{1o_0} \cdot \frac{d_{sr}}{m}}{I_{II}} \cdot z \qquad \sigma_{s2ring.pos} := \alpha \cdot \frac{M_{2o_0} \cdot \frac{d_{sr}}{m}}{I_{II}} \cdot z$$

$\sigma_{s1ring.pos} = -2.559 \times 10^7\,Pa$ $\sigma_{s2ring.pos} = -7.136 \times 10^7\,Pa$

Stress range for top reinforcement and compressed concrete

Fatigue due to negative moment (top reinforcement in tension)

$A_s := \frac{b_1}{a_o} \cdot A_{sio} = 3.272 \times 10^{-3} \cdot m^2$ $A'_s := \frac{b_1}{a_u} \cdot A_{siu} = 4.462 \times 10^{-3} \cdot m^2$

$d := d_{mo} = \begin{pmatrix} 1.555 \\ 1.555 \\ 1.521 \\ 1.473 \end{pmatrix} m$ $d'_i := c_{soil} + \phi_u + \frac{\phi_u}{2}$

$x_{II} := 0.23m$ Guess

$x_{II_i} := root\left[b_1 \frac{x_{II}^2}{2} + (\alpha - 1) \cdot A'_s \cdot \left(x_{II} - d'_i\right) + \alpha \cdot A_s \cdot \left(x_{II} - d_i\right), x_{II} \right]$

$x_{II} = \begin{pmatrix} 213.716 \\ 213.716 \\ 211.214 \\ 207.724 \end{pmatrix} \cdot mm$

$I_{II} := \frac{b_1 \cdot x_{II}^3}{12} + b_1 \cdot x_{II} \cdot \left(\frac{x_{II}}{2}\right)^2 + (\alpha - 1) \cdot A'_s \cdot \left(x_{II} - d'\right)^2 + \alpha \cdot A_s \cdot \left(d - x_{II}\right)^2$

$I_{II} = \begin{pmatrix} 0.043 \\ 0.043 \\ 0.042 \\ 0.039 \end{pmatrix} \cdot m^4$

Steel stress top (o) reinforcement

$z := d - x_{II}$

$\sigma_{s1nego_i} := \alpha \cdot \frac{\left|M_{1o_i}\right|}{I_{II_i}} \cdot z_i$ $\sigma_{s2nego_i} := \alpha \cdot \frac{\left|M_{2o_i}\right|}{I_{II_i}} \cdot z_i$

$\sigma_{s1nego} = \begin{pmatrix} 28.056 \\ 18.522 \\ 9.575 \\ 2.751 \end{pmatrix} \cdot MPa$ $\sigma_{s2nego} = \begin{pmatrix} 78.227 \\ 49.169 \\ 24.469 \\ 6.82 \end{pmatrix} \cdot MPa$

Steel stress bottom (u) reinforcement

$z := d' - x_{II}$

$\sigma_{s1negu_i} := \alpha \cdot \frac{\left|M_{1o_i}\right|}{I_{II_i}} \cdot z_i$ $\sigma_{s2negu_i} := \alpha \cdot \frac{\left|M_{2o_i}\right|}{I_{II_i}} \cdot z_i$

$$\sigma_{s1negu} = \begin{pmatrix} -1.594 \\ -1.052 \\ -0.539 \\ -0.153 \end{pmatrix} \cdot MPa \qquad \sigma_{s2negu} = \begin{pmatrix} -4.445 \\ -2.794 \\ -1.378 \\ -0.379 \end{pmatrix} \cdot MPa$$

Concrete stress bottom (u), check bottom fibre on safe side

$z := -x_{II}$

$$\sigma_{c1negu_i} := \frac{\left|M_{1o_i}\right|}{I_{II_i}} \cdot z_i \qquad \sigma_{c2negu_i} := \frac{\left|M_{2o_i}\right|}{I_{II_i}} \cdot z_i$$

$$\sigma_{c1negu} = \begin{pmatrix} -0.805 \\ -0.531 \\ -0.278 \\ -0.081 \end{pmatrix} \cdot MPa \qquad \sigma_{c2negu} = \begin{pmatrix} -2.243 \\ -1.41 \\ -0.71 \\ -0.202 \end{pmatrix} \cdot MPa$$

Star reinforcement on the top (o)

$$M_{2o_0} \cdot \frac{d_{sr}}{m} - M_{1o_0} \cdot \frac{d_{sr}}{m} = -1.161 \times 10^3 \cdot kN \cdot m \qquad M_{2o_0} - M_{1o_0} = -290.306 \cdot kN \cdot m$$

$A_s := A_{s_eqv} \qquad A'_s := \frac{d_{sr}}{a_u} \cdot A_{siu} = 0.018 \cdot m^2$

$d := d_{mo_0} = 1.555\,m \qquad d' := c + \phi_o + \frac{\phi_o}{2}$

$x_{II} := 0.23m$ Guess

$$x_{II} := root\left[d_{sr}\frac{x_{II}^2}{2} + (\alpha - 1)\cdot A'_s\cdot\left(x_{II} - d'\right) + \alpha\cdot A_s\cdot\left(x_{II} - d\right), x_{II}\right]$$

$x_{II} = 147.416 \cdot mm$

$$I_{II} := \frac{d_{sr}\cdot x_{II}^3}{12} + d_{sr}\cdot x_{II}\cdot\left(\frac{x_{II}}{2}\right)^2 + (\alpha - 1)\cdot A'_s\cdot\left(x_{II} - d'\right)^2 + \alpha\cdot A_s\cdot\left(d - x_{II}\right)^2$$

$z := d' - x_{II}$

$$\sigma_{s1ring.neg} := \alpha\cdot\frac{M_{1o_0}\cdot\frac{d_{sr}}{m}}{I_{II}}\cdot z \qquad \sigma_{s2ring.neg} := \alpha\cdot\frac{M_{2o_0}\cdot\frac{d_{sr}}{m}}{I_{II}}\cdot z$$

$\sigma_{s1ring.neg} = 2.977 \times 10^6\,Pa$

$\sigma_{s2ring.neg} = 8.301 \times 10^6\,Pa$

Fatigue verification reinforcement

stress range top reinforcement

$$\Delta\sigma_{so_i} := \max\left(\left|\sigma_{s2nego_i} - \sigma_{s1nego_i}\right|, \left|\sigma_{s2poso_i} - \sigma_{s1poso_i}\right|\right)$$

$$\Delta\sigma_{so} = \begin{pmatrix} 50.171 \\ 30.647 \\ 14.894 \\ 4.069 \end{pmatrix} \cdot \text{MPa}$$

stress range bottom reinforcement

$$\Delta\sigma_{su_i} := \max\left(\left|\sigma_{s2negu_i} - \sigma_{s1negu_i}\right|, \left|\sigma_{s2posu_i} - \sigma_{s1posu_i}\right|\right)$$

$$\Delta\sigma_{su} = \begin{pmatrix} 37.276 \\ 22.77 \\ 11.055 \\ 3.016 \end{pmatrix} \cdot \text{MPa}$$

The bottom reinforcement amount is constant. The reinforce under the anchor ring "between" section zero and zero is included in this check

$\gamma_{s.fat} := 1.15$ For straight reinforcement bars

$\gamma_{F.fat} := 1.0$

$\Delta\sigma_{Rsk} := 162.5\text{MPa}$

$$\frac{\Delta\sigma_{Rsk}}{\gamma_{s.fat}} = 141.304 \cdot \text{MPa}$$

Stress range star reinforcement

$$\Delta\sigma_{sring} := \max\left(\left|\sigma_{s2ring.pos} - \sigma_{s1ring.pos}\right|, \left|\sigma_{s2ring.neg} - \sigma_{s1ring.neg}\right|\right)$$

$$\Delta\sigma_{sring} = 45.765 \cdot \text{MPa}$$

$\Delta\sigma_{Rsk} := 162.5\text{MPa}$

$$\frac{\Delta\sigma_{Rsk}}{\gamma_{s.fat}} = 141.304 \cdot \text{MPa}$$

Verification of fatigue from equivalent load

[EN1992-1-1:2005 6.8.5]

$$\max\left(\Delta\sigma_{su}\right) \cdot \gamma_{F.fat} \le \frac{\Delta\sigma_{Rsk}}{\gamma_{s.fat}} = 1$$

$$\max\left(\Delta\sigma_{so}\right) \cdot \gamma_{F.fat} \le \frac{\Delta\sigma_{Rsk}}{\gamma_{s.fat}} = 1$$

$$UR_{fat.b.u} := \frac{\Delta\sigma_{su}\cdot\gamma_{F.fat}}{\frac{\Delta\sigma_{Rsk}}{\gamma_{s.fat}}} = \begin{pmatrix} 26.38 \\ 16.114 \\ 7.823 \\ 2.134 \end{pmatrix}\cdot\%$$

$$UR_{fat.b.o} := \frac{\Delta\sigma_{so}\cdot\gamma_{F.fat}}{\frac{\Delta\sigma_{Rsk}}{\gamma_{s.fat}}} = \begin{pmatrix} 35.505 \\ 21.689 \\ 10.54 \\ 2.88 \end{pmatrix}\cdot\%$$

Utilisation degree of bending reinforcement bottom (u) and top (o) (fatigue)

$$\Delta\sigma_{sring}\cdot\gamma_{F.fat} \le \frac{\Delta\sigma_{Rsk}}{\gamma_{s.fat}} = 1$$

$$U_{fat.star} := \frac{\Delta\sigma_{sring}\cdot\gamma_{F.fat}}{\frac{\Delta\sigma_{Rsk}}{\gamma_{s.fat}}} = 32.388\cdot\%$$

Utilisation degree of star reinforcement (fatigue)

Fatigue verification of concrete

Fatigue in compressed concrete, concrete stress range [EN 1992-1-1:2005 6.8.7]

$\Delta\sigma_{co} := \left|\sigma_{c2poso} - \sigma_{c1poso}\right| = 1.551\cdot MPa$

$\Delta\sigma_{cu} := \left|\sigma_{c2negu} - \sigma_{c1negu}\right| = 1.745\cdot MPa$

$t_0 := 28$ Assumed concrete age when fatigue loading starts

$s_c := 0.25$ Depending on cement type CEM 42.5 N

$\beta_{cc} := \exp\left[s_c\cdot\left(1 - \sqrt{\frac{28}{t_0}}\right)\right]$ $\beta_{cc} = 1$

$f_{cm} := \beta_{cc}\cdot\left(f_{ck} - 8MPa\right)$

$f_{cd} = 3 \times 10^7\ Pa$

$k_1 := 1$ For N=10^6 cycles

$$f_{cd.fat} := k_1\cdot\beta_{cc}\cdot f_{cd}\cdot\left(1 - \frac{\frac{f_{ck}}{MPa}}{250}\right)$$

$f_{cd.fat} = 24.6\cdot MPa$

$\sigma_{cd.min.equ.o} := \sigma_{c1poso}$ $\sigma_{cd.min.equ.u} := \sigma_{c1negu}$

$\sigma_{cd.max.equ.o} := \sigma_{c2poso}$ $\sigma_{cd.max.equ.u} := \sigma_{c2negu}$

$$E_{cd.min.equ.o} := \frac{\sigma_{cd.min.equ.o}}{f_{cd.fat}}$$ Lowest compressive stress level in a cycle

$$E_{cd.max.equ.o} := \frac{\sigma_{cd.max.equ.o}}{f_{cd.fat}}$$ Highest compressive stress level in a cycle

$$E_{cd.min.equ.u} := \frac{\sigma_{cd.min.equ.u}}{f_{cd.fat}}$$ Lowest compressive stress level in a cycle

$$E_{cd.max.equ.u} := \frac{\sigma_{cd.max.equ.u}}{f_{cd.fat}}$$ Highest compressive stress level in a cycle

$$R_{equ.o_i} := \frac{E_{cd.min.equ.o_i}}{E_{cd.max.equ.o_i}}$$ Stress ratio $$R_{equ.o} = \begin{pmatrix} 0.63 \\ 0.623 \\ 0.618 \\ 0.613 \end{pmatrix}$$

$$R_{equ.u_i} := \frac{E_{cd.min.equ.u_i}}{E_{cd.max.equ.u_i}}$$ Stress ratio $$R_{equ.u} = \begin{pmatrix} 0.359 \\ 0.377 \\ 0.391 \\ 0.403 \end{pmatrix}$$

$$\left|E_{cd.max.equ.o_i}\right| + 0.43 \cdot \sqrt{1 - R_{equ.o_i}} \le 1$$

$$\left|E_{cd.max.equ.u_i}\right| + 0.43 \cdot \sqrt{1 - R_{equ.u_i}} \le 1$$

$\left|E_{cd.max.equ.o_i}\right| + 0.43 \cdot \sqrt{1 - R_{equ.o_i}} =$

0.402
0.348
0.307
0.279

$\left|E_{cd.max.equ.u_i}\right| + 0.43 \cdot \sqrt{1 - R_{equ.u_i}} =$

0.436
0.397
0.364
0.34

$$UR_{fat.c.u_i} := \left(\left|E_{cd.max.equ.u_i}\right| + 0.43 \cdot \sqrt{1 - R_{equ.u_i}}\right)$$

$$UR_{fat.c.o_i} := \left(\left|E_{cd.max.equ.o_i}\right| + 0.43 \cdot \sqrt{1 - R_{equ.o_i}}\right)$$

$$UR_{fat.c.u} = \begin{pmatrix} 43.556 \\ 39.681 \\ 36.436 \\ 34.033 \end{pmatrix} \cdot \%$$

$$UR_{fat.c.o} = \begin{pmatrix} 40.211 \\ 34.826 \\ 30.672 \\ 27.877 \end{pmatrix} \cdot \%$$ Utilisation ratio of compressed concrete

E3. Fatigue control of local effects

Compressed concrete around the embedded steel ring

$$F_{xydfat} := \begin{pmatrix} F_{xydf1} \\ F_{xydf2} \end{pmatrix} \quad M_{dsfat} := \begin{pmatrix} M_{df1} \\ M_{df2} \end{pmatrix} \quad F_{dfat} := \begin{pmatrix} F_{zdf1} \\ F_{zdf2} \end{pmatrix}$$

$$M_{dafat} := F_{xydfat} \cdot h_4 + M_{dsfat} = \begin{pmatrix} 1.545 \times 10^4 \\ 2.913 \times 10^4 \end{pmatrix} \cdot kN \cdot m$$

$$\sigma_{mean.Fc.fat} := \left(\frac{F_{dfat}}{\pi \cdot d_{sr} \cdot d_1} + \frac{M_{dafat}}{I_0} \cdot r_1 + \frac{F_{dfat}}{\pi \cdot d_{sr} \cdot d_1} + \frac{M_{dafat}}{I_0} \cdot r_2 \right) \cdot \frac{1}{2} = \begin{pmatrix} 4.117 \\ 7.296 \end{pmatrix} \cdot MPa$$ Min/max stress

$$\sigma_{mean.Ft.fat} := \left(\frac{F_{dfat}}{\pi \cdot d_{sr} \cdot d_1} - \frac{M_{dafat}}{I_0} \cdot r_1 + \frac{F_{dfat}}{\pi \cdot d_{sr} \cdot d_1} - \frac{M_{dafat}}{I_0} \cdot r_2 \right) \cdot \frac{1}{2} = \begin{pmatrix} -3.065 \\ -6.244 \end{pmatrix} \cdot MPa$$ Min/max stress

Fatigue in compressed concrete at flange, concrete stress range

[EN 1992-1-1:2005 6.8.7]

Stress under and over the flange

$$\sigma_{anchor_Fc} := \begin{pmatrix} |\sigma_{mean.Fc.fat_0}| \\ |\sigma_{mean.Fc.fat_1}| \end{pmatrix} = \begin{pmatrix} 4.117 \\ 7.296 \end{pmatrix} \cdot MPa$$

$$\sigma_{anchor_Ft} := \begin{pmatrix} |\sigma_{mean.Ft.fat_0}| \\ |\sigma_{mean.Ft.fat_1}| \end{pmatrix} = \begin{pmatrix} 3.065 \\ 6.244 \end{pmatrix} \cdot MPa$$

$$\Delta\sigma_{c_bottom} := |\sigma_{anchor_Fc_1} - \sigma_{anchor_Fc_0}| = 3.179 \cdot MPa$$

$$\Delta\sigma_{c_top} := |\sigma_{anchor_Fc_1} - \sigma_{anchor_Fc_0}| = 3.179 \cdot MPa$$

$\Delta\sigma_{c_bottom} := \Delta\sigma_{c_top}$

$t_0 := 28$ Assumed concrete age when fatigue loading starts

$s_c := 0.25$ Depending on cement type CEM 42.5 N

$$\beta_{cc} := \exp\left[s_c \cdot \left(1 - \sqrt{\frac{28}{t_0}} \right) \right] \qquad \beta_{cc} = 1$$

$$f_{cm} := \beta_{cc} \cdot (f_{ck} - 8MPa)$$

$f_{cd} = 3 \times 10^7 \, Pa$

$k_1 := 1$ For N=10^6 cycles

$$f_{cd.fat} := k_1 \cdot \beta_{cc} \cdot f_{cd} \cdot \left(1 - \frac{\frac{f_{ck}}{MPa}}{250} \right)$$

$f_{cd.fat} = 24.6 \cdot MPa$

$$E_{cd.max.equ} := \frac{\sigma_{anchor_Ft_1}}{f_{cd.fat}} = 0.254$$ Highest ratio in a cycle

$$E_{cd.min.equ} := \frac{\sigma_{anchor_Ft_0}}{f_{cd.fat}} = 0.125$$ Lowest ratio in a cycle

$$R_{equ} := \frac{E_{cd.min.equ}}{E_{cd.max.equ}} = 0.491$$

$\left|E_{cd.max.equ}\right| + 0.43 \cdot \sqrt{1 - R_{equ}} \le 1 = 1$

$UR_{fat.cc.ring} := \left(\left|E_{cd.max.equ}\right| + 0.43 \cdot \sqrt{1 - R_{equ}}\right)$

$UR_{fat.cc.ring} = 56.066 \cdot \%$ Utilisation ration for fatigue in compressed concrete under embedded steel ring

U-bows

Fatigue U-bow [EN 1992-1-1:2005 6.8.5]

$a_{ubow} = 100 \cdot mm$ Spacing of U-bows

$$\sigma_{Ubow.max} := \begin{bmatrix} \left| \frac{\sigma_{mean.Fc.fat_0} \cdot a_{ubow} \cdot d_1}{2\left(\frac{\pi \cdot \phi_{Ubow}^2}{4}\right)} \right| \\ \left| \frac{\sigma_{mean.Fc.fat_1} \cdot a_{ubow} \cdot d_1}{2\left(\frac{\pi \cdot \phi_{Ubow}^2}{4}\right)} \right| \end{bmatrix} = \begin{pmatrix} 142.564 \\ 252.671 \end{pmatrix} \cdot MPa$$

$\Delta\sigma_{st} := \left|\sigma_{Ubow.max_1} - \sigma_{Ubow.max_0}\right|$ $\Delta\sigma_{st} = 110.107 \cdot MPa$

$D := 600mm$ Bending diameter

$\phi_w = 25 \cdot mm$ Diameter U-bow

$\zeta := 0.35 + 0.026 \cdot \frac{D}{\phi_w} = 0.974$ Reduction factor due to bent reinforcement bars

$\Delta\sigma_{Rsk} := 162.5MPa \cdot \zeta = 158.275 \cdot MPa$

$\gamma_{F.fat} = 1$ $\gamma_{s.fat} = 1.15$

$\Delta\sigma_{st} = 110.107 \cdot MPa$

Verification of fatigue from equivalent load

$\frac{\Delta\sigma_{Rsk}}{\gamma_{s.fat}} = 137.63 \cdot MPa$

$\Delta\sigma_{st} \cdot \gamma_{F.fat} \le \frac{\Delta\sigma_{Rsk}}{\gamma_{s.fat}}$

$U_{fat.Ubow} := \frac{\Delta\sigma_{st} \cdot \gamma_{F.fat}}{\frac{\Delta\sigma_{Rsk}}{\gamma_{s.fat}}} = 80.002 \cdot \%$ Utilisation ration for fatigue in U-bow reinforcement

G Fatigue verification with the full load spectra

Fatigue calculations for the full load spectra given by the wind turbine supplier.

G1. Loads and sectional forces

Loads

Amplitudes from load spectra:

Input of load spectra from excel, Appendix I:

$\Delta M_input :=$ Mxy.xls $\Delta F_{xy_input} :=$ Fxy.xls $n :=$ number of cycles.xls

$\Delta M := \Delta M_input \cdot kN \cdot m$

$\Delta F_{xy} := \Delta F_{xy_input} \cdot kN$

$\Delta F_z := 0kN$

Mean loads

$F_{xmean} := 316kN \qquad F_{ymean} := 4kN$

$F_{xymean} := \sqrt{F_{xmean}^2 + F_{ymean}^2} = 316.025 \cdot kN$

$M_{xmean} := 1888kN \cdot m$

$M_{xymean} := \sqrt{M_{xmean}^2 + M_{ymean}^2} = 2.138 \times 10^4 \cdot kN \cdot m$

$F_{zmean} := 2247kN$

Min/max fatigue load

$rows(\Delta M_input) = 280$ Total 280 loads

Due to technical functionality in Mathcad the loads initially can not be on vector form.

$k := 0 .. rows(\Delta M_input) - 1$

$M_{xydf1} := M_{xymean} - \frac{\Delta M_0}{2}$

$M_{xydf2} := M_{xymean} + \frac{\Delta M_0}{2}$

$F_{xydf1} := F_{xymean} - \frac{\Delta F_{xy_0}}{2}$

$F_{xydf2} := F_{xymean} + \frac{\Delta F_{xy_0}}{2}$

$$F_{zdf1} := F_{zmean} - \frac{\Delta F_z}{2}$$

$$F_{zdf2} := F_{zmean} + \frac{\Delta F_z}{2}$$

Sectional forces

$$e_{f1} := \frac{M_{df1} + F_{xydf1} \cdot h_4}{F_{zdf1} + G_d} \qquad e_{f2} := \frac{M_{df2} + F_{xydf2} \cdot h_4}{F_{zdf2} + G_d}$$

Depending on load-magnitude the soil pressure will distribute triangular over the full length or part of the full length. Smaller load result in a small eccentricity and the distribution is as follows:

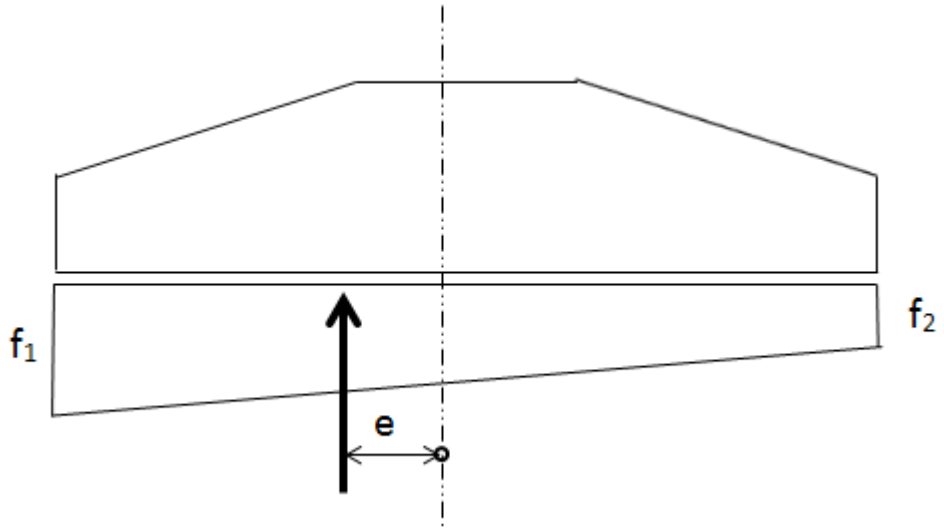

The fatigue loads are small and the soil pressure is spread over the full length. The distribution can be solved, two equations and two unknowns.

The following index system is used:

f_{11} - Max soil pressure (left side in figure above) and min fatigue load (load 1)

f_{12} - Max soil pressure (left side in figure above) and max fatigue load (load 2)

f_{21}- Min soil pressure (right side in figure above) and min fatigue load (load 1)

f_{22} - Min soil pressure (right side in figure above) and max fatigue load (load 2)

The gravity center must be equal to the eccentricity

$$\frac{\left[\frac{2\cdot\left(G_d + F_{zdf1} - \frac{f_{11}\cdot l}{2}\right)}{l}\right]\cdot\frac{l^2}{2} + \left[f_{11} - \left[\frac{2\cdot\left(G_d + F_{zdf1} - \frac{f_{11}\cdot l}{2}\right)}{l}\right]\right]\cdot\frac{2l^2}{6}}{l\cdot\frac{\left[f_{11} + \left[\frac{2\cdot\left(G_d + F_{zdf1} - \frac{f_{11}\cdot l}{2}\right)}{l}\right]\right]}{2}}$$

$$\frac{1}{3} + \frac{f_{11} \cdot l^2}{6 \cdot (G_d + F_{zdf1})}$$ Simplified expression

Equilibrium (for load 1)

$$f_{11} := \frac{1}{3} + \frac{f_{11} \cdot l^2}{6 \cdot (G_d + F_{zdf1})} = \left(e_{f1} + \frac{1}{2}\right) \left| \begin{array}{l} \text{explicit} \\ \text{solve}, f_{11} \rightarrow \end{array} \right.$$

$$f_{11}(e_{f1}, F_{zdf1}) := \frac{\left(e_{f1} + \frac{1}{6}\right) \cdot (6 \cdot G_d + 6 \cdot F_{zdf1})}{l^2}$$

$$f_{12} := \frac{f_{11} + f_{12}}{2} \cdot l = G_d + F_{zdf1} \left| \begin{array}{l} \text{explicit} \\ \text{solve}, f_{12} \rightarrow \end{array} \right.$$

$$f_{12}(e_{f1}, F_{zdf1}) := \left[(G_d + F_{zdf1}) \cdot \frac{2}{l} - \frac{\left(e_{f1} + \frac{1}{6}\right) \cdot (6 \cdot G_d + 6 \cdot F_{zdf1})}{l^2} \right]$$

Max load (load 2)

$$f_{21} := \frac{1}{3} + \frac{f_{21} \cdot l^2}{6 \cdot (G_d + F_{zdf2})} = \left(e_{f2} + \frac{1}{2}\right) \left| \begin{array}{l} \text{explicit} \\ \text{solve}, f_{21} \rightarrow \end{array} \right.$$

$$f_{21}(e_{f2}, F_{zdf2}) := \frac{\left(e_{f2} + \frac{1}{6}\right) \cdot (6 \cdot G_d + 6 \cdot F_{zdf2})}{l^2}$$

$$f_{22}(e_{f2}, F_{zdf2}) := (G_d + F_{zdf2}) \cdot \frac{2}{l} - f_{21}$$

$$f_{22}(e_{f2}, F_{zdf2}) := (G_d + F_{zdf2}) \cdot \frac{2}{l} - \frac{\left(e_{f2} + \frac{1}{6}\right) \cdot (6 \cdot G_d + 6 \cdot F_{zdf2})}{l^2}$$

For larger loads the soil pressure is spread over **a smaller** part of the length.
When the soil pressure is less then the full length, the width is a function of the eccentricity.

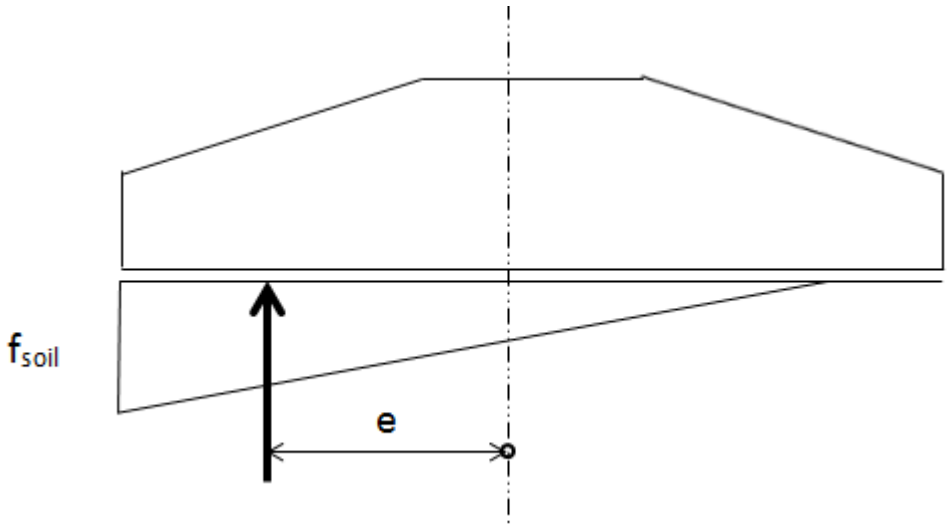

The width of the soil pressure assuming triangular distribution is:

$$b_{f1}(e_{f1}) := 3\left(\frac{1}{2} - e_{f1}\right) \qquad b_{f2}(e_{f2}) := 3\left(\frac{1}{2} - e_{f2}\right)$$

Where b_{f1} is for load 1 and b_{f2} for load 2

The soil pressure can be calculated:

$$f_{soil1}\left(b_{f1}(e_{f1}), F_{zdf1}\right) := \frac{F_{zdf1} + G_d}{\frac{b_{f1}(e_{f1})}{2}} \quad .\Rightarrow \quad f_{soil1}(e_{f1}, F_{zdf1}) := \frac{F_{zdf1} + G_d}{\frac{3\left(\frac{1}{2} - e_{f1}\right)}{2}}$$

$$f_{soil2}\left(b_{f2}(e_{f2}), F_{zdf2}\right) := \frac{F_{zdf2} + G_d}{\frac{b_{f2}(e_{f2})}{2}} \quad .\Rightarrow \quad f_{soil2}(e_{f2}, F_{zdf2}) := \frac{F_{zdf2} + G_d}{\frac{3\left(\frac{1}{2} - e_{f2}\right)}{2}}$$

The moment distribution can be calculated as a function of the eccentricity and loads

Moment distribution

$x := 0, 0.01m .. 15.5m$

Moment distribution when the soil pressure is spread over the full length

$F_{11}(x, e_{f1}, F_{zdf1})$ is the moment from soil pressure

$$F_{11}(x, e_{f1}, F_{zdf1}) := \left(f_{11}(e_{f1}, F_{zdf1}) - f_{12}(e_{f1}, F_{zdf1})\right) \cdot \frac{x^2}{2} - \frac{\left(f_{11}(e_{f1}, F_{zdf1}) - f_{12}(e_{f1}, F_{zdf1})\right)}{1} \cdot \frac{x^3}{6}$$

$$M_{f1}(x, e_{f1}, F_{zdf1}, F_{cf1}, F_{tf1}) := \begin{cases} F_{11}(x, e_{f1}, F_{zdf1}) + f_{12}(e_{f1}, F_{zdf1}) \cdot \frac{x^2}{2} - g_d \cdot \frac{x^2}{2} & \text{if } x < \frac{l - d_s}{2} \\ F_{11}(x, e_{f1}, F_{zdf1}) + f_{12}(e_{f1}, F_{zdf1}) \cdot \frac{x^2}{2} \ldots & \text{if } \frac{l - d_s}{2} \le x < \frac{l}{2} \\ + -g_d \cdot \frac{x^2}{2} - F_{cf1}\left(x - \frac{l - d_s}{2}\right) & \\ F_{11}(x, e_{f1}, F_{zdf1}) + f_{12}(e_{f1}, F_{zdf1}) \cdot \frac{x^2}{2} \ldots & \text{if } \frac{l}{2} \le x < \frac{l + d_s}{2} \\ + -g_d \cdot \frac{x^2}{2} - F_{cf1}\left(x - \frac{l - d_s}{2}\right) \ldots & \\ + -\frac{F_{zdf1}}{2} \cdot \left(x - \frac{l}{2}\right) & \\ F_{11}(x, e_{f1}, F_{zdf1}) + f_{12}(e_{f1}, F_{zdf1}) \cdot \frac{x^2}{2} - g_d \cdot \frac{x^2}{2} \ldots & \text{if } \frac{l + d_s}{2} \le x \le \\ + -F_{cf1}\left(x - \frac{l - d_s}{2}\right) - \frac{F_{zdf1}}{2} \cdot \left(x - \frac{l}{2}\right) \ldots & \\ + F_{tf1} \cdot \left(x - \frac{l + d_s}{2}\right) & \end{cases}$$

$$F_{21}(x, e_{f2}, F_{zdf2}) := \left(f_{21}(e_{f2}, F_{zdf2}) - f_{22}(e_{f2}, F_{zdf2})\right) \cdot \frac{x^2}{2} - \frac{\left(f_{21}(e_{f2}, F_{zdf2}) - f_{22}(e_{f2}, F_{zdf2})\right)}{l} \cdot \frac{x^3}{6}$$

$$M_{f2}(x, e_{f2}, F_{zdf2}, F_{cf2}, F_{tf2}) := \begin{cases} F_{21}(x, e_{f2}, F_{zdf2}) + f_{22}(e_{f2}, F_{zdf2}) \cdot \frac{x^2}{2} - g_d \cdot \frac{x^2}{2} & \text{if } x < \frac{l - d_s}{2} \\ F_{21}(x, e_{f2}, F_{zdf2}) + f_{22}(e_{f2}, F_{zdf2}) \cdot \frac{x^2}{2} \ldots & \text{if } \frac{l - d_s}{2} \le x < \frac{l}{2} \\ + -g_d \cdot \frac{x^2}{2} - F_{cf2}\left(x - \frac{l - d_s}{2}\right) & \\ F_{21}(x, e_{f2}, F_{zdf2}) + f_{22}(e_{f2}, F_{zdf2}) \cdot \frac{x^2}{2} \ldots & \text{if } \frac{l}{2} \le x < \frac{l + d_s}{2} \\ + -g_d \cdot \frac{x^2}{2} - F_{cf2}\left(x - \frac{l - d_s}{2}\right) \ldots & \\ + -\frac{F_{zdf2}}{2} \cdot \left(x - \frac{l}{2}\right) & \\ F_{21}(x, e_{f2}, F_{zdf2}) + f_{22}(e_{f2}, F_{zdf2}) \cdot \frac{x^2}{2} \ldots & \text{if } \frac{l + d_s}{2} \le x \le \\ + -g_d \cdot \frac{x^2}{2} - F_{cf2}\left(x - \frac{l - d_s}{2}\right) - \frac{F_{zdf2}}{2} \cdot \left(x - \frac{l}{2}\right) \ldots & \\ + F_{tf2} \cdot \left(x - \frac{l + d_s}{2}\right) & \end{cases}$$

Moment distribution when the soil pressure is spread over part of the length

$$F_{soil1}\left(x, e_{f1}, F_{zdf1}\right) := f_{soil1}\left(e_{f1}, F_{zdf1}\right)\cdot\frac{x^2}{2} - \frac{f_{soil1}\left(e_{f1}, F_{zdf1}\right)}{b_{f1}\left(e_{f1}\right)}\cdot\frac{x^3}{6}$$ moment from soil pressure

$$M'_{f1}\left(x, e_{f1}, F_{zdf1}, F_{cf1}, F_{tf1}\right) := \begin{cases} F_{soil1}\left(x, e_{f1}, F_{zdf1}\right) - g_d\cdot\frac{x^2}{2} & \text{if } x < \frac{l - d_s}{2} \\ F_{soil1}\left(x, e_{f1}, F_{zdf1}\right) - g_d\cdot\frac{x^2}{2} - F_{cf1}\left(x - \frac{l - d_s}{2}\right) & \text{if } \frac{l - d_s}{2} \le x < \\ F_{soil1}\left(x, e_{f1}, F_{zdf1}\right) - g_d\cdot\frac{x^2}{2} \ldots & \text{if } \frac{l}{2} \le x < \frac{l + d_s}{2} \\ \quad + -F_{cf1}\left(x - \frac{l - d_s}{2}\right) - \frac{F_{zdf1}}{2}\cdot\left(x - \frac{l}{2}\right) & \\ F_{soil1}\left(x, e_{f1}, F_{zdf1}\right) - g_d\cdot\frac{x^2}{2} \ldots & \text{if } \frac{l + d_s}{2} \le x < b_{f1}\left(e_{f1}\right) \\ \quad + -F_{cf1}\left(x - \frac{l - d_s}{2}\right) - \frac{F_{zdf1}}{2}\cdot\left(x - \frac{l}{2}\right) \ldots & \\ \quad + F_{tf1}\cdot\left(x - \frac{l + d_s}{2}\right) & \\ f_{soil1}\left(e_{f1}, F_{zdf1}\right)\cdot\frac{b_{f1}\left(e_{f1}\right)}{2}\cdot\left(x - \frac{b_{f1}\left(e_{f1}\right)}{3}\right) \ldots & \text{if } b_{f1}\left(e_{f1}\right) \le x \le l \\ \quad + -g_d\cdot\frac{x^2}{2} - F_{cf1}\cdot\left(x - \frac{l - d_s}{2}\right) \ldots & \\ \quad + -\frac{F_{zdf1}}{2}\cdot\left(x - \frac{l}{2}\right) + F_{tf1}\cdot\left(x - \frac{l + d_s}{2}\right) & \end{cases}$$

$$F_{soil2}\left(x, e_{f2}, F_{zdf2}\right) := f_{soil2}\left(e_{f2}, F_{zdf2}\right)\cdot\frac{x^2}{2} - \frac{f_{soil2}\left(e_{f2}, F_{zdf2}\right)}{b_{f2}\left(e_{f2}\right)}\cdot\frac{x^3}{6}$$

$$M'_{f2}(x, e_{f2}, F_{zdf2}, F_{cf2}, F_{tf2}) := \begin{cases} F_{soil2}(x, e_{f2}, F_{zdf2}) - g_d \cdot \frac{x^2}{2} & \text{if } x < \frac{l - d_s}{2} \\ F_{soil2}(x, e_{f2}, F_{zdf2}) - g_d \cdot \frac{x^2}{2} - F_{cf2}\left(x - \frac{l - d_s}{2}\right) & \text{if } \frac{l - d_s}{2} \le x < \\ F_{soil2}(x, e_{f2}, F_{zdf2}) - g_d \cdot \frac{x^2}{2} \ldots & \text{if } \frac{l}{2} \le x < \frac{l + d_s}{2} \\ + -F_{cf2}\left(x - \frac{l - d_s}{2}\right) - \frac{F_{zdf2}}{2} \cdot \left(x - \frac{l}{2}\right) & \\ F_{soil2}(x, e_{f2}, F_{zdf2}) - g_d \cdot \frac{x^2}{2} \ldots & \text{if } \frac{l + d_s}{2} \le x < b_{f2}(e_{f2}) \\ + -F_{cf2}\left(x - \frac{l - d_s}{2}\right) \ldots & \\ + -\frac{F_{zdf2}}{2} \cdot \left(x - \frac{l}{2}\right) + F_{tf2} \cdot \left(x - \frac{l + d_s}{2}\right) & \\ f_{soil2}(e_{f2}, F_{zdf2}) \cdot \frac{b_{f2}(e_{f2})}{2} \cdot \left(x - \frac{b_{f2}(e_{f2})}{3}\right) \ldots & \text{if } b_{f2}(e_{f2}) \le x \le l \\ + -g_d \cdot \frac{x^2}{2} - F_{cf2} \cdot \left(x - \frac{l - d_s}{2}\right) \ldots & \\ + -\frac{F_{zdf2}}{2} \cdot \left(x - \frac{l}{2}\right) + F_{tf2} \cdot \left(x - \frac{l + d_s}{2}\right) & \end{cases}$$

Use correct moment distribution, i.e. depending on soil pressure distribution

$$M_{fat1}(x, e_{f1}, F_{zdf2}, F_{cf1}, F_{tf1}) := \begin{cases} M_{f1}(x, e_{f1}, F_{zdf2}, F_{cf1}, F_{tf1}) & \text{if } b_{f1}(e_{f1}) \ge l \\ M'_{f1}(x, e_{f1}, F_{zdf2}, F_{cf1}, F_{tf1}) & \text{if } b_{f1}(e_{f1}) < l \end{cases}$$

$$M_{fat2}(x, e_{f2}, F_{zdf2}, F_{cf2}, F_{tf2}) := \begin{cases} M_{f2}(x, e_{f2}, F_{zdf2}, F_{cf2}, F_{tf2}) & \text{if } b_{f2}(e_{f2}) \ge l \\ M'_{f2}(x, e_{f2}, F_{zdf2}, F_{cf2}, F_{tf2}) & \text{if } b_{f2}(e_{f2}) < l \end{cases}$$

Calculate moments in four different sections in order to calculate stress variation

$$M_{df1} := M_{xymean} - \frac{\Delta M}{2} \qquad M_{df2} := M_{xymean} + \frac{\Delta M}{2}$$

$$F_{xydf1} := F_{xymean} - \frac{\Delta F_{xy}}{2} \qquad F_{xydf2} := F_{xymean} + \frac{\Delta F_{xy}}{2}$$

$$F_{zdf1} := F_{zmean} - \frac{\Delta F_z}{2} \qquad F_{zdf2} := F_{zmean} + \frac{\Delta F_z}{2}$$

$$F_{cf1_k} := \frac{M_{df1_k} + F_{xydf1_k} \cdot h4}{d_s} + \frac{F_{zdf1}}{4} \qquad F_{cf2_k} := \frac{M_{df2_k} + F_{xydf2_k} \cdot h4}{d_s} + \frac{F_{zdf2}}{4}$$

$$F_{tf1_k} := \frac{M_{df1_k} + F_{xydf1_k} \cdot h4}{d_s} - \frac{F_{zdf1}}{4} \qquad F_{tf2_k} := \frac{M_{df2_k} + F_{xydf2_k} \cdot h4}{d_s} - \frac{F_{zdf2}}{4}$$

$$e_{fl_k} := \frac{M_{dfl_k} + F_{xydfl_k} \cdot h_4}{F_{zdfl} + G_d} \qquad e_{fl_k} := \frac{M_{df2_k} + F_{xydf2_k} \cdot h_4}{F_{zdf2} + G_d}$$

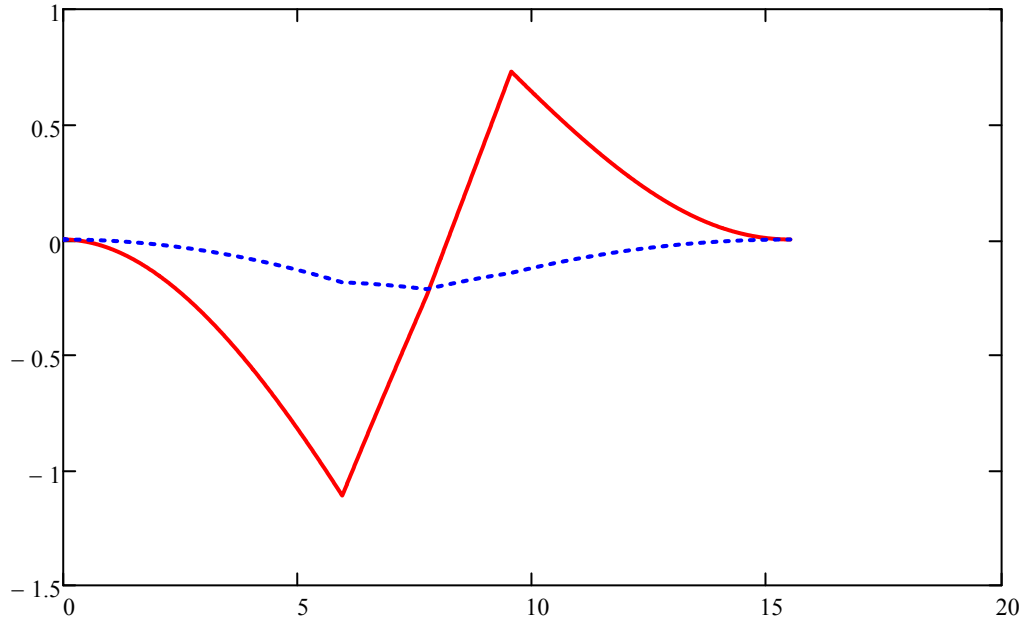

Largest moment amplitude

Control fatigue in different sections

The fatigue control is performed in the section described in C.1. Since reinforcement should be controll for both tension and compression both negative and positive moment is considered.

Minimum moment in section 0-3, fatigue

$$M_{10u_k} := M_{fatl}\left(l_x, e_{fl_k}, F_{zdfl}, F_{cfl_k}, F_{tfl_k}\right) \cdot \frac{b_1}{l}$$

$$M_{11u_k} := M_{fatl}\left(\frac{3l_x}{4}, e_{fl_k}, F_{zdfl}, F_{cfl_k}, F_{tfl_k}\right) \cdot \frac{b_1}{l}$$

$$M_{12u_k} := M_{fatl}\left(\frac{2l_x}{4}, e_{fl_k}, F_{zdfl}, F_{cfl_k}, F_{tfl_k}\right) \cdot \frac{b_1}{l}$$

$$M_{13u_k} := M_{fatl}\left(\frac{l_x}{4}, e_{fl_k}, F_{zdfl}, F_{cfl_k}, F_{tfl_k}\right) \cdot \frac{b_1}{l}$$

$$M_{10o_k} := M_{fatl}\left[\left(l_x + d_s\right), e_{fl_k}, F_{zdfl}, F_{cfl_k}, F_{tfl_k}\right] \cdot \frac{b_1}{l}$$

$$M_{11o_k} := M_{fatl}\left[\left(l_x + d_s + \frac{l_x}{4}\right), e_{fl_k}, F_{zdfl}, F_{cfl_k}, F_{tfl_k}\right] \cdot \frac{b_1}{l}$$

$$M_{12o_k} := M_{fatl}\left[\left(l_x + d_s + \frac{2l_x}{4}\right), e_{fl_k}, F_{zdfl}, F_{cfl_k}, F_{tfl_k}\right] \cdot \frac{b_1}{l}$$

$$M_{13o_k} := M_{fat1}\left[\left(l_x + d_s + \frac{3l_x}{4}\right), e_{f1_k}, F_{zdf1}, F_{cf1_k}, F_{tf1_k}\right]\cdot\frac{b_1}{l}$$

Maximum moment in section 0-3, fatigue

$$M_{20u_k} := M_{fat2}\left(l_x, e_{f2_k}, F_{zdf2}, F_{cf2_k}, F_{tf2_k}\right)\cdot\frac{b_1}{l}$$

$$M_{21u_k} := M_{fat2}\left(\frac{3l_x}{4}, e_{f2_k}, F_{zdf2}, F_{cf2_k}, F_{tf2_k}\right)\cdot\frac{b_1}{l}$$

$$M_{22u_k} := M_{fat2}\left(\frac{2l_x}{4}, e_{f2_k}, F_{zdf2}, F_{cf2_k}, F_{tf2_k}\right)\cdot\frac{b_1}{l}$$

$$M_{23u_k} := M_{fat2}\left(\frac{l_x}{4}, e_{f2_k}, F_{zdf2}, F_{cf2_k}, F_{tf2_k}\right)\cdot\frac{b_1}{l}$$

$$M_{20o_k} := M_{fat2}\left[\left(l_x + d_s\right), e_{f2_k}, F_{zdf2}, F_{cf2_k}, F_{tf2_k}\right]\cdot\frac{b_1}{l}$$

$$M_{21o_k} := M_{fat2}\left[\left(l_x + d_s + \frac{l_x}{4}\right), e_{f2_k}, F_{zdf2}, F_{cf2_k}, F_{tf2_k}\right]\cdot\frac{b_1}{l}$$

$$M_{22o_k} := M_{fat2}\left[\left(l_x + d_s + \frac{2l_x}{4}\right), e_{f2_k}, F_{zdf2}, F_{cf2_k}, F_{tf2_k}\right]\cdot\frac{b_1}{l}$$

$$M_{23o_k} := M_{fat2}\left[\left(l_x + d_s + \frac{3l_x}{4}\right), e_{f2_k}, F_{zdf2}, F_{cf2_k}, F_{tf2_k}\right]\cdot\frac{b_1}{l}$$

Stress variation due to moment

Fatigue due to bending. Check top and bottom reinforcement and compressive concrete

Use Navier's formula to calculate stresses, determine neutral axis and moment of inertia. Assume fully cracked member (stage II). According to EC compressive stresses must be checked as well. For concrete only compressive stresses is checked.

Bar spacing :	Bar diameter:	Concrete cover:
$a_{ov} := 150mm$	$\phi_u = 25\cdot mm$	$c_{soil} = 0.1\,m$
$a_{uv} := 110mm$	$\phi_o = 25\cdot mm$	$c = 50\cdot mm$

$\alpha = 5.556$

$\gamma_{s.fat} := 1.15$ For straight reinforcement bars

$\gamma_{F.fat} = 1$

$\Delta\sigma_{Rsk} := 162.5MPa$ [EC-1992-1-1:2005 6.8.4]

G.2 Fatigue in bending reinforcement

Fatigue due to positive moment (bottom reinforcement in tension)

$i := 0 .. 3$

$A_{sio} := \frac{\pi \cdot \phi_o^{\,2}}{4} = 490.874 \cdot mm^2$

$A_{siu} := \frac{\pi \cdot \phi_u^{\,2}}{4} = 490.874 \cdot mm^2$

$A_s := \frac{b_1}{a_u} \cdot A_{siu} = 4.462 \times 10^{-3} \cdot m^2 \qquad A'_s := \frac{b_1}{a_o} \cdot A_{sio} = 3.272 \times 10^{-3} \cdot m^2$

$d'_i := c + \phi_o + \frac{\phi_o}{2}$

$d_{mu} := \begin{pmatrix} 1.505 \\ 1.505 \\ 1.471 \\ 1.423 \end{pmatrix} m \qquad d := d_{mu}$

$x_{II} := 0.23m$ Guess

$x_{II_i} := \text{root}\left[b_1 \frac{x_{II}^{\,2}}{2} + (\alpha - 1) \cdot A'_s \cdot \left(x_{II} - d'_i\right) + \alpha \cdot A_s \cdot \left(x_{II} - d_i\right), x_{II} \right]$

$x_{II} = \begin{pmatrix} 241.027 \\ 241.027 \\ 238.009 \\ 233.69 \end{pmatrix} \cdot mm$

$I_{II} := \frac{b_1 \cdot x_{II}^{\,3}}{12} + b_1 \cdot x_{II} \cdot \left(\frac{x_{II}}{2}\right)^2 + (\alpha - 1) \cdot A'_s \cdot \left(x_{II} - d'\right)^2 + \alpha \cdot A_s \cdot \left(d - x_{II}\right)^2$

$I_{II} = \begin{pmatrix} 0.055 \\ 0.055 \\ 0.053 \\ 0.05 \end{pmatrix} \cdot m^4$

Steel stress top (o) reinforcement

$z := d' - x_{II}$

section 0

$\Delta\sigma_{SO0pos_k} := \left| \alpha \cdot \frac{M_{20u_k} - M_{10u_k}}{I_{II_0}} \cdot z_0 \right|$

$$\max\left(\Delta\sigma_{SO0pos}\right) = 14.438\cdot MPa$$

$$N_{O0pos_k} := \begin{cases} 1\cdot 10^6 \cdot \left(\frac{\frac{\Delta\sigma_{Rsk}}{\gamma_{s.fat}}}{\gamma_{F.fat}\cdot\Delta\sigma_{SO0pos_k}} \right)^5 & \text{if } \frac{\Delta\sigma_{Rsk}}{\gamma_{s.fat}} \le \gamma_{F.fat}\cdot\Delta\sigma_{SO0pos_k} \\ 1\cdot 10^6 \cdot \left(\frac{\frac{\Delta\sigma_{Rsk}}{\gamma_{s.fat}}}{\gamma_{F.fat}\cdot\Delta\sigma_{SO0pos_k}} \right)^9 & \text{if } \frac{\Delta\sigma_{Rsk}}{\gamma_{s.fat}} > \gamma_{F.fat}\cdot\Delta\sigma_{SO0pos_k} \end{cases}$$

$$d_{O0pos_k} := \frac{n_k}{N_{O0pos_k}} = \ldots$$

$$D_{Opos_0} := \sum_k d_{O0pos_k} = 7.313 \times 10^{-13}$$

section 1

$$\Delta\sigma_{SO1pos_k} := \left| \alpha\cdot\frac{M_{21u_k} - M_{11u_k}}{I_{II_1}}\cdot z_1 \right|$$

$$\max\left(\Delta\sigma_{SO1pos}\right) = 8.834\cdot MPa$$

$$N_{O1pos_k} := \begin{cases} 1\cdot 10^6 \cdot \left(\frac{\frac{\Delta\sigma_{Rsk}}{\gamma_{s.fat}}}{\gamma_{F.fat}\cdot\Delta\sigma_{SO1pos_k}} \right)^5 & \text{if } \frac{\Delta\sigma_{Rsk}}{\gamma_{s.fat}} \le \gamma_{F.fat}\cdot\Delta\sigma_{SO1pos_k} \\ 1\cdot 10^6 \cdot \left(\frac{\frac{\Delta\sigma_{Rsk}}{\gamma_{s.fat}}}{\gamma_{F.fat}\cdot\Delta\sigma_{SO1pos_k}} \right)^9 & \text{if } \frac{\Delta\sigma_{Rsk}}{\gamma_{s.fat}} > \gamma_{F.fat}\cdot\Delta\sigma_{SO1pos_k} \end{cases}$$

$$d_{O1pos_k} := \frac{n_k}{N_{O1pos_k}} = \ldots$$

$$D_{Opos_1} := \sum_k d_{O1pos_k} = 8.672 \times 10^{-15}$$

section 2

$$\Delta\sigma_{SO2pos_k} := \left| \alpha\cdot\frac{M_{22u_k} - M_{12u_k}}{I_{II_2}}\cdot z_2 \right|$$

$$\max\left(\Delta\sigma_{SO2pos}\right) = 4.315\cdot MPa$$

$$N_{O2pos_k} := \begin{cases} 1\cdot10^6\cdot\left(\dfrac{\frac{\Delta\sigma_{Rsk}}{\gamma_{s.fat}}}{\gamma_{F.fat}\cdot\Delta\sigma_{SO2pos_k}}\right)^5 & \text{if } \dfrac{\Delta\sigma_{Rsk}}{\gamma_{s.fat}} \le \gamma_{F.fat}\cdot\Delta\sigma_{SO2pos_k} \\ 1\cdot10^6\cdot\left(\dfrac{\frac{\Delta\sigma_{Rsk}}{\gamma_{s.fat}}}{\gamma_{F.fat}\cdot\Delta\sigma_{SO2pos_k}}\right)^9 & \text{if } \dfrac{\Delta\sigma_{Rsk}}{\gamma_{s.fat}} > \gamma_{F.fat}\cdot\Delta\sigma_{SO2pos_k} \end{cases}$$

$$d_{O2pos_k} := \frac{n_k}{N_{O2pos_k}} = \ldots$$

$$D_{Opos_2} := \sum_k d_{O2pos_k} = 0$$

section 3

$$\Delta\sigma_{SO3pos_k} := \left|\alpha\cdot\frac{M_{23u_k} - M_{13u_k}}{I_{II_3}}\cdot z_3\right|$$

$$\max\left(\Delta\sigma_{SO3pos}\right) = 1.187\cdot MPa$$

$$N_{O3pos_k} := \begin{cases} 1\cdot10^6\cdot\left(\dfrac{\frac{\Delta\sigma_{Rsk}}{\gamma_{s.fat}}}{\gamma_{F.fat}\cdot\Delta\sigma_{SO3pos_k}}\right)^5 & \text{if } \dfrac{\Delta\sigma_{Rsk}}{\gamma_{s.fat}} \le \gamma_{F.fat}\cdot\Delta\sigma_{SO3pos_k} \\ 1\cdot10^6\cdot\left(\dfrac{\frac{\Delta\sigma_{Rsk}}{\gamma_{s.fat}}}{\gamma_{F.fat}\cdot\Delta\sigma_{SO3pos_k}}\right)^9 & \text{if } \dfrac{\Delta\sigma_{Rsk}}{\gamma_{s.fat}} > \gamma_{F.fat}\cdot\Delta\sigma_{SO3pos_k} \end{cases}$$

$$d_{O3pos_k} := \frac{n_k}{N_{O3pos_k}} = \ldots$$

$$D_{Opos_3} := \sum_k d_{O3pos_k} = 0$$

Steel stress bottom (u) reinforcement

$$z := d - x_{II}$$

section 0

$$\Delta\sigma_{SU0pos_k} := \left|\alpha\cdot\frac{M_{20u_k} - M_{10u_k}}{I_{II_0}}\cdot z_0\right|$$

$$\max\left(\Delta\sigma_{SU0pos}\right) = 118.863\cdot MPa$$

$$N_{U0pos_k} := \begin{cases} 1\cdot 10^6 \cdot \left(\frac{\frac{\Delta\sigma_{Rsk}}{\gamma_{s.fat}}}{\gamma_{F.fat}\cdot\Delta\sigma_{SU0pos_k}} \right)^5 & \text{if } \frac{\Delta\sigma_{Rsk}}{\gamma_{s.fat}} \le \gamma_{F.fat}\cdot\Delta\sigma_{SU0pos_k} \\ 1\cdot 10^6 \cdot \left(\frac{\frac{\Delta\sigma_{Rsk}}{\gamma_{s.fat}}}{\gamma_{F.fat}\cdot\Delta\sigma_{SU0pos_k}} \right)^9 & \text{if } \frac{\Delta\sigma_{Rsk}}{\gamma_{s.fat}} > \gamma_{F.fat}\cdot\Delta\sigma_{SU0pos_k} \end{cases}$$

$$d_{U0pos_k} := \frac{n_k}{N_{U0pos_k}} = \ldots$$

$$D_{Upos_0} := \sum_k d_{U0pos_k} = 1.271 \times 10^{-4}$$

section 1

$$\Delta\sigma_{SU1pos_k} := \left| \alpha\cdot\frac{M_{21u_k} - M_{11u_k}}{I_{II_1}}\cdot z_1 \right|$$

$$\max\left(\Delta\sigma_{SU1pos}\right) = 72.729\cdot MPa$$

$$N_{U1pos_k} := \begin{cases} 1\cdot 10^6 \cdot \left(\frac{\frac{\Delta\sigma_{Rsk}}{\gamma_{s.fat}}}{\gamma_{F.fat}\cdot\Delta\sigma_{SU1pos_k}} \right)^5 & \text{if } \frac{\Delta\sigma_{Rsk}}{\gamma_{s.fat}} \le \gamma_{F.fat}\cdot\Delta\sigma_{SU1pos_k} \\ 1\cdot 10^6 \cdot \left(\frac{\frac{\Delta\sigma_{Rsk}}{\gamma_{s.fat}}}{\gamma_{F.fat}\cdot\Delta\sigma_{SU1pos_k}} \right)^9 & \text{if } \frac{\Delta\sigma_{Rsk}}{\gamma_{s.fat}} > \gamma_{F.fat}\cdot\Delta\sigma_{SU1pos_k} \end{cases}$$

$$d_{U1pos_k} := \frac{n_k}{N_{U1pos_k}} = \ldots$$

$$D_{Upos_1} := \sum_k d_{U1pos_k} = 1.507 \times 10^{-6}$$

section 2

$$\Delta\sigma_{SU2pos_k} := \left| \alpha\cdot\frac{M_{22u_k} - M_{12u_k}}{I_{II_2}}\cdot z_2 \right|$$

$$\max\left(\Delta\sigma_{SU2pos}\right) = 35.353\cdot MPa$$

$$N_{U2pos_k} := \begin{cases} 1\cdot10^6\cdot\left(\dfrac{\dfrac{\Delta\sigma_{Rsk}}{\gamma_{s.fat}}}{\gamma_{F.fat}\cdot\Delta\sigma_{SU2pos_k}}\right)^5 & \text{if } \dfrac{\Delta\sigma_{Rsk}}{\gamma_{s.fat}} \le \gamma_{F.fat}\cdot\Delta\sigma_{SU2pos_k} \\ 1\cdot10^6\cdot\left(\dfrac{\dfrac{\Delta\sigma_{Rsk}}{\gamma_{s.fat}}}{\gamma_{F.fat}\cdot\Delta\sigma_{SU2pos_k}}\right)^9 & \text{if } \dfrac{\Delta\sigma_{Rsk}}{\gamma_{s.fat}} > \gamma_{F.fat}\cdot\Delta\sigma_{SU2pos_k} \end{cases}$$

$$d_{U2pos_k} := \frac{n_k}{N_{U2pos_k}} = \ldots$$

$$D_{Upos_2} := \sum_k d_{U2pos_k} = 2.257 \times 10^{-9}$$

section 3

$$\Delta\sigma_{SU3pos_k} := \left|\alpha\cdot\frac{M_{23u_k} - M_{13u_k}}{I_{II_3}}\cdot z_3\right|$$

$$\max\left(\Delta\sigma_{SU3pos}\right) = 9.657\cdot MPa$$

$$N_{U3pos_k} := \begin{cases} 1\cdot10^6\cdot\left(\dfrac{\dfrac{\Delta\sigma_{Rsk}}{\gamma_{s.fat}}}{\gamma_{F.fat}\cdot\Delta\sigma_{SU3pos_k}}\right)^5 & \text{if } \dfrac{\Delta\sigma_{Rsk}}{\gamma_{s.fat}} \le \gamma_{F.fat}\cdot\Delta\sigma_{SU3pos_k} \\ 1\cdot10^6\cdot\left(\dfrac{\dfrac{\Delta\sigma_{Rsk}}{\gamma_{s.fat}}}{\gamma_{F.fat}\cdot\Delta\sigma_{SU3pos_k}}\right)^9 & \text{if } \dfrac{\Delta\sigma_{Rsk}}{\gamma_{s.fat}} > \gamma_{F.fat}\cdot\Delta\sigma_{SU3pos_k} \end{cases}$$

$$d_{U3pos_k} := \frac{n_k}{N_{U3pos_k}} = \ldots$$

$$d_{U3pos_k} := \frac{n_k}{N_{U3pos_k}} = \ldots$$

$$D_{Upos_3} := \sum_k d_{U3pos_k} = 1.891 \times 10^{-14}$$

Fatigue due to negative moment (bottom reinforcement in tension)

$$A_{sv} := \frac{b_1}{a_o}\cdot A_{sio} = 3.272 \times 10^{-3}\cdot m^2 \qquad A'_{sv} := \frac{b_1}{a_u}\cdot A_{siu} = 4.462 \times 10^{-3}\cdot m^2$$

$$d_{mo} := \begin{pmatrix} 1.555 \\ 1.555 \\ 1.521 \\ 1.473 \end{pmatrix} m \quad d := d_{mo} \qquad d'_i := c_{soil} + \phi_u + \frac{\phi_u}{2}$$

$x_{II} := 0.23m$ Guess

$$x_{II_i} := root\left[b_1 \frac{x_{II}^2}{2} + (\alpha - 1)\cdot A'_s\cdot\left(x_{II} - d'_i\right) + \alpha\cdot A_s\cdot\left(x_{II} - d_i\right), x_{II}\right]$$

$$x_{II} = \begin{pmatrix} 213.71 \\ 213.71 \\ 211.247 \\ 207.729 \end{pmatrix}\cdot mm$$

$$I_{II} := \frac{b_1\cdot x_{II}^3}{12} + b_1\cdot x_{II}\cdot\left(\frac{x_{II}}{2}\right)^2 + (\alpha - 1)\cdot A'_s\cdot\left(x_{II} - d'\right)^2 + \alpha\cdot A_s\cdot\left(d - x_{II}\right)^2$$

$$I_{II} = \begin{pmatrix} 0.043 \\ 0.043 \\ 0.042 \\ 0.039 \end{pmatrix}\cdot m^4$$

Steel stress top (o) reinforcement

$z := d - x_{II}$

section 0

$$\Delta\sigma_{SO0neg_k} := \left|\alpha\cdot\frac{M_{20u_k} - M_{10u_k}}{I_{II_0}}\cdot z_0\right|$$

$\max\left(\Delta\sigma_{SO0neg}\right) = 159.983\cdot MPa$

$$N_{O0neg_k} := \begin{cases} 1\cdot 10^6\cdot\left(\dfrac{\dfrac{\Delta\sigma_{Rsk}}{\gamma_{s.fat}}}{\gamma_{F.fat}\cdot\Delta\sigma_{SO0neg_k}}\right)^5 & \text{if } \dfrac{\Delta\sigma_{Rsk}}{\gamma_{s.fat}} \le \gamma_{F.fat}\cdot\Delta\sigma_{SO0neg_k} \\ 1\cdot 10^6\cdot\left(\dfrac{\dfrac{\Delta\sigma_{Rsk}}{\gamma_{s.fat}}}{\gamma_{F.fat}\cdot\Delta\sigma_{SO0neg_k}}\right)^9 & \text{if } \dfrac{\Delta\sigma_{Rsk}}{\gamma_{s.fat}} > \gamma_{F.fat}\cdot\Delta\sigma_{SO0neg_k} \end{cases}$$

$$d_{O0neg_k} := \frac{n_k}{N_{O0neg_k}} = \ldots$$

$$D_{Oneg_0} := \sum_k d_{O0neg_k} = 1.806 \times 10^{-3}$$

section 1

$$\Delta\sigma_{SO1neg_k} := \left| \alpha \cdot \frac{M_{21u_k} - M_{11u_k}}{I_{II_1}} \cdot z_1 \right|$$

$$\max\left(\Delta\sigma_{SO1neg}\right) = 97.89 \cdot MPa$$

$$N_{O1neg_k} := \begin{cases} 1 \cdot 10^6 \cdot \left(\frac{\frac{\Delta\sigma_{Rsk}}{\gamma_{s.fat}}}{\gamma_{F.fat} \cdot \Delta\sigma_{SO1neg_k}} \right)^5 & \text{if } \frac{\Delta\sigma_{Rsk}}{\gamma_{s.fat}} \le \gamma_{F.fat} \cdot \Delta\sigma_{SO1neg_k} \\ 1 \cdot 10^6 \cdot \left(\frac{\frac{\Delta\sigma_{Rsk}}{\gamma_{s.fat}}}{\gamma_{F.fat} \cdot \Delta\sigma_{SO1neg_k}} \right)^9 & \text{if } \frac{\Delta\sigma_{Rsk}}{\gamma_{s.fat}} > \gamma_{F.fat} \cdot \Delta\sigma_{SO1neg_k} \end{cases}$$

$$d_{O1neg_k} := \frac{n_k}{N_{O1neg_k}} = \ldots$$

$$D_{Oneg_1} := \sum_k d_{O1neg_k} = 2.184 \times 10^{-5}$$

section 2

$$\Delta\sigma_{SO2neg_k} := \left| \alpha \cdot \frac{M_{22u_k} - M_{12u_k}}{I_{II_2}} \cdot z_2 \right|$$

$$\max\left(\Delta\sigma_{SO2neg}\right) = 47.63 \cdot MPa$$

$$N_{O2neg_k} := \begin{cases} 1 \cdot 10^6 \cdot \left(\frac{\frac{\Delta\sigma_{Rsk}}{\gamma_{s.fat}}}{\gamma_{F.fat} \cdot \Delta\sigma_{SO2neg_k}} \right)^5 & \text{if } \frac{\Delta\sigma_{Rsk}}{\gamma_{s.fat}} \le \gamma_{F.fat} \cdot \Delta\sigma_{SO2neg_k} \\ 1 \cdot 10^6 \cdot \left(\frac{\frac{\Delta\sigma_{Rsk}}{\gamma_{s.fat}}}{\gamma_{F.fat} \cdot \Delta\sigma_{SO2neg_k}} \right)^9 & \text{if } \frac{\Delta\sigma_{Rsk}}{\gamma_{s.fat}} > \gamma_{F.fat} \cdot \Delta\sigma_{SO2neg_k} \end{cases}$$

$$d_{O2neg_k} := \frac{n_k}{N_{O2neg_k}} = \ldots$$

$$D_{Oneg_2} := \sum_k d_{O2neg_k} = 3.3 \times 10^{-8}$$

section 3

$$\Delta\sigma_{SO3neg_k} := \left| \alpha \cdot \frac{M_{23u_k} - M_{13u_k}}{I_{II_3}} \cdot z_3 \right|$$

$$\max\left(\Delta\sigma_{SO3neg}\right) = 13.03 \cdot MPa$$

$$N_{O3neg_k} := \begin{cases} 1 \cdot 10^6 \cdot \left(\frac{\frac{\Delta\sigma_{Rsk}}{\gamma_{s.fat}}}{\gamma_{F.fat} \cdot \Delta\sigma_{SO3neg_k}} \right)^5 & \text{if } \frac{\Delta\sigma_{Rsk}}{\gamma_{s.fat}} \le \gamma_{F.fat} \cdot \Delta\sigma_{SO3neg_k} \\ 1 \cdot 10^6 \cdot \left(\frac{\frac{\Delta\sigma_{Rsk}}{\gamma_{s.fat}}}{\gamma_{F.fat} \cdot \Delta\sigma_{SO3neg_k}} \right)^9 & \text{if } \frac{\Delta\sigma_{Rsk}}{\gamma_{s.fat}} > \gamma_{F.fat} \cdot \Delta\sigma_{SO3neg_k} \end{cases}$$

$$d_{O3neg_k} := \frac{n_k}{N_{O3neg_k}} = \ldots$$

$$D_{Oneg_3} := \sum_k d_{O3neg_k} = 2.804 \times 10^{-13}$$

Steel stress bottom (u) reinforcement

$z := d' - x_{II}$

section 0

$$\Delta\sigma_{SU0neg_k} := \left| \alpha \cdot \frac{M_{20u_k} - M_{10u_k}}{I_{II_0}} \cdot z_0 \right|$$

$$\max\left(\Delta\sigma_{SU0neg}\right) = 9.09 \cdot MPa$$

$$N_{U0neg_k} := \begin{cases} 1 \cdot 10^6 \cdot \left(\frac{\frac{\Delta\sigma_{Rsk}}{\gamma_{s.fat}}}{\gamma_{F.fat} \cdot \Delta\sigma_{SU0neg_k}} \right)^5 & \text{if } \frac{\Delta\sigma_{Rsk}}{\gamma_{s.fat}} \le \gamma_{F.fat} \cdot \Delta\sigma_{SU0neg_k} \\ 1 \cdot 10^6 \cdot \left(\frac{\frac{\Delta\sigma_{Rsk}}{\gamma_{s.fat}}}{\gamma_{F.fat} \cdot \Delta\sigma_{SU0neg_k}} \right)^9 & \text{if } \frac{\Delta\sigma_{Rsk}}{\gamma_{s.fat}} > \gamma_{F.fat} \cdot \Delta\sigma_{SU0neg_k} \end{cases}$$

$$d_{U0neg_k} := \frac{n_k}{N_{U0neg_k}} = \ldots$$

$$D_{Uneg_0} := \sum_k d_{U0neg_k} = 1.137 \times 10^{-14}$$

section 1

$$\Delta\sigma_{SU1neg_k} := \left| \alpha \cdot \frac{M_{21u_k} - M_{11u_k}}{I_{II_1}} \cdot z_1 \right|$$

$$\max\left(\Delta\sigma_{SU1neg}\right) = 5.562 \cdot MPa$$

$$N_{U1neg_k} := \begin{cases} 1 \cdot 10^6 \cdot \left(\frac{\frac{\Delta\sigma_{Rsk}}{\gamma_{s.fat}}}{\gamma_{F.fat} \cdot \Delta\sigma_{SU1neg_k}} \right)^5 & \text{if } \frac{\Delta\sigma_{Rsk}}{\gamma_{s.fat}} \le \gamma_{F.fat} \cdot \Delta\sigma_{SU1neg_k} \\ 1 \cdot 10^6 \cdot \left(\frac{\frac{\Delta\sigma_{Rsk}}{\gamma_{s.fat}}}{\gamma_{F.fat} \cdot \Delta\sigma_{SU1neg_k}} \right)^9 & \text{if } \frac{\Delta\sigma_{Rsk}}{\gamma_{s.fat}} > \gamma_{F.fat} \cdot \Delta\sigma_{SU1neg_k} \end{cases}$$

$$d_{U1neg_k} := \frac{n_k}{N_{U1neg_k}} = \ldots$$

$$D_{Uneg_1} := \sum_k d_{U1neg_k} = 0$$

section 2

$$\Delta\sigma_{SU2neg_k} := \left| \alpha \cdot \frac{M_{22u_k} - M_{12u_k}}{I_{II_2}} \cdot z_2 \right|$$

$$\max\left(\Delta\sigma_{SU2neg}\right) = 2.682 \cdot MPa$$

$$N_{U2neg_k} := \begin{cases} 1 \cdot 10^6 \cdot \left(\frac{\frac{\Delta\sigma_{Rsk}}{\gamma_{s.fat}}}{\gamma_{F.fat} \cdot \Delta\sigma_{SU2neg_k}} \right)^5 & \text{if } \frac{\Delta\sigma_{Rsk}}{\gamma_{s.fat}} \le \gamma_{F.fat} \cdot \Delta\sigma_{SU2neg_k} \\ 1 \cdot 10^6 \cdot \left(\frac{\frac{\Delta\sigma_{Rsk}}{\gamma_{s.fat}}}{\gamma_{F.fat} \cdot \Delta\sigma_{SU2neg_k}} \right)^9 & \text{if } \frac{\Delta\sigma_{Rsk}}{\gamma_{s.fat}} > \gamma_{F.fat} \cdot \Delta\sigma_{SU2neg_k} \end{cases}$$

$$d_{U2neg_k} := \frac{n_k}{N_{U2neg_k}} = \ldots$$

$$D_{Uneg_2} := \sum_k d_{U2neg_k} = 0$$

section 3

$$\Delta\sigma_{SU3neg_k} := \left| \alpha \cdot \frac{M_{23u_k} - M_{13u_k}}{I_{II_3}} \cdot z_3 \right|$$

$$\max\left(\Delta\sigma_{SU3neg}\right) = 0.723 \cdot MPa$$

$$N_{U3neg_k} := \begin{cases} 1 \cdot 10^6 \cdot \left(\frac{\frac{\Delta\sigma_{Rsk}}{\gamma_{s.fat}}}{\gamma_{F.fat} \cdot \Delta\sigma_{SU3neg_k}} \right)^5 & \text{if } \frac{\Delta\sigma_{Rsk}}{\gamma_{s.fat}} \le \gamma_{F.fat} \cdot \Delta\sigma_{SU3neg_k} \\ 1 \cdot 10^6 \cdot \left(\frac{\frac{\Delta\sigma_{Rsk}}{\gamma_{s.fat}}}{\gamma_{F.fat} \cdot \Delta\sigma_{SU3neg_k}} \right)^9 & \text{if } \frac{\Delta\sigma_{Rsk}}{\gamma_{s.fat}} > \gamma_{F.fat} \cdot \Delta\sigma_{SU3neg_k} \end{cases}$$

$$d_{U3neg_k} := \frac{n_k}{N_{U3neg_k}} = \ldots$$

$$D_{Uneg_3} := \sum_k d_{U3neg_k} = 0$$

Star reinforcement on the top (o)

$A_{s_eqv} := 6.181 \times 10^3 \ mm^2$

$A_s := A_{s_eqv}$ $\quad A'_s := \frac{b_1}{a_o} \cdot A_{sio} = 3.272 \times 10^{-3} \cdot m^2$

$d := d_{mo_0} = 1.555 \ m$ $\quad d' := c + \phi_o + \frac{\phi_o}{2}$

$x_{II} := 0.23m$ $\quad$ Guess

$$x_{II} := root\left[b_1 \frac{x_{II}^2}{2} + (\alpha - 1) \cdot A'_s \cdot \left(x_{II} - d'\right) + \alpha \cdot A_s \cdot \left(x_{II} - d\right), x_{II} \right]$$

$x_{II} = 285.16 \cdot mm$

$$I_{II} := \frac{b_1 \cdot x_{II}^3}{12} + b_1 \cdot x_{II} \cdot \left(\frac{x_{II}}{2}\right)^2 + (\alpha - 1) \cdot A'_s \cdot \left(x_{II} - d'\right)^2 + \alpha \cdot A_s \cdot \left(d - x_{II}\right)^2$$

Steel stress star reinforcement

$z := d' - x_{II}$

$$\Delta\sigma_{SSTAR_k} := \left| \alpha \cdot \frac{M_{20o_k} - M_{10o_k}}{I_{II}} \cdot z \right|$$

$$\max\left(\Delta\sigma_{SSTAR}\right) = 15.071\cdot MPa$$

$$N_{STAR_k} := \begin{cases} 1\cdot 10^6 \cdot \left(\dfrac{\dfrac{\Delta\sigma_{Rsk}}{\gamma_{s.fat}}}{\gamma_{F.fat}\cdot\Delta\sigma_{SSTAR_k}} \right)^5 & \text{if } \dfrac{\Delta\sigma_{Rsk}}{\gamma_{s.fat}} \le \gamma_{F.fat}\cdot\Delta\sigma_{SSTAR_k} \\ 1\cdot 10^6 \cdot \left(\dfrac{\dfrac{\Delta\sigma_{Rsk}}{\gamma_{s.fat}}}{\gamma_{F.fat}\cdot\Delta\sigma_{SSTAR_k}} \right)^9 & \text{if } \dfrac{\Delta\sigma_{Rsk}}{\gamma_{s.fat}} > \gamma_{F.fat}\cdot\Delta\sigma_{SSTAR_k} \end{cases}$$

$$d_{STAR_k} := \frac{n_k}{N_{STAR_k}} = \ldots$$

$$D_{star} := \sum_k d_{STAR_k} = 1.738 \times 10^{-12}$$

Damage results :

$$D_{Upos} = \begin{pmatrix} 0.013 \\ 1.507 \times 10^{-4} \\ 2.257 \times 10^{-7} \\ 1.891 \times 10^{-12} \end{pmatrix} \cdot \%$$

$$D_{Opos} = \begin{pmatrix} 7.313 \times 10^{-11} \\ 8.672 \times 10^{-13} \\ 1.358 \times 10^{-15} \\ 0 \end{pmatrix} \cdot \%$$

$$D_{Uneg} = \begin{pmatrix} 1.137 \times 10^{-12} \\ 1.348 \times 10^{-14} \\ 0 \\ 0 \end{pmatrix} \cdot \%$$

$$D_{Oneg} = \begin{pmatrix} 0.181 \\ 2.184 \times 10^{-3} \\ 3.3 \times 10^{-6} \\ 2.804 \times 10^{-11} \end{pmatrix} \cdot \%$$

$$D_{star} = 1.738 \times 10^{-10} \cdot \%$$

G.3 Shear force distribution

Shear force distribution fatigue loading

$$V_{f1}\left(x, e_{f1}, F_{zdf1}, F_{cf1}, F_{tf1}\right) := \begin{cases} f_{11}\left(e_{f1}, F_{zdf1}\right)\cdot x \ldots & \text{if } x < \frac{l - d_s}{2} \\ \quad + -\frac{f_{11}\left(e_{f1}, F_{zdf1}\right) - f_{12}\left(e_{f1}, F_{zdf1}\right)}{l}\cdot\frac{x^2}{2} \ldots & \\ \quad + -g_d\cdot x & \\ f_{11}\left(e_{f1}, F_{zdf1}\right)\cdot x \ldots & \text{if } \frac{l - d_s}{2} \le x < \frac{l}{2} \\ \quad + -\frac{f_{11}\left(e_{f1}, F_{zdf1}\right) - f_{12}\left(e_{f1}, F_{zdf1}\right)}{l}\cdot\frac{x^2}{2} \ldots & \\ \quad + -g_d\cdot x - F_{cf1} & \\ f_{11}\left(e_{f1}, F_{zdf1}\right)\cdot x \ldots & \text{if } \frac{l}{2} \le x < \frac{l + d_s}{2} \\ \quad + -\frac{f_{11}\left(e_{f1}, F_{zdf1}\right) - f_{12}\left(e_{f1}, F_{zdf1}\right)}{l}\cdot\frac{x^2}{2} \ldots & \\ \quad + -g_d\cdot x - F_{cf1} - \frac{F_{zdf1}}{2} & \\ f_{11}\left(e_{f1}, F_{zdf1}\right)\cdot x \ldots & \text{if } \frac{l + d_s}{2} \le x < l \\ \quad + -\frac{f_{11}\left(e_{f1}, F_{zdf1}\right) - f_{12}\left(e_{f1}, F_{zdf1}\right)}{l}\cdot\frac{x^2}{2} \ldots & \\ \quad + -g_d\cdot x - F_{cf1} - \frac{F_{zdf1}}{2} + F_{tf1} & \end{cases}$$

$$V'_{f1}\left(x, e_{f2}, F_{zdf2}, F_{cf2}, F_{tf2}\right) := \begin{cases} f_{soil1}\left(e_{f1}, F_{zdf1}\right)\cdot x - \dfrac{f_{soil1}\left(e_{f1}, F_{zdf1}\right)}{b_{f1}\left(e_{f1}\right)}\cdot\dfrac{x^2}{2} - g_d\cdot x \quad \text{if } x < \dfrac{l - d_s}{2} \\ f_{soil1}\left(e_{f1}, F_{zdf1}\right)\cdot x - \dfrac{f_{soil1}\left(e_{f1}, F_{zdf1}\right)}{b_{f1}\left(e_{f1}\right)}\cdot\dfrac{x^2}{2} \ldots \quad \text{if } \dfrac{l - d_s}{2} \le x < \dfrac{l}{2} \\ \quad + -g_d\cdot x - F_{cf1} \\ f_{soil1}\left(e_{f1}, F_{zdf1}\right)\cdot x - \dfrac{f_{soil1}\left(e_{f1}, F_{zdf1}\right)}{b_{f1}\left(e_{f1}\right)}\cdot\dfrac{x^2}{2} \ldots \quad \text{if } \dfrac{l}{2} \le x < \dfrac{l + d_s}{2} \\ \quad + -g_d\cdot x - F_{cf1} - \dfrac{F_{zdf1}}{2} \\ f_{soil1}\left(e_{f1}, F_{zdf1}\right)\cdot x \ldots \quad \text{if } \dfrac{l + d_s}{2} \le x < b_{f1}\left(e_{f1}\right) \\ \quad + -\dfrac{f_{soil1}\left(e_{f1}, F_{zdf1}\right)}{b_{f1}\left(e_{f1}\right)}\cdot\dfrac{x^2}{2} \ldots \\ \quad + -g_d\cdot x - F_{cf1} - \dfrac{F_{zdf1}}{2} + F_{tf1} \\ f_{soil1}\left(e_{f1}, F_{zdf1}\right)\cdot\dfrac{b_{f1}\left(e_{f1}\right)}{2} - g_d\cdot x \ldots \quad \text{if } b_{f1}\left(e_{f1}\right) \le x < l \\ \quad + -F_{cf1} - \dfrac{F_{zdf1}}{2} + F_{tf1} \end{cases}$$

$$V_{f2}\left(x, e_{f2}, F_{zdf2}, F_{cf2}, F_{tf2}\right) := \begin{cases} f_{21}\left(e_{f2}, F_{zdf2}\right)\cdot x \ldots \quad \text{if } x < \dfrac{l - d_s}{2} \\ \quad + -\dfrac{f_{21}\left(e_{f2}, F_{zdf2}\right) - f_{22}\left(e_{f2}, F_{zdf2}\right)}{l}\cdot\dfrac{x^2}{2} - g_d\cdot x \\ f_{21}\left(e_{f2}, F_{zdf2}\right)\cdot x \ldots \quad \text{if } \dfrac{l - d_s}{2} \le x < \dfrac{l}{2} \\ \quad + -\dfrac{f_{21}\left(e_{f2}, F_{zdf2}\right) - f_{22}\left(e_{f2}, F_{zdf2}\right)}{l}\cdot\dfrac{x^2}{2} \ldots \\ \quad + -g_d\cdot x - F_{cf2} \\ f_{21}\left(e_{f2}, F_{zdf2}\right)\cdot x \ldots \quad \text{if } \dfrac{l}{2} \le x < \dfrac{l + d_s}{2} \\ \quad + -\dfrac{f_{21}\left(e_{f2}, F_{zdf2}\right) - f_{22}\left(e_{f2}, F_{zdf2}\right)}{l}\cdot\dfrac{x^2}{2} \ldots \\ \quad + -g_d\cdot x - F_{cf2} - \dfrac{F_{zdf2}}{2} \\ f_{21}\left(e_{f2}, F_{zdf2}\right)\cdot x \ldots \quad \text{if } \dfrac{l + d_s}{2} \le x < l \\ \quad + -\dfrac{f_{21}\left(e_{f2}, F_{zdf2}\right) - f_{22}\left(e_{f2}, F_{zdf2}\right)}{l}\cdot\dfrac{x^2}{2} \ldots \\ \quad + -g_d\cdot x - F_{cf2} - \dfrac{F_{zdf2}}{2} + F_{tf2} \end{cases}$$

$$V'_{f2}(x, e_{f2}, F_{zdf2}, F_{cf2}, F_{tf2}) := \begin{cases} f_{soil2}(e_{f2}, F_{zdf2}) \cdot x - \dfrac{f_{soil2}(e_{f2}, F_{zdf2})}{b_{f2}(e_{f2})} \cdot \dfrac{x^2}{2} - g_d \cdot x & \text{if } x < \dfrac{l - d_s}{2} \\ f_{soil2}(e_{f2}, F_{zdf2}) \cdot x - \dfrac{f_{soil2}(e_{f2}, F_{zdf2})}{b_{f2}(e_{f2})} \cdot \dfrac{x^2}{2} \ldots & \text{if } \dfrac{l - d_s}{2} \le x < \dfrac{l}{2} \\ \quad + -g_d \cdot x - F_{cf2} & \\ f_{soil2}(e_{f2}, F_{zdf2}) \cdot x - \dfrac{f_{soil2}(e_{f2}, F_{zdf2})}{b_{f2}(e_{f2})} \cdot \dfrac{x^2}{2} \ldots & \text{if } \dfrac{l}{2} \le x < \dfrac{l + d_s}{2} \\ \quad + -g_d \cdot x - F_{cf2} - \dfrac{F_{zdf2}}{2} & \\ f_{soil2}(e_{f2}, F_{zdf2}) \cdot x \ldots & \text{if } \dfrac{l + d_s}{2} \le x < b_{f2}(e_{f2}) \\ \quad + -\dfrac{f_{soil2}(e_{f2}, F_{zdf2})}{b_{f2}(e_{f2})} \cdot \dfrac{x^2}{2} \ldots & \\ \quad + -g_d \cdot x - F_{cf2} - \dfrac{F_{zdf2}}{2} + F_{tf2} & \\ f_{soil2}(e_{f2}, F_{zdf2}) \cdot \dfrac{b_{f2}(e_{f2})}{2} - g_d \cdot x \ldots & \text{if } b_{f2}(e_{f2}) \le x < l \\ \quad + -F_{cf2} - \dfrac{F_{zdf2}}{2} + F_{tf2} & \end{cases}$$

$$V_{fat1}(x, e_{f2}, F_{zdf2}, F_{cf2}, F_{tf2}) := \begin{cases} V_{f1}(x, e_{f2}, F_{zdf2}, F_{cf2}, F_{tf2}) & \text{if } b_{f2}(e_{f2}) > l \\ V'_{f1}(x, e_{f2}, F_{zdf2}, F_{cf2}, F_{tf2}) & \text{if } b_{f2}(e_{f2}) \le l \end{cases}$$

$$V_{fat2}(x, e_{f2}, F_{zdf2}, F_{cf2}, F_{tf2}) := \begin{cases} V_{f2}(x, e_{f2}, F_{zdf2}, F_{cf2}, F_{tf2}) & \text{if } b_{f2}(e_{f2}) > l \\ V'_{f2}(x, e_{f2}, F_{zdf2}, F_{cf2}, F_{tf2}) & \text{if } b_{f2}(e_{f2}) \le l \end{cases}$$

Minimum shear force in section 0-3, fatigue

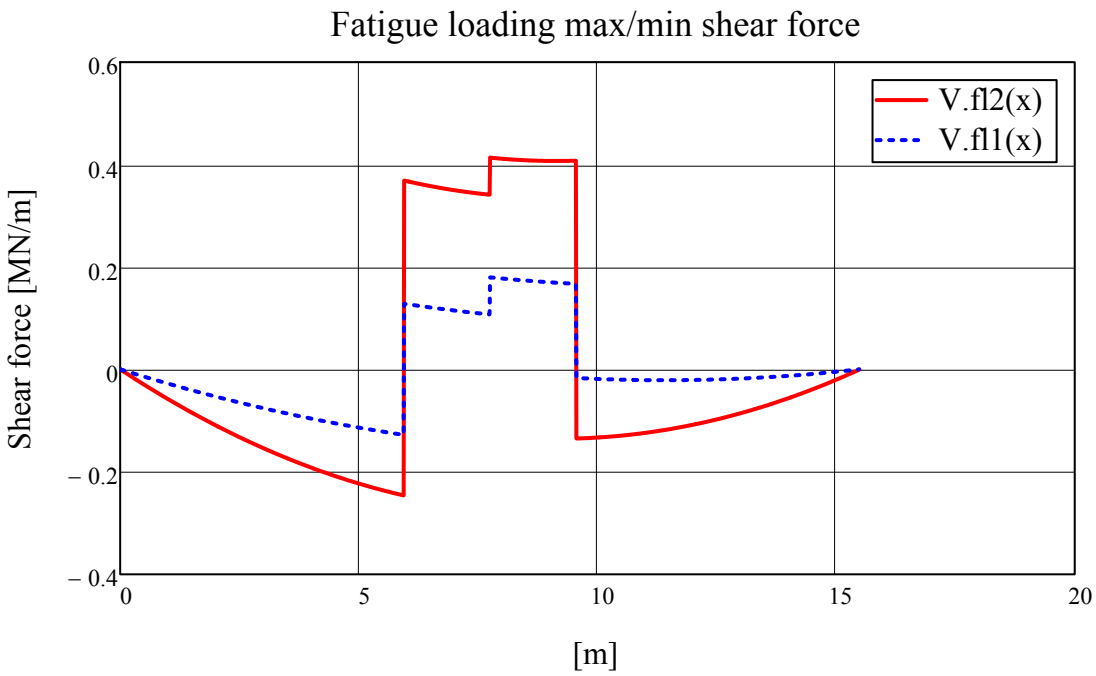

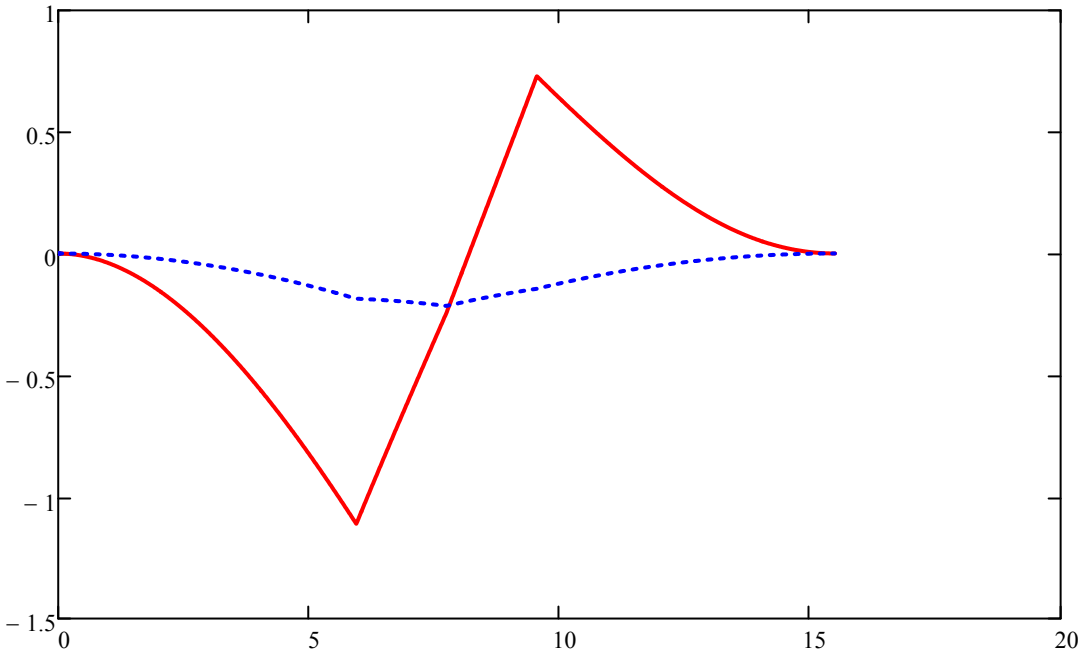

G.4 Fatigue in U-bows

Fatigue U-bow [EN 1992-1-1:2005 6.8.5]

$a_{ubow} := 100mm$ $d_{sr} := 4m$ $d_1 := 340mm$ $\phi_{Ubow} := 25mm$

$$I_0 := \frac{1}{4}\cdot\pi\cdot\left(r_2^{\,4} - r_1^{\,2}\right)$$

$d_{sr} = 4\,m$

$r_2 := \frac{d_{sr}}{2} + \frac{d_1}{2} = 2.17\,\text{m}$

$r_1 := \frac{d_{sr}}{2} - \frac{d_1}{2} = 1.83\,\text{m}$

$I_0 := \frac{\pi}{4}\cdot\left(r_2^{\,4} - r_1^{\,4}\right) = 8.607\,\text{m}^4$

$W_{annulus} := \frac{I_0}{r_2} = 3.966\cdot\text{m}^3$

$$\sigma_{mean.pos.fat1} := \left(\frac{F_{zdf1}}{\pi\cdot d_{sr}\cdot d_1} + \frac{M_{df1}}{I_0}\cdot r_1 + \frac{F_{zdf1}}{\pi\cdot d_{sr}\cdot d_1} + \frac{M_{df1}}{I_0}\cdot r_2\right)\cdot\frac{1}{2}$$

$$\sigma_{mean.pos.fat2} := \left(\frac{F_{zdf2}}{\pi\cdot d_{sr}\cdot d_1} + \frac{M_{df2}}{I_0}\cdot r_1 + \frac{F_{zdf2}}{\pi\cdot d_{sr}\cdot d_1} + \frac{M_{df2}}{I_0}\cdot r_2\right)\cdot\frac{1}{2}$$

$$\sigma_{mean.neg.fat1} := \left(\frac{F_{zdf1}}{\pi\cdot d_{sr}\cdot d_1} - \frac{M_{df1}}{I_0}\cdot r_1 + \frac{F_{zdf1}}{\pi\cdot d_{sr}\cdot d_1} - \frac{M_{df1}}{I_0}\cdot r_2\right)\cdot\frac{1}{2}$$

$$\sigma_{mean.neg.fat2} := \left(\frac{F_{zdf2}}{\pi\cdot d_{sr}\cdot d_1} - \frac{M_{df2}}{I_0}\cdot r_1 + \frac{F_{zdf2}}{\pi\cdot d_{sr}\cdot d_1} - \frac{M_{df2}}{I_0}\cdot r_2\right)\cdot\frac{1}{2}$$

$$\Delta\sigma_{Ubow.pos} := \frac{\left(\sigma_{mean.pos.fat2} - \sigma_{mean.pos.fat1}\right)\cdot a_{ubow}\cdot d_1}{2\left(\frac{\pi\cdot\phi_{Ubow}^{\,2}}{4}\right)}$$

$$\Delta\sigma_{Ubow.neg} := \frac{\left(\sigma_{mean.neg.fat2} - \sigma_{mean.neg.fat1}\right)\cdot a_{ubow}\cdot d_1}{2\left(\frac{\pi\cdot\phi_{Ubow}^{\,2}}{4}\right)}$$

$\max\left(\left|\Delta\sigma_{Ubow.pos}\right|\right) = 2.18\times 10^3\cdot\text{MPa}$

$\max\left(\left|\Delta\sigma_{Ubow.neg}\right|\right) = 2.18\times 10^3\cdot\text{MPa}$

$D := 600\text{mm}$ Bending diameter

$\zeta := 0.35 + 0.026\cdot\frac{D}{\phi_{Ubow}} = 0.974$ Reduction factor due to bent reinforcement bars

$\Delta\sigma_{Rsk} := 162.5\text{MPa}\cdot\zeta = 158.275\cdot\text{MPa}$

$\gamma_{F.fat} := 1.0$ $\gamma_{s.fat} := 1.15$

$$N_{Ubow_k} := \begin{cases} 1 \cdot 10^6 \cdot \left(\dfrac{\dfrac{\Delta\sigma_{Rsk}}{\gamma_{s.fat}}}{\gamma_{F.fat} \cdot \Delta\sigma_{Ubow.pos_k}} \right)^5 & \text{if } \dfrac{\Delta\sigma_{Rsk}}{\gamma_{s.fat}} \le \gamma_{F.fat} \cdot \Delta\sigma_{Ubow.pos_k} \\ 1 \cdot 10^6 \cdot \left(\dfrac{\dfrac{\Delta\sigma_{Rsk}}{\gamma_{s.fat}}}{\gamma_{F.fat} \cdot \Delta\sigma_{Ubow.pos_k}} \right)^9 & \text{if } \dfrac{\Delta\sigma_{Rsk}}{\gamma_{s.fat}} > \gamma_{F.fat} \cdot \Delta\sigma_{Ubow.pos_k} \end{cases}$$

$$N_{Ubow_k} := \frac{n_k}{N_{Ubow_k}} = \ldots$$

$$D_{Ubow} := \sum_k N_{Ubow_k} = 1.064$$

H Utilisation degree

Utilisation degree of bending reinforcement top (o) and bottom (u)

$$UR_{b.u} = \begin{pmatrix} 30.355 \\ 17.415 \\ 7.929 \\ 2.052 \end{pmatrix} \cdot \%$$

$$UR_{b.o} = \begin{pmatrix} 31.316 \\ 17.615 \\ 8.006 \\ 2.066 \end{pmatrix} \cdot \%$$

Utilisation degree of shear capacity **without** shear reinforcement

$$UR_{shear.VRdc} = \begin{pmatrix} 90.676 \\ 64.919 \\ 44.09 \\ 22.63 \end{pmatrix} m \cdot \%$$

Utilisation degree of shear capacity **with** shear reinforcement spacing 500mm

$$UR_{shear} = \begin{pmatrix} 73.612 \\ 52.702 \\ 35.96 \\ 18.582 \end{pmatrix} \cdot \%$$

Utilisation degree of bending in star reinforcement

$$UR_{b.star} = 66.324 \frac{1}{m} \cdot \%$$

Utilisation degree of U-bow reinforcement , tensile side (t), compressive side (c)

Compressive:

$$UR_{shear.Ubow_0} = 93.628 \cdot \%$$

Tensile:

$$UR_{shear.Ubow_1} = 87.697 \cdot \%$$

Utilisation degree of crack width in the different sections top (o) and bottom (u)

$$UR_{crack.width.u} = \begin{pmatrix} 96.453 \\ 58.625 \\ 28.332 \\ 7.696 \end{pmatrix} \cdot \%$$

$$UR_{crack.width.o} = \begin{pmatrix} 85.539 \\ 50.133 \\ 22.788 \\ 5.804 \end{pmatrix} \cdot \%$$

Utilisation degree of compressed concrete under the steel ring

$$UR_{cc.ring} = \begin{pmatrix} 50.888 \\ 47.909 \end{pmatrix} \cdot \%$$

Utilisation degree of bending reinforcement top (o) and bottom (u) for **fatigue loading**

Equivalent load

$$UR_{fat.b.u} = \begin{pmatrix} 26.38 \\ 16.114 \\ 7.823 \\ 2.134 \end{pmatrix} \cdot \%$$

$$UR_{fat.b.o} = \begin{pmatrix} 35.505 \\ 21.689 \\ 10.54 \\ 2.88 \end{pmatrix} \cdot \%$$

ac damage summation

$$D_{Upos} = \begin{pmatrix} 0.013 \\ 1.507 \times 10^{-4} \\ 2.257 \times 10^{-7} \\ 1.891 \times 10^{-12} \end{pmatrix} \cdot \%$$

$$D_{Oneg} = \begin{pmatrix} 0.181 \\ 2.184 \times 10^{-3} \\ 3.3 \times 10^{-6} \\ 2.804 \times 10^{-11} \end{pmatrix} \cdot \%$$

Utilisation degree of compressed concrete top (o) and bottom (u) for **fatigue loading**

$$UR_{fat.c.u} = \begin{pmatrix} 43.556 \\ 39.681 \\ 36.436 \\ 34.033 \end{pmatrix} \cdot \%$$

$$UR_{fat.c.o} = \begin{pmatrix} 40.211 \\ 34.826 \\ 30.672 \\ 27.877 \end{pmatrix} \cdot \%$$

Utilisation degree of compressed concrete under steel ring for **fatigue loading**

$$UR_{fat.cc.ring} = 56.066 \cdot \%$$

Utilisation degree of shear reinforcement closest to the steel ring for **fatigue loading**

Equivalent load

$$U_{fat.Ubow} = 80.002 \cdot \%$$

ac damage summation

$$D_{Ubow} = 106.368 \cdot \%$$

Utilisation degree of star reinforcement for **fatigue loading**

Equivalent load

$$U_{fat.star} = 32.388 \cdot \%$$

ac damage summation

$$D_{star} = 1.738 \times 10^{-10} \cdot \%$$

I Fatigue Loads

$$S_{r,eq} = \left(\sum_{i=0}^{n} \frac{S_{r,i}^{m}}{N_{eq}} \right)^{\frac{1}{m}}$$

					Neq= 10^7 m= 7	
Load nr	Sr,Fi=Fxy [kN]	Sr,Mi=Mxy [kNm]	ni	n acc	Sr,Mi= (sum(ni*Sr,Mi^m/10^7)	Sr,Fi= =(sum(ni*Sr,Fi^m/10^7)
1	601	40 922	30	30	5,76526E+26	8,49655E+13
2	509	34 827	100	130	6,21459E+26	8,85165E+13
3	490	33 957	60	190	3,12361E+26	4,06934E+13
4	470	31 780	76	266	2,48823E+26	3,85034E+13
5	470	31 780	253	519	8,28319E+26	1,28176E+14
6	464	28 297	266	785	3,86424E+26	1,23171E+14
7	457	27 426	220	1005	2,56779E+26	9,15875E+13
8	457	27 426	46	1051	5,36902E+25	1,91501E+13
9	444	27 426	63	1114	7,35322E+25	2,143E+13
10	444	26 991	266	1380	2,77597E+26	9,0482E+13
11	425	26 991	260	1640	2,71335E+26	6,51172E+13
12	418	26 991	43	1683	4,48747E+25	9,58743E+12
13	418	26 991	20	1703	2,08719E+25	4,45927E+12
14	418	26 120	301	2004	2,49677E+26	6,7112E+13
15	418	26 120	231	2235	1,91613E+26	5,15046E+13
16	411	26 120	81	2316	6,71889E+25	1,60464E+13
17	411	26 120	340	2656	2,82027E+26	6,73553E+13
18	411	26 120	36	2692	2,98617E+25	7,13174E+12
19	411	26 120	13	2705	1,07834E+25	2,57535E+12
20	411	25 250	188	2893	1,23023E+26	3,72435E+13
21	405	25 250	97	2990	6,34748E+25	1,73363E+13
22	405	24 814	232	3222	1,3439E+26	4,14642E+13
23	398	24 814	34	3256	1,9695E+25	5,37849E+12
24	398	24 379	354	3610	1,81182E+26	5,59996E+13
25	398	24 379	353	3963	1,8067E+26	5,58414E+13
26	398	24 379	25	3988	1,27953E+25	3,95477E+12
27	398	23 044	210	4198	7,24643E+25	3,32201E+13
28	392	23 944	66	4264	2,97797E+25	9,38742E+12
29	392	23 508	340	4604	1,34893E+26	4,83595E+13
30	392	23 073	106	4710	3,69007E+25	1,50768E+13
31	385	23 073	266	4976	9,25998E+25	3,33508E+13
32	379	23 073	322	5298	1,12095E+26	3,61685E+13
33	379	23 073	71	5369	2,47165E+25	7,97504E+12
34	379	23 073	496	5865	1,72667E+26	5,57129E+13
35	379	23 073	74	5939	2,57608E+25	8,31201E+12
36	379	23 073	13	5952	4,52555E+24	1,46022E+12
37	379	22 638	439	6391	1,33761E+26	4,93105E+13
38	372	22 638	377	6768	1,1487E+26	3,71657E+13
39	372	22 202	376	7144	9,99845E+25	3,70671E+13
40	366	22 202	676	7820	1,79759E+26	5,94722E+13
41	366	22 202	699	8519	1,85875E+26	6,14957E+13
42	359	22 202	287	8806	7,63179E+25	2,20568E+13

43	359	22 202	393	9199	1,04505E+26	3,02033E+13
44	359	22 202	148	9347	3,93556E+25	1,13743E+13
45	359	22 202	73	9420	1,94119E+25	5,61027E+12
46	359	21 767	200	9620	4,63042E+25	1,53706E+13
47	353	21 767	923	10543	2,13694E+26	6,30412E+13
48	353	21 767	414	10957	9,58496E+25	2,82763E+13
49	353	21 767	156	11113	3,61172E+25	1,06549E+13
50	353	21 767	830	11943	1,92162E+26	5,66893E+13
51	353	21 767	244	12187	5,64911E+25	1,66653E+13
52	353	21 767	329	12516	7,61703E+25	2,24708E+13
53	353	21 767	150	12666	3,47281E+25	1,02451E+13
54	346	21 767	345	13011	7,98747E+25	2,0481E+13
55	346	21 767	835	13846	1,9332E+26	4,957E+13
56	346	21 767	767	14613	1,77576E+26	4,55332E+13
57	346	21 767	1 996	16609	4,62116E+26	1,18493E+14
58	346	21 767	5	16614	1,1576E+24	2,96827E+11
59	346	21 767	69	16683	1,59749E+25	4,09621E+12
60	346	21 707	415	17098	9,42425E+25	2,46366E+13
61	340	21 767	1 133	18231	2,62313E+26	5,9509E+13
62	340	21 767	1 258	19489	2,91253E+26	6,60744E+13
63	333	21 767	1 682	21171	3,89418E+26	7,63723E+13
64	333	21 332	345	21516	6,9349E+25	1,56649E+13
65	333	21 332	1 062	22578	2,13474E+26	4,82208E+13
66	333	21 332	226	22804	4,54286E+25	1,02617E+13
67	333	20 896	1 057	23861	1,83873E+26	4,79937E+13
68	333	20 461	4472	28333	6,71413E+26	2,03054E+14
69	333	20 461	1 422	29755	2,13495E+26	6,45668E+13
70	333	20 461	925	30680	1,38877E+26	4,20002E+13
71	333	20 461	2 488	33168	3,73541E+26	1,12969E+14
72	333	20 461	2 272	35440	3,41111E+26	1,03162E+14
73	333	20 461	83	35523	1,24614E+25	3,76867E+12
74	327	20 461	2846	38369	4,2729E+26	1,13781E+14
75	327	20 461	207	38576	3,10784E+25	8,2757E+12
76	327	20 461	1314	39890	1,9728E+26	5,25327E+13
77	327	20 020	4 051	43941	5,22169E+26	1,61956E+14
78	327	20 026	490	44431	6,3293E+25	1,95898E+13
79	320	20 026	3 891	48322	5,02598E+26	1,33694E+14
80	320	20 026	5308	53630	6,85631E+26	1,82381E+14
81	320	20 026	1 631	55261	2,10675E+26	5,60407E+13
82	320	19 690	922	56183	1,05792E+26	3,16797E+13
83	313	19 590	2275	58458	2,51897E+26	6,69563E+13
84	313	19 590	1 445	59903	1,59996E+26	4,25283E+13
85	313	19590	8 413	68316	9,31519E+26	2,47606E+14
86	313	19 690	7804	76120	8,95442E+26	2,29682E+14
87	313	19 590	2732	78852	3,02497E+26	8,04065E+13
88	313	19 590	5 177	84029	5,73217E+26	1,52366E+14
89	313	19 590	1 629	85658	1,80369E+26	4,79437E+13
90	313	19 166	3 581	89239	3,40192E+26	1,05394E+14
91	313	10 155	6747	95986	7,51398E+24	1,98573E+14
92	313	10 155	1 660	97646	1,8487E+24	4,88561E+13

93	313	19 155	3422	101068	3,23784E+26	1,00714E+14
94	307	19 155	16 307	117375	1,54294E+27	4,19124E+14
95	307	19 155	7285	124660	6,89294E+26	1,8724E+14
96	307	19 155	13032	137692	1,23307E+27	3,3495E+14
97	307	10 155	7266	144958	8,09198E+24	1,86751E+14
98	307	19 155	2 512	147470	2,37681E+26	6,45637E+13
99	300	19 155	2403	149873	2,27368E+26	5,25536E+13
100	300	19 155	16 882	166755	1,59735E+27	3,69209E+14
101	300	19 155	7820	174575	7,39915E+26	1,71023E+14
102	300	18 720	3320	177895	2,67472E+26	7,26084E+13
103	300	18 720	3597	181492	2,89789E+26	7,86664E+13
104	300	18 284	243	181735	1,65999E+25	5,31441E+12
105	294	18 284	24 387	206122	1,66593E+27	4,63009E+14
106	294	18 284	12 945	219067	8,84302E+26	2,45773E+14
107	294	18284	10 381	229448	7,09149E+26	1,97093E+14
108	294	18 284	13 987	243435	9,55483E+26	2,65556E+14
109	287	18284	2244	245679	1,53293E+26	3,59912E+13
110	287	18 284	3307	248986	2,25909E+26	5,30405E+13
111	287	17 849	2934	251920	1,69339E+26	4,7058E+13
112	287	17 849	42 095	294015	2,42956E+27	6,75155E+14
113	287	17 849	8 791	302806	5,07383E+26	1,40998E+14
114	287	17 849	12 695	315501	7,32706E+26	2,03613E+14
115	281	17 849	5669	321170	3,27193E+26	7,84243E+13
116	281	17 414	18332	339502	8,90225E+26	2,53603E+14
117	281	16 978	399	339901	1,62248E+25	5,51972E+12
118	281	16 978	31 650	371551	1,287E+27	4,37843E+14
119	281	16 978	21 053	392604	8,56091E+26	2,91245E+14
120	281	16 978	24 043	416647	9,77675E+26	3,32608E+14
121	274	16 978	9753	426400	3,96592E+26	1,13082E+14
122	274	16 543	13 375	439775	4,53517E+26	1,55077E+14
123	274	16 543	25 031	464806	8,48747E+26	2,90223E+14
124	274	16 543	48 180	512986	1,63368E+27	5,58625E+14
125	274	16 543	12 163	525149	4,12421E+26	1,41025E+14
126	274	16 543	961	526110	3,25854E+25	1,11424E+13
127	274	16 108	21 220	547330	5,97086E+26	2,46036E+14
128	268	16 108	22 873	570203	6,43598E+26	2,27126E+14
129	268	15 672	10 060	580263	2,33598E+26	9,98945E+13
130	268	15 672	51 243	631506	1,18989E+27	5,08836E+14
131	268	15 672	24 561	656067	5,70318E+26	2,43888E+14
132	261	15672	28 993	685060	6,73231E+26	2,39209E+14
133	261	15 672	1 418	686478	3,29266E+25	1,16993E+13
134	261	15 237	90 359	776837	1,72293E+27	7,45513E+14
135	261	15 237	7003	783840	1,3353E+26	5,77787E+13
136	261	14 802	21 868	805708	3,40449E+26	1,80423E+14
137	261	14 802	3076	808784	4,78883E+25	2,53787E+13
138	255	14 802	73 503	882287	1,14432E+27	5,15331E+14
139	255	14 802	13 922	896209	2,16743E+26	9,76074E+13
140	255	14 802	22 830	919039	3,55426E+26	1,60062E+14
141	248	14 802	1 679	920718	2,61393E+25	9,68752E+12
142	248	14 366	115566	1036284	1,45942E+27	6,66794E+14

143	248	14 366	22 825	1059109	2,88245E+26	1,31696E+14
144	248	14 366	5329	1064438	6,72972E+25	3,07473E+13
145	242	14 366	45 993	1110431	5,80822E+26	2,23563E+14
146	242	13 931	561	1110992	5,71267E+24	2,72691E+12
147	242	13 931	55 594	1166586	5,66114E+26	2,70231E+14
148	235	13 931	90 065	1256651	9,17133E+26	3,56477E+14
149	235	13 496	15 367	1272018	1,25321E+26	6,08225E+13
150	235	13 496	38 837	1310855	3,16724E+26	1,53717E+14
151	235	13 496	54311	1365166	4,42918E+26	2,14963E+14
152	220	13 496	38 337	1403503	3,12647E+26	9,56262E+13
153	229	13 060	16 017	1419520	1,03797E+26	5,28968E+13
154	220	13 060	100 323	1519843	6,50134E+26	2,50241E+14
155	220	13 060	14 581	1534424	9,44908E+25	3,63702E+13
156	229	12 625	14 908	1549332	7,62148E+25	4,92343E+13
157	229	12 025	25 289	1574621	9,19448E+25	8,3518E+13
158	222	12 625	121 469	1696090	6,20991E+26	3,22802E+14
159	216	12 625	3969	1700059	2,02909E+25	8,70678E+12
160	216	12 625	145 025	1845084	7,41417E+26	3,18141E+14
161	216	12 190	45 710	1890794	1,82826E+26	1,00274E+14
162	216	12 190	371	1891165	1,48388E+24	8,13861E+11
163	209	12 190	105 848	1997013	4,23359E+26	1,84377E+14
164	209	12 190	70 745	2067758	2,82958E+26	1,23231E+14
165	209	11754	132 770	2200528	4,11528E+26	2,31272E+14
166	209	11 764	51 513	2252041	1,60621E+26	8,97307E+13
167	202	11 754	40 562	2292603	1,25724E+26	5,56646E+13
168	202	11754	112298	2404901	3,48074E+26	1,5411E+14
169	202	11 319	132 399	2537300	3,15167E+26	1,81696E+14
170	202	11 319	158 321	2695621	3,76873E+26	2,17269E+14
171	202	10 883	12 388	2708009	2,23997E+25	1,70005E+13
172	196	10 883	68 321	2776330	1,23536E+26	7,59183E+13
173	196	10 883	49 153	2825483	8,88772E+25	5,46188E+13
174	196	10 083	259 889	3085372	2,7537E+26	2,88789E+14
175	189	10 883	59 565	3144937	1,07704E+26	5,13126E+13
176	189	10 448	3959	3148896	5,38044E+24	3,4105E+12
177	189	10 448	218564	3367460	2,97037E+26	1,88283E+14
178	189	10 448	122 754	3490214	1,66828E+26	1,05747E+14
179	189	10 013	64 698	3554912	6,52891E+25	5,57344E+13
180	183	10 013	104 123	3659035	1,05074E+26	7,15656E+13
181	183	10 013	267 752	3926787	2,70198E+26	1,84031E+14
182	176	10 013	111 893	4038680	1,12915E+26	5,85318E+13
183	176	9 577	3297	4041977	2,43627E+24	1,72468E+12
184	176	9 577	17202	4059179	1,27112E+25	8,99845E+12
185	176	9577	490 524	4549703	3,62465E+26	2,56595E+14
186	170	9 577	68 943	4618646	5,09444E+25	2,829E+13
187	170	9 142	23 335	4641981	1,24536E+25	9,57525E+12
188	170	9 142	174 022	4816003	9,28737E+25	7,1408E+13
189	170	9 142	261 543	5077546	1,39583E+26	1,07321E+14
190	163	9 142	159 337	5236883	8,50365E+25	4,87113E+13
191	163	9 142	212 047	5448930	1,13167E+26	6,48254E+13
192	163	8707	512 520	5961450	1,94442E+26	1,56684E+14

193	163	8707	4 136	5965586	1,56914E+24	1,26443E+12
194	157	8707	95 537	6061123	3,62453E+25	2,24631E+13
195	157	8707	126 081	6187204	4,78332E+25	2,96447E+13
196	157	8 271	647 033	6834237	1,7133E+26	1,52133E+14
197	150	8 271	5466	6839703	1,44736E+24	9,33917E+11
198	150	8 271	303 972	7143675	8,04896E+25	5,19365E+13
199	150	7836	196636	7340311	3,56717E+25	3,35971E+13
200	150	7836	478 593	7818904	8,68215E+25	8,17721E+13
201	144	7836	121 027	7939931	2,19555E+25	1,55389E+13
202	144	7836	245 871	8185802	4,46034E+25	3,15678E+13
203	144	7 401	838 015	9023817	1,01926E+26	1,07594E+14
204	144	7 401	81 855	9105672	9,95584E+24	1,05095E+13
205	137	7 401	1 078 602	10184274	1,31188E+26	9,77024E+13
206	137	7 401	93 477	10277751	1,13694E+25	8,46737E+12
207	137	6965	348 486	10626237	2,77098E+25	3,15667E+13
208	137	6965	292 930	10919167	2,32923E+25	2,65343E+13
209	131	6965	1 228 141	12147308	9,76554E+25	8,13106E+13
210	131	6530	49 788	12197096	2,52068E+24	3,29628E+12
211	131	6530	633 679	12830775	3,2082E+25	4,19535E+13
212	131	6530	1 810	12832585	9,1637E+22	1,19833E+11
213	124	6530	1 577 253	14409838	7,98534E+25	7,10973E+13
214	124	6530	751 919	15161757	3,80683E+25	3,3894E+13
215	124	6095	471 655	15633412	1,47381E+25	2,12606E+13
216	118	6095	4 196	15637608	1,31115E+23	1,33662E+11
217	118	6095	1 389 759	17027367	4,34266E+25	4,42704E+13
218	118	6095	1 747 266	18774633	5,45978E+25	5,56587E+13
219	118	5659	212 919	18987552	3,95724E+24	6,78248E+12
220	111	5659	251 632	19239184	4,67675E+24	5,22428E+12
221	111	5659	1 357 019	20596203	2,52211E+25	2,81739E+13
222	111	5659	2 143 991	22740194	3,98475E+25	4,45127E+13
223	104	5659	242 040	22982234	4,49847E+24	3,18508E+12
224	104	5224	1 438 488	24420722	1,52731E+25	1,89295E+13
225	104	5224	527 488	24948210	5,6006E+24	6,94138E+12
226	104	5224	3 255 502	28203712	3,45653E+25	4,28402E+13
227	98	5224	130 915	28334627	1,38999E+24	1,13651E+12
228	98	4789	2 041 740	30376367	1,17954E+25	1,77249E+13
229	98	4789	1 409 785	31786152	8,14454E+24	1,22387E+13
230	98	4789	2 387 859	34174011	1,3795E+25	2,07296E+13
231	91	4789	2 213 673	36387684	1,27887E+25	1,14394E+13
232	91	4353	443 103	36830787	1,31228E+24	2,28978E+12
233	91	4353	4 670 926	41501713	1,38332E+25	2,41375E+13
234	91	4353	1 243 664	42745377	3,68319E+24	6,42677E+12
235	85	4353	1 695 202	44440579	5,02044E+24	5,43443E+12
236	85	4353	423 857	44864436	1,25528E+24	1,35879E+12
237	85	3 018	8 816 545	53680981	2,01063E+24	2,82638E+13
238	85	3 918	168 697	53849678	2,39088E+23	5,40804E+11
239	78	3 918	1 979 437	55829115	2,80539E+24	3,47699E+12
240	78	3 918	1 079 800	56908915	1,53036E+24	1,89673E+12
241	78	3 483	8 095 667	65004582	5,03416E+24	1,42205E+13
242	78	3 483	4 261 486	69266068	2,64994E+24	7,48554E+12

243	72	3 483	3 294 897	72560965	2,04888E+24	3,30498E+12
244	72	3 047	4 235 916	76796881	1,03289E+24	4,24888E+12
245	72	3047	2 553 974	79350855	6,22764E+23	2,56179E+12
246	72	3047	8 424 894	87775749	2,05434E+24	8,45069E+12
247	65	3047	4 381 578	92157327	1,06841E+24	2,14795E+12
248	65	2 612	3 428 399	95585726	2,84383E+23	1,68068E+12
249	65	2 612	9 830 576	1,05E+08	8,15438E+23	4,81917E+12
250	65	2 612	7 463 256	1,13E+08	6,19071E+23	3,65866E+12
251	59	2 612	2 831 244	1,16E+08	2,34849E+23	7,04598E+11
252	59	2 612	4 253 985	1,2E+08	3,52865E+23	1,05867E+12
253	59	2 177	18 393 799	1,38E+08	4,26266E+23	4,57758E+12
254	59	2 177	6 040 264	1,44E+08	1,3998E+23	1,50321E+12
255	52	2 177	3 360 670	1,48E+08	7,78816E+22	3,45501E+11
256	52	2 177	7 427 643	1,55E+08	1,72131E+23	7,63615E+11
257	52	1 741	840838	1,56E+08	4,07665E+21	86444175421
258	46	1 741	20 387 687	1,76E+08	9,88461E+22	8,88531E+11
259	46	1 741	8 375 957	1,85E+08	4,06093E+22	3,65039E+11
260	46	1 741	6 979 848	1,92E+08	3,38405E+22	3,04194E+11
261	46	1 306	4 162 644	1,96E+08	2,69756E+21	1,81415E+11
262	46	1 306	20 892 214	2,17E+08	1,3539E+22	9,1052E+11
263	39	1 306	12 137 496	2,29E+08	7,86559E+21	1,66564E+11
264	39	1 306	21 431 118	2,5E+08	1,38882E+22	2,94101E+11
265	39	871	602 078	2,51E+08	2,28971E+19	8262377004
266	39	871	14 682 390	2,66E+08	5,58372E+20	2,01488E+11
267	39	871	20 617 202	2,86E+08	7,84074E+20	2,82932E+11
268	33	871	12 178 782	2,98E+08	4,6316E+20	51904072620
269	33	871	26 708 068	3,25E+08	1,01571E+21	1,13826E+11
270	33	871	33 217 769	3,58E+08	1,26327E+21	1,41569E+11
271	33	871	5 080 469	3,63E+08	1,93211E+20	21652167837
272	33	435	3 886 909	3,67E+08	1,14559E+18	16565400957
273	26	435	24 595 279	3,92E+08	7,24897E+18	19754461215
274	26	435	35 676 560	4,28E+08	1,0515E+19	28654735765
275	26	435	53 733 980	4,81E+08	1,5837E+19	43158112736
276	26	435	39 497 474	5,21E+08	1,16411E+19	31723621360
277	20	435	30 235 443	5,51E+08	8,9113E+18	3870136704
278	20	435	104 158 265	6,55E+08	3,06986E+19	13332257920
279	20	435	45 226 296	7E+08	1,33296E+19	5788965888
280	13	435	36 674 024	7,37E+08	1,08089E+19	230124061,8
				sum Sr,Xi=	6,44495E+28	2,34462E+16

Mxyeq=sum(S.Mi)^(1/m)=		13049,76938
	Fxyeq=sum(S.Fi)^(1/m)=	218,0628346

J Sections of strut-and-tie model 1

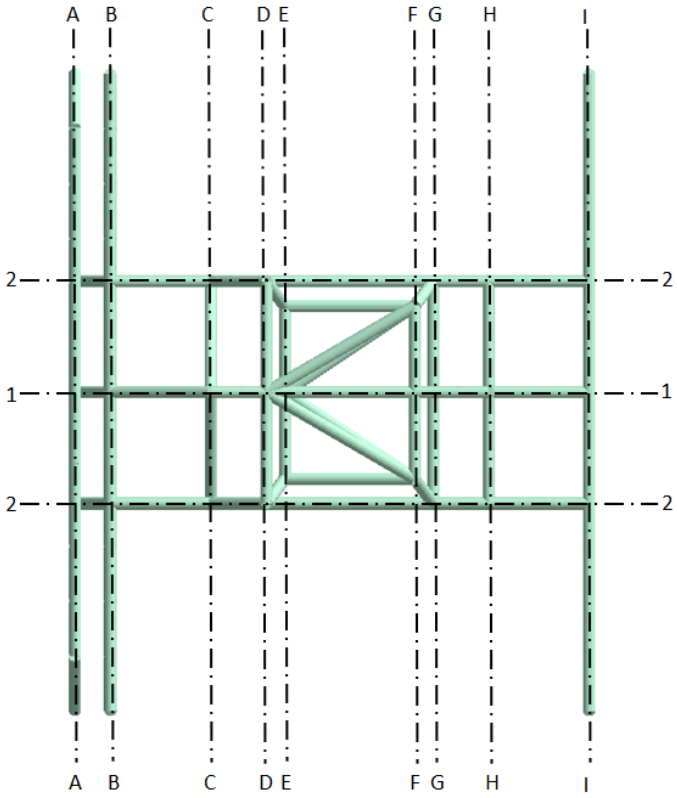

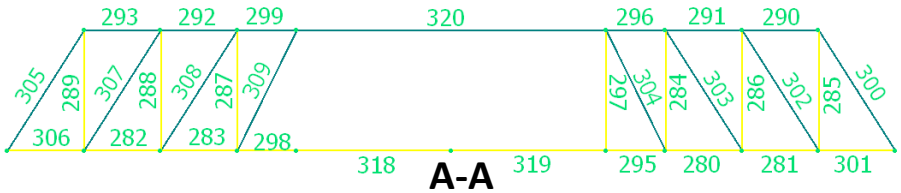

A-A

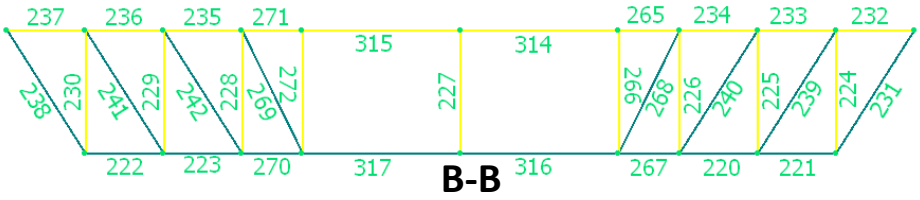

B-B

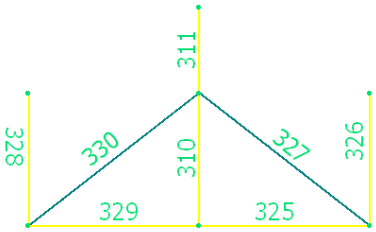

C-C

D-D

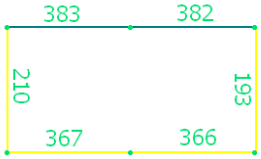

E-E

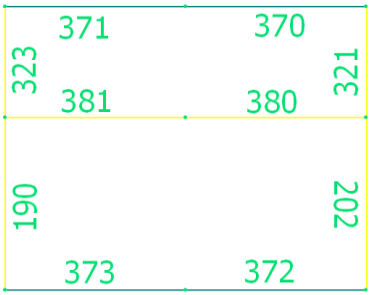

F-F

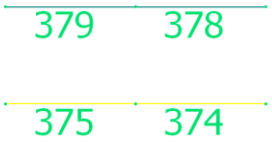

G-G

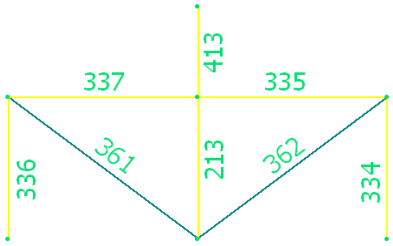

H-H

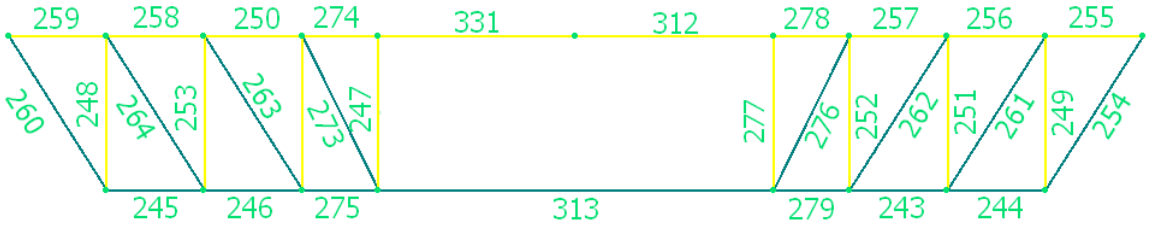

I-I

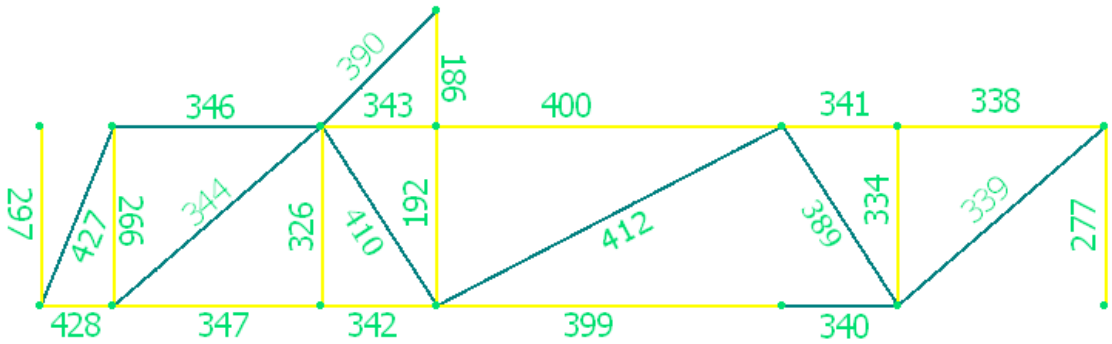

2-2

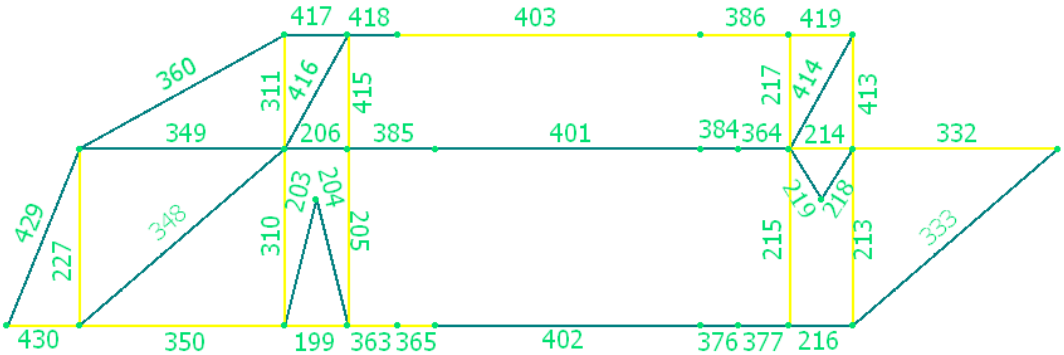

1-1

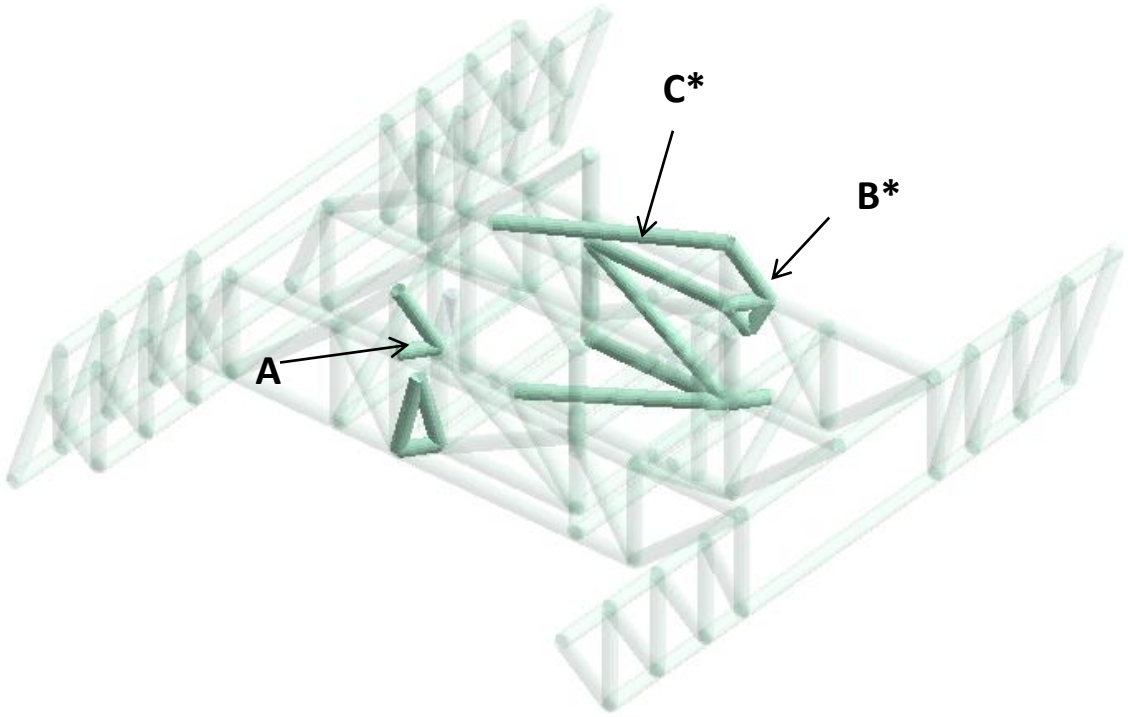

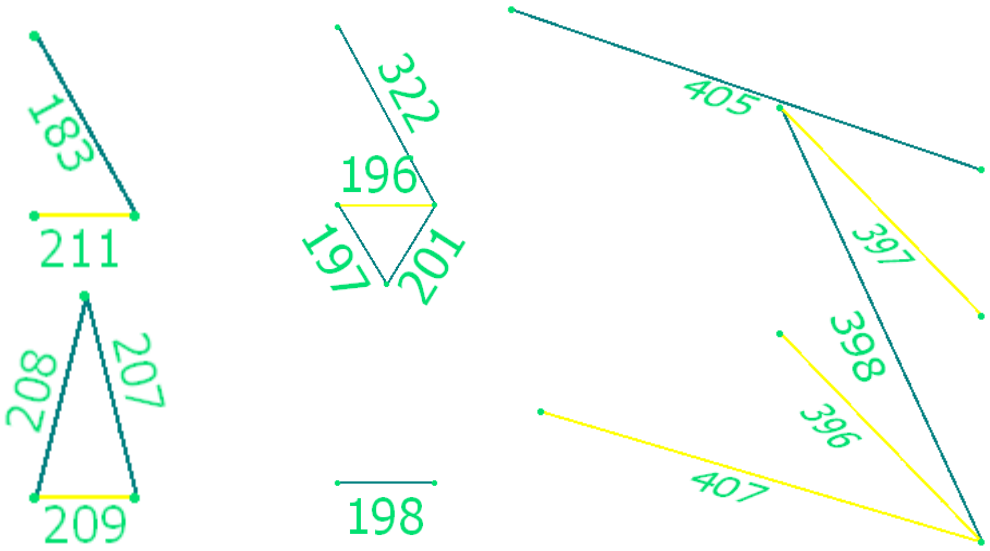

A* B* C*

K Reinforcement calculations and forces in struts and ties

Bar diameter [m]	0,025
f.yd [Pa]	521739130
A,si (phi=25) [m^2]	0,0004906
f.cd	30MPa

minimum required width with minimum spacing (one bar diameter)

chosen with regard to load distribution (only applicable on some ties)

ID	L [m]	N [kN*10^-2]	A,s req /concrete area [m^2]	Needed Bars/diameter of strut[m]	Section (see App. J)	Remark	Min spread	Spread over	Required spacing
199	0,5	50,726	0,0097225	19,81652654	1	Ubow	0,96583		
203	1,031	-46,781	0,1559367	0,251521127	1				
204	1,031	-46,781	0,1559367	0,251521127	1				
205	1,4	45,384	0,0086986	17,72963057	1	Ubow	0,86148		0
206	0,5	-1,97	0,0065667	0,051614632	1				
214	0,5	48,735	0,0093409	19,03872611	1	Ubow	0,92694		0
215	1,4	0	0	0	1				
216	0,5	-21,891	0,07297	0,172057069	1				
217	0,9	0	0	0	1				
332	1,625	21,891	0,0041958	8,551898089	1	Middle	0,40259	1,8	210
333	2,145	-28,895	0,0963167	0,197674691	1				
348	2,145	-28,321	0,0944033	0,195701436	1				
349	1,625	-5,727	0,01909	0,088004182	1				
350	1,625	39,38	0,0075478	15,3841189	1	Bottom	0,74421	1,8	117
360	1,858	-13,942	0,0464733	0,137310029	1				
363	0,4	39,38	0,0075478	15,3841189	1	Bottom	0,74421	1,8	117
364	0,4	-1,97	0,0065667	0,051614632	1				
365	0,3	39,38	0,0075478	15,3841189	1	Bottom	0,74421	1,8	117
376	0,3	-21,891	0,07297	0,172057069	1				
377	0,4	-21,891	0,07297	0,172057069	1				
384	0,3	-1,97	0,0065667	0,051614632	1				
385	0,7	-1,97	0,0065667	0,051614632	1				
386	0,7	23,861	0,0045734	9,321494692	1	Top	0,44107	1,8	193
401	2,1	-1,97	0,0065667	0,051614632	1				
402	2,1	-21,891	0,07297	0,172057069	1				
403	2,4	23,861	0,0045734	9,321494692	1	Top	0,44107	1,8	193
414	1,03	-49,133			1				
415	0,9	45,384	0,0086986	17,72963057	1	Ubow	0,86148		0
416	1,03	-51,918	0,17306	0,264971215	1				
417	0,5	-12,196	0,0406533	0,128424661	1				
418	0,4	-37,41	0,1247	0,224922848	1				
419	0,5	23,861	0,0045734	9,321494692	1	Top	0,44107	1,8	193
429	1,511	-47,603	0,1586767	0,253721273	1				
430	0,569	17,923	0,0034352	7,001766454	1	Bottom	0,32509	1,8	257
338	1,625	21,891	0,0041958	8,551898089	2	Middle	0,40259	1,8	210
339	2,145	-28,895	0,0963167	0,197674691	2				
340	0,9	-12,466	0,0415533	0,129838438	2				
341	0,9	21,891	0,0041958	8,551898089	2	Middle	0,40259	1,8	210

342	0,9	47,22	0,0090505	18,44687898	2	Bottom	0,89734	1,8	97
343	0,9	5,993	0,0011487	2,341214437	2	Middle	0,09206	1,8	768
344	2,145	-38,67	0,1289	0,228679275	2				
346	1,625	-17,923	0,0597433	0,155684391	2				
347	1,625	47,22	0,0090505	18,44687898	2	Bottom	0,89734	1,8	97
389	1,664	-17,428	0,0580933	0,153519482	2				
390	1,273	-41,642	0,1388067	0,237304247	2				
399	2,7	55,954	0,0107245	21,85888747	2	Bottom	1,06794	1,8	82
400	2,7	5,993	0,0011487	2,341214437	2	Middle	0,09206	1,8	768
410	1,664	-43,949	0,1464967	0,243789064	2				
412	3,041	-118,599	0,39533	0,400479448	2				
427	1,511	-47,603	0,1586767	0,253721273	2				
428	0,569	17,923	0,0034352	7,001766454	2	Bottom	0,32509	1,8	257
280	0,892	84,269	0,0161516	32,92037367	A	Bottom	1,62102	6,6	200
281	0,892	56,18	0,0107678	21,94717622	A	Bottom	1,07236	6,6	300
282	0,892	56,18	0,0107678	21,94717622	A	Bottom	1,07236	6,6	300
283	0,892	84,269	0,0161516	32,92037367	A	Bottom	1,62102	6,6	200
284	1,4	44,1	0,0084525	17,22802548	A		0,8364	6,6	383
285	1,4	44,1	0,0084525	17,22802548	A		0,8364	6,6	383
286	1,4	44,1	0,0084525	17,22802548	A		0,8364	6,6	383
287	1,4	44,1	0,0084525	17,22802548	A		0,8364	6,6	383
288	1,4	44,1	0,0084525	17,22802548	A		0,8364	6,6	383
289	1,4	44,1	0,0084525	17,22802548	A		0,8364	6,6	383
290	0,892	-28,09	0,0936333	0,194901683	A			6,6	
291	0,892	-56,18	0,1872667	0,275632604	A			6,6	
292	0,892	-56,18	0,1872667	0,275632604	A			6,6	
293	0,892	-28,09	0,0936333	0,194901683	A			6,6	
295	0,692	106,059	0,020328	41,43281529	A		2,04664	6,6	159
296	0,692	-84,269	0,2808967	0,337577615	A			6,6	
297	1,4	44,1	0,0084525	17,22802548	A		0,8364	6,6	383
298	0,692	106,059	0,020328	41,43281529	A	Bottom	2,04664	6,6	159
299	0,692	-84,269	0,2808967	0,337577615	A			6,6	
300	1,66	-52,286	0,1742867	0,265908628	A			6,6	
301	0,892	28,09	0,0053839	10,97358811	A	Bottom	0,52368	6,6	601
302	1,66	-52,286	0,1742867	0,265908628	A			6,6	
303	1,66	-52,286	0,1742867	0,265908628	A			6,6	
304	1,562	-49,189	0,1639633	0,257913287	A			6,6	
305	1,66	-52,286	0,1742867	0,265908628	A			6,6	
306	0,892	28,09	0,0053839	10,97358811	A	Bottom	0,52368	6,6	601
307	1,66	-52,286	0,1742867	0,265908628	A			6,6	
308	1,66	-52,286	0,1742867	0,265908628	A			6,6	
309	1,562	-49,189	0,1639633	0,257913287	A			6,6	
318	1,8	106,059	0,020328	41,43281529	A	Bottom	2,04664	6,6	159
319	1,8	106,059	0,020328	41,43281529	A	Bottom	2,04664	6,6	159
320	3,6	-106,059	0,35353	0,378715852	A			6,6	
220	0,892	-24,026	0,0800867	0,180252151	B				
221	0,892	-12,013	0,0400433	0,127457518	B				
222	0,892	-12,013	0,0400433	0,127457518	B				
223	0,892	-24,026	0,0800867	0,180252151	B				
224	1,4	18,86	0,0036148	7,367813163	B		0,34339	7,5	1017

225	1,4	18,86	0,0036148	7,367813163	B		0,34339	7,5	1017
226	1,4	18,86	0,0036148	7,367813163	B		0,34339	7,5	1017
227	1,4	18,485	0,003543	7,221316348	B		0,33607	7,5	1038
228	1,4	18,86	0,0036148	7,367813163	B		0,34339	7,5	1017
229	1,4	18,86	0,0036148	7,367813163	B		0,34339	7,5	1017
230	1,4	18,86	0,0036148	7,367813163	B		0,34339	7,5	1017
231	1,66	-22,361	0,0745367	0,173894294	B				
232	0,892	12,013	0,0023025	4,692976645	B	Top	0,20965	7,5	1598
233	0,892	24,026	0,004605	9,385953291	B	Top	0,4443	7,5	799
234	0,892	36,039	0,0069075	14,07892994	B	Top	0,67895	7,5	532
235	0,892	36,039	0,0069075	14,07892994	B	Top	0,67895	7,5	532
236	0,892	24,026	0,004605	9,385953291	B	Top	0,4443	7,5	799
237	0,892	12,013	0,0023025	4,692976645	B	Top	0,20965	7,5	1598
238	1,66	-22,361	0,0745367	0,173894294	B			7,5	
239	1,66	-22,361	0,0745367	0,173894294	B			7,5	
240	1,66	-22,361	0,0745367	0,173894294	B			7,5	
241	1,66	-22,361	0,0745367	0,173894294	B			7,5	
242	1,66	-22,361	0,0745367	0,173894294	B			7,5	
265	0,692	45,358	0,0086936	17,71947346	B	Top	0,86097	7,5	423
266	1,4	22,05	0,0042263	8,614012739	B		0,4057	7,5	870
267	0,692	-36,039	0,12013	0,220762898	B			7,5	
268	1,562	-21,037	0,0701233	0,168667584	B			7,5	
269	1,562	-21,037	0,0701233	0,168667584	B			7,5	
270	0,692	-36,039	0,12013	0,220762898	B			7,5	
271	0,692	45,358	0,0086936	17,71947346	B	Top	0,86097	7,5	423
272	1,4	22,1	0,0042358	8,633545648	B		0,40668	7,5	868
314	1,8	45,358	0,0086936	17,71947346	B	Top	0,86097	7,5	423
315	1,8	45,358	0,0086936	17,71947346	B	Top	0,86097	7,5	423
316	1,8	-45,358	0,1511933	0,247666159	B			7,5	
317	1,8	-45,358	0,1511933	0,247666159	B			7,5	
310	1,4	45,384	0,0086986	17,72963057	C		0,86148		
311	0,9	6,755	0,0012947	2,638895966	C		0,10694		
325	1,8	42,126	0,0080742	16,45686624	C	Bottom	0,79784		
326	1,4	32,764	0,0062798	12,79952442	C		0,61498		
327	2,28	-53,368	0,1778933	0,26864588	C				
328	1,4	32,764	0,0062798	12,79952442	C		0,61498		
329	1,8	42,126	0,0080742	16,45686624	C	Bottom	0,79784		
330	2,28	-53,368	0,1778933	0,26864588	C				
184	0,9	117,786	0,0225757	46,01406369	D		2,2757		
186	0,9	117,786	0,0225757	46,01406369	D		2,2757		
192	1,4	117,786	0,0225757	46,01406369	D		2,2757		
212	1,4	117,786	0,0225757	46,01406369	D		2,2757		
368	1,8	-97,052	0,3235067	0,362278003	D		-0,0069		
369	1,8	-97,052	0,3235067	0,362278003	D		-0,0069		
387	1,8	39,264	0,0075256	15,33880255	D	Top	0,74194		
388	1,8	39,264	0,0075256	15,33880255	D	Top	0,74194		
193	1,4	26,223	0,0050261	10,2442293	E		0,48721		
210	1,4	26,223	0,0050261	10,2442293	E		0,48721		
366	1,4	97,052	0,0186016	37,91415711	E	Bottom	1,87071		
367	1,4	97,052	0,0186016	37,91415711	E		1,87071		

382	1,4	-39,264	0,13088	0,230428923	E				
383	1,4	-39,264	0,13088	0,230428923	E				
190	1,4	114,565	0,0219583	44,75575372	F		2,21279		
202	1,4	114,565	0,0219583	44,75575372	F		2,21279		
321	0,9	91,91	0,0176161	35,90539278	F		1,77027		
323	0,9	91,91	0,0176161	35,90539278	F		1,77027		
370	1,4	-22,978	0,0765933	0,176277074	F				
371	1,4	-22,978	0,0765933	0,176277074	F				
372	1,4	-111,658	0,3721933	0,388583757	F				
373	1,4	-111,658	0,3721933	0,388583757	F				
380	1,4	189,871	0,0363919	74,17465817	F	Top	3,68373		
381	1,4	189,871	0,0363919	74,17465817	F	Top	3,68373		
374	1,8	91,233	0,0174863	35,6409172	G		1,75705		
375	1,8	91,233	0,0174863	35,6409172	G		1,75705		
378	1,8	-149,021	0,4967367	0,448914318	G				
379	1,8	-149,021	0,4967367	0,448914318	G				
213	1,4	85,9	0,0164642	33,55753715	H		1,65288		
334	1,4	33,52	0,0064247	13,094862	H		0,62974		
335	1,8	43,098	0,0082605	16,83658599	H	Top	0,81683		
336	1,4	33,52	0,0064247	13,094862	H		0,62974		
337	1,8	43,098	0,0082605	16,83658599	H	Top	0,81683		
361	2,28	-54,599	0,1819967	0,271726544	H				
362	2,28	-54,599	0,1819967	0,271726544	H				
413	0,9	42,95	0,0082321	16,77876858	H		0,81394		
243	0,892	-24,026	0,0800867	0,180252151	I				
244	0,892	-12,013	0,0400433	0,127457518	I				
245	0,892	-12,013	0,0400433	0,127457518	I				
246	0,892	-24,026	0,0800867	0,180252151	I				
247	1,4	18,86	0,0036148	7,367813163	I		0,34339		
248	1,4	18,86	0,0036148	7,367813163	I		0,34339		
249	1,4	18,86	0,0036148	7,367813163	I		0,34339		
250	0,892	36,039	0,0069075	14,07892994	I		0,67895		
251	1,4	18,86	0,0036148	7,367813163	I		0,34339		
252	1,4	18,86	0,0036148	7,367813163	I		0,34339		
253	1,4	18,86	0,0036148	7,367813163	I		0,34339		
254	1,66	-22,361	0,0745367	0,173894294	I				
255	0,892	12,013	0,0023025	4,692976645	I		0,20965		
256	0,892	24,026	0,004605	9,385953291	I		0,4443		
257	0,892	36,039	0,0069075	14,07892994	I		0,67895		
258	0,892	24,026	0,004605	9,385953291	I		0,4443		
259	0,892	12,013	0,0023025	4,692976645	I		0,20965		
260	1,66	-22,361	0,0745367	0,173894294	I				
261	1,66	-22,361	0,0745367	0,173894294	I				
262	1,66	-22,361	0,0745367	0,173894294	I				
274	0,692	45,358	0,0086936	17,71947346	I		0,86097		
275	0,692	-36,039	0,12013	0,220762898	I				
276	1,562	-21,037	0,0701233	0,168667584	I				
277	1,4	18,86	0,0036148	7,367813163	I		0,34339		
278	0,692	45,358	0,0086936	17,71947346	I		0,86097		
279	0,692	-36,039	0,12013	0,220762898	I				

312	1,8	45,358	0,0086936	17,71947346	I		0,86097		
313	3,6	-45,358	0,1511933	0,247666159	I				
331	1,8	45,358	0,0086936	17,71947346	I		0,86097		
183	1,03	-101,06	0,3368667	0,369682904	A*				
207	1,031	-27,03	0,0901	0,19118893	A*				
208	1,031	-27,03	0,0901	0,19118893	A*				
209	0,5	127,868	0,024508	49,95267941	A*		2,47263		
211	0,5	0	0	0	A*				
196	0,5	251,493	0,0482028	98,24779618	B*		4,88739		
197	0,472	-26,716	0,0890533	0,190075192	B*				
198	0,5	-114,038	0,3801267	0,392703269	B*				
201	0,472	-26,716	0,0890533	0,190075192	B*				
322	1,03	-105,141	0,35047	0,377073291	B*				
396	2,1	72,785	0,0139505	28,4340552	C*		1,3967		
397	2,1	142,394	0,0272922	55,62738004	C*	Top	2,75637		
398	2,524	-206,529	0,68843	0,52848205	C*				
405	2,778	-35,467	0,1182233	0,21900395	C*				
407	2,524	36,82	0,0070572	14,38403397	C*	Bottom	0,6942		